

**Molecular mechanism of influenza**  
**A virus restriction by human**  
**annexin A6**

Submitted by

**Stefan Diaz Gaisenband**

for the Doctor of Philosophy at

Brunel University London

in March 2017

## **ABSTRACT**

Influenza A virus (IAV) is a major threat to human health with seasonal epidemics, occasional pandemics and emergence of new highly pathogenic strains from the animal reservoir. Our laboratory has shown that the human Annexin A6 (AnxA6) interacts with the IAV M2 proton channel and limits production of progeny IAV from infected cells. We have found that overexpression of AnxA6 impairs morphogenesis and release of progeny viruses. These findings are supported by another study showing that AnxA6 has a critical role in the late endosomal cholesterol balance and affects IAV replication and propagation in AnxA6-overexpressing cells. However, the molecular mechanism responsible for restriction of IAV morphogenesis by AnxA6 is still unclear. AnxA6 is a calcium-dependent phospholipid-binding protein which plays a major role in cellular events such as regulation of cholesterol homeostasis and membrane organisation or repair. AnxA6 is also implicated in the regulation of intracellular signalling pathways required for IAV infection. In this study, we used a combination of virology, cellular biology and biochemistry approaches to decipher the restriction mechanism of IAV by human AnxA6. We found that AnxA6 down-regulates M2 viral protein expression and impairs viral morphogenesis and budding. We also found that AnxA6 regulates chemokines and cytokines expression during viral infection, suggesting that AnxA6 triggers an innate immune response to IAV by modulating signalling pathways required for viral replication. Finally, we observed that IAV down-regulates AnxA6 expression at mRNA level during early stages of infection and at protein level during late infection, suggesting that IAV has developed a strategy to respond to AnxA6 restriction mechanism during viral infection. We conclude that it is essential to better understand the interaction between human AnxA6 and IAV to elucidate the potential of AnxA6 as an antiviral candidate.

## DECLARATION

I declare that this thesis is a presentation of my own original research work, except where due acknowledgement is made, and that it has not been previously submitted for any other degree, diploma or other qualification.

Signed:



Stefan Diaz Gaisenband

## ACKNOWLEDGEMENTS

This piece of work has not been possible without the help and support of many amazing people who deserve to be acknowledged and thanked.

I would like to firstly thank my first supervisor Dr Beatrice Nal-Rogier for giving me the opportunity to work in the exciting field of Virology. Thank you for your great supervision, constant support, advice and also for all the stimulating discussions about my research project. Thank you as well for the critical evaluation of my thesis and my work. Also, my second supervisor Dr Anthony Tsolaki for his support and contribution to the progress of my research work, providing me with helpful advice and interesting suggestions for the work to come. Also, Dr Gudrun Stenbeck and Dr Jeremy Rossman for agreeing to act as examiners and give me the opportunity to discuss in details my research findings: it was an enjoyable time!

Dr Alan Reynolds and Dr Ashley Howkins for their training and advice while performing electron microscopy procedures at the ETC. Thanks to the fantastic technicians' team: Helen, Gerry and Matt... You have all helped me out whenever I needed your help! Also, a big thank you to all people involved in the research carried out by our group: Zainab, Luis, Yasmin, Maria and Luc. You have all made my life much easier with your friendship and technical support.

Then, thanks to all PhD students who have now become my friends. It has been great pleasure to get to know you all and be able to share our endless days in labs with you. Christianah, Parissa, Dimple, Sheila, Ezgi, Haroon... And Amir, of course, we have also shared the excitement but also all our frustrations (much more often!) during our projects. You've been an amazing friend during these past years!

Last but not least, my good friend Juanka, who has always been there for me when I needed him! Of course, my parents and my brother for their love and trust. You have been an amazing help and support for me during all this time and I will always be grateful for all your sacrifice during this long way. Finally, Dasha, there is no words to describe how thankful I am for all your love, constant support and advice. You have pushed me out of my comfort zone and have made me a stronger person. Thank you for being by my side every day during these last years.

# TABLE OF CONTENTS

ABSTRACT .....	i
DECLARATION.....	ii
ACKNOWLEDGEMENTS .....	iii
TABLE OF CONTENTS .....	v
LIST OF FIGURES.....	x
LIST OF TABLES.....	xiii
ABBREVIATIONS .....	xiv
1 INTRODUCTION.....	1
1.1 Influenza A virus.....	1
1.1.1 Transmission, clinical manifestations and circulation .....	1
1.1.2 Classification and subtypes .....	1
1.1.3 Virion morphology.....	4
1.1.4 Genome organisation .....	4
1.1.5 Cell tropism.....	5
1.1.6 Structural proteins: from structure to function during virus infection .....	6
1.1.7 Virus life cycle.....	23
1.1.8 Assembly and budding .....	26
1.1.9 Regulation of cellular pathways during virus life cycle .....	28
1.1.10 Innate immune response .....	30
1.2 Interactions of influenza A virus with host cellular factors .....	43
1.2.1 Interest of host factors as antiviral targets .....	43
1.2.2 Extensive network of interactions between influenza A virus and the host .....	44
1.2.3 High-throughput approaches to study virus-host interactions .....	45
1.2.4 Interactions between influenza A virus and the host during last stages of the virus life cycle lead to morphogenesis of new virions.....	52

1.3	Human annexin A6 is a cellular factor interacting with M2 cytoplasmic tail of influenza A virus .....	62
1.3.1	Interaction of human Annexin A6 with M2 viral protein.....	62
1.3.2	Overexpression of Annexin A6 negatively modulates IAV infection and affects virus morphogenesis and release from infected cells .....	65
1.3.3	Classification, tissue expression and structure of Annexin A6.....	69
1.3.4	Annexin A6 biological functions .....	71
1.3.5	Modulation of important intracellular signalling pathways by annexin A6 . .....	75
1.4	Hypothesis .....	82
1.5	Aims of the study.....	82
2	MATERIALS AND METHODS .....	83
2.1	Materials .....	83
2.1.1	Virus strains.....	83
2.1.2	Cell lines .....	83
2.1.3	Oligonucleotides for quantitative Real Time-Polymerase Chain Reaction .....	83
2.1.4	Primary antibodies.....	85
2.1.5	Secondary antibodies .....	86
2.1.6	Kits .....	86
2.2	Methods .....	87
2.2.1	Cell amplification .....	87
2.2.2	Expression of AnxA6 in the A431 and A549 stable cell lines.....	87
2.2.3	Virus amplification and purification .....	88
2.2.4	Plaque assay .....	89
2.2.5	Median tissue culture infectious dose - TCID50 .....	89
2.2.6	Scanning electron microscopy.....	90
2.2.7	Transmission electron microscopy .....	90

2.2.8	Immunofluorescence Assay.....	90
2.2.9	Imagestream - Flow cytometry .....	91
2.2.10	Western blot .....	91
2.2.11	Real-Time Polymerase chain reaction (RT-PCR) .....	93
2.2.12	Proteome Profiler – Human Phospho-MAPK Array .....	94
3	RESULTS .....	96
3.1	Annexin A6 overexpression impairs morphogenesis and release of influenza A virus.....	97
3.1.1	Expression levels of AnxA6 in the cell lines used for our study .....	97
3.1.2	Annexin A6 over-expression restricts influenza A virus .....	98
3.1.3	Filamentous influenza A virus particles are readily observed at the surface of infected human epithelial cells .....	99
3.1.4	Patterns of expression of viral H3 and M2 proteins and cellular human annexin A6 protein .....	101
3.1.5	AnxA6 is not enriched together with M2 at the plasma membrane where viral particles bud .....	102
3.1.6	M2 and annexin A6 could colocalize in intracellular vesicular-like compartments. ....	105
3.1.7	AnxA6 expression does not alter the subcellular localisation of M1 during viral infection .....	107
3.1.8	Protein composition of released viral particles.....	109
3.1.9	Annexin A6 over-expression leads to M2 down-regulation and a defect in expression of viral proteins at the cell surface .....	110
3.1.10	Alteration of normal expression and subcellular compartmentalisation of viral proteins by annexin A6 .....	114
3.1.11	Identification of pathway targeting degradation of M2 .....	116
3.1.12	Anx6 overexpression impairs morphogenesis of filamentous influenza A virus .....	119

3.2	Annexin A6 is implicated in the modulation of important cellular pathways required for viral infection and induction of the anti-IAV innate immune response ...	123
3.2.1	Annexin A6 regulates important signalling kinases during early IAV infection.....	123
3.2.2	Annexin A6 regulates expression of ERK and AKT signalling pathways during early infection.....	133
3.2.3	Overexpression of Annexin A6 leads to differential profile of cytokines in A549 human lung epithelial cells.....	134
3.2.4	Over-expression of annexin A6 in A549 lung epithelial cells is associated with higher levels of NF- $\kappa$ B nuclear translocation in IAV infected cells .....	138
3.3	Influenza A virus down-regulates Annexin A6 expression.....	142
3.3.1	Annexin A6 is down-regulated upon IAV infection at the mRNA level	142
3.3.2	Annexin A6 protein is also down-regulated during IAV infection.....	145
3.3.3	Influenza A virus does not down-regulate exogenous annexin A6 protein during infection.....	148
4	DISCUSSION.....	151
4.1	Molecular mechanism of influenza A virus restriction by Annexin A6.....	151
4.2	Annexin A6 modulates important intracellular signalling pathways required for influenza A virus infection .....	159
4.3	Influenza A virus down-regulates annexin A6 .....	164
5	CONCLUSIONS AND PERSPECTIVES.....	167
6	BIBLIOGRAPHY .....	170
7	APPENDIX: Study of an engineered Annexin A1-derived peptide as a modulator of influenza A virus infection.....	189
7.1	Introduction .....	189
7.2	Hypothesis and aim of the study .....	190
7.3	Materials and methods.....	190
7.3.1	Haemagglutination assay .....	190

7.3.2	Haemagglutination assay inhibition .....	191
7.4	Results .....	191
7.5	Discussion and conclusion .....	194

## LIST OF FIGURES

Figure 1.1. Classification of all influenza A virus haemagglutinin and neuraminidase subtypes.....	3
Figure 1.2. Genome of influenza A virus.....	5
Figure 1.3. Cleavage of HA is necessary for membrane fusion.. ..	8
Figure 1.4. Propeller structure of the NA globular head .....	10
Figure 1.5. Structural organisation of an M1 matrix protein monomer.. ..	12
Figure 1.6. Structural organisation of an M2 matrix protein. ....	15
Figure 1.7. Structure of influenza A virus M2 proton channel.....	16
Figure 1.8. M2 mutants of filamentous Udorn and spherical WSN influenza viruses exhibit incomplete scission.....	18
Figure 1.9. Three-dimensional model of all vRNPs packaged together within a virion .....	23
Figure 1.10. Influenza A virus life cycle.. ..	24
Figure 1.11. Proposed model of budding of influenza viruses.....	27
Figure 1.12. The vast innate immune response against influenza virus is orchestrated by soluble and cellular mediators but also by viral components .....	31
Figure 1.13. Innate immune recognition of IAV is transduced through several pathways in lung epithelial cells. ....	34
Figure 1.14. Influenza A virus escapes innate immunity by preventing its recognition through cellular receptors.. ..	40
Figure 1.15. Map of interactions between the host and influenza A virus .....	44
Figure 1.16. Genome-wide RNAi screens identify new host factors important for influenza infectious life cycle in human cells. ....	47
Figure 1.17. Yeast two-hybrid system.....	49
Figure 1.18. Methodology for the design of a map of interactions between the host and influenza virus. ....	51
Figure 1.19. Interactions between the human host cell and influenza virus. ....	55
Figure 1.20. AnxA6 interacts with the M2 CT of influenza A virus.....	63
Figure 1.21. Human AnxA6 and M2 virus proteins interact in human infected cells. ....	64
Figure 1.22. AnxA6 negatively modulates influenza A virus infection. ....	65
Figure 1.23. Influenza virus budding is impaired by AnxA6 over-expression. ....	66

Figure 1.24. AnxA6 regulates late endosomal cholesterol balance to limit influenza A virus infection	68
Figure 1.25. Representation of the crystal structure of AnxA6 .....	70
Figure 1.26. AnxA6 plays an important role in intracellular cholesterol homeostasis and formation of caveolae.....	73
Figure 1.27. Regulation of EGFR/Ras by AnxA6.....	77
Figure 1.28. AnxA6 is involved in T cell receptor signalling.....	79
Figure 1.29. AnxA6 interacts with p65 in chondrocytes.....	80
Figure 1.30. AnxA6 induces ERK and p38 activation in chondrocytes through regulation of PKC $\alpha$ ...	81
Figure 2.1. Cloning system used to establish stable A431 and A549 cell lines expressing AnxA6. ....	88
Figure 3.1 Expression of annexin A6 in A431 and A549 cells.. .....	97
Figure 3.2. AnxA6 expression leads to a reduction in titres of influenza A/Udorn/72 (H3N2). .....	98
Figure 3.3. SEM and IFA enable observation of budding of filamentous virions from infected A431 and A431-AnxA6 cells.....	100
Figure 3.4. Observation of subcellular localisation of viral H3 and M2 proteins and cellular AnxA6 protein in infected cells by immunofluorescence assay .....	102
Figure 3.5. M2 was observed at the basis of budding filamentous particles .....	103
Figure 3.6. AnxA6 is not enriched together with M2 at the plasma membrane where viral particles bud.. .....	104
Figure 3.7. Analysis of annexin A6 subcellular localisation in infected cells .....	106
Figure 3.8. M2 and annexin A6 colocalised in vesicular-like compartments.. .....	107
Figure 3.9. Subcellular localisation of viral M1 protein in infected cells is not altered by AnxA6 expression .....	108
Figure 3.10. Annexin A6 is not detected in released viral particles. ....	110
Figure 3.11. Study of the trafficking of viral proteins to the cell surface by flow cytometry. ....	112
Figure 3.12. Trafficking of viral proteins to the cell surface by imaging flow cytometry.....	113
Figure 3.13. Trafficking of M2 viral protein to the cell surface by imaging flow cytometry. ....	114
Figure 3.14. Expression of AnxA6 leads to changes in detection of viral proteins in detergent soluble and insoluble fractions of IAV infected cells.....	115
Figure 3.15. AnxA6 targets M2 degradation through the lysosomal pathway. ....	119
Figure 3.16. Annexin A6 overexpression impairs morphogenesis of filamentous influenza A virus. .	120

Figure 3.17. Annexin A6 overexpression leads to budding of interconnected filamentous influenza A virus.....	122
Figure 3.18. Study of MAPKs and other signalling kinases activation during early influenza infection..	125
Figure 3.19. Detection of activated/phosphorylated kinases during influenza infection. ....	125
Figure 3.20. Normalisation of activated/phosphorylated kinases during influenza infection .....	130
Figure 3.21. Annexin A6 regulates expression of ERK and AKT signalling pathways during early infection of influenza virus in A549 human lung epithelial cells. ....	133
Figure 3.22. Differential profile of cytokines is expressed upon viral infection in A549 human lung epithelial cells over-expressing Annexin A6.....	136
Figure 3.23. Differential profile of cytokines is expressed upon viral infection in A549 human lung epithelial cells over-expressing Annexin A6.....	137
Figure 3.24. Over-expression of annexin A6 in A549 lung epithelial cells is associated with higher levels of NF- $\kappa$ B nuclear translocation in IAV infected cells. ....	140
Figure 3.25. Endogenous annexin A6 is down-regulated upon IAV infection at the mRNA level. ....	142
Figure 3.26. Endogenous annexin A6 is down-regulated upon IAV infection at the mRNA level.. ....	143
Figure 3.27. Exogenous annexin A6 gene expression is up-regulated by influenza A virus.....	145
Figure 3.28. Annexin A6 is slightly down-regulated upon IAV infection at the protein level during early infection.....	146
Figure 3.29. Annexin A6 protein is down-regulated at very late IAV infection.....	147
Figure 3.30. Exogenous annexin A6 protein is not down-regulated during early IAV infection.....	148
Figure 3.31. Exogenous annexin A6 protein is not down-regulated during late viral infection.....	149
Figure 4.1. Suggested model of the restriction molecular mechanism of influenza A virus by human annexin A6 .....	157
Figure 4.2. Targeting intracellular pathways to clarify the role of AnxA6 in their regulation during influenza infection.. ....	163
Figure 4.3. Map of the AnxA6-related region on chromosome 5 .....	165

## LIST OF TABLES

Table 1. Current approved antiviral drugs against influenza viruses.....	43
Table 2. Yeast two-hybrid screening for the interaction of AnxA6 and M2 CT.....	62

## ABBREVIATIONS

<b>IAV</b> - Influenza A virus	<b>HPAI</b> - Highly pathogenic avian influenza
<b>AnxA6</b> - Annexin A6	<b>AnxA1</b> - Annexin A1
<b>HA</b> - Haemagglutinin	<b>NA</b> - Neuraminidase
<b>M1</b> - Matrix protein 1	<b>M2</b> - Matrix protein 2
<b>NS1</b> - Non-structural protein 1	<b>NS2</b> - Non-structural protein 2
<b>NEP</b> - Nuclear export protein	<b>NP</b> - Nucleoprotein
<b>PB1</b> - Polymerase basic protein 1	<b>PB2</b> - Polymerase basic protein 2
<b>PA</b> - Polymerase acid protein	<b>SA</b> - Sialic acid
<b>TGN</b> - Trans-Golgi network	<b>FPR2</b> - Formyl peptide receptor 2
<b>RBCs</b> – Red blood cells	<b>CT</b> - Cytoplasmic tail
<b>TM</b> - Transmembrane	<b>NGC</b> - Negative Gaussian Curvature
<b>CRAC</b> - Cholesterol recognition aa consensus	<b>vRNA</b> - Viral RNA
<b>mRNA</b> – RNA messenger	<b>cRNA</b> - Complementary RNA
<b>vRNP</b> - Viral ribonucleoprotein	<b>MAPK</b> - Mitogen-activated protein kinase
<b>CRM1</b> - Chromosome region maintenance 1	<b>UTRs</b> - Untranslated regions
<b>NLS</b> - Nuclear Localisation Signal	<b>NES</b> - Nuclear export signal
<b>VLP</b> - Virus-like particle	<b>SP-A</b> - Surfactant protein A
<b>SP-D</b> - Surfactant protein D	<b>MBL</b> - Mannose-binding lectin
<b>CRD</b> - Carbohydrate-recognition domain	<b>HNP</b> - Human neutrophil peptide
<b>PRR</b> - Pattern recognition receptor	<b>APC</b> - Antigen presenting cells
<b>PAMP</b> - Pathogen-associated molecular pattern	<b>DAMP</b> - Damage-associated molecular pattern
<b>TLR</b> - Toll-like receptor	<b>RLR</b> - RIG-like receptor
<b>RLH</b> - RIG-I- like helicase	<b>NOD</b> - Nucleotide oligomerization domain
<b>NLR</b> - NOD-like receptor	<b>TIR</b> - Toll-interleukin 1 receptor
<b>TRIF</b> -TIR containing adapter inducing IFN- $\beta$	<b>NF-<math>\kappa</math>B</b> - Nuclear factor – kappa B
<b>TANK</b> - TRAF family member associated NFKB activator	<b>TBK1</b> - TANK binding kinase 1
<b>IRF</b> - Interferon regulatory factor	<b>IKK-I</b> - Inducible I $\kappa$ B kinase
<b>IFN</b> - Type I interferons	<b>CARD</b> - Caspase recruiting domain
	<b>RD</b> - Repressor domain

**FADD** - FAS-associated death domain-containing protein

**VISA** - Virus-induced signalling adaptor

**CCL** - Chemokine (C-C motif) ligand

**TNF $\alpha$**  - Tumor necrosis factor  $\alpha$

**RANTES** - Regulated on activation normal T cells expressed and secreted

**P58IPK** - 58 kilo Dalton cellular inhibitor

**OAS** - 2'-5'oligoadenylate synthetase

**eIF4B** - Eukaryotic translation initiation factor 4B

**RNAi** - RNA interference

**Y2H** - Yeast two-hybrid

**CBP** - Calmodulin-binding domain

**LC-MS** - Liquid chromatography tandem mass spectrometry

**AD** - Activating domain

**hNup98** - Human nucleoporin 98

**MTOC** - Microtubule organizing centre

**ER** - Endoplasmic reticulum

**siRNA** - Small interference RNA

**PE** – Phosphatidylethanolamine

**Cav1** - Caveolin-1

**LE** - Late endosomes

**NPC1** - Niemann-Pick C1

**TCR** - T cell receptor

**ERK** - Extracellular signal-regulated kinase

**LAT** - Linker for activation of T cell

**MOI** - Multiplicity of infection

**PS** - Penicillin/ Streptomycin

**TRIM25** - Tripartite motif 25

**MAVS** - Mitochondrial anti-viral signalling

**Cardif** - CARD adaptor inducing interferon- $\beta$

**IL** - Interleukin

**NK**- Natural killer

**JNK** - c-Jun N-terminal kinase

**PKR** - Protein kinase R

**Hsp** - Heat shock protein

**PABII** - Poly(A)-binding protein II

**IFITM3** - Interferon-induced transmembrane protein 3

**PPI** - Protein-protein interactions

**TAP** - Tandem affinity purification

**ProtA** - Protein A of Staphylococcus aureus

**TEV** - Tobacco etch virus

**BD** - Binding domain

**NPC** - Nuclear pore complex

**HRB** - Human immunodeficiency virus rev-binding

**COPI** - Coat protein I

**FPPS** - Farnesyl diphosphate synthase

**PS** - Phosphatidylserine

**cPLA2** - Cytoplasmic phospholipase A2

**t-SNARE** - Target membrane SNAP receptors

**MVB** - Multivesicular bodies

**EGF** - Epidermal growth factor

**SOCE** - Store-operated calcium entry

**PI3K** - Phosphoinositide 3-kinase

**WT** - Wild-type

**FBS** - Foetal bovine serum

**DMEM** - Dulbecco's modified Eagle's medium

<b>BSA</b> - Bovine serum albumin	<b>PFU</b> - Plaque forming unit
<b>MAb</b> - Monoclonal antibody	<b>PAb</b> - Polyclonal antibody
<b>BCA</b> - Bicinchoninic acid	<b>PVDF</b> - Polyvinylidene difluoride
<b>SEM</b> - Scanning electron microscopy	<b>IFA</b> - Immunofluorescence assay
<b>RT-PCR</b> - Real-Time Polymerase chain reaction	<b>RQ</b> - Relative quantities
$\Delta\Delta$ <b>CT</b> - Comparative CT method	<b>A431-AnxA6</b> - A431 cells expressing AnxA6
<b>A549-Anx6</b> - A549 cells expressing AnxA6	<b>ANDV</b> - Andes Virus
<b>SCP-2</b> - Sterol carrier protein-2	<b>PI(4,5)P2</b> - Phosphatidylinositol 4,5 biphosphate
<b>OSBP</b> - Oxysterol-binding protein	<b>VAMP</b> - Vesicle-associated membrane protein
<b>VAPA</b> - VAMP-associated protein A	<b>CERT</b> - Ceramide-transfer protein
<b>DRM</b> - Detergent resistant membrane	<b>PITRF</b> - Polymerase I and transcript release factor
<b>LDL</b> - Low-density lipoproteins	<b>PTEN</b> - Phosphatase and tensin homology
<b>ANT3</b> - Adenine nucleotide translocator 3	<b>VDAC1</b> – Voltage-dependent anion channel 1
<b>iNOS</b> - Inducible nitric oxide synthase	<b>EM</b> - Electron microscopy

# 1 INTRODUCTION

## 1.1 Influenza A virus

### 1.1.1 Transmission, clinical manifestations and circulation

Influenza is a viral infection of the respiratory tract spread worldwide and transmitted by direct contact with infected people or surfaces and by inhalation of aerosols containing small viral particles. Illness can be mild to severe, leading to death at times in groups at high risk such as young children, elderly and those with serious medical conditions. Most common symptoms observed in sick people are fever, headache and other body aches, cough and rhinitis, which usually last for about one week. Influenza A viruses (IAV) represent a major threat to human health with seasonal epidemics, occasional pandemics and emergence of new highly pathogenic strains from the animal reservoir. Every year, three to five million people are severely ill and 250.000 to 500.000 people die worldwide because of circulating seasonal influenza viruses, being H1N1 and H3N2 subtypes among the most common (WHO, 2016). Besides seasonal illness, a general concern is that more pathogenic viruses can appear after reassortment of human seasonal viruses with circulating highly pathogenic avian influenza (HPAI). Several zoonotic transmissions to humans have already been reported over the last years: the swine-origin pandemic influenza H1N1 virus, which spread worldwide in 2009, the avian-origin H5N1 HPAI circulating since 1997 and the recently reported H7N9, H9N2 and H10N8 avian viruses. Likely, new influenza strains transmitted from animals to humans are to arise in the coming years (WHO, 2016, Medina and Garcia-Sastre, 2011, Kalthoff et al., 2010, Itoh et al., 2009, Peiris et al., 2007).

### 1.1.2 Classification and subtypes

Influenza viruses are classified into types A, B, and C on the basis of their core proteins (IAV, IBV and ICV, respectively). However, a new influenza virus identified in 2011 was proposed as a new member of the *Orthomyxoviridae* family and named influenza D virus (IDV), this new type has been found in swine, goat, sheep and cattle (Ferguson et al., 2016, Hause et al.,

2013). IAV infects a range of mammalian and avian species in addition to humans, whereas IBV and ICV mainly affect humans (Iha et al., 2016, Medina and Garcia-Sastre, 2011). IBV and ICV express slightly different proteins when compared to IAV. IBV express 9 proteins also found in IAV and two proteins which are exclusive to the B type virus, NB and BM2. NB is a protein encoded by the RNA segment 6 highly expressed at the surface of IBV infected cells and involved in ion channel activity (Hatta and Kawaoka, 2003). BM2 is a protein encoded by the RNA segment 7, expressed during late infection and transported to plasma membrane of infected cells through TGN. As M2 protein of IAV, BM2 is a proton channel involved in uncoating of viral particles and is essential for IBV morphogenesis. Also, BM2 has been suggested to contribute to virus assembly and budding by promoting M1-vRNPs incorporation into newly-forming virions (Pinto and Lamb, 2006b, Imai et al., 2004). ICV encodes for 9 proteins expressed also in IAV and IBV, but in addition it also expresses an exclusive haemagglutinin-esterase-fusion (HEF) glycoprotein which has a combined IAV haemagglutinin/neuraminidase-like function: it binds to surface receptors in an HA fashion during entry and cleaves surface cell receptors to promote ICV propagation in an NA manner (Wang and Veit, 2016, Gao et al., 2008b). In addition, IAV are classified into subtypes based on the spike envelope glycoproteins haemagglutinin (HA) or neuraminidase (NA), which are essential for entry and egress of virus particles at the plasma membrane of infected cells. Influenza virus presents a wide variability in antigens due to minor and major changes in its genome which are caused by frequent mutations and rearrangement of its genetic material. Minor changes, also called “antigenic drift”, occur in the amino acid sequence of proteins and enable the virus to escape immune recognition causing outbreaks very frequently (Medina and Garcia-Sastre, 2011). Major changes, also called “antigenic shift”, are very common and have an impact on virulence and severity of pathology. They have been described in several viral proteins such as HA, NA or the polymerase basic protein 1 (PB1) and are caused by reassortment from viruses of different origin such as animal and human subtypes occasionally causing large regional or pandemic outbreaks. These constant changes in the genomic structure lead to classification of influenza A viruses into different groups and clades (Medina

and Garcia-Sastre, 2011). Currently, 18 subtypes of HA and 11 subtypes of NA have been identified and characterised enabling the classification of influenza virus strains in groups, only H1 and H3 subtypes circulate among humans (figure 1.1) (Wu et al., 2014).

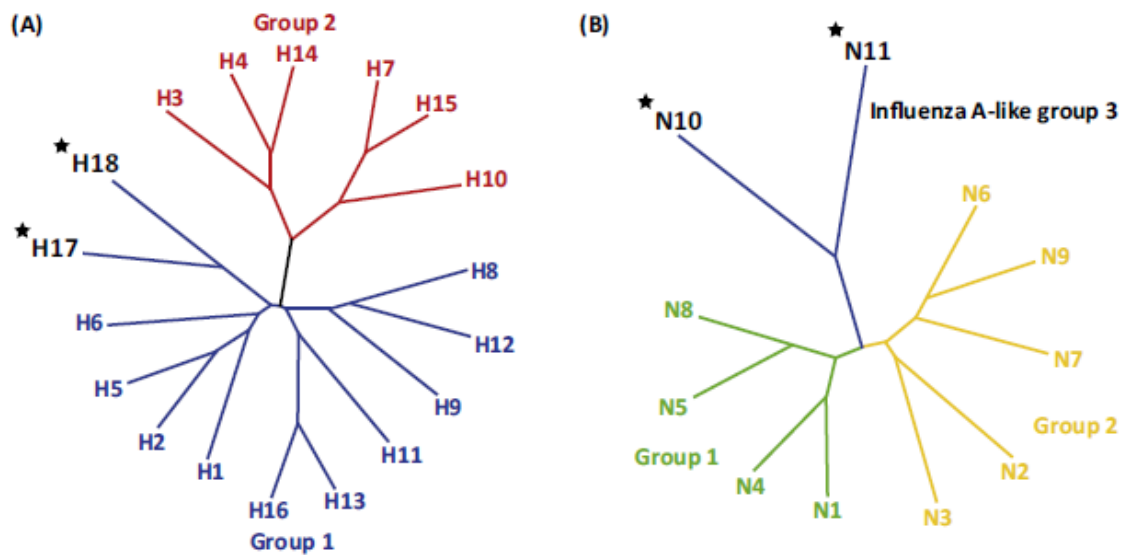


**Figure 1.1. Classification of all influenza A virus haemagglutinin and neuraminidase subtypes.**

(A) All characterised HAs are grouped into two groups, and the new H17/H18 subtypes recently found in bats are included in the first group and marked with a star (B) All described NAs were also originally classified into two groups but recently a new ‘influenza A-like group 3’ has been proposed including the new N10/N11 subtypes found in bats, again marked with a star. From Wu et al., 2014.

The HA subtypes are very well described and are divided into two main groups. The first group includes H1 and H9 clades which contain the H1 subtypes with all H1N1 human seasonal strains and both H1N1 strains that caused pandemics in 1918 and 2009, and also the H5 subtype that gave rise to the HPAI H5N1 strains. The second group comprises the H3 and H7 clades, which include all human seasonal H3N2 strains and also the HPAI H7N7 strains. NA subtypes were also classified into two groups: the first group includes N1, N4, N5, and N8, and the second group N2, N3, N6, N7, and N9 (Medina and Garcia-Sastre, 2011). Recently, the discovery of H17N10 and H18N11 strains in bats has expanded the range of natural IAV reservoirs and as a result a new NA influenza A-like group 3 has been suggested. Both H17 and H18 subtypes are included in the HA group 1 whereas both N10 and N11 were included

in this new NA influenza A-like group 3 as they presented different characteristics to all NA previously described (Wu et al., 2014, Tong et al., 2013, Tong et al., 2012).

### 1.1.3 Virion morphology

IAV strains are pleomorphic and can exhibit different morphologies, filaments are predominant in human respiratory tract and spherical virions are frequently observed after adaptation to laboratory conditions (Rossman et al., 2012, Rossman and Lamb, 2011, Sieczkarski and Whittaker, 2005). In a recent study, both filamentous and spherical virions were used to further understand the link between the morphology and the specificity for a specific substrate. It was demonstrated that a spherical laboratory-adapted strain was exhibiting a filamentous shape after being passaged 12 times in guinea pigs; conversely, it was also found that two filamentous viruses showed a spherical shape after 10 passages in embryonated chicken eggs and Madin-Darby canine kidney (MDCK) cells (Seladi-Schulman et al., 2013). These results suggested that filamentous strains are likely to have an advantage for infection in the host and are selected in vivo over spherical strains but also that spherical morphology is not required for increased growth in eggs and MDCK cells. Finally, Seladi-Schulman and collaborators found that changes in morphology could correspond to mutations in the M1 protein; however, they suggested that these mutations are not the only explanation for efficient switch in the shape and adaptation of viruses to new conditions (Seladi-Schulman et al., 2013).

### 1.1.4 Genome organisation

Influenza A virus is an enveloped virus belonging to the Orthomyxoviridae family and contains a segmented negative single-stranded RNA genome encoding 11-12 proteins (figure 1.2). The viral envelope is derived from the plasma membrane of the host cell (Sun and Whittaker, 2003). The RNA segments encode for the structural proteins haemagglutinin (HA), neuraminidase (NA), matrix protein 1 (M1) and proton channel M2, the non-structural proteins 1 and 2 (NS1 and NS2, the latter also known as nuclear export protein, NEP), the nucleoprotein (NP), the also non-structural mitochondrial protein PB1-F2 derived from the PB1 segment, the 3 components of the viral RNA polymerase complex (PB1, PB2 and PA) and the

later reported protein named N40 which limits virus replication *in vitro* and *in vivo* when PB1-F2 is absent (Medina and Garcia-Sastre, 2011, Wise et al., 2009, Sieczkarski and Whittaker, 2005, Chen et al., 2001, Tauber et al., 2012).

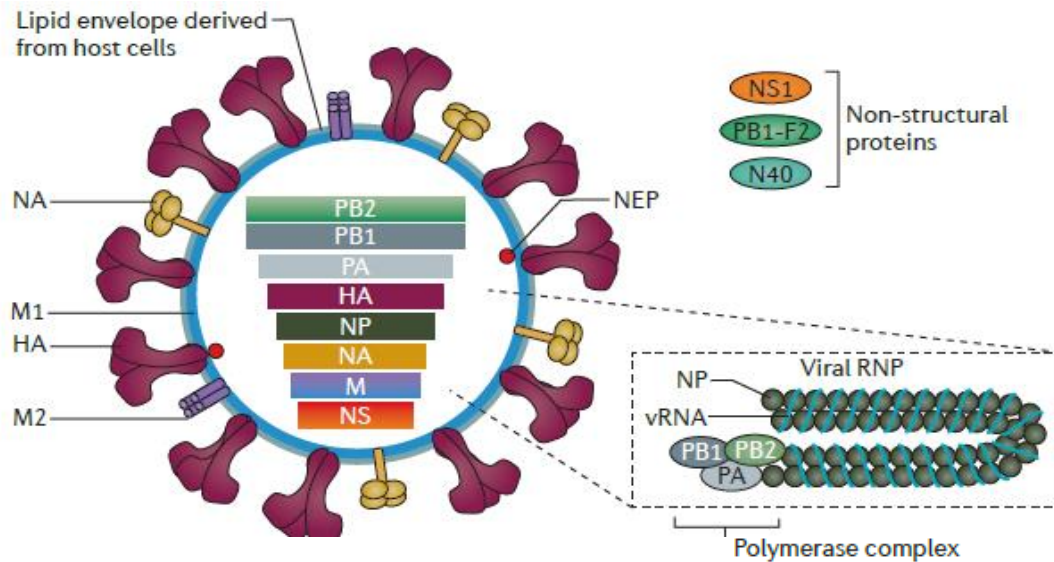


**Figure 1.2. Genome of influenza A virus.** IAV possess a single-stranded negative RNA genome formed of 8 segments encoding for 11-12 proteins which are: the structural proteins haemagglutinin (HA), neuraminidase (NA), matrix protein 1 (M1) and proton channel M2, the non-structural proteins 1 and 2 (NS1 and NS2, the latter also known as nuclear export protein, NEP) and PB1-F2, the nucleoprotein (NP), the 3 components of the viral RNA polymerase complex PB1, PB2 and PA, and finally the recently reported proteins named N40. The RNA polymerase complex consists of the 3 protein subunits (PB1, PB2 and PA), viral RNA and monomers of NP protein and is responsible for the replication and transcription of the virus genome. From Medina and Garcia-Sastre, 2011.

### 1.1.5 Cell tropism

As already mentioned above, IAV are classified into subtypes based on the spike envelope glycoproteins, which exhibit different antigenic properties in the different groups. HA has an essential role in early infection as it is responsible for the first contact between the virus and the host cell: it binds to sialic acid (SA)-containing receptors at the surface of host cell and promotes virus-cell membranes fusion for the entry of the virus. HA recognises glycoproteins terminating with  $\alpha$ -2,6-linked or  $\alpha$ -2,3-linked SA moieties expressed in airway epithelial cells

and is responsible for the specificity and affinity of cell tropism. In other words, it determines which cells and tissues support virus replication (Medina and Garcia-Sastre, 2011, Ibricevic et al., 2006). Also, this specificity of HA facilitates propagation of IAV in specific regions of the respiratory tract and leads to infection of the upper or the lower respiratory tract. It is now well known that avian viruses bind to  $\alpha$ -2,3-linked SA and human viruses bind  $\alpha$ -2,6-linked SA receptors. In vitro experiments using cultures of ciliated and non-ciliated human airway epithelial cells showed that human viruses were able to bind to and infect non-ciliated cells expressing predominantly  $\alpha$ -2,6-linked SA receptors, whereas avian viruses were able to infect mainly ciliated cells expressing most importantly  $\alpha$ -2,3-linked SA (Matrosovich et al., 2004). Also, HA is important not only for cell and tissue tropism but also to define spread and severity of infection. To enable viral entry after binding the cell receptor, HA is cleaved by host proteases in its cleavage site and changes in the amino acid sequence of this site leads to different manifestations of the disease (Medina and Garcia-Sastre, 2011). Interestingly, it has been described that the cleavage site in HA amino acid sequence of H5 and H7 HPAI contains a multibasic cleavage site cleaved by intracellular ubiquitous furin-like proteases present in the trans-Golgi network (TGN) of most cells which leads to a systemic infection and increased pathogenesis, whereas most of low-pathogenic influenza viruses possess only a single arginine amino acid in HA cleavage site recognised by extracellular trypsin-like proteases of intestinal and respiratory mucosal regions limiting their propagation to these regions (Suguitan et al., 2012). A study revealed that animals infected with an H5N1 HPAI not only exhibited neurological damage such as encephalitis and coma but also that HPAI could travel from peripheral to central nervous system (Jang et al., 2009). Therefore, rapid determination of changes in protein sequences is essential to understand the ability for viruses to adapt to new environment and to be spread to new species (Medina and Garcia-Sastre, 2011).

#### 1.1.6 Structural proteins: from structure to function during virus infection

Influenza A virus encodes for structural proteins enabling the efficient assembly and formation of new virions, which then bud from infected host cells to spread the infection. These important

viral proteins are the haemagglutinin, the neuraminidase, the matrix protein 1 (M1) and the proton channel M2 (Rossman and Lamb, 2011). These proteins have all been described to participate in many stages of the virus life cycle, however some of their specific roles are still not entirely clear (Chlanda et al., 2015).

### 1.1.6.1 Haemagglutinin

The haemagglutinin consists of 566 amino acids and is derived from the RNA segment 4 (Palese and Schulman, 1976). It is a type 1 membrane-associated glycoprotein with a 529 amino-acid ectodomain, a 27 amino-acid membrane anchoring domain near the C-terminus and a 10 amino-acid short cytoplasmic tail facing the host cell cytosol (Rossman and Lamb, 2011, Zambon, 2011, Steinhauer, 1999). HA forms homotrimers and each monomer contains a native precursor HA<sub>0</sub> which is cleaved at a conserved arginine residue by host proteases into two polypeptides, HA<sub>1</sub> and HA<sub>2</sub> (figure 1.3).

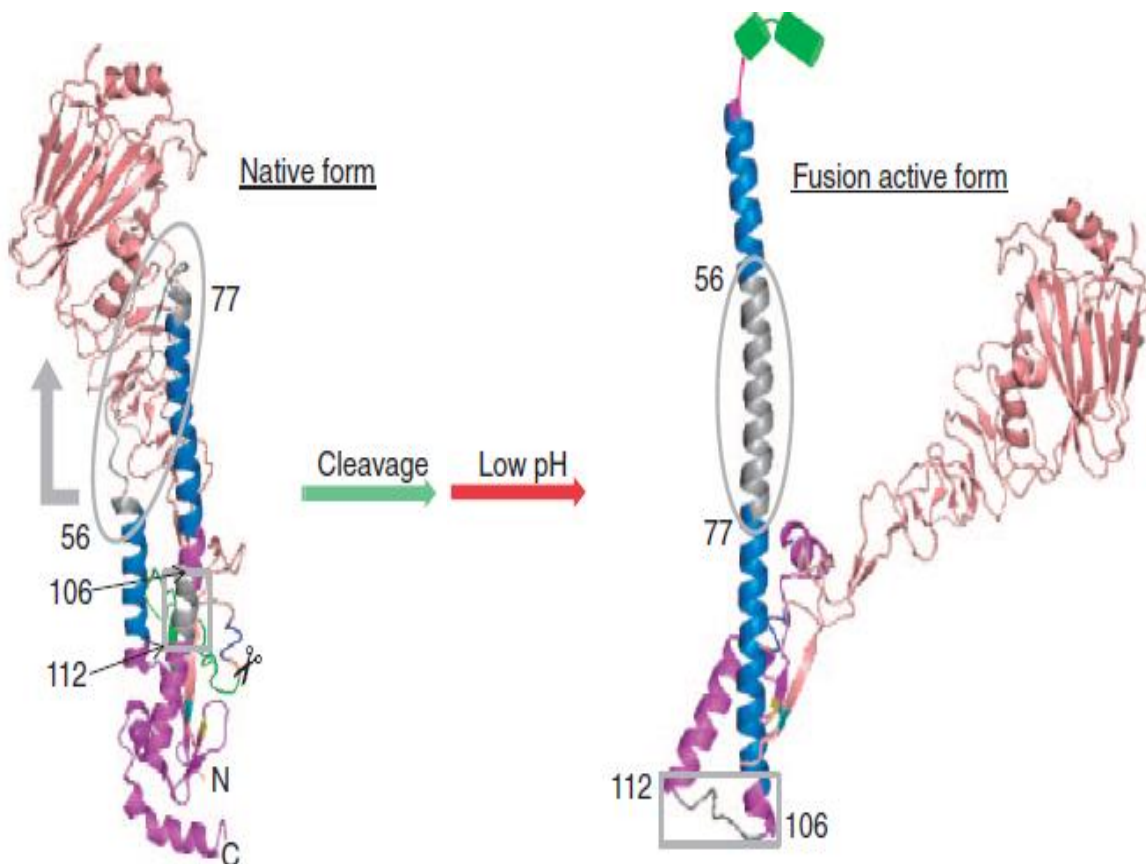


**Figure 1.3. Cleavage of HA is necessary for membrane fusion.** Native HA<sub>0</sub> is cleaved by host proteases at the cleavage site and suffers a conformational change. This change enables unfolding of the protein at low pH and formation of the fusion active form containing a fusion peptide (shown in green) which will be inserted into the host membrane to promote fusion of virus-host membranes. In an active form, HA<sub>1</sub> (pink) and HA<sub>2</sub> (purple) subunits are interconnected by a disulphide bond. Regions suffering a conformational change are located in the HA<sub>2</sub> subunit (shown in grey). From Sriwilaijaroen and Suzuki, 2012.

Firstly, HA is responsible for the first contact of the virus with the host cell and binds to a sialic-acid receptor at the cell surface. Then, IAV enters the cell by endocytosis and travels to the endosomal compartment, where HA is cleaved to promote fusion of viral-endosomal membranes when exposed to a low pH. Cleavage of HA<sub>0</sub> into the two subdomains HA<sub>1</sub> and HA<sub>2</sub>, linked by a disulphide bond, induces a conformational change that releases the fusion peptide (Skehel and Wiley, 2000, Wiley and Skehel, 1987). Firstly, HA<sub>1</sub> contacts with the sialic acid receptor at the cellular surface and then insertion of HA<sub>2</sub> N-terminus site in the cell membrane brings together host cell and virus membranes (McCullough et al., 2012, Hu, 2010, Steinhauer, 1999). Interaction of HA<sub>1</sub> with the receptor occurs through the receptor-binding site, located at the membrane-distal tip of each monomer. Each receptor-binding site is formed by several conserved residues in the base, Tyr-98, Trp-153, His-183, and Tyr-195, surrounded by three secondary structure elements, which are the 130-loop (residues 135 to 138), the 220-loop (residues 221 to 228) and the 190-helix (residues 190 to 198) (Gamblin et al., 2004). Due to the critical role in initial stages of the virus life cycle, HA has received much attention and its receptor binding site is at the moment a target for neutralizing antibodies and for therapeutic strategies (McCullough et al., 2012). Interestingly, the HA<sub>1</sub> polypeptide contains several highly conserved domains playing an important role in receptor binding specificity. In the past decade, several studies have been carried out to identify and characterise these conserved motifs in the HA<sub>1</sub> region. Also, bioinformatic methods have been used to elucidate the importance of these domains in receptor binding specificity and to identify mutations affecting HA affinity (Hu, 2010, Veljkovic et al., 2009). It was suggested that investigation of the key

regions of the protein playing a role in receptor affinity is necessary to better understand the virus tropism (Hu, 2010). It is clear that HA is mainly involved in the first stages of infection by establishing the first contact of IAV with the receptor at the host cell surface and by promoting membranes fusion for viral entry; however, it has been described to play a role in other stages of the life cycle such as assembly and release. It has been described that HA travels together with NA to lipid rafts to initiate the budding events (Veit and Thaa, 2011). In a study recently published, it was found that expression of HA alone or with NA leads to budding of viral particles and HA was found located in areas of membrane curvature, providing evidence that it could also be involved in the release of newly formed virions (Chlanda et al., 2015). Similarly, it had already been described that NA alone was sufficient to produce VLPs and promote their budding from the cell surface suggesting that NA also is important for morphogenesis and release of IAV (Lai et al., 2010).

#### 1.1.6.2 Neuraminidase

The neuraminidase is a type II integral membrane protein derived from the RNA segment 6 and at the surface of viral particles, monomers linked by disulfide bonds form tetramers with a mushroom-like shape (Medina and Garcia-Sastre, 2011, Shtyrya et al., 2009). Each monomer is a 470 amino acid polypeptide formed by an N-terminal cytoplasmic tail, a transmembrane domain and a C-terminal globular head (Shtyrya et al., 2009, Barman et al., 2004). The globular head contains the enzyme active site constituted by very conserved functional and structural residues which is responsible for stability of the enzyme at low pH, and also the calcium binding site located under the active site formed by the oxygens of many residues in the main and side chains. The head of NA is constituted of six identical antiparallel  $\beta$ -sheets which are assembled in a propeller-like structure and interconnected by numerous loops (figure 1.4) (Shtyrya et al., 2009).

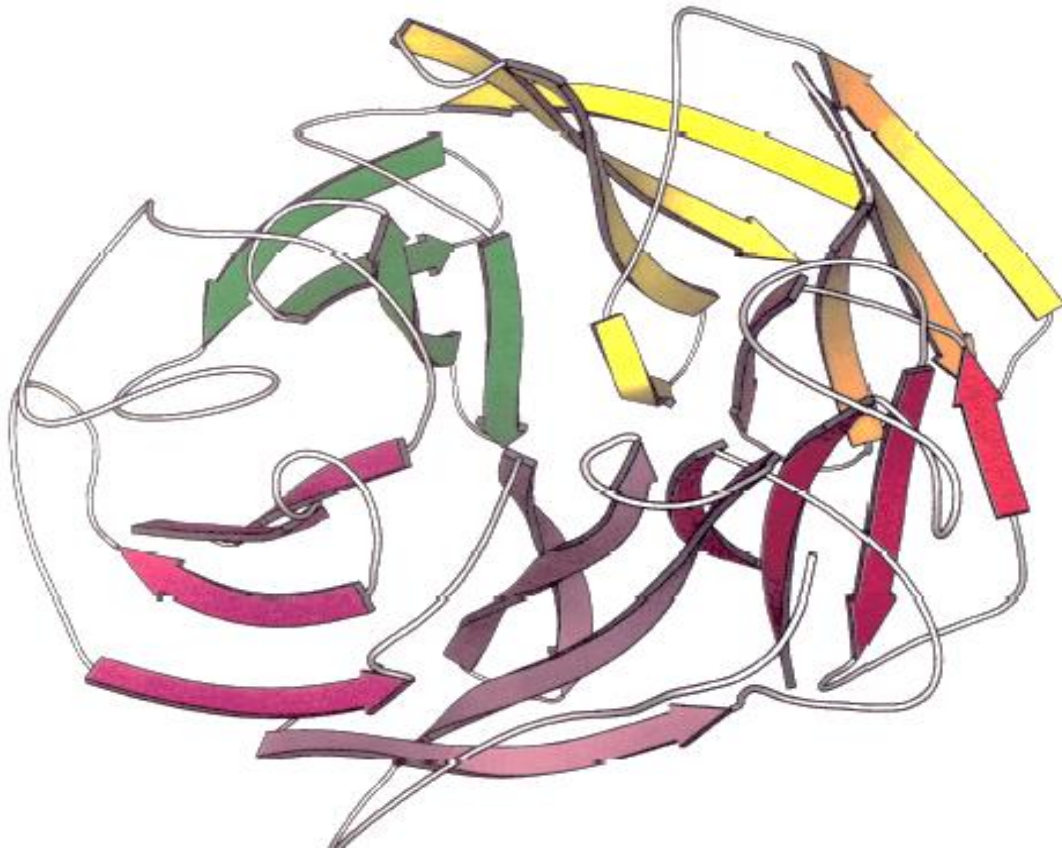


**Figure 1.4. Propeller structure of the NA globular head.** Six identical  $\beta$ -sheets are interconnected by numerous loops and assembled in a propeller-like structure. Loops are indicated in grey and  $\beta$ -sheets in colours. From Shtyrya et al., 2009.

Little information is available on the function of both cytoplasmic tail and transmembrane domain but it is very well known that they are both highly conserved, and for instance the cytoplasmic tail contains a 6 amino acid sequence - MNPNQK - which is identical in all NA subtypes (Barman et al., 2004). The transmembrane domain contains necessary elements to enable the apical transport to plasma membrane undergone by NA in polarized MDCK cells and is also responsible for NA anchoring to the cell membrane through its interaction with detergent-resistant lipid rafts (Kundu et al., 1996). Polarity is fundamental for normal cellular physiology and is responsible for the spatial segregation of compartments fulfilling specialised functions (Richardson and Simmons, 1979). In epithelial cells such as MDCK, polarity results in the separation of apical and baso-lateral membranes by tight junctions. The apical membrane interacts with the extracellular milieu and contains microvilli involved in cell

absorption, secretion and adhesion. The baso-lateral membrane faces the extracellular matrix and communicates with the rest of neighbouring cells (Balcarova-Stander et al., 1984). These cellular regions differ from each other in lipid and protein composition in order to execute their different functions (McCaffrey and Macara, 2012). When newly lipids and proteins are synthesized in the endoplasmic reticulum (ER), they are sorted into cargo vesicles at the TGN and are delivered to the appropriate plasma membrane to fulfil their function. A common route to transport lipids and proteins to plasma membrane is through the endosomal system, proteins contain basolateral or apical specific signals that enable them to be recognised and included in early or recycling endosomes before being delivered to the cell surface, if not transported to lysosomes for degradation. One important mechanism for influenza virus biology is lipid raft-dependent apical sorting, which constitutes a platform for virus assembly and budding and is based on the affinity of proteins for microdomains enriched in sphingolipids and cholesterol (Cao et al., 2012). As already mentioned, HA has already been shown to associate with lipid rafts and it was demonstrated that depletion of cholesterol and sphingolipids from membrane microdomains leads to missorting of HA during its transport to apical membrane in MDCK cells (Keller and Simons, 1998). Therefore, it is not surprising NA undergoes apical transport to plasma membrane in MDCK cells. It has been shown that both cytoplasmic tail and transmembrane domain participate in the late stages of the virus life cycle: it was found that specific residues play an important role in the protein structure and its association with lipid rafts for efficient virus assembly and morphogenesis (Barman et al., 2004). Neuraminidase may play different roles during IAV infection but its best known function is the cleavage of sialic acid from glycans on the host cell surface to enable virus spread to surrounding cells (Shtyrya et al., 2009). NA is an exosialidase responsible for cleavage of a sialic acid and an adjacent sugar at the surface of an infected cell which facilitates the budding of newly formed virions and also prevents their attachment to the host cell surface due to the recognition of sialic acids by haemagglutinin (Gamblin and Skehel, 2010, Shtyrya et al., 2009). This idea is supported by a recent study which demonstrated the presence of NA with HA in areas of membrane curvature and it was suggested to be involved in the initiation of assembly

and budding (Chlanda et al., 2015). Finally, an other role which was also proposed for NA is that it could assist in virus propagation and movement in human airway epithelium by cleaving sialic acids from mucins (Matrosovich et al., 2004). However, it is also important for HA trafficking to plasma mebrane, potentially by cleaving early interactions with sialic acid receptors in TGN (Tong et al., 2012).

### 1.1.6.3 M1 matrix protein

Influenza matrix protein (M1) is the major component of the virus and is responsible for its integrity and morphology (Noton et al., 2007). M1 protein consists of 252 amino acids and can form oligomers, most importantly dimers. It contains three domains which are interconnected by short linkers: the N-terminal domain (1-67 residues), the middle domain (87-164 residues) which is connected to the N-terminal by a linker region and the C-terminal domain (165-252 residues) (figure 1.5) (Tsfasman et al., 2015, Noton et al., 2007). Chrystallography studies determined that N-terminal and middle domains both contain 9  $\alpha$ -helices connected by loops and 4  $\alpha$ -helices are predicted for the C-terminal domain (Tsfasman et al., 2015).

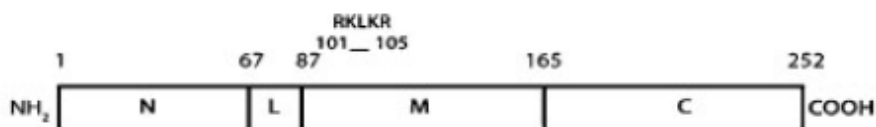


**Figure 1.5. Structural organisation of an M1 matrix protein monomer.** N-terminal (N), middle (M), C-terminal (C) domains and the linker (L) region are shown together with the RKLKR sequence, which is important for M1 binding to vRNA and NEP and is located between residues 101 and 105. Numbers represent the position of residues. From Noton et al., 2007.

Currently, the role of the different domains of M1 protein is still unclear; however, recent studies have provided some insight in this matter. In a study recently published it was found that the N-terminal domain, and especially residues 1-20, are critical for M1 and swine importin  $\alpha$ 1 interaction which results in M1 nuclear translocation (Liu et al., 2014b). In addition, Noton and co-workers found that the middle domain is the main motif for M1 binding to NP protein

during viral ribonucleoproteins (vRNPs) trafficking inside the cell and also, that it is the dominant element in self-association yet N-terminal and C-terminal domains were also involved in protein oligomerisation (Noton et al., 2007). Very little is known about the C-terminal domain but it was thought to have a weak structure. By using bioinformatics in a previously published study, a model of spatial arrangement of this domain was predicted and it was suggested to be organised in an almost flat layer containing 3  $\alpha$ -helices (Shishkov et al., 2011). A latter study demonstrated that the C-domain was less compact but more flexible compared to other domains of M1 (Shtykova et al., 2013). This study and others suggested that the versatility of this domain was important for the multifunctionality and interaction of M1 matrix protein with host cell machineries, facilitating its role in virus structural organisation and morphogenesis (Shtykova et al., 2013, Shishkov et al., 2011). Furthermore, it has been recently published that polar residues serine-183 and threonine-185 play a critical role in M1 oligomerisation and formation of the virion: single mutation led to a disrupted morphology of the virus but double mutation of these residues completely blocked virus production (Zhang et al., 2015). Finally, several studies have shown that M1 travels along other viral glycoproteins to sites of assembly and budding to orchestrate late stages during viral infection; however, no evidence of interaction with lipid rafts where these stages happen has been provided. For this reason, Tsfasman et al. performed X-ray and computational analysis of M1 protein structure to identify motifs involved in interactions with membrane rafts. They identified 6 amphipathic  $\alpha$ -helices containing cholesterol recognition amino acid consensus (CRAC) motifs which could explain M1 interaction and binding to cholesterol and other lipids at the membrane of infected cells (Tsfasman et al., 2015). It is then clear that M1 matrix protein is a multifunctional protein which plays a role in many stages of the virus life cycle. As mentioned above, M1 is the core protein of the viral envelope and is located in its inner side. It constitutes not only the link between the envelope and the vRNP complexes but also between all viral and cellular components that are present at the plasma membrane for efficient virus formation (Chlanda et al., 2015, Veit and Thaa, 2011, Barman et al., 2004, Nayak et al., 2004, Baudin et al., 2001, Ali et al., 2000, Bui et al., 2000). M1 interacts with cytoplasmic tails of mature HA and NA and

they travel all together along the secretory pathway to the budzone, an area of coalescent lipid raft domains which constitutes a platform for the recruitment of all necessary components to initiate assembly and budding (Schmitt and Lamb, 2005). The Rab11-dependent recycling endosome pathway is also involved in trafficking of viral components to plasma membrane for completion of the final stages of virus life cycle, it regulates transport of vRNPs to cell surface (Eisfeld et al., 2011a). Interaction between HA, NA and M1 is key for internalisation of M1 into the forming virion and also its association with lipid rafts, where late stages of the virus life cycle occur (Rossman and Lamb, 2011, Barman et al., 2001, Ali et al., 2000). Also, Bui et al. had found that M1 expression is essential for export of vRNPs from the nucleus to the cytosol (Bui et al., 2000). In a latter study, full-length and individual domains of M1 were tested for binding to liposomes and RNP and it was found that both full length and C-terminal domain were able to interact with RNP (Baudin et al., 2001). In addition, M1 interacts not only with viral components but also with lipids present at the plasma membrane. In a recent study it was found by quantitative microscopy approaches that M1 oligomerisation required for driving the assembly and budding of influenza virus is enhanced upon binding to lipids present at the plasma membrane (Hilsch et al., 2014). Finally, many studies have shown the involvement of M1 in virus morphology (Rossman and Lamb, 2011, Calder et al., 2010, Elleman and Barclay, 2004, Ruigrok et al., 2001). Ruigrok suggested that polymerisation of M1 at budding sites is responsible for elongation of virus filaments (Ruigrok et al., 2001). An other study found that changes in the M1 protein sequence led to alterations in shape but suggested that other elements could be involved in morphology, which is in agreement with other studies where M2 was found to also contribute to virion morphology (Roberts et al., 2013, Elleman and Barclay, 2004, Roberts et al., 1998). Finally, Calder and collaborators studied by electron cryomicroscopy the structural basis of influenza A/Udorn/72 filamentous morphology: they found that its matrix protein is highly ordered with a helical organization and suggested that the sequence of M1 is responsible for stabilising the overall structure and therefore also the filamentous shape (Calder et al., 2010).

## 1.1.6.4 M2 viroporin

### 1.1.6.4.1 Protein structure

M2 belongs to the family of viroporins, which are proteins expressed by viruses with ion channel activity. The IAV M2 protein is the best characterised viroporin (Pinto et al., 1992). It is a 97-amino acid type III transmembrane protein originated after mRNA splicing of genomic segment 7 and contains 3 domains: a 24-residue N-terminal ectodomain, a 19-residue single-helical domain integrated in the membrane and a 54-residue C-terminal cytoplasmic tail (CT) (figure 1.6) (Holsinger et al., 1994). At the plasma membrane of infected cells, M2 consists of homotetramers formed by the tetramerisation of 4 hydrophobic transmembrane (TM) helices and the link of the different monomers by disulphide bonds. This tetramerization provides the organisation for a pH-dependent functional proton channel with N-terminal and C-terminal domains facing the outside and the inside of the virion respectively.

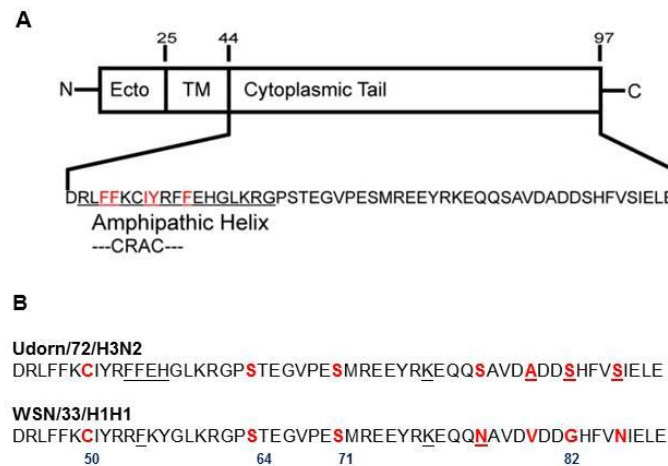


**Figure 1.6. Structural organisation of an M2 matrix protein.** (A) M2 consists of a 24-residue N-terminal extracellular domain, a 19-residue transmembrane domain and a 54-residue C-terminal cytoplasmic domain. In the cytoplasmic tail, residues underlined form the amphipathic helix which plays a role in M2 binding to cholesterol (CRAC motif), membrane localisation and budding and scission of viral particles. (B) Alignment of CT of Udorn and WSN viruses. Important amino acids are labelled in red: cysteine at position 50 is important for palmitoylation and lipid binding, serines at positions 64 and 71 are important for phosphorylation as well as serine in Udorn and asparagine in WSN at position 82. From Rossman et al., 2010.

Also, M2 CT contains a cholesterol recognition amino acid consensus (CRAC) motif, which enables M2 recruitment to virus budding sites by binding to cholesterol and may participate in membrane curvature prior to scission (Schroeder et al., 2005).

#### 1.1.6.4.2. Channel activity

Currently, investigation on characterising the molecular mechanism of M2 ion channel activity is still ongoing. However, it is already known that the wild-type M2 protein is activated below pH 6.2, its activity in the A/Udorn/72 strain is about 100 protons per second at this pH (Cady et al., 2009). Also, several amino acids and domains have already been shown to be essential for its structure and the channel activity. Overall, residues Val-27, His-37 and Trp-41 have been described to be important for proton transport in the transmembrane domain, whilst the cytoplasmic tail flexible loop (residues 47-50) and amphipathic helix (residues 51-59) reinforce the tetramerization by intermolecular interaction (figure 1.7) (Pielak and Chou, 2011).

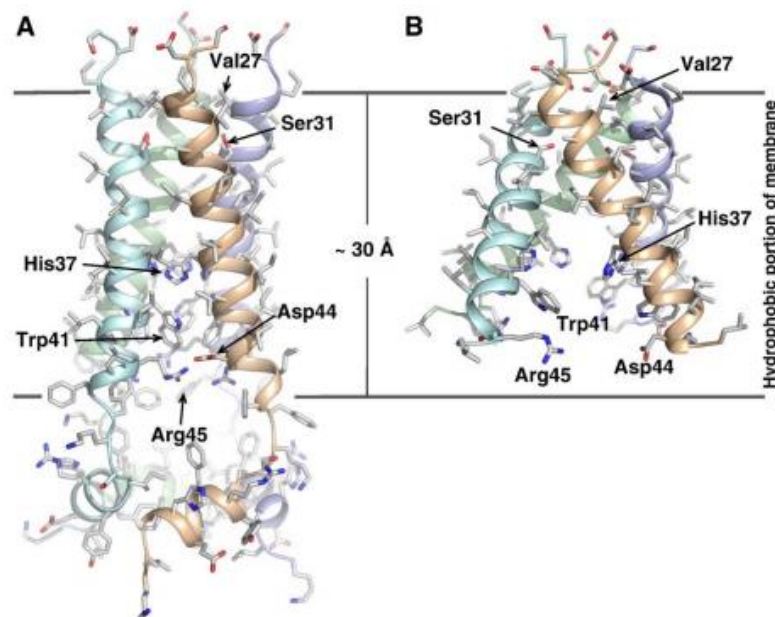


**Figure 1.7. Structure of influenza A virus M2 proton channel.** (A) Structure of M2 from residues 18-60. (B) Crystal structure of the hydrophobic portion of the membrane including residues 22-46. The residues Val-27, His-37 and Trp-41 which are important for proton transport are represented. Tetramerization of 4 TM helices leads to the formation of a pH-gated proton channel. From Pielak and Chou, 2011.

Firstly, Wang et al. recorded membrane voltage of wildtype and mutated M2 proteins expressed in oocytes of *Xenopus laevis* at different physiological pH and showed that histidine residue 37 protonation in the TM domain is critical for activation of M2 ion channel activity, playing also a role in the specific activity of ion transport (Wang et al., 1995). Then, a later study determined by using a similar approach that an indole moiety in a single chain of the tryptophan residue 41 functions as the gate of the channel and is responsible for regulating the pH-dependent aperture and closure of the pore (Tang et al., 2002). Above external pH 6.2, tetramerization of the 4 hydrophobic TM helices forming the channel is very compact and the gate is closed. Below pH 6.2, protons are able to bind histidine residues 37 present in the 4 TM helices causing their protonation and a conformational change which is essential for opening the pore, channel activation and subsequent proton transport (Cady et al., 2009). In addition, valine residue 27 was described to be able to act as a secondary gate for channel conductance and selectivity, which is also involved in M2 proton channel inhibition by the antiviral drug amantadine by forming an extended blockage of the pore when interacting with the molecule (Yi et al., 2008)

#### 1.1.6.4.3. Roles during virus infection

The M2 protein is a multifunctional protein which is critical in many early and late stages of the IAV life cycle. It regulates uncoating of endocytosed viral particles at early stages, its proton-selective activity acidifies the interior of viral particles and enables their uncoating in late endosomes where vRNPs dissociate from M1 protein (Pinto and Lamb, 2006a). It also plays a role in processing and trafficking of newly expressed HA to the lipid rafts: M2 regulates pH in the trans-Golgi network to promote correct maturation of HA which is essential for its efficient intracellular transport to budding site (Henkel and Weisz, 1998, Sakaguchi et al., 1996). In addition, it is now clear that M2 participates in final stages of the virus life cycle: it was suggested that M2 may associate with M1, HA, NA and vRNPs to stabilize the budding sites and to allow assembly of new virions (Kien et al., 2013, Rossman and Lamb, 2011, Takeda et al., 2003). Moreover, the role of M2 in filamentous formation and in scission of

filamentous and spherical IAV particles was explained by its location to the neck of budding viral particles, in low cholesterol-containing membrane domains, at the basis of the bud (figure 1.8) (Roberts et al., 2013).

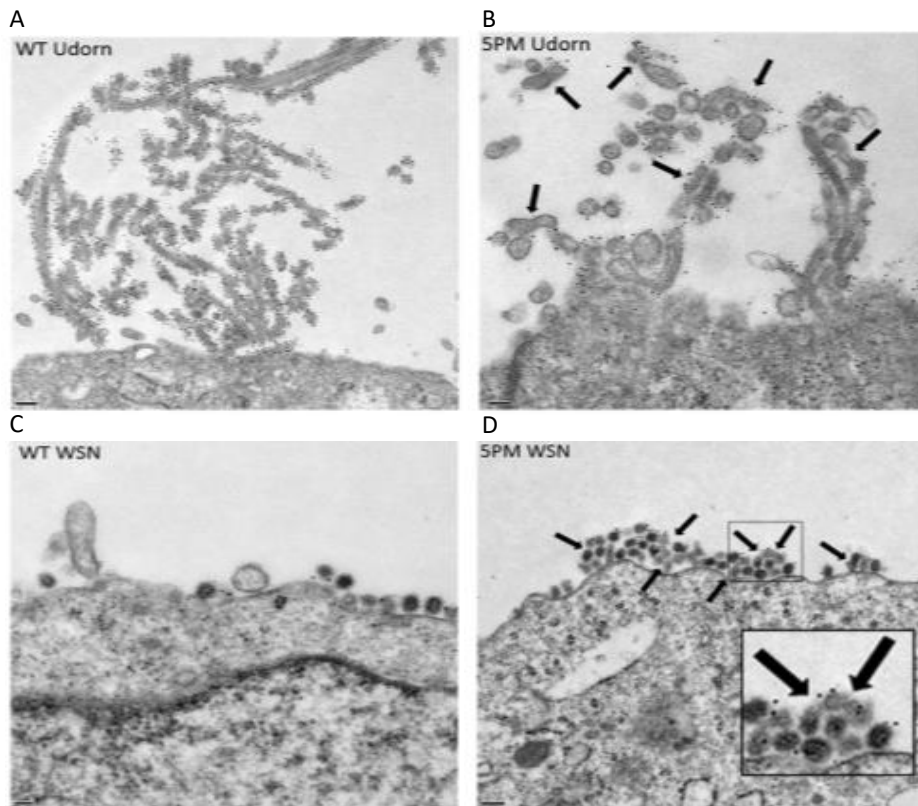


**Figure 1.8. M2 mutants of filamentous Udon and spherical WSN influenza viruses exhibit incomplete scission.** Thin sections of Udon- and WSN-infected MDCK cells for 12h and 6h respectively were labelled with gold-conjugated antibodies, indicating HA (12 nm) and M2 (6 nm) localisation. M2 was found at the basis of budding virions. Arrows show a joined membrane between two virus particles. Scale bars, 0.2 μm (A and D) and 0.1 μm (B and C). Adapted from Roberts et al., 2013.

Rossman and collaborators had previously postulated that IAV budding is an ESCRT-independent mechanism (Rossman et al., 2010). In agreement with this hypothesis, *in silico* experiments suggested that the amphipathic helix of M2 is able to alter the cell membrane leading to Negative Gaussian Curvature (NGC) and hence the pinching off of virus particles budding from the cellular surface (Schmidt et al., 2013). Furthermore, M2 has been shown to be involved together with NS1 and HA in the regulation of autophagy. It was suggested that

after stimulation of M2 and HA synthesis by NS1, M2 interacts at early stages of influenza infection with host factor beclin 1 to stimulate the formation of autophagosomes and promote autophagy. However, M2 was also able to block the final stages of autophagy during late stages of infection by inhibiting the fusion of autophagosome and lysosome for degradation of their content and to delay apoptosis. This process allows host cell survival upon infection and supports virus replication (Zhirnov and Klenk, 2013). Finally, a study performed in mice showed that M2 is involved in pathogenesis during infection and it was suggested that an IAV lacking the M2 protein would be a promising live attenuated vaccine (Watanabe et al., 2009). In addition, the M2 ectodomain (M2e) is currently used as a universal vaccine IAV as it is conserved among most virus subtypes (El Bakkouri et al., 2011).

#### 1.1.6.5 Viral ribonucleoprotein

##### 1.1.6.5.1. Structure

The eight genomic viral RNA (vRNA) segments together with multiple copies of nucleoprotein (NP) and the RNA polymerase complex form the viral ribonucleoprotein (vRNP), which is responsible for virus replication and transcription (Coloma et al., 2009). vRNP structure and organisation has been well studied for many decades; however, investigation on the structure of the different structural elements is still ongoing to better understand their function during the virus life cycle such as replication and transcription, transport of the genome, assembly and packaging. Electron microscopy (EM) analysis determined that vRNPs were 10 nm wide flexible helical rod-shaped structures and that their length depends on the associated vRNA interacting with the polymerase complex (Compans et al., 1972). The RNA polymerase complex consists of PB1, PB2 and PA monomers and is well organised in the cell nucleus to achieve the synthesis of complementary RNA (cRNA) from original vRNA during replication and messenger RNA molecules (mRNA) during transcription. The 5' and 3' ends of all RNA segments contain a highly conserved 12-13 nucleotide sequence corresponding to their binding site to the polymerase complex (Zheng and Tao, 2013, Desselberger et al., 1980,

Robertson, 1979). The polymerase complex also binds through interaction with PB1 and PB2 to NP, a small rod-shaped protein that regulates viral RNA folding into the vRNP and is found in polymeric forms to reinforce the stabilisation of the complete vRNP structure (Zheng and Tao, 2013, Ruigrok and Baudin, 1995). After analysis by cryo-EM of the RNP hairpin by two different groups, it was suggested that the polymerase complex is located at the open end whereas three to eight NP molecules are located in a small loop at the closed end (Zheng and Tao, 2013, Arranz et al., 2012, Moeller et al., 2012). Also, they suggested that flexible C-terminal of the PA subunit is responsible for connecting the vRNA template with the polymerase active site (Zheng and Tao, 2013, Moeller et al., 2012). As mentioned above, NP is an important element for structure of vRNP which exhibits a tendency to self-polymerise and a study performed by cryo-EM provided interesting information on the atomic composition of NP to further understand vRNP structure (Coloma et al., 2009). This study revealed the first three-dimensional structure of a biologically active RNP from a negative-stranded RNA with ability to synthesise viral RNA. It was proposed that NP monomers form a ring with two monomers being the link to the polymerase complex but not contacting with each other and that vRNA is distributed uniformly for binding to vRNP structure in different sites. Taking into account that NP protein has an upper head domain, a main body domain and a tail loop or linker region, analysis of the interaction between NP monomers and the biological activity of vRNP after mutations of several conserved and non-conserved residues in the loop identified the amino acids that are important for NP-NP interactions and for viral RNA replication (Ng et al., 2009, Coloma et al., 2009).

#### 1.1.6.5.2. Assembly

When dissociation of vRNPs from M1 protein occurs during early stages of IAV infection, vRNPs are released in the host cell cytoplasm, transported to the nucleus for replication and transcription, and later on packaged into viral particles. Firstly, vRNPs reach the host cell nucleus; however, it is not known whether they enter the nucleus individually or as a whole structure. There, replication and transcription starts to actively produce new vRNPs and mRNA

that will be then translated into proteins in the cytoplasm. Newly synthesized proteins that are important for replication travel back to the host cell nucleus to support virus replication and RNP assembly. It has been defined that NP, PA, PB1 and PB2 viral proteins are essential to accomplish assembly and formation of a newly formed vRNP, which is a rod-shaped RNP with a regular helical symmetry. All proteins which are imported back to the nucleus contain nuclear localization signals (NLS) required for nuclear import (Zheng and Tao, 2013). NP is found in a favourable state for encapsidation and is phosphorylated to self-polymerise and interact with the RNA and the polymerase complex (Chenavas et al., 2013, Zheng and Tao, 2013, Arrese and Portela, 1996, Almond and Felsenreich, 1982). Recent studies suggested that interaction between NP and the polymerase complex is sufficient for initiation of viral RNA replication, however the later interaction of NP and vRNA is essential for vRNA encapsidation into vRNP (Zheng and Tao, 2013, Newcomb et al., 2009). Newcomb's findings provide some insight into how IAV is able to switch from RNA-primed transcription to unprimed replication when no RNA template is present and they suggested that the NP-polymerase interaction could lead to a change in the polymerase to start unprimed replication (Newcomb et al., 2009). In addition, it was found that polymerisation of NP becomes more stable when RNA is present in the nucleus suggesting that RNA-dependent NP polymerisation is necessary for preservation of the overall vRNP structure (Tarus et al., 2012). However, it is still not known how the three functional components of a vRNP interact to succeed in their assembly into the final structure (Zheng and Tao, 2013).

#### 1.1.6.5.3. Export

Once assembly is finalised, newly formed vRNPs are exported from the nucleus to the cytoplasm of the infected cell to fulfil next stages in the IAV life cycle. Due to lack of nuclear export signal (NES) in component proteins of vRNPs, the M1 matrix protein and the non-structural protein 2 (NS2) (also called nuclear export protein-NEP) play an important role in vRNP translocation to the cytoplasm (Zheng and Tao, 2013, Baudin et al., 2001, Bui et al., 2000, O'Neill et al., 1998). No NES were thought to be present in NP, PA, PB1 and PB2;

however, Yu and co-workers found three NES in the NP protein and their mutation was leading to NP accumulation in the nucleus and impaired replication (Yu et al., 2012). Recently, a comparative analysis of seven viral NES revealed an important role for the third NES of NP (NP-NES3) in viral production and replication. NP-NES3 was also found to be highly conserved in human, avian and swine influenza A viruses (Chutiwitoonchai et al., 2014). However, it was suggested that M1 is the link between vRNPs and NEP, the latter which contains two NES that regulate the interaction of the vRNP-M1-NEP complex with the chromosome region maintenance 1 (CRM1) for their translocation to the cell cytoplasm (Zheng and Tao, 2013, Huang et al., 2013, Fukuda et al., 1997). Also, HA accumulation at the membrane of the infected cell activates the Raf/MEK/ERK mitogen-activated protein kinase (MAPK) signalling cascade that leads to induction of vRNP export (Marjuki et al., 2006). In a later study, Marjuki compared the replication efficiency of seasonal H1N1 and H3N2 viruses, associated HA expression at the cell surface and induction of MAPK signalling cascade. It was found that the H3N2 virus used in the study exhibited a higher replication rate compared to the H1N1 strain, resulting in a higher membrane expression of HA and an increased in MAPK activation. Interestingly, an H1N1 virus encoding a PB1 protein of the H3N2 led to increased ERK activation. Increased ERK activation translated in increased vRNP nuclear export and higher viral titers (Marjuki et al., 2007).

#### 1.1.6.5.4. Packaging

After vRNPs are assembled and translocated to the cytoplasm, they have to travel to the host cell membrane, where they are packaged together with other viral components into infective viral particles. In the past years, electron tomography and fluorescence in situ hybridization studies have provided interesting information on the mode the eight vRNPs are organised in the budding virions. It was found that all eight viral genomic fragments are aligned but interconnected to each other at the end of the budding virion and can exhibit different length (figure 1.9) (Zheng and Tao, 2013, Chou et al., 2012, Fournier et al., 2012, Noda et al., 2012).

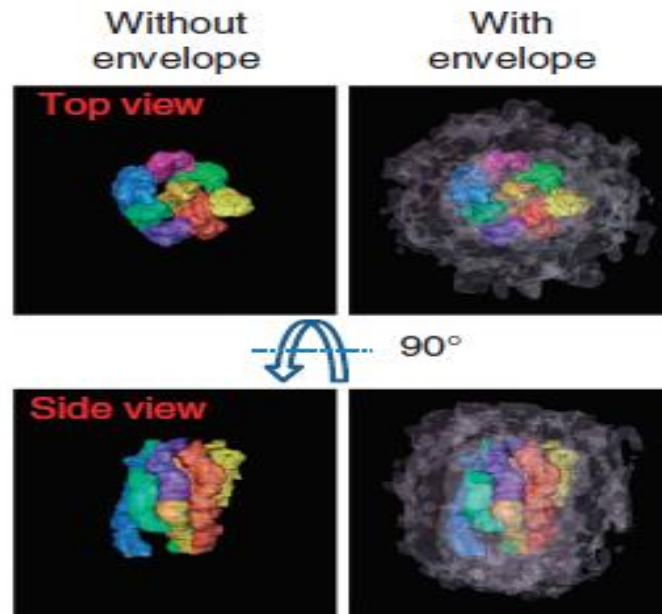


**Figure 1.9. Three-dimensional model of all vRNPs packaged together within a virion.** The eight vRNP are shown by a different color whereas the viral envelope is indicated in grey. Virion containing all eight packaged vRNPs can be observed from the top and the side and differences in length can be appreciated. From Noda et al., 2012.

Each genomic RNA fragment contains a sequence-specific signal for influenza packaging, consisting of the untranslated regions (UTRs) of both ends and the adjacent coding sequences of the open reading frame (Zheng and Tao, 2013, Hutchinson et al., 2010). Analysis of these signals have determined that both UTR and coding regions were conserved in all RNAs and contribute to genome packaging into forming virions (Zheng and Tao, 2013, Gog et al., 2007, Fujii et al., 2003). However, a more recent study suggested that the noncoding regions of each vRNA have a virion incorporation signal and that the terminal coding regions have a clustering signal to incorporate all eight vRNA into the virion (Goto et al., 2013).

### 1.1.7 Virus life cycle

The influenza virus life cycle is divided into early and late stages which include entry into the host cell, uncoating, translocation of vRNPs into the nucleus, replication and transcription of the viral genome, transport of newly formed vRNPs and proteins to sites of budding, assembly



Filamentous viruses enter the cell by macropinocytosis while spherical viruses are internalised through a clathrin-mediated endocytosis (Rossman et al., 2012). When internalisation has occurred, the virus traffics in the cytoplasm towards the nucleus and eventually reaches the endosomes. There, the low pH in endosomes causes a conformational change in HA causing the fusion of the viral and the endosomal membrane (Rossman and Lamb, 2011, Sieczkarski and Whittaker, 2005). Also, the proton-selective activity of M2 channel acidifies the interior of internalised viral particles and enables their uncoating at early stages in late endosomes, leading to the release of the vRNP complexes containing the viral RNA genome, NP protein and the RNA polymerase complex in the cell cytoplasm (Medina and Garcia-Sastre, 2011, Pinto and Lamb, 2006). vRNP complexes bind to importin receptors and translocate to the nucleus for replication and transcription (Wu et al., 2007). Briefly, three types of RNA molecules are synthesized in the nucleus by the RNA polymerase complex upon replication and transcription of vRNA.

During replication, the RNA polymerase complex produces cRNA using vRNA as a template, which is then copied to generate new vRNA molecules. Transcription leads to the synthesis of mRNA molecules that will be exported to the cytoplasm for translation into new viral proteins (Matsuoka et al., 2013, Zheng and Tao, 2013, Medina and Garcia-Sastre, 2011). Replication and translation lead to cell damage and result in apoptosis and antiviral inflammatory response. This cellular responses can be regulated by IAV through NS1 and PB1-F2 proteins, the main immune antagonists (Varga and Palese, 2011, Medina and Garcia-Sastre, 2011). RNA polymerase subunits PA, PB1 and PB2 together with NP are important for replication and transcription and are imported back to the nucleus together with NS1 and a small population of M1 which play an important role in export of RNPs once translation has occurred. As previously introduced, import and export of RNA or proteins into and from the nucleus to the cytoplasm is determined by the presence of the specific signals NLS and NES respectively, which consist of specific amino acids located at the surface of the protein enabling their interaction with the nuclear transport machinery (Boulo et al., 2007). Then, HA, NA, M2 and

M1 together with newly synthesized vRNP travel along the secretory pathway to reach the plasma membrane for the efficient assembly and budding. M1 is important in these final stages of the virus life cycle since it interacts with lipid membranes together with viral proteins and cross-links all the elements required for efficient completion of virus assembly. It has been shown that M1 contains a late domain which enables recruitment of host components participating in bud completion and virus release (Hui et al., 2003). Finally, NA is responsible for the cleavage of sialic acid receptors at the surface of infected cells enabling the release of virions (Matsuoka et al., 2013, Medina and Garcia-Sastre, 2011, Rossman and Lamb, 2011).

#### 1.1.8 Assembly and budding

As in the case of many other enveloped viruses like human immunodeficiency virus (HIV), the budding of IAV occurs at the apical plasma membrane of polarised epithelial cells, specifically in specialised domains called lipid rafts. Lipid raft microdomains, described as small (10-200 nm diameter), highly dynamic and enriched in sphingolipids and cholesterol membrane domains, constitute platforms for an efficient assembly and budding of virus particles (Veit et al., 2013, Medina and Garcia-Sastre, 2011, Rossman and Lamb, 2011, Takeda et al., 2003). Coalescence of these microdomains on the cell surface leads to formation of the 'viral budzone' (Schmitt and Lamb, 2005). Various models to better understand the structure and function of lipid rafts in cellular processes have been suggested in the last years, nevertheless one has been better described and suggests that rafts are composed of cholesterol-enriched lipids coexisting with cholesterol-poor liquid-disordered domains in the membrane (Kenworthy, 2008). Before release of the progeny, viral assembly and budding take place in rafts and lead to morphogenesis of new virions. These late stages correspond to the transport of viral structural proteins and genome to the budzone, assembly, membrane curvature and scission leading to the release of viral particles. A model of influenza viruses budding has been proposed by Rossman and Lamb (figure 1.11) (Rossman and Lamb, 2011).

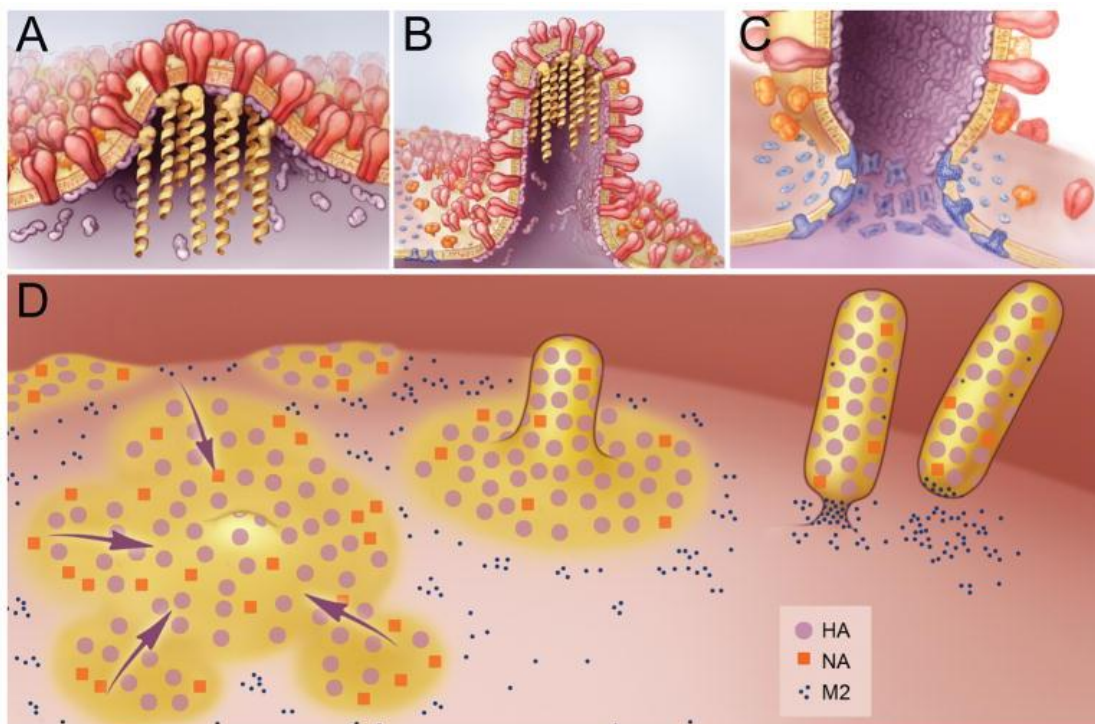


**Figure 1.11. Proposed model of budding of influenza viruses.** (A) Commencement of budding. (B) Formation of virions. (C) Curvature and scission of the membrane. (D) Review of the budding process. M2 is shown in blue, it concentrates at the neck of the bud, surrounding the lipid raft-associated budding zone where HA and NA viral proteins accumulate. From Rossman and Lamb, 2011.

To initiate the bud, both HA and NA are targeted to lipid rafts and travel to the cell surface through the secretory pathway (Veit and Thaa, 2011). HA has been shown to concentrate in lipid rafts and initiate the bud in an artificial virus-like particle (VLP) system. Expression of NA, M2 and M1 enhanced the budding of VLP. These results suggested that HA has an intrinsic ability to initiate the budding event and other viral proteins were then recruited to lipid rafts for proper assembly. M1 plays an important role in assembly and morphogenesis of new virions as it has the ability to cross-link HA and NA cytoplasmic tails and to interact as well with M2, vRNP and membranes. Finally, M2 binds to cholesterol at the periphery of lipid rafts and induces negative curvature of cell membrane leading to membrane scission and therefore to the release of virus progeny (Rossman and Lamb, 2011). The role of viral proteins and their interaction has been described in this chapter; however, it is now well known that host factors also play a critical role in many stages of the virus life cycle and therefore the numerous

interactions between host and viral proteins during the different steps of IAV infection will be explained later on.

#### 1.1.9 Regulation of cellular pathways during virus life cycle

It is very clear that interactions between IAV and the host occur during infection. While IAV uses the cellular machinery on its own benefit to replicate and propagate infection, the host induces cellular responses to limit viral spread to surrounding cells and tissues. Investigations are still ongoing to decipher the role of signaling pathways during viral infection and the mechanisms underlying their activation; however, it has been suggested that both autophagy and apoptosis are tightly regulated during IAV infection and necessary for virus replication and proliferation (Zhang et al., 2014). On the one hand, several stimuli can induce apoptosis through receptor stimulation, activation of protein kinase/phosphatase cascades or cysteine proteases (Kidd et al., 2000). Apoptotic response can vary depending on the cell line and stimulus, and is thought to help the host to counteract virus replication and propagation providing a protective role. PB1-F2, a protein encoded in most influenza strains from an alternative open reading frame in PB1 gene segment, has been described to translocate to mitochondria and induce apoptosis (Chen et al., 2001). PB1-F2 interacts with the inner mitochondrial membrane adenine nucleotide translocator 3 (ANT3) and the outer mitochondrial membrane voltage-dependent anion channel 1 (VDAC1) to induce mitochondrial permeabilisation and release of mitochondrial components for cell death activation (Zamarin et al., 2005). In a later study, Zamarin and collaborators used a recombinant virus with a knocked out PB1-F2 protein to study its role in viral pathogenesis. They found that PB1-F2 knock out did not affect virus replication but accelerated IAV clearance from lungs of infected mice, suggesting that PB1-F2 plays an important role in viral pathogenesis (Zamarin et al., 2006). Activation of cell death pathways during IAV infection is a mechanism used by the virus to interfere with and prevent activation of antiviral immune responses (Zamarin et al., 2006, Chen et al., 2001). Le Goffic has performed several studies to better understand the role of PB1-F2 in the regulation of the host immune response: he first

found that expression of PB1-F2 leads to increased Nuclear Factor – Kappa B (NF- $\kappa$ B) activation and a strain-dependent PB1-F2-mediated up-regulation of interferon  $\beta$  (IFN $\beta$ ) during infection (Le Goffic et al., 2010). In a transcriptomic study of host immune and cell death responses to PB1-F2, he confirmed PB1-F2-mediated increased NF- $\kappa$ B activity and he also found a higher activation of genes linked to cell death and inflammatory responses (Le Goffic et al., 2011). In addition, PB2 and NS1 viral proteins also can regulate the host immune response and apoptosis. PB2 was found to interact with mitochondria to induce mitochondrial damage (Woodfin and Kazim, 1993). PB2 especially binds to the mitochondrial antiviral signaling (MAVS) protein, which was previously linked to apoptosis activation during viral infection, and inhibits IFN $\beta$  signalling (Graef et al., 2010, Iwai et al., 2010, Lei et al., 2009). NS1 is also able to induce apoptosis, as its expression translated in cell death in MDCK and HeLa cells (Schultz-Cherry et al., 2001). However, further investigations have showed that NS1 plays a pivotal role during IAV infection as it has also been described to be an anti-apoptotic factor. Zhirnov found that IAV with deletion of NS1 protein induced apoptosis faster than a wildtype virus through the inhibition of IFN response (Zhirnov et al., 2002). NS1 can also down-regulate apoptosis by interacting with and preventing activation of signalling pathways such as protein kinase R and PI3K/Akt (Ehrhardt et al., 2007, Li et al., 2006). On the other hand, autophagy is just another cellular mechanism activated during viral infection. Autophagy is a catabolic process for the recycling and degradation of cytoplasmic macromolecules, including protein aggregates and entire organelles, during cellular stress (Wirawan et al., 2012). During viral infection, it is responsible for the removal of viral protein aggregates in order to limit virus propagation, as in the case of IAV it plays an important role in host defence (Dreux and Chisari, 2010). Autophagy activation leads to the formation of a double-membrane vesicle called autophagosome as a result of engulfment of a portion of cytoplasm by a membrane. The material in the autophagosome is degraded by hydrolysis after the fusion of its outer membrane with a lysosome (Wirawan et al., 2012). Many studies have already demonstrated that IAV has the ability to hijack the autophagic machinery and use it for its own purposes. It was first observed an increased expression of LC3-II, an

autophagy marker, during infection (Zhou et al., 2009, Tanida et al., 2008). Also, another study showed the presence of numerous small autophagosomes ubiquitously distributed in the cytoplasm of infected cells when compared to non-infected cells (Gannage et al., 2009). IAV encodes many proteins which can induce autophagy; but only M2 proton channel has the intrinsic ability to activate initial stages of autophagy (Zhirnov et al., 2013, Zhou et al., 2009). Interestingly, M2 is able to induce initial steps of autophagy leading to formation of autophagosomes, but it can also block the final steps by preventing the maturation of autophagosomes (Gannage et al., 2009). Autophagy activation leads to accumulation of viral RNA and proteins for efficient replication and assembly and to reduce antigenicity in order to evade host immune response. However, IAV can also manipulate autophagy to induce apoptosis and propagate infection at late stages of the virus life cycle. Again, M2, NS1 and PB1-F2 have been described as the main viral players in the regulation of apoptosis. Therefore, IAV encodes viral proteins which regulate activation and suppression of autophagy and apoptosis pathways and it is evident that further investigation is required to better understand their implication during IAV virus life cycle. Clearly, IAV hijacks these cellular machineries and tightly regulates these pathways to ensure its propagation (Zhang et al., 2014).

#### 1.1.10 Innate immune response

##### 1.1.10.1 Respiratory tract is the main target of influenza A virus

##### 1.1.10.1.1 Structure and function - gas exchange

Influenza virus causes an infection of the respiratory tract, which develops mainly in the lungs. Lung is a well-designed and structured organ in charge of the gas exchange between internal and external environment and has developed several strategies to protect airways of the respiratory system from invasion of pathogens. However, some microorganisms, including viruses, are able to evade host defence mechanisms and infect lung epithelial cells (Yoo et al., 2013). Upon infection of a new influenza virus strain, immunity depends entirely on the innate response, which corresponds to the first mechanism of defence and is critical for fate

of disease as adaptive immune cells only appear in the lungs after 5 days (Tripathi et al., 2015, Unterholzner and Bowie, 2008). Here, I only describe several innate immune mechanisms activated against IAV as the response to viral invasion is vast and complex.

#### 1.1.10.1.2 Chemical and physical barriers to restrict viral invasion

Upon infection, IAV needs to overcome the lung and other defence mechanisms to pathogen invasion. The lung acts as a physical and chemical barrier which contains a wide range of soluble and cellular innate mediators conferring a protective role to the host (figure 1.12) (Tripathi et al., 2015, Sanders et al., 2011).

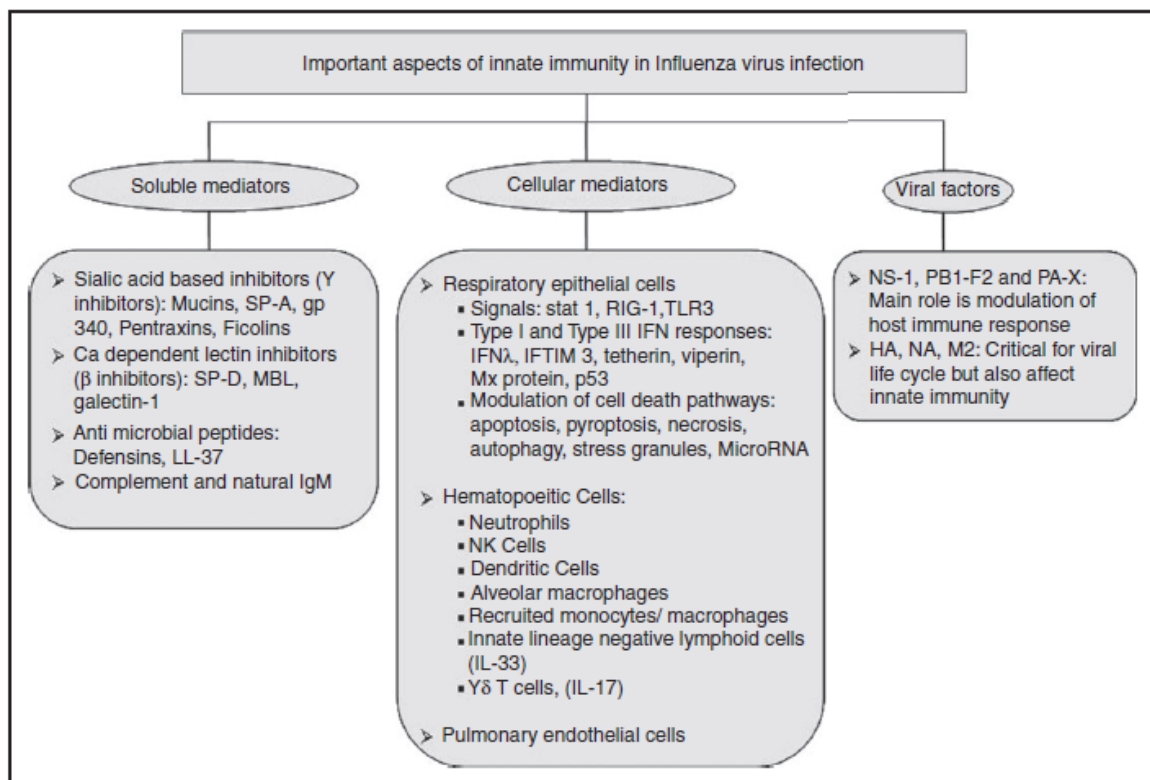


**Figure 1.12. The vast innate immune response against influenza virus is orchestrated by soluble and cellular mediators but also by viral components.** Soluble mediators in the lung are the first barrier that influenza viruses need to overcome. Then, cellular mediators take action to activate innate intracellular signalling cascades, interferon response and expression of cytokines regulating the pro-inflammatory response. From Tripathi et al., 2015.

Firstly, the mucus secreted in the lung forms a dense physical barrier against virus infection. It consists of glycosylated mucins enriched with sialic acids that simulate receptors at the cell

surface, they recognise and capture viral particles to prevent infection as they will be cleared together with the mucus (Cohen et al., 2013, Knowles and Boucher, 2002). In addition, many soluble mediators found in the respiratory tract are well known to inhibit influenza infection, among them members of lectin and collectin families such as surfactant protein A (SP-A), surfactant protein D (SP-D), mannose-binding lectin (MBL), which fulfil their anti-viral activity in different ways (Tripathi et al., 2015). The  $\gamma$ -inhibitors, also called sialic acid inhibitors, are able to block viral propagation by inhibition of sialic-acid and they prevent binding of virus to epithelial cells but also the cleavage of sialic acid by neuraminidase. The scavenger receptor-rich glycoprotein 340 (gp-340) is a protein found in lungs and saliva which possesses sialic acid-containing receptors that bind to the virus to promote its aggregation and to reduce its infectivity (Hartshorn et al., 2003). Gp-340 binds to SP-A and SP-D, which also contain anti-IAV activities. SP-A is able to neutralize IAV by a similar mechanism as it blocks the attachment of HA viral protein to the sialic acid receptor at the cell surface and prevents virus entry inside the cell (Hawgood et al., 2004). SP-D acts in a similar way to SP-A and gp-340, however it belongs to the class of  $\beta$ -inhibitors that exhibit their anti-IAV activity through binding to carbohydrates located on the viral envelope. SP-D binds to mannose residues present on haemagglutinin through its carbohydrate-recognition domain (CRD) and blocks its recognition by cell surface receptors to prevent infection (Tripathi et al., 2015, Tecle et al., 2008, Hawgood et al., 2004). Another  $\beta$ -inhibitor is the MBL, which also binds to mannose-containing glycans of HA and NA viral proteins to neutralise the virus, reduce infectivity and inhibit NA activity (Job et al., 2010). However, it has been shown that SP-D is the main responsible for anti-viral activity in human bronchoalveolar lavage fluid during IAV infection, exhibiting an effect 10-fold more potent than other collectins present in the lung (Hartshorn et al., 1994). Other proteins have been described to play an important role in innate immune response against IAV. For example, the H-ficolin binds to acetylated glycans and proteins in a calcium-dependent manner and exhibit lectin activity to block IAV as  $\gamma$ -inhibitors (Pan et al., 2012, Verma et al., 2012). Also, the galectin-1 which is a galactose-binding lectin was shown to interact with the envelope of the virus to inhibit infection and reduce IAV susceptibility in mice, it was found that

galectin-1 reduces viral load and inflammation in the lungs (Yang et al., 2011). Furthermore, another class of activators of the innate immunity upon IAV infection are the defensins, a group of antimicrobial peptides found in the lungs that are classified into  $\alpha$ -,  $\beta$ -defensins and retrocyclins (Tripathi et al., 2015). The most potent  $\alpha$ -defensins are the human neutrophil peptides (HNPs) which are found in the lung when inflammation occurs. They exhibit anti-viral activity by promoting viral aggregation and can also bind to surface of cells to block infection.  $\beta$ -defensins are less potent than HNPs but they have been suggested to play a role in the regulation of the response to IAV infection. Retrocyclins are defensins only present in primates, however they exhibit an even more powerful anti-viral activity against IAV than HNPs which is promoted by viral aggregation (Doss et al., 2009). Finally, complement activation is now known to be important for the modulation of IAV infection, which can be initiated by activation of the C3 component of the complement or also by natural IgMs (O'Brien et al., 2011, Jayasekera et al., 2007).

#### 1.1.10.1.3 Infection of the lung activates a general antiviral state

When IAV penetrates the first barrier in the lung, epithelial cells also trigger an anti-viral response which is initiated through innate immune recognition pathways. Briefly, once inside the host, viral components such as proteins and nucleic acids are detected through pattern recognition receptors (PRRs), expressed by many cell types such as epithelial, endothelial and antigen presenting cells (APC) circulating in the lung, which recognise specific pathogen-associated molecular patterns (PAMPs) to activate a host anti-viral response (Kawai and Akira, 2007). In addition, infection leads to release of damage-associated molecular patterns (DAMPs) which are molecules released from intracellular milieu during cellular stress and act as damage signals recognised by surrounding cells to further initiate the innate immune response. Detection of PAMPs and DAMPs by PRRs upon IAV infection can also trigger inflammasome activation, which was recently suggested to play a role in the modulation of a protective inflammatory response and to accomplish a more efficient recovery (Yoo et al., 2013).

#### 1.1.10.1.4 Innate recognition pathways

It is now well known that IAV is recognised by host innate immune cells through PRRs, which can be classified into different families depending on their subcellular localisation and recognition of viral ligands. For IAV, recognition happens through Toll-like receptors (TLRs), RIG-like receptors (RLRs) and nucleotide oligomerization domain (NOD)-like receptors (NLRs) (figure 1.13). Firstly, the TLRs belong to a family of PRRs located in intracellular compartments like endosomes or endoplasmic reticulum and also at the cell surface, they are transmembrane receptors that recognise viral nucleic acids and proteins to trigger the innate response (Takeuchi and Akira, 2009, Kawai and Akira, 2007). TLR2 and TLR4 are found at the plasma membrane and are responsible for recognition of viral envelope glycoproteins, whereas TLR3 and TLR7 detect double stranded viral RNA (dsRNA) and single stranded RNA (ssRNA) respectively as they are located in intracellular compartments (Tuvim et al., 2012, Imai et al., 2008, Hashimoto et al., 2007, Guillot et al., 2005, Diebold et al., 2004, Lee et al., 2003). Viral RNA recognition by TLR3 in macrophages and dendritic cells activates downstream signalling through the Toll-interleukin 1 receptor (TIR) containing adapter inducing IFN- $\beta$  (TRIF). TRIF then binds to and phosphorylates both TRAF family member-associated nuclear factor – kappa B (NF- $\kappa$ B) activator (TANK) binding kinase 1 (TBK1) and inducible I $\kappa$ B kinase (IKK-I) to activate interferon regulatory factor 3 (IRF3) and NF- $\kappa$ B transcription factors. Simultaneously, recognition of viral RNA by TLR7 in dendritic cells initiates downstream signalling through the adaptor protein myeloid differentiation factor 88 (MyD88), which is responsible for activation of IRF7 and NF- $\kappa$ B. Activation of both IRFs and NF- $\kappa$ B transcription factors leads to their translocation into the nucleus to initiate production of chemokines, type I interferons (IFNs) and other pro-inflammatory cytokines (Tripathi et al., 2015, Yoo et al., 2013). Interferons are the first host antiviral defence mechanism and target several stages of the virus life cycle to restrict infection and propagation. When viral infection occurs inside a cell, IFN system is induced and its components bind to specific receptors at the cell surface to stimulate transcription of IFN-stimulated genes (ISGs) that will block virus spread (Sen, 2001). Then,

the RIG-I- like helicases (RLH) such as RIG-I and Mda5 are cytoplasmic PRRs belonging to the family of RLRs, which are also involved in the activation of innate immunity responses. They recognise both viral ssRNA and dsRNA through the helicase/repressor domain (RD) to activate signalling pathways (figure 1.13) (Unterholzner and Bowie, 2008, Kawai and Akira, 2007).

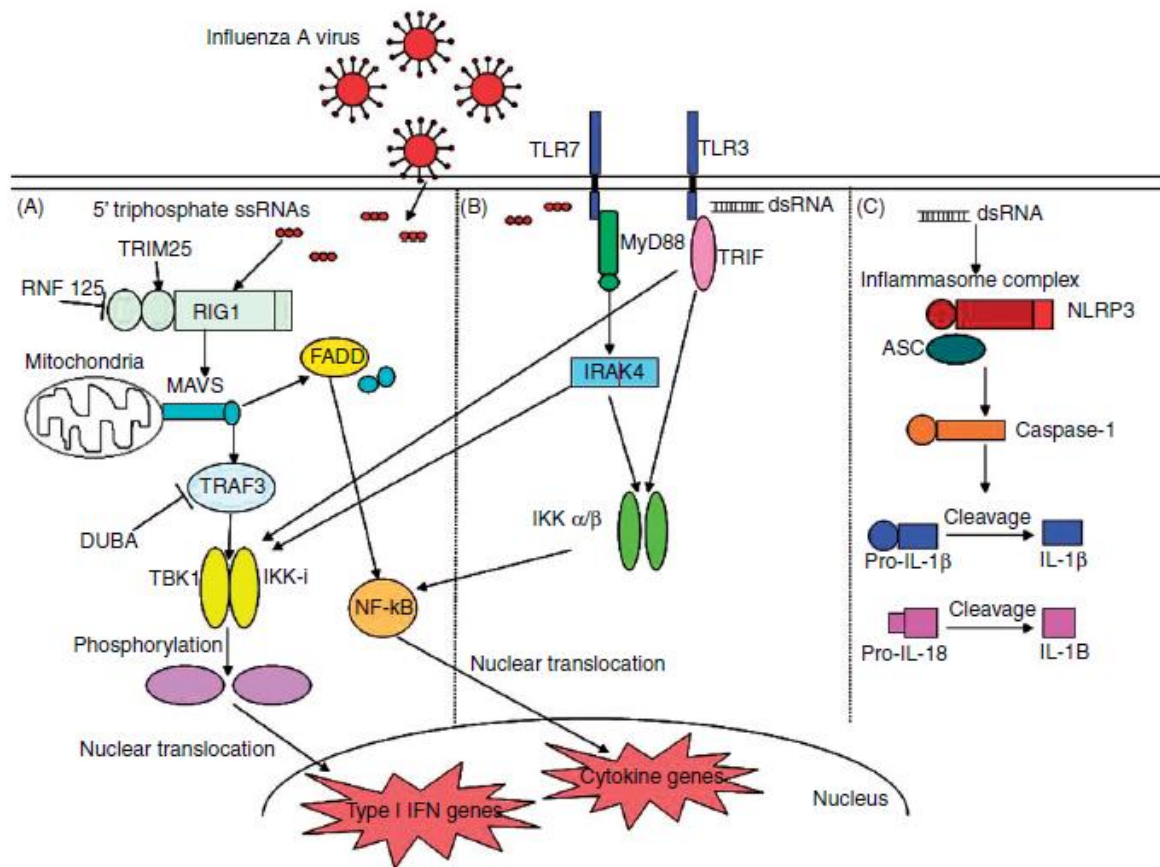


**Figure 1.13. Innate immune recognition of IAV is transduced through several pathways in lung epithelial cells.** (A) RLR pathway: RIG-I is a cytoplasmic protein that regulates production of type 1 IFN or pro-inflammatory cytokines by activating MAVS or Fas-associated death domain containing protein (FADD) upon recognition of viral sRNA. (B) TLR pathway: TLR3 and TLR7 also control production of type 1 IFN and pro-inflammatory cytokines by activating downstream signalling pathways through MyD88 and TRIF upon recognition of dsRNA and ssRNA respectively. (C) NLR pathway: the inflammasome is a multi-protein complex activated upon infection which induces caspase-1 activation leading to production of IL-1 $\beta$  and IL-18 pro-inflammatory cytokines. From Tripathi et al., 2015.

Upon recognition of viral RNA, their caspase recruiting domain (CARD)-like domains suffer a conformational change and become exposed for their ubiquitination by tripartite motif 25 (TRIM25), an E3 ubiquitin ligase (van de Sandt et al., 2012, Gack et al., 2007).

Then, both RIG-1 and Mda5 interact with CARD-like domains of the adaptor protein interferon- $\beta$  promoter stimulator-1 (IPS-1), resulting in the activation of IRF3 and NF- $\kappa$ B transcription factors regulating the type I IFN and cytokine response to reduce viral replication (van de Sandt et al., 2012, Unterholzner and Bowie, 2008, Kawai and Akira, 2007). IPS-1 interacts with FAS-associated death domain-containing protein (FADD) to activate NF- $\kappa$ B (Takahashi et al., 2006, Kawai et al., 2005). The IPS-1 adaptor protein has also been called mitochondrial anti-viral signalling (MAVS), virus-induced signalling adaptor (VISA) or CARD adaptor inducing interferon- $\beta$  (Cardif) (Unterholzner and Bowie, 2008). It is now evident that TLRs and RLRs work together to provide the host with a fast innate immune response.

Finally, a third mechanism of IAV recognition is the activation of the inflammasome through transcription of nuclear oligomerisation domain (NOD)-like receptor protein 3 (NLRP3), pro-IL-1 $\beta$  and pro-IL-18. NLRP3 belongs to the NOD-like receptors (NLR) family and is a class of cytosolic PRR, which oligomerises upon activation to form together with apoptosis speck-like domain and procaspase-1 the inflammasome multi-protein complex. Activation of NLRP3-dependent inflammasome leads to activation of caspase-1 and subsequent maturation and release of IL-1 $\beta$  and IL-18 pro-inflammatory cytokines (figure 1.13). It was recently suggested that activation of NLRP3 inflammasome may play a role in modulating a protective inflammatory response and accomplishing a more efficient recovery (Yoo et al., 2013). Also, influenza M2 protein produces a proton and nucleotide efflux into the cell cytosol that activates inflammasome through the activation of caspase-1 (Ichinohe et al., 2010).

All together, these different pathways activated through PRRs during IAV infection lead to the activation of interferons antiviral response and expression of other cytokines regulating the pro-inflammatory response.

#### 1.1.10.1.5 Cell types involved in the innate immune response

During IAV infection, numerous cell types contribute to the innate immune response. Resident alveolar macrophages and dendritic cells circulate inside the lung and maintain low levels of cytokines; however, other cells are then recruited to activate an anti-viral state when infection occurs. Infection of lung resident alveolar macrophages does not translate into effective viral production, however they play an essential role in inhibition of infection (Tripathi et al., 2015, van de Sandt et al., 2012). They express many different receptors which recognise viral particles to be phagocytosed together with infected apoptotic cells. Infected cells produce chemokine (C-C motif) ligand 2 (CCL2), which drives recruitment of other alveolar macrophages and monocytes to site of infection through recognition of their CCR2 receptor and their activation. Alveolar macrophages are an important source of chemokines and cytokines and their activation leads to production of pro-inflammatory cytokines such as IFNs, interleukin-6 (IL-6) and tumor necrosis factor  $\alpha$  (TNF $\alpha$ ) (Tripathi et al., 2015, van de Sandt et al., 2012, Sanders et al., 2011, Yu et al., 2011). In addition, natural killer (NK) cells are recruited to the lung upon viral infection by IL-15 (Verbist et al., 2012). They are cytotoxic lymphocytes and contribute to the control of replication targeting the lysis of infected cells upon recognition of viral HA by their NKp44 and NKp46 receptors (Ho et al., 2008, Mandelboim et al., 2001, Arnon et al., 2001). It has been reported that NK cells are able to link the innate and humoral adaptive responses as they express CD16 receptors recognising the Fc region of antibodies on infected cells to activate the called antibody dependent cellular cytotoxicity, resulting in lysis of infected cells (van de Sandt et al., 2012, Anegon et al., 1988, Hashimoto et al., 1983). Similarly, dendritic cells can also be recruited to sites of infection and help to establish the bridge between innate and adaptive immune responses (Tripathi et al., 2015, van de Sandt et al., 2012). Two types of dendritic cells co-exist in the lung, however they execute different functions. First, myeloid or conventional dendritic cells circulate in the lung, detect viral antigens and mature into antigen presenting cells. Cell maturation leads to their migration to the draining lymph nodes and presentation of processed antigens to T and B

lymphocytes, which proliferate and differentiate to produce specific antibodies (Tripathi et al., 2015, van de Sandt et al., 2012, Grayson and Holtzman, 2007). Then, plasmacytoid dendritic cells are responsible for the synthesis of IFNs during IAV infection (Jewell et al., 2007). Interestingly, both types of dendritic cells cooperate in the production of chemokines to recruit different immune effectors to sites of infection. They trigger 3 waves of distinct chemokines that take place during infection and that will attract the cell types involved in each phase of infection (Piqueras et al., 2006). Finally, pulmonary endothelial cells are also an important source of pro-inflammatory chemokines and cytokines and contribute to recruitment of monocytes, macrophages and NK cells to sites of infection (Tripathi et al., 2015).

#### 1.1.10.1.6 Production of chemokines and cytokines to limit viral propagation

As already mentioned, different cell types contribute to innate immune response and inhibit viral infection by producing pro-inflammatory chemokines and cytokines. In our study, we have studied expression of many cytokines during influenza infection, among them the type I interferon, TNF $\alpha$ , IL-1, IL-6, IL-8 and regulated on activation normal T cells expressed and secreted (RANTES, also called CCL5). Some of the main roles of type I IFNs described during infection are the activation of ISG to limit viral replication, the increase in T and NK cell responses to viral infection and the regulation of anti-inflammatory response through inhibition of IL-1, IL-18, or IL-12 and/or enhancement of IL-10 production (Arimori et al., 2013, Gonzalez-Navajas et al., 2012, Guarda et al., 2011, Sadler and Williams, 2008, Billiau, 2006, Honda et al., 2005, Kolumam et al., 2005, Nguyen et al., 2002). TNF $\alpha$  has also been found to be involved in the inhibition of viral replication and in the activation of NF- $\kappa$ B and IRF transcription factors to enhance cytokine and chemokine production (Veckman et al., 2006, Seo and Webster, 2002). Then, IL-1 controls viral-induced acute lung inflammation and is able to increase survival by promoting enhanced IgM antibody responses and migration of CD4 $^{+}$  T cells to the lung (Schmitz et al., 2005). Also, IL-6 is responsible for an increased neutrophil survival in the lung and viral clearance, the regulation of viral-induced inflammation and protection against fatal lung failure but also it regulates long-term CD4 $^{+}$  T-cell memory

responses (Lauder et al., 2013, Dienz et al., 2012, Longhi et al., 2008). IL-8 is involved in the recruitment of neutrophils to the infection site (Schumacher et al., 1992). Finally, RANTES has been shown to play a role in the attraction of monocytes, T lymphocytes, basophils and eosinophils to the lung and also to control bronchial asthma exacerbation during viral infection (Asai et al., 2001, Matsukura et al., 1998).

#### 1.1.10.2 Evasion of the innate immune response by influenza A viruses

Viruses have developed strategies to counteract the host innate and adaptive immune responses. Influenza virus encodes proteins that can bind to cellular factors participating in the activation of immunity to evade their antiviral mechanism such as non-structural protein 1 (NS1), both PB2 and PB1-F2 components of the polymerase complex, and finally M2 (figure 1. 14) (Goraya et al., 2015, van de Sandt et al., 2012).

NS1 is the main antagonist to the host immune response induced during infection, which is inhibited at different levels but most importantly through inhibition of the RIG-I signalling pathway resulting in a reduction of IFN- $\beta$  production (Goraya et al., 2015, van de Sandt et al., 2012). Firstly, NS1 binds viral ssRNA and prevents its recognition by TLRs and RIG-I receptor. Also, NS1 can bind to TRIM25 and blocks its E3 ubiquitin ligase activity essential for activation of RIG-I. Altogether, NS1 downregulates IAV antiviral RIG-I-dependent mechanisms by manipulating IRF3, NF- $\kappa$ B and c-Jun N-terminal kinase (JNK) (Gack et al., 2009, Ludwig et al., 2002, Talon et al., 2000, Wang et al., 2000). However, other interactions of NS1 and cellular factors having an impact on immune regulation have been reported. It has been found that NS1 blocks E3 ubiquitin ligase TRIM25 to limit viral replication by inhibiting protein kinase R (PKR), a cellular protein which is activated by dsRNA involved in protein translation, responsible for initiation of an antiviral response. PKR is also inhibited by NP and M2 which both inhibit the 58 kilo Dalton cellular inhibitor (P58IPK), a cellular regulator of the pathway that interacts with the human heat shock 40 protein (Hsp40). Similarly, another cellular factor called 2'-5'-oligoadenylate synthetase (OAS) which blocks viral replication is inhibited upon

NS1 binding to RNA to prevent its activation (Goraya et al., 2015, van de Sandt et al., 2012, Sharma et al., 2011, Guan et al., 2011, Li et al., 2006).

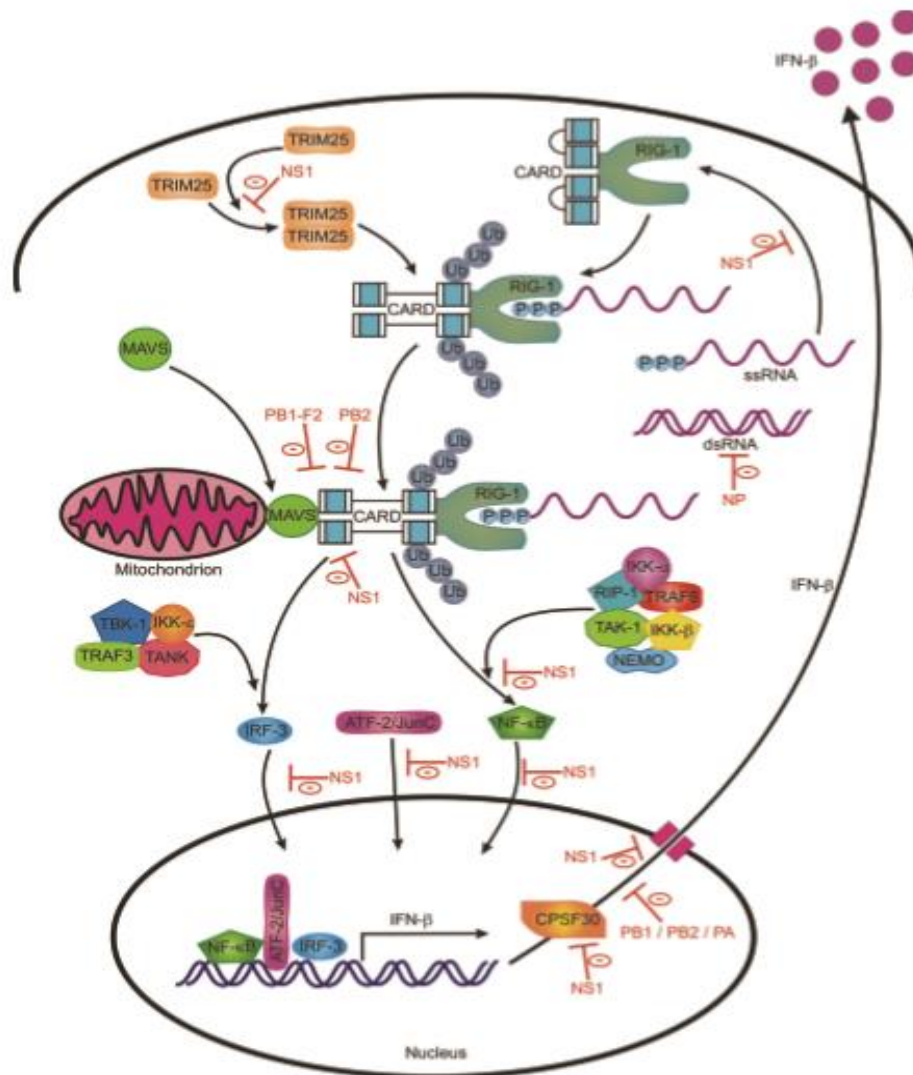


**Figure 1.14. Influenza A virus escapes innate immunity by preventing its recognition through cellular receptors.** Influenza virus has developed strategies to counteract immune responses and promote successful propagation within the host. As an example, NS1 is the main antagonist of the host immune system. NS1 is able to inhibit innate responses at different levels of RLR and TLR pathways, it is considered the most efficient inhibitor of the interferon response. PB1-F2 also limits interferon production by inhibiting RLR and TLR signalling pathways. Points where viral proteins interfere with innate recognition pathways are indicated in red. From Van de Sandt et al., 2012.

Then, NS1 interacts with the cleavage and polyadenylation specificity factor 30 (CPSF30) and the poly(A)-binding protein II (PABII), both essential components of the 3' end processing machinery of cellular pre-mRNAs, which results in the selective blockage of elongation and nuclear export of cellular mRNA but not in translocation to the cytoplasm of viral mRNA (Chen et al., 1999, Nemeroff et al., 1998). Furthermore, a recent study demonstrated that NS1 interacts with the eukaryotic translation initiation factor 4B (eIF4B), a component of the mRNA-to-protein translation machinery. NS1 targets eIF4B for lysosomal degradation which results in inhibition of the host restriction factor interferon-induced transmembrane protein 3 (IFITM3) (Wang et al., 2014). IFITM3 provides resistance to IAV by blocking its entry into the cytoplasm (Feeley et al., 2011). It is obvious that NS1 is the main immune antagonist as it interacts with many factors involved in the innate immune response; however, it has also been reported to regulate important events which are essential to build the innate cellular response. For instance, NS1 impairs the differentiation of IAV-infected monocytes into dendritic cells resulting in a defective endocytosis of antigens and a dysregulation of cytokines normally produced during infection (Boliar and Chambers, 2010). Interestingly, NS1 also limits dendritic cells maturation, inhibits synthesis of type I IFN and reduces the T cell response (Fernandez-Sesma et al., 2006).

In addition, seasonal IAV encoding PB2 containing aspartic acid in position 9 and PB1-F2 containing a serine in position 66 are able to evade the IFN-related innate immune response. Both PB2 and PB1-F2 interact with IPS-1 to prevent activation of RLR and TLR signalling pathways and inhibit production of IFN- $\beta$  (Goraya et al., 2015, Varga et al., 2011, Graef et al., 2010, Iwai et al., 2010).

Finally, M2 protein also plays a role in immune evasion by IAV. As already mentioned, M2 inhibits the PKR-dependent antiviral response through its interaction with P58IPK for preventing its release. This way, M2 protein promotes inhibition of protein synthesis, apoptosis and possibly increases release of viral particles (Goraya et al., 2015, van de Sandt et al., 2012, Guan et al., 2011). M2 was also found to be involved in macroautophagy, a cellular

mechanism of degradation and linked to innate and adaptive immunity for viral antigen release. Infection with IAV led to accumulation of autophagosomes and blockage of their fusion with lysosomes (Gannage et al., 2009). Several studies have found that M2 is responsible for inhibiting this step of fusion; it was observed that M2 promotes autophagosomes formation in early stages of infection but then inhibits fusion of phagosomes with lysosomes at late stages of infection (Zhirnov and Klenk, 2013, Gannage et al, 2009). More recently, a study determined that M2 CT interacts with LC3, an essential factor for autophagy. M2 interaction with LC3 resulted in LC3 transport to plasma membrane and was suggested to promote stability of newly formed viral particles and to determine virion morphology (Beale et al., 2014). Overall, it was suggested that M2 regulates autophagy and cell death pathways to support viral infection and to facilitate its transmission (Beale et al., 2014, Zhirnov and Klenk, 2013, Gannage et al, 2009).

## 1.2 Interactions of influenza A virus with host cellular factors

### 1.2.1 Interest of host factors as antiviral targets

Nowadays, emergence of new viral diseases and resistance to current antiviral drugs has increased the interest in developing new strategies against viral infection. Antivirals can be classified in 3 categories: direct virus-targeting antivirals (e.g. inhibitors of attachment, entry, proteases, polymerases...), indirect virus-targeting antivirals (e.g. inhibitors of replication and transcription complex, ribonucleoprotein complex and blockers of other key factors of the viral life cycle) and host-targeting antivirals (e.g. interferon and cyclophilin inhibitors); the inhibition of proteases and polymerases being still the major therapy. Current drugs reduce or eliminate very efficiently the virus presence but in some cases the virus still develops pathology since genetic traces could remain integrated in cells previously infected (Lou et al., 2014). Antigenic changes occur very frequently in IAV in comparison to type B and C viruses, enabling IAV to evade host immune recognition and develop resistance to available antiviral drugs (Iha et al., 2016, Medina and Garcia-Sastre, 2011). In the case of influenza viruses, current antiviral drugs target inhibition of M2 and NA proteins encoded by one or several influenza types; however, resistance have already been observed for both classes of drugs (table 1).

Antiviral drug	Active against	Viral target	Route	Recommended use in 2010/2011
Amantadine	Influenza A virus	M2	Oral	Not recommended because
Rimantadine	Influenza A virus	M2	Oral	of widespread resistance
Oseltamivir	Influenza A and B virus	NA	Oral	Treatment/prophylaxis
Zanamivir	Influenza A and B virus	NA	Inhalation	Treatment/prophylaxis
Peramivir*	Influenza A and B virus	NA	Intravenous	Awaiting permanent approval

\*Approved for emergency use during the 2009 pandemic only.

**Table 1. Current approved antiviral drugs against influenza viruses.** Amantadine and rimantadine target M2 viral protein and are specific of influenza A virus. Oseltamivir, zanamivir and peramivir (only been approved during 2009 pandemic) are NA inhibitors and are used against influenza A and B viruses.

## 1.2.2 Extensive network of interactions between influenza A virus and the host

In the past decade, many studies have already described numerous interactions between IAV viral proteins and host factors which occur at the different stages of infection; however, it is evident that they represent only a minority of the complex network established to complete IAV life cycle (Shaw, 2011). For instance, a map of confirmed interactions between the host and influenza A virus during infection was created by Matsuoka and his collaborators by using the FluMap tool (figure 1.15) (Matsuoka et al., 2013).

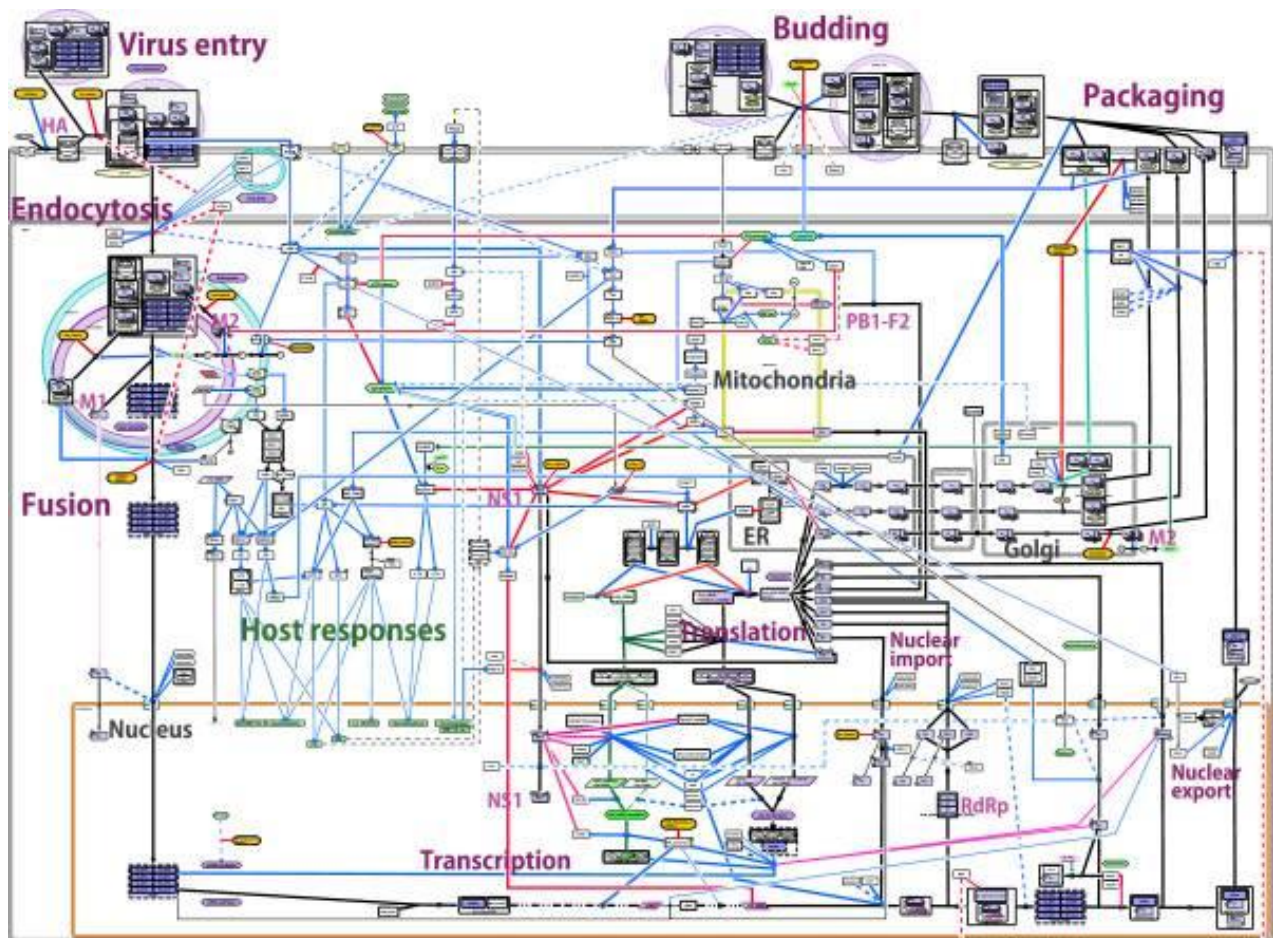


**Figure 1.15. Map of interactions between the host and influenza A virus.** Global view of interactions generated with FluMap, a software designed to be a tool for creating interaction maps applying the knowledge that is available in scientific databases such as Reactome, KEGG and Panther Pathway database. Host and viral factors together with their role during infection are indicated with different colours: virus factors in purple, host factors in green, antiviral factors in orange, which inhibit or activate viral replication in red and blue respectively. From Matsuoka et al., 2013.

### 1.2.3 High-throughput approaches to study virus-host interactions

The many studies investigating the extensive network of interactions between the host and influenza viruses have described many different approaches which can be classified into RNA interference (RNAi) screens, protein-protein interactions (PPI) and proteome analysis. However, it is evident that new approaches involving progress and development of new technologies will appear in coming years and will allow a more comprehensive study of interactions between the host and viruses.

#### 1.2.3.1 RNAi screening

Firstly, RNAi has become an experimental tool which aims at identification of gene products associated with phenotypic changes in a genome wide or an individual gene scale. In virology, RNAi technology enables identification of host proteins in a particular function during viral infection, but more importantly, genome-wide RNAi screens provide a global view of these interactions. This technology enables to decipher the global network of interactions between the host and the virus during the virus life cycle, but also during particular stages of infection. Taken together, it enables to identify signalling and transduction pathways but also individual host factors of cellular machineries hijacked by the virus to spread infection. However, this approach has also limitations as studies can differ from one to another in different aspects as each one was performed with the use of different cells types, siRNA libraries, viral strains or experimental procedures. For IAV, four studies used this approach to determine the cellular network required by the virus for an efficient replication; yet each one was performed with different assays (Shaw, 2011). First, Hao and collaborators performed a genome-wide RNAi screen in *Drosophila* which aimed at identifying host genes important for influenza virus replication (Hao et al., 2008). Then, a second study led by Brass investigated host factors involved in virus replication and also genes involved in all stages of viral infection which require HA viral protein, from binding at the cell surface to assembly and budding. In this study, they used several influenza strains to infect the U2OS osteosarcoma cell line previously transfected

with siRNAs targeting 17,877 genes (Brass et al., 2009). In a latter study led by Karlas, a two-step genome-wide RNAi was also performed to identify host factors important not only for replication but for all stages of the infectious virus life cycle in humans. In their study, A549 lung epithelial cells were transfected with specific siRNAs targeting approximately 23,000 human genes and infected with influenza A H1N1 virus (AWSN/33). Supernatants from siRNA-transfected and virus-infected A549 cells were transferred onto 293T human embryonic kidney reporter cells to assess luciferase activity correlating to levels of infection (Karlas et al., 2010). Finally, a fourth study carried out by König and his collaborators used a very similar approach. They also performed a human genome-wide RNAi screening in human lung A549 cells using a siRNA library against ~19,000 genes to identify host cellular factors that are involved in viral replication (König et al., 2010). Megan Shaw, from the Mount Sinai School of Medicine in New York, reviewed and discussed the main findings of these four studies to understand their importance for the development of new anti-IAV drugs. She found that, when comparing the list of primary hits from each study, the functional categories which scored highly vary whether hits were classified individually from the lower confidence list or combined from the list with higher confidence hits (common to two or more studies). A classification of hits from the low confidence list unravelled functional categories for essential genes during virus infection; however, when analysed combined from the list with higher confidence the new categories which scored highly provided insight into essential cellular pathways required for infection. Also, Megan Shaw found surprising that no one hit was found in all studies, suggesting that limitations could come from the fact that each group used different RNAi libraries. Altogether, 1077 genes were tested between all studies and it was found that 992 genes were unique hits to one of the screens, 72 genes were common hits to two of the four screens, 8 were common to three screens and 5 were common to four of the screens (figure 1.16). Interestingly, it is evident that the vATPase and COPI complexes, the ribosomal, mRNA splicing and nuclear trafficking machinery, and also the kinase signalling are all essential for IAV replication (Shaw, 2011).

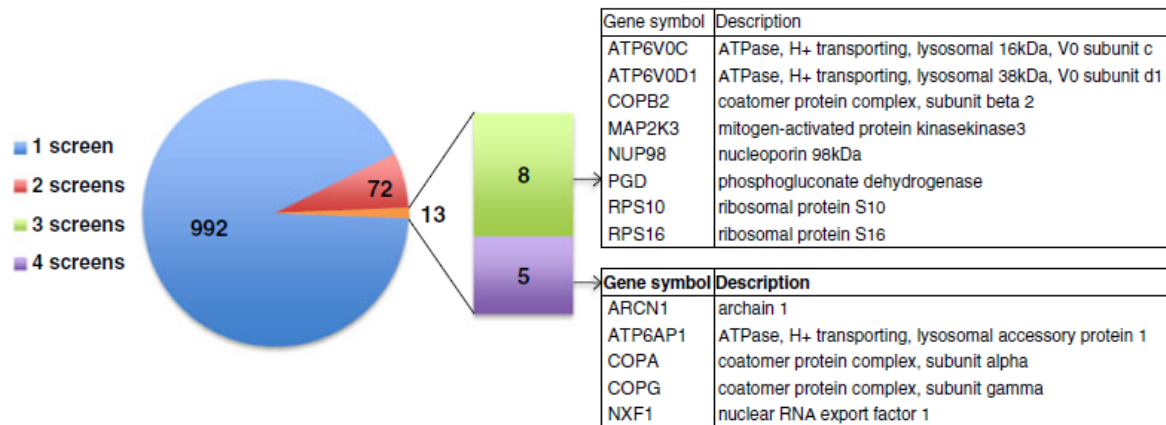


**Figure 1.16. Genome-wide RNAi screens identify new host factors important for influenza infectious life cycle in human cells.** Similar approaches were used in four different studies which enabled identification of essential host factors during virus replication: 992 genes were unique hits to one screen only, 72 genes were common hits in two screens, 8 were common to three screens and 5 were common in all four screens. Nomenclature and name of the 13 factors common to at least 3 screens are indicated. From Shaw, 2011.

### 1.2.3.2 Study of protein-protein interactions

In addition to RNAi, other approaches have been used to study interactions between influenza virus and the host. For instance, the study of protein-protein interactions (PPI) is also vastly used and aims at predicting the role of target proteins and their identification as drug targets. They can be performed by a combination of *in vitro*, *in vivo* and *in silico* methods, which provide insight into the function of a target protein in different conditions: *in vitro* provides information on the role of a protein outside a living organism, *in vivo* on an entire organism and *in silico* suggests a role for the protein based on computer-based analysis. These latter methods provide information on protein function which are not always confirmed as they lack the understanding of an entire cell or organism behaviour. Also, *in silico* studies lead to models that are often predicted from individual domains but not from the full-length protein and have to be verified empirically. Some of the most common techniques used for identification of PPIs, which are available currently due to the progress witnessed in the field, are described below. They consist of the tandem affinity purification (TAP), proteomic testing and yeast two-hybrid

system (Y2H). After identification, PPIs are required to be validated by using different approaches which include spectroscopy, coimmunoprecipitation or colocalisation study by confocal microscopy (Rao et al., 2014, Berggard et al., 2007).

#### 1.2.3.2.1 Tandem affinity purification

TAP approach is very often used in the study of PPIs, and in combination with mass spectrometry, it enables to identify protein complexes and study their role inside the cell. Briefly, it consists of the fusion of a TAP tag to proteins of interest which are then transformed into desired organisms for purification of complexes formed by the TAP-tagged protein and interacting partners. Originally, the TAP tag contained two binding domains, the protein A of *Staphylococcus aureus* and a calmodulin-binding domain, containing a cleavage site for the tobacco etch virus protease between them and which can be added either at the C-terminal site or at the N-terminal site (Puig et al., 2001). This method has many advantages for the study of protein complexes and interactions as it allows purification of complexes in their natural state without requiring previous knowledge on protein structure or function. Also, specificity during the purification process leads to a reduction of non-specific binding and therefore problems of contaminant proteins are not very common (Xu et al., 2010, Berggard et al., 2007).

#### 1.2.3.2.2 Proteomics

In addition, proteomics is also a common approach to identify PPIs. It consists of the global study of cellular protein structure, function, localisation and interactions and can help to understand their contribution to normal or pathological conditions. Progress in this technology enables to analyse the expression of thousands of proteins and protein complexes in a sample (Kinoshita et al., 2006). Currently, this approach has expanded to a wide range of disciplines and it has led to the publication of many studies in the context of viral infection (Coombs et al., 2010, Shaw et al., 2008). Upon virus replication, numerous interactions with the host occur to accomplish the viral life cycle and viral proteins are able to manipulate cellular machineries to support its propagation. Several studies have analysed the proteomes of a large number of

viruses infecting humans, monkeys, mice, etc. (Zhou et al., 2011). Interestingly, Shaw and collaborators used mass spectrometry-based proteomics to analyse composition of IAV particles and they found that 9 viral proteins and 36 cellular proteins suggesting that all factors are essential for the production of infective influenza virions (Shaw et al., 2008).

#### 1.2.3.2.3 Two-hybrid screening

Finally, another strategy to identify new PPIs is the two-hybrid system, which is based on the detection of transcription of a reporter gene when two proteins interact with each other. The original method is the system used in yeast (Y2H), which requires transport of interacting partners inside the nucleus (figure 1.17).

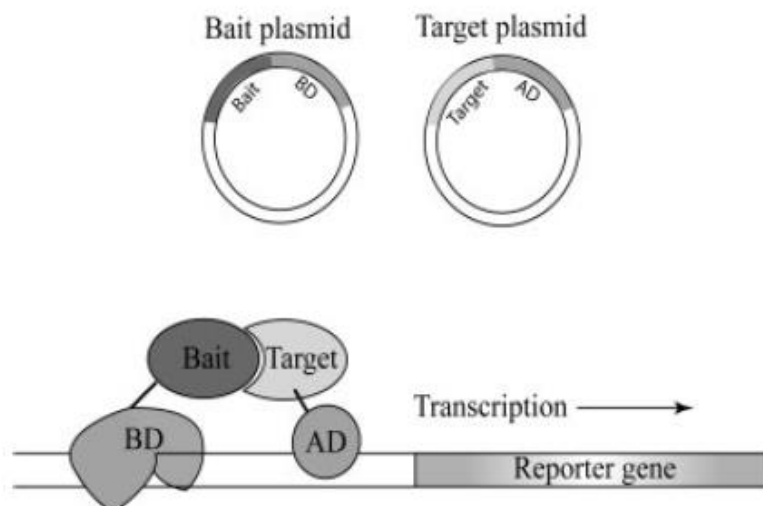


**Figure 1.17. Yeast two-hybrid system.** Bait and target plasmids are co-expressed in yeast cells and interaction of their respective BD and AD domains inside the nucleus initiate transcription of the downstream reporter gene. From Berggård et al., 2007.

However, many other variants have been developed for its use in other organisms and also to decipher interactions on a genome-wide scale, in the cytoplasm or between integral membrane proteins (Rao et al., 2014, Berggard et al., 2007, Stagljär et al., 1998). In eukaryotes, a large number of transcription activators possess two essential domains that are required to interact with each other to initiate transcription, the DNA binding domain (BD) that binds to the DNA promoter region and the activating domain (AD). This property is exploited

in the two-hybrid system, where two plasmids are expressed together in the same yeast cell, one bait plasmid encoding a known protein of interest fused to a BD and a target bait encoding an unknown protein fused to an AD. The target plasmid contains a mixture of unknown proteins selected from an expression library which are tested against the bait protein to identify interacting partners. Upon interaction of bait and target proteins, BD and AD travel inside the nucleus and connect with each other to form a functional transcription activator which activates transcription of the reporter gene located downstream of the promoter (Berggard et al., 2007). This approach was used by Shapira and his collaborators to identify host cellular factors interacting with influenza virus and responsible for the regulation of pathways during viral infection. They combined the traditional yeast two-hybrid analysis and a genome-wide RNAi expression profiling to decipher interactions between human factors and viral proteins of influenza virus (figure 1.18). First, they performed a yeast-2-hybrid screen to identify binary interactions between host factors and the 10 major viral proteins (all but PB1-F2) of an H1N1 influenza virus. They looked for interactions between each viral protein and a collection of ~12,000 human proteins available in the Human ORFeome v3.1. 1745 host genes which were identified as interacting partners, involved in a transcriptional response and also contributing in the regulation of antiviral cellular pathways were targeted with specific siRNAs in primary human bronchial epithelial cells for 72h and amplification of influenza A/PR/8/34 virus in these cells was monitored after transferring supernatants at 48h post-infection onto 293T cells containing an influenza polymerase-dependent reporter.

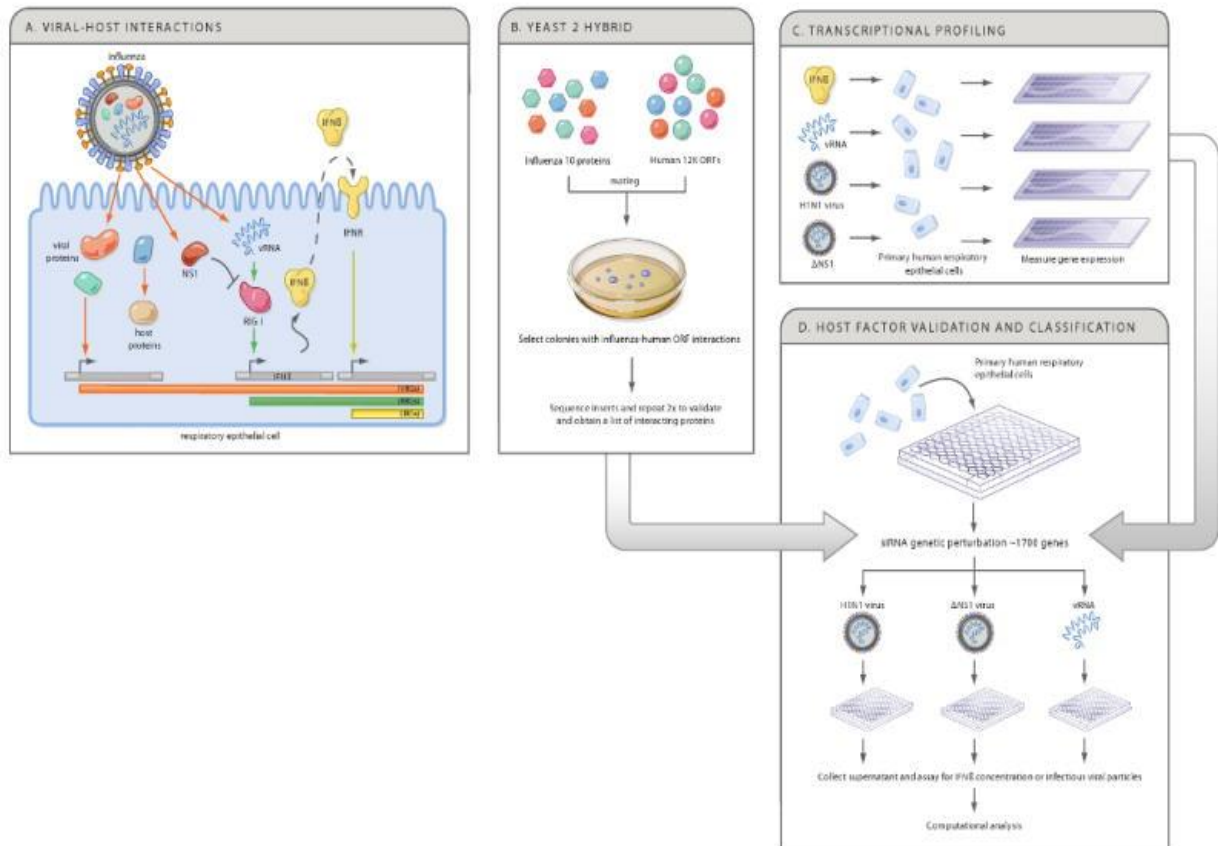


**Figure 1.18. Methodology for the design of a map of interactions between the host and influenza virus.** (A) During influenza infection, numerous interactions between host and viral components lead to changes in host gene and cellular behaviour. Viral components regulate a wide range of cellular responses including host gene expression and signalling pathways which induce an antiviral state in infected cells. (B, C and D) Investigation of these interactions were performed by a strategy including a yeast-2-hybrid system for their identification, analysis of transcriptional changes of identified host factors upon exposure to viral stimuli and study of their role in replication and interferon induction in lung epithelial cells during virus infection. From Shapira et al., 2009.

In addition to the wild-type virus, virus propagation was analysed when cells were exposed to a virus lacking NS1 virus protein and to viral RNA. In the end, 220 genes were found to be important for influenza virus replication and for the regulation of signalling pathways such as apoptosis, NF- $\kappa$ B, p53, PML, MAPK and WNT signalling (Shapira et al., 2009).

#### 1.2.4 Interactions between influenza A virus and the host during last stages of the virus life cycle lead to morphogenesis of new virions

As discussed earlier, last stages of the virus life cycle lead to morphogenesis and release of newly formed virions. Interactions between all the necessary viral components are essential for efficient virus morphogenesis and were already described above; however, it is now clear that interaction between viral proteins and host factors is also critical for production of infective progeny (Rossman and Lamb, 2011, Nayak et al., 2004). Interactions between viral components and the host have already been identified. In this chapter, I will briefly describe interactions during early infection; however, I will describe in details interactions happening during the late stages of infection as our study focuses mainly on these final events leading to virus morphogenesis (figure 1.19).

Host factors play a critical role at many stages of the virus life cycle, from IAV attachment and entry into susceptible cells to release from the cell surface for propagation of infection. Initially, HA interacts with SA receptors at the cell surface to promote IAV attachment. Upon HA binding to SA, epidermal growth factor receptor (EGFR) activation triggers IAV uptake through dynamin-dependent clathrin-mediated endocytosis which requires virus interaction with epsin-1, a clathrin-interacting protein acting as a cargo adaptor on clathrin coated pits (Chen and Zhuang, 2008, Rust et al., 2004, Eierhoff et al., 2010). Alternatively, entry may also occur through macropinocytosis in a myosin-2 dependent mechanism (de Vries et al., 2011). Transport of viral particles to endosomes for uncoating is regulated by Rab GTPases 5/7/10 and dependent on coat protein I (COPI) vesicular transport (Brass et al., 2009, Sieczkarski and Whittaker, 2003). Acidification of endosomes by vacuolar ATPases (vATPase) activates cellular serine proteases (SPs), which cleave HA to promote fusion of viral envelope and the endosomal membrane (Kohio and Adamson, 2013, Bottcher-Friebertshauser et al., 2010). Also, M2 ion channel acidifies the interior of viral particles enabling uncoating of vRNPs into the cytoplasm: the cellular ubiquitin proteasome system (UPS) disintegrates M1 coat from M1-NEP-vRNP complexes and promotes vRNPs release (Widjaja et al., 2010, Pinto and Lamb,

2006b). Then, importins  $\alpha/\beta$  and the nuclear pore complex promote transport of vRNPs into the nucleus for replication and transcription (Gabriel et al., 2011, Shaw, 2011). vRNPs encoding for each of the negative-sense vRNAs are used in the nucleus to produce positive-sense cRNAs and mRNAs. Firstly, the viral RNA-dependent RNA polymerase (RdRp) promotes cap-snatching of host pre-mRNA cellular transcripts to produce viral mRNA during transcription. Cellular pre-mRNA 5' cap is recognised by PB2, cleaved by PA at nucleotide 10–13 and used as primers for synthesis of viral mRNA (Dias et al., 2009). Human homolog of CLE (hCLE) and cyclin T1 and cyclin-dependent kinase 9 (CDK9) interact with the viral RdRp, facilitating its association with cellular RNA polymerase II (Pol II) to promote transcription. Polyadenylation of vRNA following elongation results in functional viral mRNA (Zhang et al., 2010, Perez-Gonzalez et al., 2006). Interestingly, IAV encodes all necessary elements to complete successfully transcription; however, production of viral M2 and NEP mRNAs is dependent on the host splicing machinery (Dubois et al., 2014). Polypyrimidine tract-binding protein 1 (PTBP1), NHP2-like protein 1 (NHP2L1), U1 small nuclear ribonucleoprotein 70 kDa (SNRP70), splicing factor 3B subunit 1 (SF3B1), splicing factor 3A subunit 1 (SF3A1), CDC-like kinase 1 (CLK1), 56-kDa U2AF65-associated protein (UAP56), pre-mRNA branch site protein p14 (p14) and pre-mRNA-processing splicing factor 8 (PRPF8) are examples of host factors playing a role in splicing of M and NS genes during infection (Karlas et al., 2010, König et al., 2010, Brass et al., 2009). Finally, mature viral mRNA is transported to the cytoplasm through the nuclear pore complex (NPC) for subsequent translation. Factors of the mRNA export machinery exploited by IAV during mRNA export are the nuclear mRNA export factor 1 (NXF1), heterogeneous nuclear ribonucleoprotein U-like protein 1 (E1B-AP5), mRNA export factor 1 (Rae1) and NTF2-related export protein 1 (P15) (Satterly et al., 2007). Similarly, vRNPs which form complexes with M1 and NP in the nucleus are also exported from the nucleus and travel to the cytoplasm through interactions with the NPC, the human immunodeficiency virus (HIV) rev-binding (HRB), the cellular chromosome region maintenance 1 (Crm1) and the human nucleoporin 98 (hNup98) proteins (Muller et al., 2012). At this point, NS1 viral protein plays a critical viral by regulating the switch from

transcription to replication for the generation of cRNA, which will subsequently be used to form new vRNA (Muller et al., 2012, Perez et al., 2010). NS1 IAV interferes with the host mRNA processing and polyadenylation machinery to promote virus mRNA transcription and protein translation (Kainov et al., 2011). NS1 first interacts with and inhibits host cellular factors involved in mRNA processing (Muller et al., 2012). NS1 binds to both cleavage and polyadenylation specificity factor subunit 4 (CPSF4) and polyadenylate-binding protein 2 (PAB2) to interfere with 3' cleavage of cellular pre-mRNA and inhibit its polyadenylation and processing (Chen et al., 1999, Nemeroff et al., 1998). NS1 was also found to bind host NS1-BP and to accumulate within the nucleus with many other host splicing factors during infection, suggesting an important role in interfering with normal host pre-mRNA processing (Wolff et al., 1998). NS1 is also responsible for IAV interference with host mRNA export from the nucleus to the cytoplasm as it interacts with NXF1, E1B-AP5, Rae1 and P15 and forming an inhibitory complex of the export machinery which is then used by IAV to promote export of its own mRNA (Muller et al., 2012, Satterly et al., 2007). Altogether, NS1 expression leads to retention of cellular mRNA in the nucleus and inhibits a possible antiviral response, enabling IAV to use this general host shut-off to promote its replication and spread the infection. Viral RdRp interacts with the cellular minichromosome maintenance complex (MCM) influenza replication factor 1 (IREF-1), Tat-specific factor 1 (Tat-SF1) and heat shock proteins 40/70/90 (hsp40/70/90) to form a functional complex and facilitate replication of vRNA (Batra et al., 2016, Manzoor et al., 2014, Kawaguchi et al., 2011, Jorba et al., 2009, Naito et al., 2007, Momose et al., 2002). Once replication and transcription have occurred inside the nucleus, newly processed viral mRNAs translocate to the cell cytoplasm for translation into viral proteins that will execute different functions. Translation is a selective cap-dependent mechanism initiated with recognition of the 5'-untranslated regions (UTR) within the viral mRNAs (Garfinkel and Katze, 1992). The G-rich sequence factor 1 (GRSF1) is a host factor that binds to 5'-UTRs of viral mRNAs to stimulate and control viral protein translation. It selectively recruits mRNAs to ribosomes following infection and regulates virus protein synthesis (Kash et al., 2002). NS1 forms a complex with eukaryotic initiation factor 4GI

(eIF4GI), polyadenylate-binding protein 1 (PAB1) and stauferin-1 (Stau) to stabilize active ribosomes (Burgui et al., 2003, Falcon et al., 1999). Other interactions between viral and host proteins are necessary to complete viral protein translation and folding of newly synthesized viral proteins. For instance, the T complex polypeptide 1 (TCP-1) interacts with PB2 and could act as a chaperone mediating efficient folding of PB2 protein (Fislova et al., 2010).

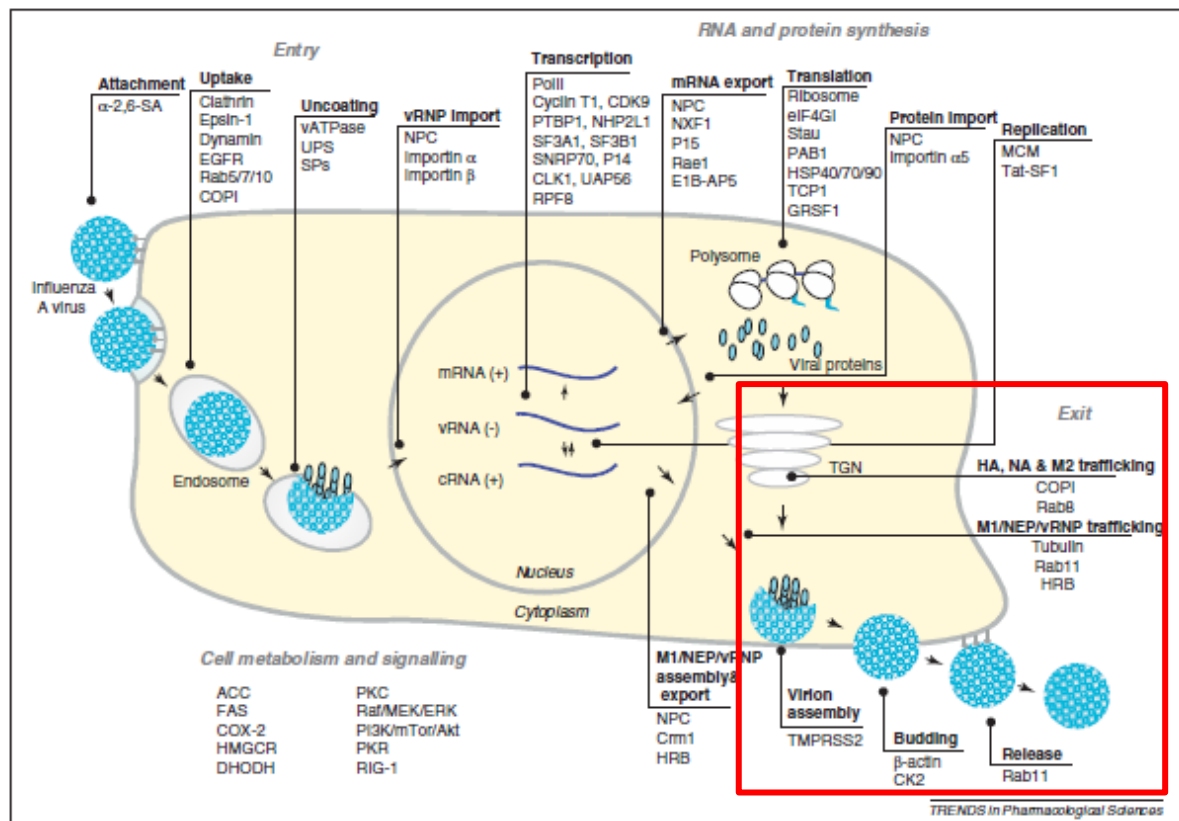


**Figure 1.19. Interactions between the human host cell and influenza virus.** Many interactions between the host and influenza A virus have been already described, which can either assist or restrict during viral infection. Interactions during late stages of the virus life cycle are indicated with a red frame. From Muller et al., 2012.

When translation ends, all necessary elements for completion of the virus life cycle such as vRNPs and viral proteins are transported to the plasma membrane along the secretory pathway. On one hand, vRNP complexes are transported to the plasma membrane along the microtubule network (Eisfeld et al., 2011, Amorim et al., 2011, Momose et al., 2007). Momose and collaborators used anti-NP antibody against specific viral RNAs to specifically precipitate

vRNPs from infected MDCK cells. Staining against NP showed a punctate pattern in the cytoplasm near the microtubule organizing centre (MTOC). Further analysis determined that NP co-localised with  $\alpha$ -tubulin, suggesting NP association with microtubules. The treatment of infected cells with nocodazole, an agent interfering with polymerization of microtubules, resulted in a random distribution of NP within the cytoplasm and providing more evidence to the microtubule-dependent transport of vRNPs to cell periphery (Momose et al., 2007). Two studies published almost simultaneously determined that viral genome interacts with Rab11 GTPase to be transported to cell membrane in Rab11-positive vesicles. Amorim and collaborators suggested that vRNPs concentrate on recycling endosomes in proximity to the MTOC, where they associate with Rab11-associated recycling endosomes for their transport to plasma membrane through the microtubule network on Rab11-positive vesicles (Eisfeld et al., 2011a, Amorim et al., 2011). Amorim and collaborators performed a co-transfection of GFP-tagged constitutively active Rab11 and components of vRNPs individually, which resulted in immunoprecipitation of both GFP-Rab11 and PB2 after GFP-affinity pull-down. In this study, authors also found by performing FISH experiments that vRNAs accumulate in perinuclear bodies in cells infected with several influenza strains at 6 hours post-infection. Staining of each vRNA and cellular  $\gamma$ -tubulin determined that perinuclear bodies containing vRNAs were localised around the MTOC. Then, colocalisation of vRNAs and Rab11 was also observed in the perinuclear region of infected cells around the MTOC. Drug perturbation of MTOC and vesicular trafficking affected normal RNP cellular localisation at late stages of infection. Altogether, Amorim suggested that vRNPs traffic to the plasma membrane in a Rab11-dependent mechanism through microtubule network, which could be possible due to the recruitment of vRNPs onto Rab11-positive vesicles by PB2 protein (Amorim et al., 2011). In agreement with Amorim findings, Eisfeld and collaborators used a monoclonal antibody against NP viral protein to confirm the previously observed association of Rab11A with vRNPs. Then, vRNPs Rab11-dependent travel to plasma membrane was monitored over infection: it was found that vRNPs colocalised with Rab11A during late stages of infection. They observed accumulation of vRNPs with Rab11A at the MTOC when vRNPs nuclear export has occurred

at 7h post-infection and at the cell periphery or plasma membrane between 9 and 11 hours of infection. Also, cell treatment with siRNA against Rab11 and the use of Rab11 mutants led to a disrupted transport of vRNPs to plasma membrane which had an impact on virus titers. Again, a coimmunoprecipitation experiment confirmed physical interaction between Rab11A and NP protein. These results provide a stronger evidence that vRNPs interact with and are transported to the plasma membrane by RAB11A-containing vesicles (Eisfeld et al., 2011). In addition, HRB is another important host factor involved in vRNPs trafficking to plasma membrane; however, it was first described to interact with IAV in a study performed by O'Neill and collaborators. They used a yeast two-hybrid system to identify influenza interacting partners of the cellular nucleoporins: only the NEP/NS2 protein was found to bind and interact with the nuclear export machinery. NS2 was suggested to interact with nuclear pore complex and to facilitate vRNAs nuclear export through its interaction with HRB (O'Neill et al., 1998). From these findings, Eisfeld and collaborators then investigated the role of HRB in vRNPs trafficking to the plasma membrane. In their study, siRNA targeting of HRB resulted in reduced titers after several virus life cycles determining that HRB is important for viral replication. By using immunofluorescence microscopy, they found that HRB co-localises with vRNPs in a perinuclear region in close proximity of the MTOC at 7h post-infection and at the cell periphery at 9h of infection. HRB knockdown in infected cells resulted in accumulation of vRNPs in the perinuclear region and dispersed within the cytoplasm. These results suggest that HRB interacts with NS2 following vRNPs nuclear export to promote their delivery to plasma membrane (Eisfeld et al., 2011b). In the other hand, newly translated viral proteins traffic to the plasma membrane upon their interaction with Rab8 and the coat protein I (COPI) complex (Huber et al., 1993). COPI complexes are formed by multiple complex subunits that were found to be important for virus infection in many genome-wide screens (König et al., 2010, Brass et al., 2009). They are responsible for the transport of cellular components between the Golgi and the endoplasmic reticulum (ER) and vice versa but have also a role in endocytic pathway. As COPI complexes regulate transport of cargoes between different compartments, Sun and co-workers studied which steps of IAV life cycle are dependent on the formation of

COPI complexes. Meanwhile the treatment of COPI with specific siRNA resulted in reduced virus internalisation and endosomal trafficking, pharmacological disruption of COPI function resulted in reduced membrane expression of M2 and NA in a lesser extent and had an important effect on virus assembly, budding and progeny infectivity (Sun et al., 2013). Previously, Brass had also found that depletion of COPI complex formation leads to a defect in transport of HA, NA and M2 viral proteins to the plasma membrane (Brass et al., 2009). Rab8, which has a role in membrane trafficking, was identified to play a role in transport from the trans-Golgi network (TGN) to plasma membrane and was responsible for targeting active HA protein to the cell surface (Huber et al., 1993). The cellular type II trans-membrane serine proteases (e.g. TMPRSS2, TMPRSS4) and human airway trypsin-like proteases also play a role in trafficking of viral components necessary for virus assembly and spread of infection: they can activate HA on its way to the plasma membrane by inducing cleavage of polybasic sites or trypsin-like sites (Bertram et al., 2010, Bottcher et al., 2009, Wang et al., 2008). Bertman and collaborators linked the expression of TMPRSS2 and TMPRSS4 in cell lines lacking trypsin with the ability to naturally support influenza propagation and found that their depletion with siRNA led to reduced viral release (Bertman et al., 2010).

When all viral proteins and vRNPs arrive to the cell surface, other host proteins take action to complete assembly and budding of new virions (Muller et al., 2012). For instance,  $\beta$ -actin, members of G protein signalling, the casein kinase 2 (CK2), Rab11 and a large number of lipids are all cellular factors which are involved in virus budding (Muller et al., 2012, Bruce et al., 2010, Hui and Nayak, 2002, Simpson-Holley et al., 2002). Simpson-Holley showed that  $\beta$ -actin and actin cytoskeleton participate in organisation of rafts microdomains during late stages of infection and facilitate budding. The treatment with drugs disrupting actin cytoskeleton resulted in rearrangement of viral components and actin network at the cell surface, which affected virus filament formation and budding (Simpson-Holley et al., 2012). As members of the G proteins family and protein kinases have been described to participate in apical membrane dynamics, Hui and collaborators investigated their involvement role during IAV budding in MDCK cells. When using G protein signalling blockers, impaired budding was

observed. Conversely, when GTP analogues were added into the medium of permeabilised MDCK cells, virus budding increased. Also, they found that treatment with a CK2 inhibitor resulted in decreased budding, CK2 protein depletion also resulted in reduced virus release and CK2 activity was increased during infection but to a higher extent at late stages of infection. Altogether, this study determined that members of G protein signalling and CK2 participate in IAV budding (Hui and Nayak, 2002). In a later study, Bruce and collaborators investigated the role of Rab11 during IAV budding as this pathway had already been described to be important for the release of other viruses. Depletion of Rab11 with siRNA treatment resulted in decreased viral titers, abnormal morphology and accumulation of newly formed virions at the cell surface of infected cells. Interestingly, Rab11 co-localised with NP viral protein in close proximity to apical cell surface during late infection, suggesting it could be involved in the trafficking of vRNPs to plasma membrane. These results suggest that Rab11 is an important cellular factor regulating virus morphogenesis and budding (Bruce et al., 2010). Also, interaction between M1 viral protein and the cellular receptor of activated C kinase 1 (RACK1), a protein involved in chromosome segregation and completion of cytokinesis in eukaryotic cells, was found to be important for release of IAV particles (Demirov et al., 2012, Reinhardt and Wolff, 2000). Demirov and collaborators determined that treatment of A549 cells with siRNA and with a specific antibody against RACK1 both resulted in reduced virus budding. In addition, they found that mutation of proline 16 in M1 viral protein resulted in impaired interaction between M1 and RACK1, inefficient recruitment of RACK1 to plasma membrane and defective pinching-off of newly formed virions (Demirov et al., 2012). Previously, Reinhardt showed that protein kinase C (PKC) can phosphorylate M1 when interacting with RACK1 and suggested this mechanism enables anchoring of M1 to membrane during late stages of infection (Reinhardt and Wolff, 2000). Recently, another study determined that CD81, a member of the tetraspanins family, is recruited together with PB1, HA, NA and M2 in plasma membrane patches. It was observed that CD81 accumulates at both ends and all along entire filamentous virions. Also, CD81 depletion with siRNA led to defective scission and subsequent impaired budding of virions from infected cells. These

results suggest that CD81 is recruited to sites of assembly and budding and is incorporated in filamentous particles to facilitate the pinching-off of newly formed virions (He et al., 2013). Similarly, the cellular LC3 autophagy regulator was later described to interact with M2 viral protein during late stages of infection. It was found that M2 recruits LC3 to plasma membrane through a 3-residue LCR-interacting region (LIR). Through its LIR motif, LC3 promotes virion stability, filament formation and assists in the virus egress from infected cells (Beale et al., 2014). Then, another study determined that cofilin-1 participates in assembly and budding of IAV. Cofilin-1 belongs to a family of actin-depolymerizing factors, it can dissociate F-actin and regulate cytoskeleton remodelling. As cofilin-1 has previously been found to be involved in virus infection and inhibited by the natural compound pentagalloyl glucose (PGG), Liu and collaborators investigated the role of both cofilin-1 and PGG during IAV infection. In this study, microscopy analysis of F-actin organisation in infected cells revealed that IAV-induced actin aggregation to plasma membrane is inhibited after treatment with PGG. Treatment with PGG resulted in decreased total protein expression and phosphorylation of cofilin-1 during viral infection but also in reduced viral titers. In addition, treatment of IAV-infected cells with specific siRNA against cofilin-1 also led to reduced viral titers. Altogether, these results show that cofilin-1 is an important host factor which participates in the production of new virus progeny by promoting aggregation and reorganisation of the actin cytoskeleton during late stages of infection (Liu et al., 2014a).

Finally, it is now very evident that host cellular factors interact with viral proteins not only to assist viral replication and propagation but also to restrict the virus life cycle and to negatively modulate infection, they are called restriction factors. Several restricting factors have already been described to inhibit and interfere with late stages of the virus life cycle such as tetherin, viperin and AnxA6 proteins. Wang and collaborators found that the interferon-induced viperin inhibits release of IAV. They found that viperin binds to and inhibits the farnesyl diphosphate synthase (FPPS), an enzyme involved in isoprenoid lipids synthesis, to alter membrane fluidity and disrupt lipid rafts which results in inhibition of virus release (Wang et al., 2007a). Another interferon-inducible factor which exhibits antiviral activity is tetherin. Tetherin restricts release

of IAV and many other viruses such as HIV or Ebola virus by binding to viral particles at the cell surface, where it tethers them together to block spread of infection. Interestingly, NA found in specific IAV strains is able to counteract restriction by viperin and participates in virus budding (Yondola et al., 2011). Finally, the previous study of our group showed that human AnxA6 protein interacts with M2 viral protein and inhibits release of IAV in a similar manner to tetherin (Ma et al., 2012). Overall, these enhancing or restricting cellular factors were identified by biochemistry and cellular biology methods such as microscopy, coimmunoprecipitation and western blotting.

### 1.3 Human annexin A6 is a cellular factor interacting with M2 cytoplasmic tail of influenza A virus

#### 1.3.1 Interaction of human Annexin A6 with M2 viral protein

In a previous study, our group performed a genomic yeast two-hybrid screening on a random-primed human placenta cDNA library using the IAV M2 CT (from H5N1 strain A/Goose/Guangdong/1/96; GenBank accession no. 81975894) as a bait in order to identify cellular factors interacting with M2 that could either assist or restrain processes involving M2 viral protein. This screening identified the interaction between human annexin A6 (AnxA6) and M2 CT as one of the most interesting results since it was classified with the highest confidence score (table 2) (Ma et al., 2012).

Characteristic	Value or description
Bait	M2 cytoplasmic tail (aa 44–97)
Library	Random-primed human placenta cDNA
No. of interactions tested	63.89 million
Prey	AnxA6
No. of positive clones	15
Confidence score <sup>a</sup>	A
Minimal interacting domain	aa 44-147

<sup>a</sup> Predicted biological score (A to E), a statistical confidence score assigned to each interaction by Hybrigenics.

**Table 2. Yeast two-hybrid screening for the interaction of AnxA6 and M2 CT.** Screening of a random-primed human placenta cDNA library using the IAV M2 CT as a bait: a total of 63.89 million interactions were tested and 273 positive clones corresponding to 47 cellular factors were identified. One of the most interesting results was the identification of the interaction between M2 CT and human AnxA6, with 15 positive clones (5%) corresponding to this protein (GenBank accession number NM\_001155.3). This interaction was classified with the highest confidence score (predicted biological score of A by Hybrigenics). From Ma et al. 2012.

63.89 million interactions were tested and 273 positive clones corresponding to 47 cellular factors were identified. Human annexin A6 was identified as one of the most interesting factors interacting with M2 CT with 15 positive clones (5%). Sequence alignment of the positive cDNA

clones demonstrated that a small domain between repeats 2 and 3 in the first core domain of AnxA6 is necessary for interaction with M2 CT, corresponding to amino acids between positions 44 and 147 (figure 1.20) (Ma et al., 2012).

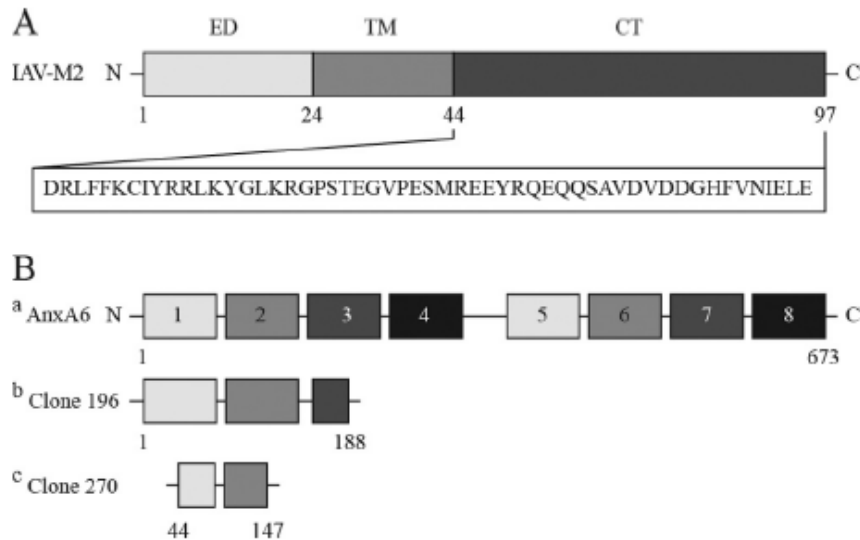


**Figure 1.20. AnxA6 interacts with the M2 CT of influenza A virus.** (A) Representation of M2 domains and the CT sequence used as bait in a yeast two-hybrid system performed on a human placenta cDNA library. Ectodomain, transmembrane and cytoplasmic tail are identified as ED, TM and CT respectively. (B) Representation of the full length AnxA6 consisting of a double 4 repeat-core and the clones 196 and 270 which contain the largest and smallest cDNA fragments of AnxA6 interacting with M2. Amino acids are shown with numbers. From Ma et al. 2012.

After identification of the interaction, it was determined that M2 and AnxA6 also interact in IAV-infected human cells. Physical interaction between AnxA6 and M2 CT during IAV life cycle was confirmed by coimmunoprecipitation experiments which showed that M2 and AnxA6 were detected together in IAV infected cells. Confocal microscopy also determined that AnxA6 and M2 colocalize in proximity of the plasma membrane in AnxA6-transfected and infected A549 cells (figure 1.21) (Ma et al., 2012).

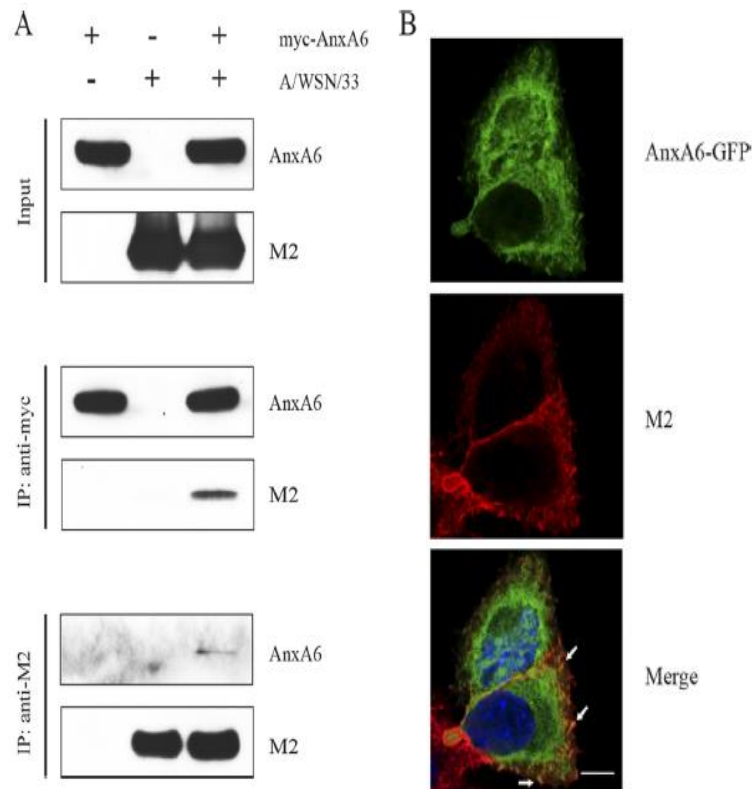


**Figure 1.21. Human AnxA6 and M2 virus proteins interact in human infected cells.** (A) 293T cells were transfected with a plasmid encoding a myc-tagged AnxA6 protein, infected with A/WSN/33 virus at an MOI=0.1, lysed at 24h post-infection and coimmunoprecipitation of AnxA6 and M2 proteins was performed with anti-myc and anti-M2 (middle and lower panels, respectively). Input samples are indicated in the upper panel. Both AnxA6-myc and M2 proteins were immunoprecipitated together and detected by western blotting with specific anti-M2 or anti-myc MAb. (B) A549 cells were transfected with a plasmid encoding an AnxA6-GFP protein, infected with A/WSN/33 virus at an MOI=5. At 14h post-infection, cells were fixed, stained with an anti-M2 MAb followed by Alexa Fluor 555-conjugated IgG and analysed by confocal microscopy. AnxA6 and M2 appeared to colocalize in discrete subdomains at the plasma membrane of infected A549 cells. Areas where AnxA6 and M2 colocalize are indicated with arrows. From Ma et al. 2012.

### 1.3.2 Overexpression of Annexin A6 negatively modulates IAV infection and affects virus morphogenesis and release from infected cells

In the same study, it was demonstrated that AnxA6 interacts with M2 at the plasma membrane of infected cells but more importantly it was shown that AnxA6 overexpression negatively modulates infection. Effect of AnxA6 expression during influenza virus infection was investigated and it was found that silencing or overexpression of AnxA6 led to differences in the propagation of IAV infection (Ma et al., 2012). Interestingly, AnxA6 overexpression negatively modulates IAV infection leading to reduced titres of progeny viruses. Conversely, silencing of AnxA6 with small interference RNA (siRNA) led to an increase in titres of newly produced viral particles (figure 1.22).

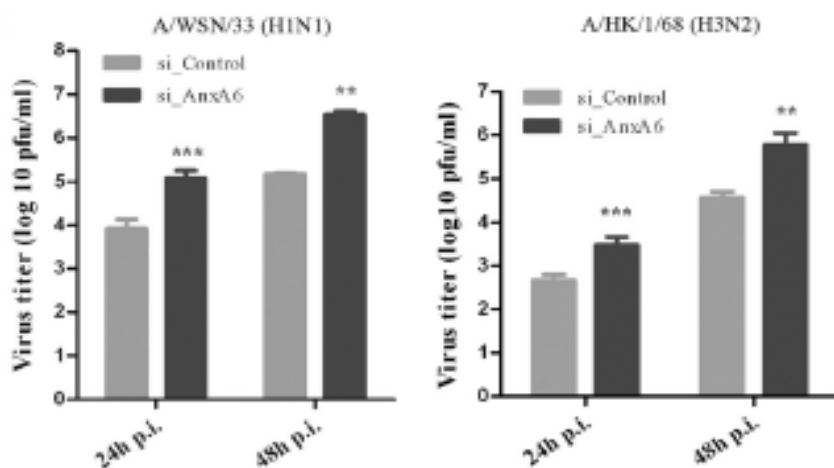


**Figure 1.22. AnxA6 negatively modulates influenza A virus infection.** Cell culture supernatants of A549 non-treated and treated with siRNA for AnxA6 were collected at 24h and 48h after infection at MOI=0.01 with influenza A/WSN/33(H1N1) (left) and A/HK/1/68(H3N2) (right) viruses and titres were determined by plaque assay on MDCK cells. Data are represented as means  $\pm$  standard deviations for triplicates from four and duplicates from three independent experiments respectively and statistical significance was calculated with an unpaired Student's t test. \*\*, P<0.01; \*\*\*, P<0.0001. From Ma et al. 2012.

Then, effect of AnxA6 overexpression during early and late stages of the virus life cycle was also investigated. No effect of AnxA6 was observed in early phases of infection such as viral

entry, replication and transcription or export of vRNPs from the nucleus; however, it was demonstrated that AnxA6 affects late stages and especially the budding of progeny viruses from infected cells. Cells expressing AnxA6 and infected with a spherical strain exhibited a defect in morphogenesis of newly produced virions, viral particles were found to have an elongated shape and to be interconnected (figure 1.23) (Ma et al., 2012).

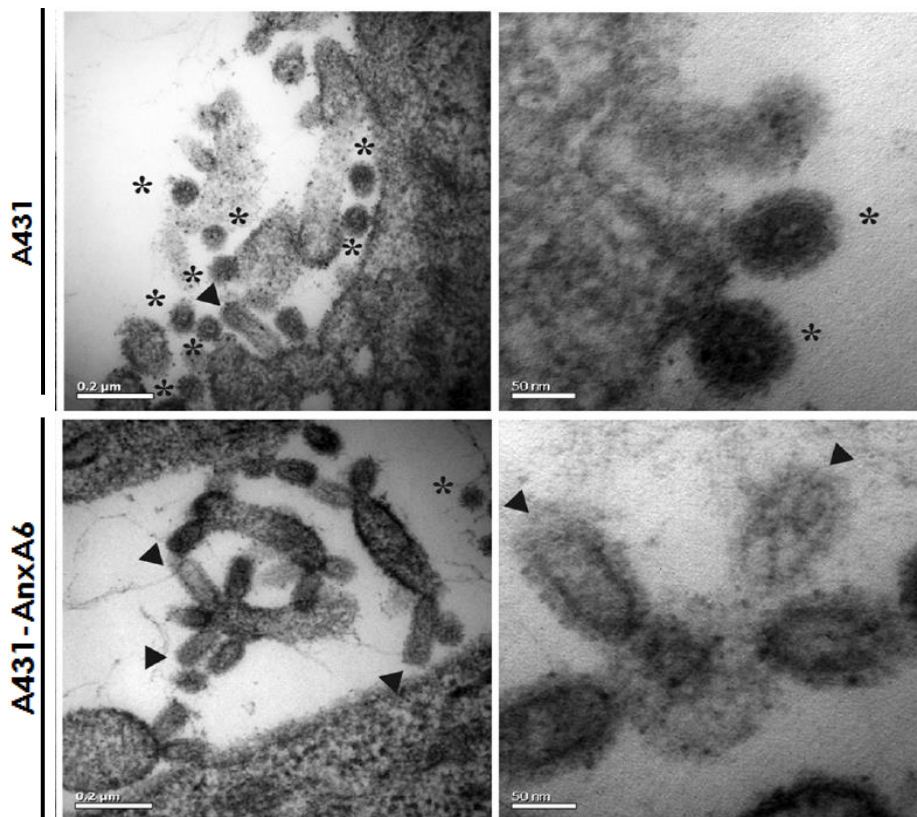


**Figure 1.23. Influenza virus budding is impaired by AnxA6 over-expression.** Cells were infected with the spherical influenza A/WSN/33 virus strain at MOI=5 for 10 hours, treated and analysed by transmission electron microscopy. Asterisks indicate spherical virions, and arrowheads indicate atypical elongated virions. From Ma et al. 2012.

These previous findings were supported by a latter study in which the AnxA6-mediated intracellular cholesterol homeostasis is shown to be critical for efficient IAV infection, they showed the link between AnxA6 overexpression and inhibited IAV propagation (Musiol et al., 2013). Musiol and collaborators found that cells treated with siRNA for AnxA6 were exhibiting higher viral titres than non-treated cells but cells overexpressing AnxA6 had reduced viral titres

and also exhibited a reduced amount of M1 viral protein, these results were in agreement with the study performed by Ma (Ma et al., 2012). They also determined that AnxA6 overexpression not only decreased the production of viral particles but also their infectivity. In addition, they demonstrated that AnxA6 has a critical role in the late endosomal cholesterol balance and affects viral replication and propagation in AnxA6-overexpressing cells infected with IAV (Musiol et al., 2013). In an earlier study performed by Cubells et al., it was shown that AnxA6 overexpression in Chinese hamster ovary (CHO) cells leads to accumulation of cholesterol in late endosomes (Cubells et al., 2007). Musiol et al. confirmed these results and also found that this effect could be reversed by addition of exogenous cholesterol or by overexpression of NPC1 (Niemann-Pick C1), a membrane protein which acts as a transporter of cholesterol inside the cell. Interestingly, cells with a mutation in NPC1 gene, treated with U18666A, a drug used to produce an abnormal accumulation of cholesterol in late endosomes or cells overexpressing AnxA6 all exhibited the same phenotype in dysregulation of the intracellular cholesterol homeostasis leading to inhibition of viral replication. Conversely, reestablishment of normal trafficking of cholesterol led to restored viral titres. Altogether, this study confirmed AnxA6 antiviral activity and suggested that IAV restriction mechanism is linked to AnxA6-mediated regulation of intracellular cholesterol pools (figure 1.24) (Musiol et al., 2013).

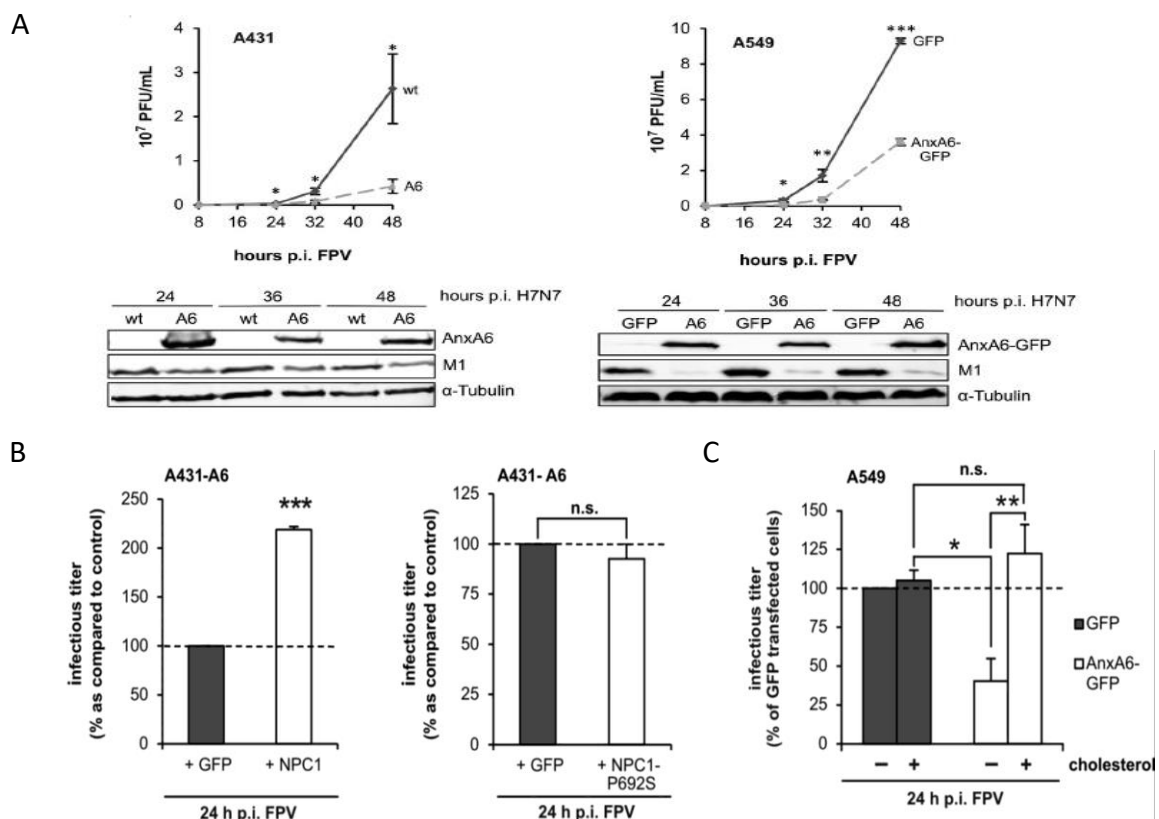


**Figure 1.24. AnxA6 regulates late endosomal cholesterol balance to limit influenza A virus infection.** (A) A431 (wt) and A431-AnxA6 (A6) cells (top left), as well as A549 cells transiently overexpressing GFP or AnxA6-GFP (top right) were infected with the avian influenza A/FPV/Bratislava/79(H7N7) at MOI=0.01 and titres were determined by plaque assay at 24h, 32h and 48h. Data are represented as means  $\pm$  standard errors of means for at least three independent experiments and statistical significance was calculated with a two-tailed t test. \*,  $P<0.05$ ; \*\*,  $P<0.01$ ; \*\*\*,  $P<0.001$ . Also, cell lysates were collected and expression levels of viral M1 and cellular AnxA6 proteins were determined by Western blotting.  $\alpha$ -tubulin was used as loading control. (B) A431-AnxA6 cells transiently expressing NPC1-YFP (bottom left) or NPC1 P692S-YFP (bottom middle) were infected with the avian influenza A/FPV/Bratislava/79(H7N7) at MOI=0.01 and titres were determined by plaque assay at 24h. (C) A549 cells transiently overexpressing GFP or AnxA6-GFP (bottom right) were infected with the avian influenza A/FPV/Bratislava/79(H7N7) at MOI=0.01, treated with exogenous cholesterol at 2h p.i and titres were determined by plaque assay at 24h. Data are represented as means  $\pm$  standard errors of means for at least three independent experiments and statistical significance was calculated with a two-tailed t test. \*,  $P<0.05$ ; \*\*,  $P<0.01$ ; \*\*\*,  $P<0.001$ . From Musiol et al. 2013.

Finally, it is clear that AnxA6 is a restricting factor of IAV and also it has a general mechanism of restriction on different viral strains as Ma et al. showed this event on viruses H1N1 and H3N2 whereas Musiol et al. on viruses H7N7 (figures 1.22 and 1.24). Furthermore, it is now evident that regulation of intracellular cholesterol pools, and especially transport of cholesterol to site of budding, is a critical step for completion of IAV life cycle. It is well known that IAV buds from lipid rafts, and cholesterol depletion with methyl- $\beta$ -cyclodextrin (M $\beta$ CD) leading to lipid microdomains disruption affects virus envelope integrity and virus morphogenesis (Barman and Nayak, 2007). However, the molecular mechanism responsible for restriction of IAV morphogenesis by AnxA6 is still not fully understood and requires to be further investigated, especially it will be crucial to understand the effect of AnxA6 overexpression on M2 expression and function during viral infection.

### 1.3.3 Classification, tissue expression and structure of Annexin A6

AnxA6 is a calcium-dependent phospholipid-binding protein which plays a major role in many cellular events such as regulation of cholesterol homeostasis and membrane organisation (Lizarbe et al., 2013). It belongs to a superfamily of membrane-binding proteins expressed in organisms from protists to higher eukaryotes, they are classified in 5 groups (A-E) and human together with vertebrate annexins constitute the group A (Enrich et al., 2011). AnxA6 is highly expressed in most cells and tissues and it also has been shown to be important in early and late endosomes, the Golgi complex and phagosomes in studies performed in rat cell lines (Cubells et al., 2007, Pons et al., 2000, Jackle et al., 1994, Desjardins et al., 1994). Nevertheless, epithelial cells of the small intestine and parathyroid gland or the A431 cell line derived from vulval squamous epithelial carcinoma do not express AnxA6, whereas others such as some human breast cancer cell lines or Chinese hamster ovary (CHO) cell line do express it but in almost undetectable levels (Cubells et al., 2007, Grewal et al., 2005, Grewal et al., 2000). Little is known about the AnxA6 gene structure and regulation; however, it was suggested that AnxA6 appeared after the fusion of duplicated AnxA5 and AnxA10 genes in the evolution of early vertebrates (Mirsaeidi et al., 2016). AnxA6 is the only annexin having a double highly conserved core formed by 8 homologous motifs of 68-amino acids, the other 12 human annexins have 4 motifs (figure 1.25) Smith and collaborators performed the analysis of sequence similarity of each motif and revealed that both cores are organised very similarly: it was found high similarity between motifs 1 and 5, 2 and 6, 3 and 7, 4 and 8 respectively. However, the two cores are 45% similar and are no more similar to each other than to the structure of other annexins. They also determined that AnxA6 gene contained 26 exons: among them 25 are translated and 1 untranslated. In addition, they found that exon 21 can be alternatively spliced and translated into an isoform lacking 6 amino acids (VAAEIL) at the start of motif 7 (Smith et al., 1994). The shorter isoform, AnxA6-2, was found to differ in cellular localisation and regulation from the main full length isoform, AnxA6-1 (Cornely et al., 2011). From hundreds of screened cDNA clones and isolation of the longest clones, they suggested

that transcription initiation could occur at a site lying 75 bp upstream of the end of the original cDNA clone. Also, some TATA and CAAT motifs were found upstream the transcription start site; however, they did not conclude that this region was the promoter of the AnxA6 gene (Smith et al., 1994). A more recent study showed that AnxA6 gene expression is down-regulated in gastric cancer cells: it was found that AnxA6 promoter region can be methylated by Ying Yang 1 (YY1), a protein involved in DNA methylation (Wang et al., 2013).

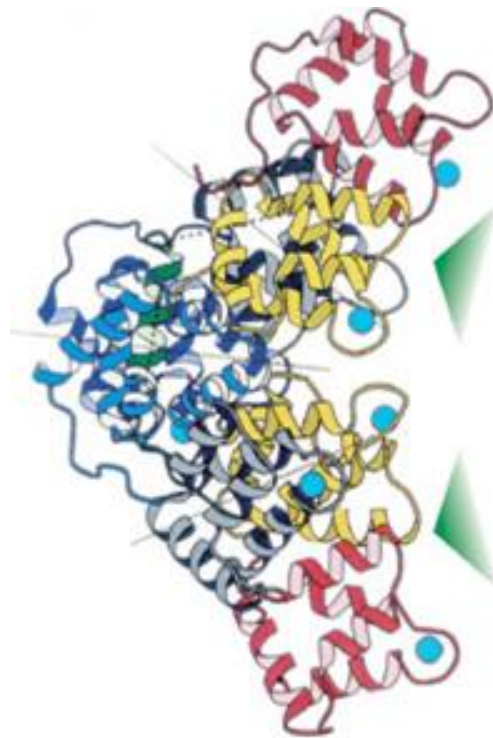


**Figure 1.25. Representation of the crystal structure of AnxA6.** AnxA6 consists of two cores connected by a linker shown in dark green. Bound calcium ions are shown with blue spheres and regions of the cores interacting with membranes are indicated with green arrows. From Gerke et al. 2005.

Over the past years, several studies have provided more insight into the many functions of AnxA6 and therefore more is known about the protein regulation. As already mentioned, AnxA6 is the only annexin having a double highly conserved core formed by 4 homologous motifs each. The 4 motifs of each core are organised around a central hydrophilic hole presumably related to the ion channel activity, each motif contains 4 alpha-helices and one extra helix being the cap of a cylindrical arrangement on the concave side of the protein.

Calcium-binding sites are located on the opposite and convex side enabling binding to cell membrane (Lizarbe et al., 2013, Gerke et al., 2005, Liemann and Lewit-Bentley, 1995). The three main calcium-binding sites of the convex face of the protein were proposed to be the sites of binding to phospholipids (Liemann and Lewit-Bentley, 1995). Crystallography study of AnxA6 on membranes showed a certain flexibility of the overall structure enabling both cores to orientate themselves for their attachment to one or two separated membranes, however a different orientation has been found in other conditions suggesting that changes in cores orientation lead to fulfil different functions (Gerke et al., 2005, Avila-Sakar et al., 1998). Unlike core domains, the N-terminal region of annexins, corresponding to the first motif, exhibits a high variability due to differences in length and amino acid sequence which can go from few to more than 200 residues. Length of this region enables the classification of annexins into 3 groups, AnxA6 being in the first one among annexins having a short N-terminal region of maximum 21 residues (Lizarbe et al., 2013). It plays an essential role in the stability of the protein and it has been suggested to be the key element in the structure and function since its post-translational modifications lead to changes in the structure of core domains despite their opposite location (Gerke and Moss, 2002). Also, the N-terminal extension has been shown to be involved in the interaction of AnxA6 with other calcium-binding proteins. After crystallography studies on AnxA5, this region has been described to arrange regions of the opposite concave face of the protein and to bind domains I and IV together in AnxA6 and other annexins with a short N-terminal region (Lizarbe et al., 2013).

#### 1.3.4 Annexin A6 biological functions

As already mentioned, AnxA6 is a calcium-dependent phospholipid-binding protein which plays an important role in several cellular events in addition to the restriction of influenza A virus life cycle (Lizarbe et al., 2013). When levels of intracellular calcium are elevated, AnxA6 is recruited to the cell plasma membrane where it interacts with phospholipids like phosphatidylserine (PS) and phosphatidylethanolamine (PE) (Lizarbe et al., 2013, Gerke et al., 2005). AnxA6 is implicated in cholesterol homeostasis, membrane organisation and repair,

vesicular trafficking and as already described also in inhibition of virus infection (Lizarbe et al., 2013, Cornely et al., 2011, Cubells et al., 2008, Cubells et al., 2007). It is member of a group of proteins capable of protecting the integrity of cell membranes after its activation when damage has occurred. It has recently been suggested that AnxA6 could control the permeability of membranes by promoting membrane-membrane contacts and by influencing the organisation and diffusion of lipids in the bilayer. AnxA6 is able to stabilize the permeability barrier of complex liposomes and to provide protection against different stresses such as the lysolipid lysophosphatidylcholine (LPC), the polyamine spermidine, the amyloid precursor protein and also toxic agent to neurons amyloid- $\beta$ , the hormone amylin and finally against osmotic shock (Creutz et al., 2012). In addition, it is now well known that AnxA6 regulates intracellular cholesterol distribution, it sequesters cholesterol in late endosomes and reduces levels of cholesterol in the Golgi complex and the plasma membrane perturbing the intracellular cholesterol homeostasis (Cubells et al., 2007) (figure 1.26). The reduction of cholesterol in the Golgi complex inhibits the activity of the cytoplasmic phospholipase A2 (cPLA2) and its association with the Golgi complex leading to the blockage of caveolin-1 (cav1) export from Golgi and reduction of caveolae at the plasma membrane (Cubells et al., 2008). It was later described by the same group that transport of cholesterol from late endosomes to the Golgi complex plays an important role in trafficking and localisation of target membrane SNAP receptors (t-SNAREs), it was shown that inhibition of cholesterol transport led to a defect in normal localisation and function of t-SNAREs due to their retention in Golgi membranes. Interestingly, they found that AnxA6 overexpression leading to accumulation of cholesterol in late endosomes and reduction in the Golgi is responsible for the retention of both SNAP23 and syntaxin-4 in the Golgi apparatus and their abnormal intracellular distribution, which are important proteins of the secretory pathway (Reverter et al., 2011). In a study recently published, Alvarez-Guaita and co-workers found evidence for AnxA6 to be capable of driving remodelling of lipid domains at the plasma membrane. They showed that AnxA6 induces membrane changes by its ability to decrease membrane order through

cholesterol homeostasis and interaction with actin cytoskeleton inside the cell, constituting a first evidence obtained from live cells that AnxA6 is a membrane organiser.

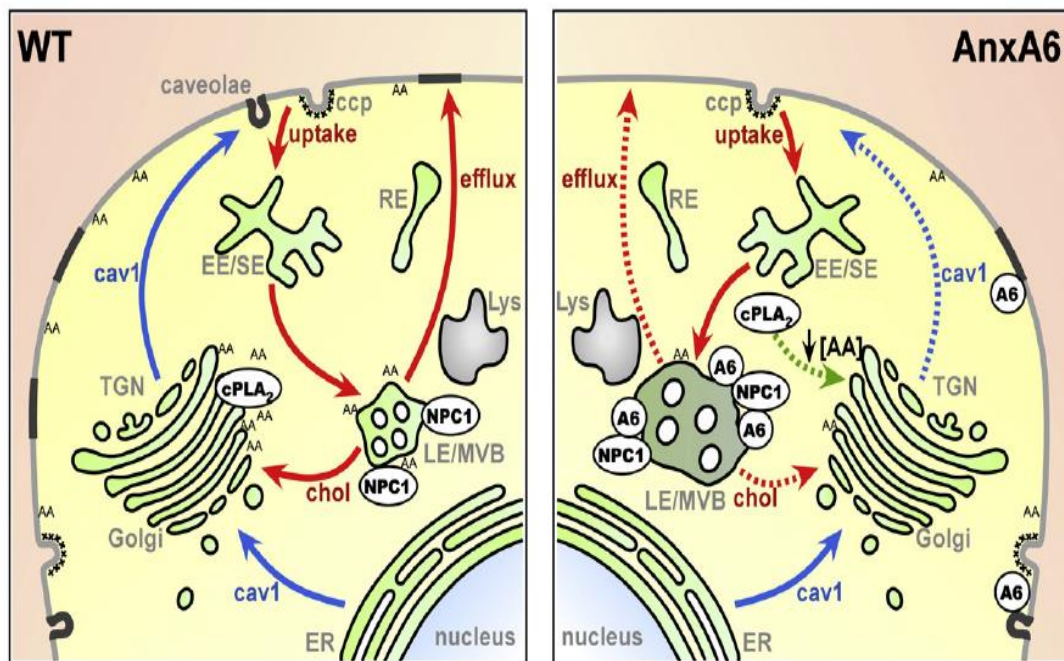


**Figure 1.26. AnxA6 plays an important role in intracellular cholesterol homeostasis and formation of caveolae.** In cells expressing low AnxA6 (left panel), caveolin travels from endoplasmic reticulum (ER) to the plasma membrane (shown with blue arrows) and cholesterol is transported from late endosomes (LE) to the Golgi and plasma membrane (shown with red arrows together with the uptake of cholesterol and the efflux to the cell surface). Arachidonic acid (AA) is synthesized by cytoplasmic phospholipase A2 (cPLA<sub>2</sub>) in the Golgi and is transported to plasma membrane. In cells expressing high AnxA6 (right panel), cholesterol is sequestered in late endosomes leading to AnxA6 translocation to LE and multivesicular bodies (LE/MVB) where it binds to Niemann-Pick C1 (NPC1) protein and inhibits cholesterol export to Golgi complex and plasma membrane (shown with red dashed arrows). Cholesterol reduction in the Golgi inhibits the activity of cPLA<sub>2</sub> and its association with the Golgi complex (shown with green dashed arrows) leading to diminution of AA production and reduction of caveolin-1 export to plasma membrane (shown with blue dashed arrows). Reduction of cholesterol and caveolin-1 at the plasma membrane due to AnxA6 overexpression leads to a reduction of caveolae. Caveolae are small invaginations of the plasma membrane enriched in cholesterol, sphingolipids and caveolin-1 which facilitate virus assembly and budding. Caveolar membranes promote recruitment of all cellular and viral proteins to sites of budding and their incorporation into newly formed virus particles released from the cell surface. From Enrich et al. 2011.

Briefly, AnxA6 overexpression leads to reduction in plasma membrane order, measured by labelling of cell membranes with the fluorescent probe di-4-ANEPPDHQ, and also to changes in the organisation of the actin cytoskeleton by reducing amounts of cortical actin and increasing stress fibres in A431 and MEF AnxA6-expressing cells. In addition, it was found to regulate clustering of raft and non-raft associated proteins, playing again a role in the organisation of membranes and their microdomains (Alvarez-Guaita et al., 2015). In agreement with these latest findings involving AnxA6 in membrane domains organisation, AnxA6 has previously been identified as a link between membrane microdomains and the organisation of the cytoskeleton, and it was suggested that AnxA6 and actin interactions could regulate events such as receptor-mediated endocytosis, cell migration or vesicle trafficking spectrin (Cornely et al., 2011, Grewal et al., 2010). It has been shown that constitutive plasma membrane AnxA6 is able to stabilise the cortical actin cytoskeleton and regulate intracellular calcium concentration leading to changes in cell proliferation and differentiation (Monastyrskaya et al., 2009). However, AnxA6 also interacts with spectrin, another important protein involved together with actin in membrane and cytoskeleton organisation, to regulate trafficking of clathrin-coated vesicles inside the cell. Therefore, it is very possible that AnxA6 regulates the traffic of endocytic vesicles to the lysosomal compartment through interaction with both actin and spectrin, possibly promoting the recruitment of calpain-1 protease to cleave spectrin for initiation of intracellular vesicular transport (Grewal et al., 2010, Grewal et al., 2000, Kamal et al., 1998, Lin et al., 1992). Indeed, AnxA6 can interact with actin to regulate through endocytic trafficking the activation and localisation of cell surface receptors such as epidermal growth factor (EGF) and T cell receptors (TCR) (Cornely et al., 2011, Grewal et al., 2010, Grewal and Enrich, 2006). Furthermore, the mechanism of plasma membrane repair accomplished by AnxA6 is still unclear but it has been suggested that AnxA6 is able to bring together plasma membrane around a gap for small injuries and in case of more important damage patch-vesicles could interact in a repairing fashion (Cornely et al., 2011). Another function of AnxA6 is its contribution to mitochondrial formation regulating calcium homeostasis and membrane potentials (Chlystun et al., 2013). Finally, AnxA6 is involved in another cellular

process of minor importance during influenza virus infection; however, it can be related to a physiopathological condition. Indeed, AnxA6 downregulation is involved in heart function and blood pressure, increasing contractility and reducing cardiovascular conditions (Grewal et al., 2010, Gerke and Moss, 2002). Indeed, overexpression of AnxA6 in mice leads to hypertrophy and heart failure (Guntjeski-Hamblin et al., 1996).

### 1.3.5 Modulation of important intracellular signalling pathways by annexin A6

In addition to the biological functions already described above, it has been demonstrated that Annexin A6 is also involved in the modulation of intracellular signalling pathways and its scaffolding role is important to recruit signalling proteins for signal transduction (Enrich et al., 2011).

#### 1.3.5.1 Calcium signalling is important for regulation of AnxA6 membrane functions

Calcium signalling has an important role in many cellular events in eukaryotic cells. For this reason, cells encode a number of proteins which are regulated by intracellular changes in calcium homeostasis; among them, our protein of interest, Annexin A6, which is recruited to cellular plasma membrane upon cellular stress and subsequent increase in calcium levels and binds to negatively charged lipids in the membrane to fulfil its membrane-associated functions (Gerke et al., 2005). AnxA6 was described more than a decade ago to translocate to membranes of smooth muscle cells in a calcium-dependent mechanism and was found to associate with raft microdomains (Babiychuk and Draeger, 2000). This finding supported the idea that AnxA6 is a calcium-regulated membrane-binding protein which organises membrane microdomains/rafts. Conversely, AnxA6 plays a role in the regulation of ion transport across the cell. Monastyrskaya et al. demonstrated that when intracellular calcium levels reach a high concentration, Annexin A6 is promoted to the plasma membrane and decrease the store-operated calcium entry (SOCE). They found that inhibition of SOCE is due to the fact that membrane-associated AnxA6 interacts with actin cytoskeleton to rearrange, accumulate and stabilize F-actin at the plasma membrane, also resulting in inhibition of cell proliferation

(Monastyrskaya et al., 2009, Monastyrskaya et al., 2007). Finally, another study performed in mice determined that AnxA6 overexpression in the heart participates in regulation of intracellular calcium and has an impact on their cardiac activity (Kaetzel and Dedman, 2004). Through its involvement in intracellular calcium homeostasis, AnxA6 interacts with many factors involved in the formation of complexes regulating other signalling pathways (Enrich et al., 2011).

#### 1.3.5.2 Annexin A6 regulation of EGFR/Ras/Raf pathway

It has already been mentioned that AnxA6 has been reported to regulate localisation and expression of cell surface receptors, one example is the epidermal growth factor receptor (EGFR) (Cornely et al., 2011). Activation of EGFR is an essential step for a diverse range of cellular processes; however its inactivation is crucial as deregulation of EGFR receptor/Ras signalling pathway leads to different pathologies such as different types of cancer. Inactivation of this pathway occurs upon endocytic transport of activated EGFR to lysosomes and subsequent degradation (Grewal et al., 2010). Interestingly, AnxA6 has been described to play a central role in the regulation of the EGFR receptor through the Ras/Raf signalling pathway (figure 1.27) (Grewal et al., 2010, Grewal and Enrich, 2009). Excessive EGFR activation in some breast cancer cell lines correlates with deregulation of Ras/Raf signalling, which is regulated by GTPase-activating proteins such as p120GAP. Grewal, Enrich and co-workers demonstrated that AnxA6 can act as tumour suppressor by modulating Ras and Raf-1 activity through recruitment of the p120GAP protein to plasma membrane in EGFR-overexpressing breast cancer cells. They found that AnxA6 is found with activated H-Ras-containing protein complexes and mediates interaction of p120GAP and Ras in a calcium-dependent manner at plasma membrane to reduce Ras and Raf-1 activation (Grewal et al., 2005).

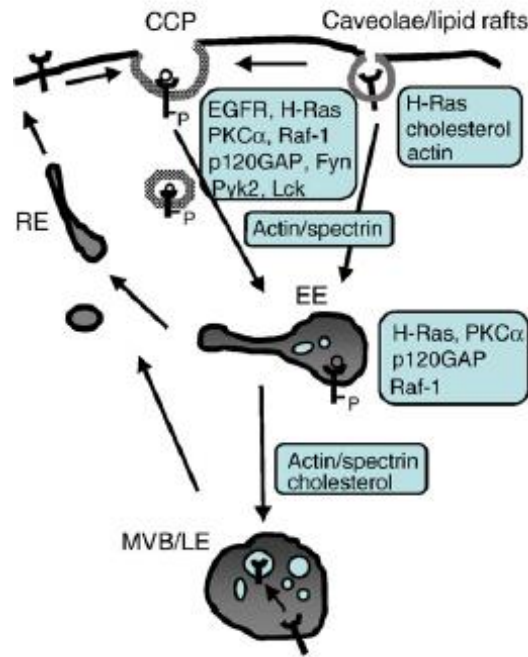


**Figure 1.27. Regulation of EGFR/Ras by AnxA6.** Intracellular cholesterol pools regulate location and expression of AnxA6, which in turn has an impact on distribution and activation of EGFR. When activated and translocated to plasma membrane, AnxA6 recruits p120GAP and PKC $\alpha$  to down-regulate the EGFR/Ras pathway. From Grewal and Enrich, 2009.

Activation of Raf-1 was shown to initiate MAPKs signalling that regulate cell differentiation and proliferation in cancer (Rentero et al., 2006). Therefore, AnxA6 regulation of this pathway is essential for EGFR inactivation and prevention of cancer (Vila de Muga et al., 2009). In addition, it was found that upon increased intracellular calcium levels, AnxA6 can bind to plasma membrane and recruit protein kinase C $\alpha$  (PKC $\alpha$ ), which binds to and inactivates EGFR (Koese et al., 2013, Rentero et al., 2006). PKC $\alpha$  is a family member of serine/threonine kinases involved in regulation of cellular events such as cell division, proliferation and differentiation, apoptosis and gene regulation. It is activated by several signals in a calcium-dependent manner, including lipids, the second messenger diacylglycerol, G-protein coupled receptors or physical stress. When activated, PKC $\alpha$  suffers a conformational change which increases its binding affinity to substrates (Nakashima, 2002). PKC $\alpha$  has been described to bind and phosphorylate threonine 654 (T654) in the tyrosine kinase domain of EGFR to down-regulate its related signalling (Wang et al., 2007b). Finally, it was found that AnxA6 regulates

extracellular signal-regulated kinase (ERK) and p38 mitogen-activated protein kinase (MAPK) activation during terminal differentiation of chondrocytes through regulation of PKC $\alpha$  activity (Minashima et al., 2012). Similarly, AnxA6 could also interact with Ras/Raf-1 pathway to regulate activation of the phosphoinositide 3-kinase (PI3K) and Akt pathways through modulation of PKC $\alpha$  activity (Rentero et al., 2006).

### 1.3.5.3 Potential role of annexin A6 in T cell receptor signalling

AnxA6 has been described to be also involved in T cell signalling; however, the mechanism is still not well understood. It is known that AnxA6 plays a role in differentiation and activation of T cells. AnxA6 binds to cellular factors involved in the formation of T cell receptor (TCR) microclusters such as Pyk2, Lck and Fyn (figure 1.28). TCR microclusters contain and interact with all necessary elements to start signalling through T cell receptors in antigen presenting cells. Also, it has been suggested that AnxA6 could reorganise the membrane cholesterol- and PS-enriched lipid domains around a TCR and interact with actin to maintain the stability of TCR complex and to regulate the receptor signalling (Cornely et al., 2011, Grewal et al., 2010, Grewal and Enrich, 2006).

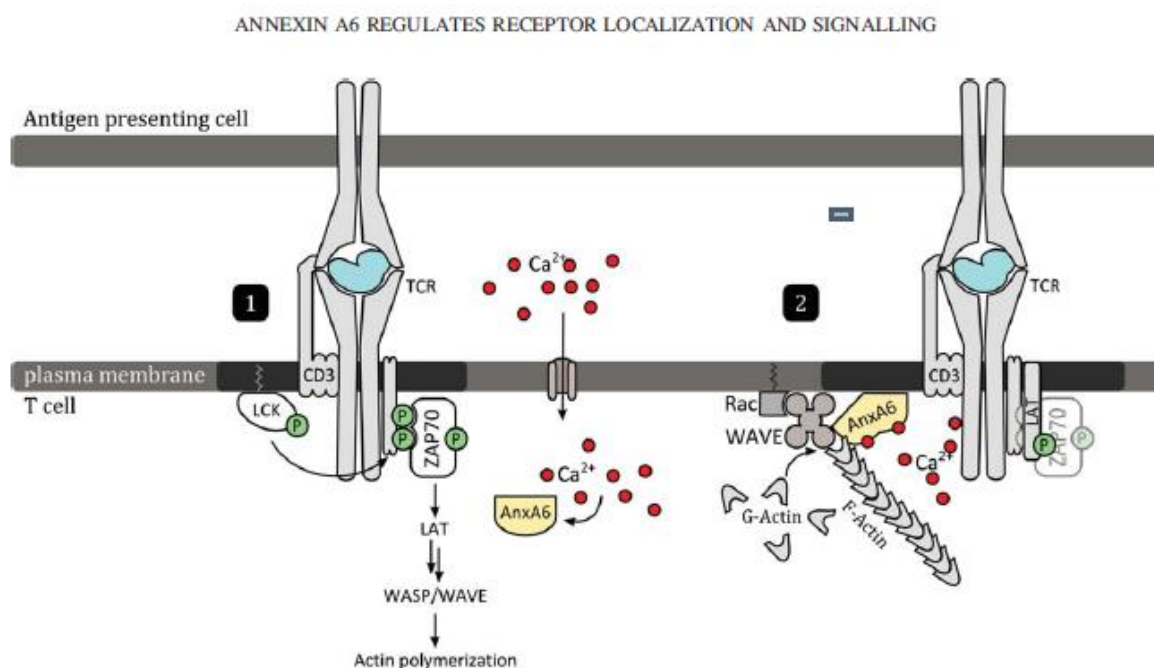


**Figure 1.28. AnxA6 is involved in T cell receptor signalling.** (1) Firstly, a TCR recognises an antigen at the surface of an antigen-presenting cell and initiates remodelling of membrane reorganisation. TCR then becomes phosphorylated by Lck kinase, which subsequently activates ZAP-70 and the transmembrane linker for activation of T cells (LAT). TCR/LAT oligomerisation and activation leads to recruitment of cellular factors involved in the receptor signalling, actin polymerisation through activation of WASP/WAVE and increase of intracellular calcium. Also, AnxA6 could bind to the plasma membrane in proximity to TCR, where it is phosphorylated by Lck and binds to Fyn kinase. (2) AnxA6 activation and recruitment to plasma membrane could participate in the organisation of F-actin and lipid rafts in proximity of the activated TCR. From Cornely et al., 2011.

#### 1.3.5.4 Annexin A6 regulates NF- $\kappa$ B and MAPK signalling in articular chondrocytes

In a recent study, AnxA6 was found to regulate Nuclear Factor kappa B (NF- $\kappa$ B) in articular chondrocytes (Campbell et al., 2013). NF- $\kappa$ B is a transcription factor which plays an important role in many physiological and pathological events like cell proliferation, cell survival, inflammation and pathogenic infections such as IAV. It consists of 5 proteins which are p65 (RelA), RelB, c-Rel, p105/p50 (NF- $\kappa$ B1) and p100/52 (NF- $\kappa$ B2). When inactivated, the inhibitory I $\kappa$ B protein retains NF- $\kappa$ B dimers in the cytosol. Upon NF- $\kappa$ B activation, I $\kappa$ B is phosphorylated by I $\kappa$ B kinase (IKK) and subsequently degraded, leading to nuclear translocation of NF- $\kappa$ B for transcription of target genes (Oeckinghaus and Ghosh, 2009). Campbell and co-workers found that AnxA6 interacts with the p65 subunit of the transcription factor NF- $\kappa$ B and that loss of AnxA6 led to a decreased nuclear translocation of NF- $\kappa$ B complex and consequently of mRNA levels of IL-1 and TNF $\alpha$  (figure 1.29) (Campbell et al., 2013).

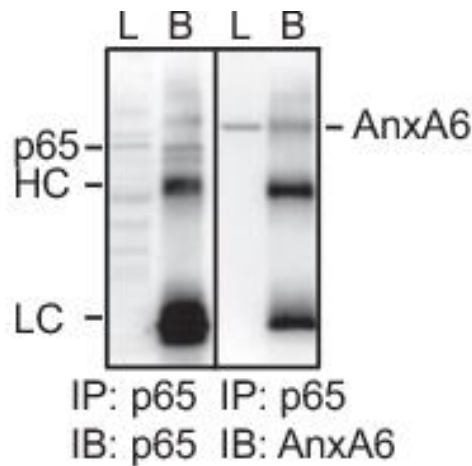


**Figure 1.29. AnxA6 interacts with p65 in chondrocytes.** Coimmunoprecipitation from cell lysates of mouse chondrocytes was performed and specific antibodies were used to label AnxA6 and p65 proteins. Both proteins were found together in the cell immunoprecipitates. L: lysate; B: beads; HC: heavy chain IgG; LC: light chain IgG. From Campbell et al., 2013.

In addition, another study revealed that lack of AnxA6 led to a reduction in ERK and p38 MAPK activities. Knockout of AnxA6 in mice translated into a reduction in intracellular  $\text{Ca}^{2+}$  levels, which subsequently led to a reduced activation of ERK and p38 MAPKs. Also, by using a specific inhibitor, they found that MAPKs regulation by AnxA6 is a  $\text{PKC}\alpha$ -dependent mechanism. They concluded that AnxA6 stimulates  $\text{PKC}\alpha$  activity to regulate  $\text{Ca}^{2+}$  homeostasis and terminal differentiation of chondrocytes through regulation of ERK and p38 MAPKs (figure 1.30) (Minashima et al., 2012).

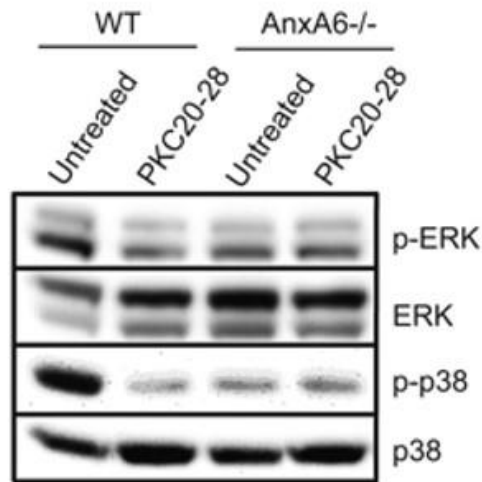


**Figure 1.30. AnxA6 induces ERK and p38 activation in chondrocytes through regulation of PKC $\alpha$ .** Cell lysates from wild-type (WT) and AnxA6<sup>-/-</sup> chondrocytes were cultured in the absence (Untreated) or presence of the PKC $\alpha$ -specific inhibitor PKC20–28 for 1 h. Lysates were analysed for MAPKs activities by immunoblotting cell lysates with antibodies specific for p-ERK and total ERK or p-p38 and total p38. From Minashima et al., 2012.

To conclude, I have now described all the important stages during IAV life cycle, from virus attachment to budding from the cell surface of infected cells. I have then introduced in detail the structure and function of all viral structural proteins and vRNPs during infection in addition to the vast host innate immune response activated upon their recognition. Also, I have described all the interactions which have been identified so far between viral proteins and cellular factors that either facilitate or restrict IAV infection. In particular, I have focused on AnxA6 as a previous study performed by our group has shown that AnxA6 is a restriction factor of IAV infection. Our laboratory has shown AnxA6 interacts with the IAV M2 proton channel and limits production of progeny IAV from infected cells. We have found that overexpression of AnxA6 impairs morphogenesis and release of progeny viruses. However, the molecular mechanism responsible for restriction of IAV morphogenesis by AnxA6 is still unclear. In this study, I present new data providing insight into this mechanism of IAV restriction by AnxA6.

## **1.4 Hypothesis**

We hypothesized that AnxA6 interferes with IAV budding through disruption of the budzone by one of the two following mechanisms. Firstly, since Ma et al. demonstrated the physical interaction between AnxA6 and M2 cytoplasmic tail, we suggested that AnxA6 could colocalize with M2 at the neck of budding particles and generate a mechanical restraint on M2 during the scission event. Secondly, we thought that reduction of cholesterol at membranes of the secretory pathway induced by AnxA6 overexpression alters the normal trafficking of viral proteins to the cell surface and indirectly disrupts the budzone. This hypothesis is supported by the latest data published by Musiol et al. showing the important role of cholesterol in IAV infection and by the better understanding of AnxA6 role in cholesterol transport and trafficking inside the cell. In addition, we know that AnxA6 is implicated in the modulation of important cellular pathways required for influenza virus infection and therefore we also hypothesized that AnxA6 may regulate a potential innate immune response against the virus. In this study, we have then investigated in one hand the mechanism underlying AnxA6 interference with IAV budding. In the other hand, we have investigated the regulation of Nuclear Factor – Kappa B (NF- $\kappa$ B), Mitogen-Activated Protein Kinase (MAPK) and Akt pathways as well as the induction of pro-inflammatory cytokines and chemokines during viral infection.

## **1.5 Aims of the study**

To understand the molecular mechanism responsible for restriction of IAV morphogenesis by AnxA6, I use a combination of virology, cellular biology and biochemistry approaches that enable me to study:

- Effect of AnxA6 overexpression on subcellular localisation, compartmentalisation and transport of viral components to the cell surface and budding of IAV
- Modulation of intracellular signalling pathways and induction of pro-inflammatory cytokines and chemokines by AnxA6 during IAV infection
- Down-regulation of AnxA6 by IAV

## 2 MATERIALS AND METHODS

### 2.1 Materials

#### 2.1.1 Virus strains

A/Udorn/72 (H3N2): filamentous strain propagated in MDCK cells, a kind gift from Dr. Jeremy Rossman

A/WSN/33 (H1N1): initially isolated from a patient in 1933 and subsequently propagated in MDCK cells, a kind gift from Drs Poon and Peiris

#### 2.1.2 Cell lines

MDCK: Madin-Darby canine kidney cell line, variant MDCK.1, purchased from ATCC

A431: human vulval squamous epithelial cell line, purchased from ATCC

A431-AnxA6: A431 stable cell line expressing recombinant human annexin A6, previously described in Ma et al., 2012

A549: human adenocarcinoma alveolar basal epithelial cell line, purchased from ATCC

A549-AnxA6: A4549 stable cell line over-expressing recombinant human annexin A6, previously described in Ma et al., 2012

#### 2.1.3 Oligonucleotides for quantitative Real Time-Polymerase Chain Reaction

Annexin A6 'Full length'      F: 5'-ATGGCCAAACCAGCACAGG-3'

R: 5'-GCCGTAGAGGGACTTGTAGC-3'

Annexin A6 'Central'      F: 5'-AGCTGTCTGGGGGAGATGAT-3'

R: 5'-TTGTGTCTTCGTCAGTCCCG-3'

Annexin A6 'ΔVAAEIL'      F: 5'-TGCCCAGGAAATAGCAGACA-3'

	R: 5'-ATGGCCACAAATGCATCCCT-3'
18S	F: 5'-ATGGCCGTTCTTAGTTGGTG-3'
	R: 5'-CGCTGAGCCAGTCAGTGTAG-3'
M1	F: 5'-AAGACCAATCCTGTCACCTCTGA-3'
	R: 5'-CAAAGCGTCTACGCTGAGTCC-3'
Interleukin-1 $\beta$	F: 5'-GGACAAGCTGAGGAAGATGC-3'
	R: 5'-TCGTTATCCCATGTGTGCGAA-3'
Interleukin-6	F: 5'-GAAAGCAGCAAAGAGGCACT-3'
	R: 5'-TTTCACCAGGCAAGTCTCCT-3'
Interleukin-8	F: 5'-GGTGCAGTTTTGCCAAGGAG-3'
	R: 5'-CACCCAGTTTTCTTGGGGT-3'
RANTES	F: 5'-TCATTGCTACTGCCCTCTGC-3'
	R: 5'-TCTTCTCTGGGTTGGCACAC-3'
Nuclear Factor- $\kappa$ B	F: 5'-GTATTTCAACCACAGATGGCACT-3'
	R: 5'-AACCTTTGCTGGTCCCACAT-3'
Tumor Necrosis Factor- $\alpha$	F: 5'-AGCCCATGTTGTAGCAAACC-3'
	R: 5'-TGAGGTACAGGCCCTCTGAT-3'
Interferon- $\beta$	F: 5'-ACGCCGCATTGACCATCTAT-3'
	R: 5'-TGCTCATGAGTTTTCCCCTGG-3'

#### 2.1.4 Primary antibodies

Monoclonal mouse anti-M1 (clone GA2B) purchased from AbD Serotec, UK

Monoclonal mouse anti-M2 (clone 14C2) purchased from Santa Cruz Biotechnology, USA

Monoclonal mouse anti-Annexin A6 (clone 73) purchased from BD Transduction Laboratories, USA

Monoclonal mouse anti-GAPDH (clone 9484) purchased from Abcam, UK

Monoclonal rabbit anti-myc purchased from Sigma Life Sciences, UK

Polyclonal goat anti-H3 purchased from BEI Resources, ATCC, USA

Polyclonal goat anti-H3 received from Dr. Jeremy Rossman, University of Kent, UK

Polyclonal rabbit anti-caveolin1 (clone N20, sc-894) purchased from Santa Cruz Biotechnology, USA

Polyclonal rabbit anti-NF- $\kappa$ B p65 (clone C20, sc-372) purchased from Santa Cruz Biotechnology, USA

Monoclonal rabbit phospho-p44/42 MAPK (Erk1/2) (Thr202/ Tyr204) (#4370) purchased from Cell Signaling, UK

Monoclonal rabbit p44/42 MAPK (Erk1/2) (clone 137F5) (#4695) purchased from Cell Signaling, UK

Monoclonal rabbit phospho-Akt (Ser473) (clone D9E) (#4060) purchased from Cell Signaling, UK

Polyclonal rabbit Akt (#9272) purchased from Cell Signaling, UK

Polyclonal rabbit phospho-SAPK/JNK (Thr183/Tyr185) (#9251) purchased from Cell Signaling, UK

Polyclonal rabbit SAPK/JNK (#9252) purchased from Cell Signaling, UK

#### 2.1.5 Secondary antibodies

Alexa Fluor 488 donkey anti-goat purchased from Stratech, UK

Alexa Fluor 488 donkey anti-goat purchased from Jackson ImmunoResearch Laboratories, USA

Alexa Fluor 488 goat anti-rabbit purchased from Invitrogen, UK

Alexa Fluor 546 donkey anti-mouse purchased from Invitrogen, UK

Alexa Fluor 647 donkey anti-rabbit purchased from Invitrogen, UK

FITC-conjugated rat anti-mouse purchased from BD Biosciences Pharmingen

HRP-conjugated anti-goat purchased from Abcam

HRP-conjugated anti-mouse purchased from SignalChem

HRP-conjugated anti-rabbit purchased from SignalChem

#### 2.1.6 Kits

GenElute Mammalian Total RNA miniprep kit (#RTN70-1KT), purchased from Sigma

## 2.2 Methods

### 2.2.1 Cell amplification

Human vulval squamous epithelial A431 cells, A431 cells stably expressing AnxA6-myc (A431-AnxA6) previously described in Ma et al., lung epithelial A549 cells, A549 cells stably over-expressing AnxA6-myc (A549-AnxA6) previously described in Ma et al and Madin-Darby Canine Kidney (MDCK) cells were amplified in complete growth medium (10% foetal bovine serum (FBS) decomplexed at 56°C for 30 minutes, Fisher scientific; 100 U/mL Penicillin/Streptomycin (P/S), Fisher Scientific; and Dulbecco's modified Eagle's medium High glucose (DMEM), sodium pyruvate, glutamine, Hyclone Fisher Scientific) and in an atmosphere of air supplied with 5% carbon dioxide and a temperature of 37°C.

### 2.2.2 Expression of AnxA6 in the A431 and A549 stable cell lines

Stable A431 and A549 cell lines expressing recombinant human AnxA6 were obtained as previously described in Ma et al. 2012. Briefly, a pLenti-Anx6 construct was obtained by AnxA6-myc tagged cDNA amplification and insertion into a pLenti vector (figure 2.1). Then, a lentiviral expression system was used for transfection of confluent 293T cells with the pLenti-Anx6 transfer vector, pGag-pol packaging plasmid and pVSV-G plasmid. At 48h post-transfection, the cell culture medium including pseudotyped lentiviral particles was collected and cell debris spun down. Confluent A431 and A549 cells were finally infected with the virus supernatant and cells expressing the recombinant human AnxA6 were selected with culture medium supplemented with 5 µg/ml blasticidin. Screening for AnxA6 expression of propagated surviving clones was then performed by Western blotting, flow cytometry and immunofluorescence assays.

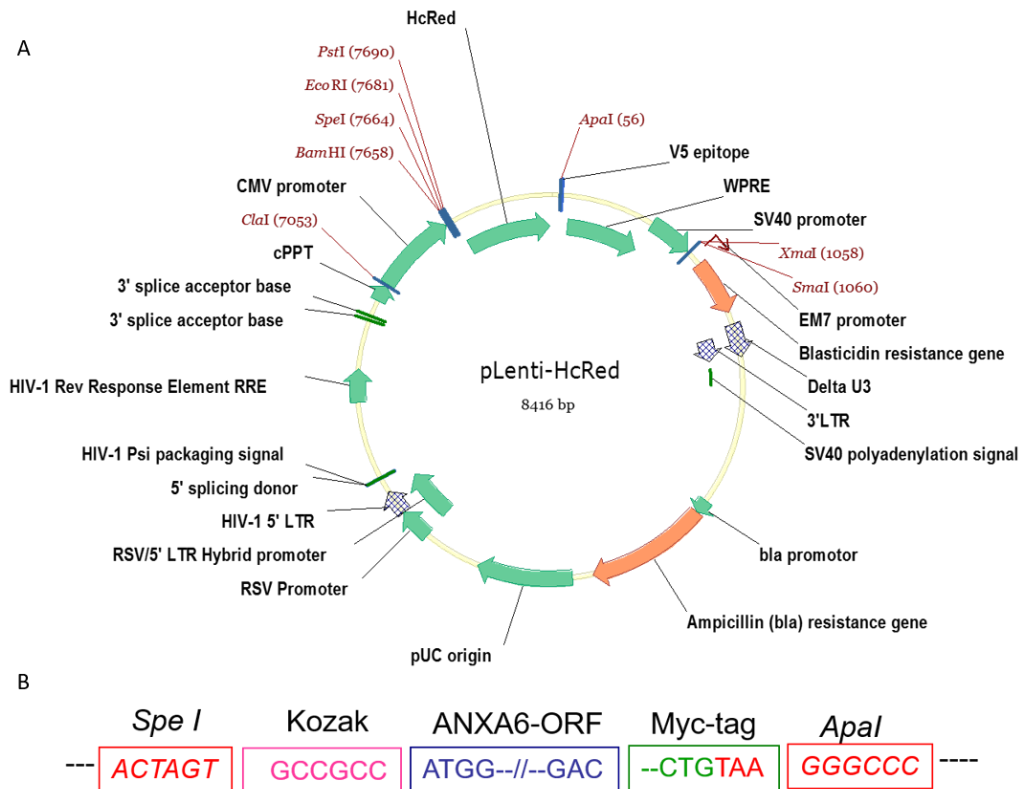


**Figure 2.1. Cloning system used to establish stable A431 and A549 cell lines expressing AnxA6.** (A) Restriction map of the pLenti vector used for insertion of an Anx6-containing construct. (B) Construct obtained from an AnxA6-myc tagged cDNA amplification and cloned into a pLenti vector.

### 2.2.3 Virus amplification and purification

Filamentous A/Udorn/72(H3N2) influenza virus was inoculated at a multiplicity of infection (MOI) of 0.001 and amplified for 3 days on MDCK cells. The cell culture medium containing the virus suspension became slightly cloudy due to cell death and 30ml of each flask were harvested into a 50ml falcon tube and centrifuged at 3.000 rpm or 1.500 g at 4°C for 10mins. This centrifuge step enabled to spin down the cell debris and harvest the amplified virus. At this stage, virus is not concentrated but can be stored at -80°C. If required, ultra-centrifugation (Beckman Coulter Ultracentrifuge) on a sucrose cushion can be performed at this stage to further purify viral particles. Then, supernatants obtained after centrifugation were collected, transferred to Ultraclear centrifuge tubes and ultra-centrifuged at 3.000 rpm or 1.500 g at 4°C for 10-15 min in the pre-cold SW32Ti rotor to spin down any cell debris left over from the

previous spin. Supernatants were re-collected, transferred to a new tube containing cold 30% sucrose and centrifuged at 25.000 rpm or 107.000 g at 4°C for 90 min in the pre-cold SW32Ti rotor with maximal acceleration and deceleration. Then, the upper phase medium and the sucrose phase were removed and a white pellet was found at the bottom of the tubes. Pellets containing the viral particles were serially resuspended in 100µl cold PBS for concentration and collected in a screw capped tube. Finally, the screw capped tube was briefly centrifuged at 2.000 rpm or 450 g for 10 min and 50µl of viral suspension aliquots were prepared in new eppendorf tubes and stored at -80°C.

#### 2.2.4 Plaque assay

After amplification and concentration, the titre of infectious virus needs to be determined by plaque assay. MDCK cells were seeded on 6 well-plates (5x10<sup>5</sup> MDCK cells per well) and grown to 100% confluence to form a monolayer. Then, 10-fold dilutions of virus stock were prepared and 300µl of every dilution were inoculated onto the susceptible cell monolayers. After a 1h incubation period at 37°C, viruses bind to cells and the infectious medium for the entry of the virus and the agar overlay solution for the formation of a gel after solidification were added to the monolayers. Final concentrations were infectious medium 1X (1% P/S, 1ug/ml Trypsin-TPCK, 0.3% bovine serum albumin (BSA) and 1,5% agar in PBS). The 6-well plates were incubated for 3 days at 37°C, cells were fixed with 4% paraformaldehyde (VWR International) in PBS for 2 hours and staining with 0, 1% crystal violet in PBS for 15 minutes was performed after the agarose removal. Infected cells produced viral progeny and their spread produced the lysis of the monolayer appearing as circular zones called plaques. Counting of plates was performed in every well and only the ones containing between 10 and 100 plaques were used in order to determine the titre of each strain in plaque forming units (PFU) per millilitre.

#### 2.2.5 Median tissue culture infectious dose - TCID<sub>50</sub>

The titre of infectious virus can also be determined by TCID<sub>50</sub>. Influenza A virus was added to DMEM in a 96-well plate for preparation of a ½ tenfold serial dilution and incubated at 37°C

for 1h. MDCK and A549 cells were then diluted in 2X infectious medium (2% P/S, 2ug/ml Trypsin-TPCK, 0.6% BSA in DMEM) and  $10^5$  cells were added into each well and incubated for 3-5 days at 37°C until cytopathic effect is observed. Visualisation under the microscope is required to identify positive or negative wells for virus infection and application of statistical methods to estimate the infectious titre.

#### 2.2.6 Scanning electron microscopy

A431 and A431-AnxA6 cells were infected with influenza A/Udorn/72(H3N2) for 6h and 18h at a MOI=1, fixed first with 2.5% glutaraldehyde in phosphate buffer 0.1M pH=7.2 for 2 hours and then with 1% osmium tetroxide in phosphate buffer 0.1M pH=7.2 for 1h at 4°C, critical point dried (K850 Critical Point Dryer) and platinum coated (Sputter Coating; 1kV, 5mA, 30sec). Samples were observed on Zeiss Supra 35VP FEG (field emission gun) scanning electron microscope.

#### 2.2.7 Transmission electron microscopy

A431 and A431-AnxA6 cells were infected with A/Udorn/72(H3N2) for 10h and 20h at a MOI=5, fixed first with 4% paraformaldehyde/1% glutaraldehyde in phosphate buffer 0.1M pH=7.2 for 2 hours and with 1% osmium tetroxide in phosphate buffer 0.1M pH=7.2 for 1h at room temperature. Cells were then dehydrated by consecutive incubations with increasing ethanol concentrations and infiltrated in LR White resin (Agar Scientific) at 50°C overnight for 24h. Samples are then prepared for sectioning: cut into 100nm-thick sections and collected on copper grids to be visualised on JEOL 2100 FEG (field emission gun) transmission electron microscope.

#### 2.2.8 Immunofluorescence Assay

A431 and A431-AnxA6 cells were infected with influenza A/Udorn/72(H3N2) for 16h at a MOI=2, fixed in 4% paraformaldehyde, blocked in 1mg/mL BSA (Sigma Life Sciences, UK) and labelled with DAPI (Invitrogen, UK), monoclonal antibody (MAb) mouse anti-M2 (clone 14C2, Santa Cruz Biotechnology), polyclonal antibody (pAb) goat anti-H3 (BEI Resources,

ATCC, USA) and MAb rabbit anti-myc (Sigma Life Sciences). Labelling was performed with DAPI 100X for nuclei (Invitrogen, UK), dilution 1:800 for the anti-M2 MAb, dilution 1:800 for the anti-myc MAb against AnxA6-myc protein and 1:3200 for the anti-H3 PAb. Alexa fluorophore-conjugated secondary antibodies were used in a 1:100 dilution: Alexa 488 donkey anti-goat (Strattech, UK), Alexa 546 donkey anti-mouse (Invitrogen, UK) and Alexa 647 donkey anti-rabbit (Invitrogen, UK). Samples were observed on Zeiss Axiovert 200M.

#### 2.2.9 Imagestream - Flow cytometry

A431 and A431-AnxA6 cells were first plated on collagen-coated dishes to promote their adherence and survival during posterior treatment, infected with influenza A/Udorn/72(H3N2) for 8 hours and 16 hours at MOI=3 or MOI=5, treated when required with either trypsin or Versene and Accutase (Fisher scientific, UK) in DMEM to promote their detachment from dishes. Collected cells were washed twice with PBS, fixed with 4% paraformaldehyde (VWR International) in PBS and blocked with 1% BSA (Sigma Life Sciences) in PBS. Before the labelling, cells were permeabilised in 0.1% Triton X-100 (Sigma Life Sciences) in PBS for 3-5 minutes in ice if required. Then, staining was performed with dilution 1:150 for the anti-M2 MAb, 1:5000 for the anti-myc MAb against AnxA6-myc protein and 1:800 for the anti-H3 PAb. Secondary antibodies were used in different concentrations: 1:200 for rat anti-mouse FITC (BD Biosciences Pharmingen), 1:500 for goat anti-rabbit Alexa fluoro 488 (Invitrogen) and 1:300 for the donkey anti-goat Alexa fluoro 488 (Jackson ImmunoResearch Laboratories, INC.). Cells were resuspended in Accumax (PAA Laboratories Ltd) and nuclei stained with 0.5mM Draq5 label DNA (Biostatus). Analysis was performed using the Imagestream multispectral imaging flow cytometer, configuration of the Imagestream defining cell parameters and collection of data was performed with the Inspire software application, Amnis Ideas software was used for the image analysis (Amnis Corporation, Seattle, WA).

#### 2.2.10 Western blot

Cells were infected with the filamentous influenza A/Udorn/72(H3N2) virus for 8h, 16h and 48h at a MOI=2. Cells were washed, lysed in lysis buffer (1% Triton X 100, 20mM Tris-HCl,

150mM NaCl, 1mM EDTA, 1% anti-proteases cocktail) for 15min on ice. We used a protease inhibitor cocktail compatible with our homemade lysis buffer in order to prevent proteolytic degradation during lysis and sample extraction. This anti-protease inhibitor cocktail was composed of protease inhibitors such as aprotinin, bestatin, E-64, leupeptin and pepstatin A, and stabilized in high-quality dimethyl sulfoxide (Fisher Scientific, UK). The medium containing cells after scrapping the surface of the flask with a scrapper was centrifuged at 10.000rpm for 10min at 4°C. This step enabled to separate the soluble and insoluble fractions of the samples. Soluble cytosolic proteins and membrane proteins which were solubilised by Triton X-100 (Sigma Life Sciences) were found in the soluble fraction, and non-solubilised membranes and nuclear fraction were found in the pellet insoluble fraction. The addition of proteases inhibitor cocktail to the lysis buffer and steps of the procedure performed on ice or at 4°C using pre-cold buffers prevent the degradation of the proteins by proteases. Total protein concentration of samples was determined with the bicinchoninic acid (BCA) protein kit assay (Thermo Scientific™ Pierce, product No. 23227) according to the manufacturer's instructions, absorbance at 562nm was read on Nano Drop and samples were loaded at same concentration. After preparation of the cell lysates, the proteins of the different fractions were separated by SDS-PAGE in an 8% resolving gel (8% acrylamide/bis, 400mM Tris-HCl pH = 8.8, 0.1% SDS, 0.01% APS, TEMED and ddH<sub>2</sub>O) and a 4% stacking gel (8% acrylamide/bis, 100mM Tris-HCl pH = 6.8, 0.1% SDS, 0.01% APS, TEMED and ddH<sub>2</sub>O) to concentrate proteins extracted from samples. Then, lysates were mixed in a loading buffer (50 mM Tris-HCl pH = 6.8, 2% SDS, 10% glycerol, 100 mM dithiothreitol, 0.1% bromophenol blue), boiled for 5min at 95°C to denature proteins and run in a 1X running gel (25 mM Tris-HCl, 200 mM glycine and 0.1% SDS). Electrophoresis was run at 110 V for 1-2h and proteins were transferred from the gel to hybond-P polyvinylidene difluoride (PVDF) membranes. The transfer step performed in a 1X transfer buffer (25 mM Tris-HCl, 192 mM glycine and 10% ethanol) enabled movement of protein samples from resolving gel to PVDF membrane for posterior probing. Blocking in PBST-milk 5% (1X PBS, Tween-20 0.1%; milk 5%) and labelling of both fractions in a dilution 1:500 with the anti-M2 MAb, the anti-myc MAb, the anti-M1 MAb

(clone GA2B, AbD Serotec), the goat anti-H3 PAb (received from Dr Jeremy Rossman, University of Kent, UK) and in a dilution 1:250 with the rabbit anti-caveolin1 PAb (clone N20, sc-894, Santa Cruz Biotechnology) were performed and then followed by the labelling in a dilution 1:1000 with the HRP-conjugated anti-rabbit (SignalChem), the HRP-conjugated anti-mouse (SignalChem) and the HRP-conjugated anti-goat (Abcam) secondary antibodies. Membranes were placed for visualisation into chromogenic solution ECL (GE Healthcare UK) for 5min at RT and then revealed. The protein size was estimated using EZ-run prestained protein ladder (Fisher BioReagents).

#### 2.2.11 Real-Time Polymerase chain reaction (RT-PCR)

A4549 and A549-AnxA6 cells were infected when required with influenza A/Udorn/72(H3N2) at MOI=1 or MOI=5 and RNA was extracted at 1h post-binding, 3 hours, 6 hours and 23/24 hours post-infection by using a GenElute Mammalian Total RNA Miniprep Kit (#RTN70-1KT, Sigma-Aldrich). Briefly, cells were lysed with a 2-mercaptoethanol-containing buffer, vortexed thoroughly until suspension was clear and diluted in equal volume of ethanol 70%. Each lysate-ethanol mixture was loaded for several times through binding columns to isolate RNA from the cell lysate and washing columns to remove impurities. Then, 45 -90  $\mu$ L of isolated and purified RNA were eluted in the flow-through after centrifugation and concentration was measured by spectrophotometry (NanoDrop 2000, Thermo Scientific, UK). RNA was then treated with AMPD1 Amplification Grade DNase I (Sigma-Aldrich, UK) for transformation into cDNA with the High Capacity RNA-to-cDNA Kit (Applied Biosystems), which contains all the reagents needed for reverse transcription (RT) of total RNA to single-stranded cDNA. For RT reaction, cDNA was obtained from a 20  $\mu$ L RT reaction consisting of 10  $\mu$ L of 2 $\times$  RT Buffer, 1  $\mu$ L of 20 $\times$  RT Enzyme Mix and 9  $\mu$ L of RNA sample, according to the supplier's instructions. Then, detection of viral M1 mRNA and mRNA of different chemokines and cytokines was performed by using a SYBR green-based RT-PCR, and total gene expression was normalised against detected levels of 18S mRNA which was used as endogenous control. The PCRs were performed on the StepOnePlus Real-Time PCR system (Applied Biosystems) from a 10

$\mu\text{L}$  reaction mix consisting of 5  $\mu\text{L}$  Power SYBR Green Master Mix 2x, 0.15  $\mu\text{L}$  of 5 $\mu\text{M}$  forward and reverse primers, 3.7  $\mu\text{L}$  of distilled water and 1  $\mu\text{L}$  of cDNA template. The amplification program for the reaction was the following: 40 cycles of 15 seconds at 95°C and 60 seconds at 60°C.

#### 2.2.12 Proteome Profiler – Human Phospho-MAPK Array

Levels of relative phosphorylation of different protein kinases during IAV infection were determined by using the Human Phospho-MAPK Array Kit (#ARY002B Proteome Profiler Array, R&D Systems), according to the manufacturer's instructions. A549 and A549-AnxA6 cells were infected at MOI=10 with influenza A/Udorn/72 (H3N2) when required and lysates were collected at 0.5h, 1h and 4h post-infection. For cell lysate collection, cells were washed twice in PBS, solubilised in Lysis Buffer 6 and resuspended lysates were rocked at 4°C for 30 minutes and centrifuged at 14,000 x g for 5 minutes. Total protein concentration of supernatants was determined with the BCA protein kit assay (Thermo Scientific Pierce, product No. 23227) and spectrophotometric analysis at 562nm (NanoDrop 2000, Thermo Scientific, UK). Nitrocellulose membranes provided by the array kit contained spotted capture and control antibodies in duplicate. Membranes were blocked in Array Buffer 5 for one hour on a rocking platform shaker, which retained the capture and control antibodies in their location. Meanwhile, all samples were adjusted to 300 $\mu\text{g}$  of total protein in up to 400  $\mu\text{L}$  Lysis Buffer 6, topped up to 1.5mL with Array Buffer 1 and incubated with 20  $\mu\text{L}$  of reconstituted Detection Antibody Cocktail for one hour at room temperature. Then, Array Buffer 5 was removed and the prepared sample/antibody mixture was added to all membranes overnight at 4°C on a rocking platform shaker. Membranes were washed three times in 1X Wash Buffer for 10 minutes on a shaker and 2mL of Streptavidin-HRP antibody diluted in Array Buffer 5 according to manufacturer's guidance were added for 30 minutes at room temperature. Membranes were then washed three times in 1X Wash Buffer for 10 minutes on a shaker, embedded in 1 mL of the prepared Chemi Reagent Mix evenly onto each membrane and

prepared for detection of phosphorylation signals. Membranes were exposed to X-ray films for 10-15 minutes and signals were analysed as advised in the Appendix of the array kit.

### 3 RESULTS

The previous study of our group determined that AnxA6 physically interacts with M2 protein and is a restriction factor of IAV, it was found that AnxA6 impairs viral morphogenesis by targeting budding and release late stages of the virus life cycle (Ma et al., 2012). In this study, we aim at understanding the molecular mechanism responsible for restriction of IAV morphogenesis and budding by AnxA6. We hypothesized that AnxA6 interferes with the formation of the IAV budzone by either one or both of the two following mechanisms. Firstly, since Ma et al. demonstrated the physical interaction between AnxA6 and M2 cytoplasmic tail, we suggested that AnxA6 could colocalize with M2 at the neck of budding particles and generate a mechanical restraint on M2 during the scission event. Secondly, we thought that reduction of cholesterol at membranes of the secretory pathway induced by AnxA6 overexpression alters the normal trafficking of viral proteins to the cell surface and interferes with the formation of the budzone. This hypothesis is supported by the latest data published by Musiol et al. showing the important role of cholesterol in IAV infection and by the better understanding of AnxA6 role in cholesterol transport and trafficking inside the cell. In addition, we know that AnxA6 is implicated in the modulation of important cellular pathways required for influenza virus infection such as NF- $\kappa$ B and MAPKs; therefore, we also hypothesized that AnxA6 may regulate a potential innate immune response against IAV. In this study, we have then investigated on the one hand the mechanism underlying AnxA6 interference with IAV budding and on the other hand the regulation of intracellular signalling pathways as well as the induction of pro-inflammatory cytokines and chemokines during IAV infection. Finally, we studied whether IAV down-regulates AnxA6 expression during infection as a mechanism of defence against viral restriction.

### 3.1 Annexin A6 overexpression impairs morphogenesis and release of influenza A virus

#### 3.1.1 Expression levels of AnxA6 in the cell lines used for our study

In our work, we used A431 cells, which do not express AnxA6, and A431 cells stably expressing AnxA6-myc (A431-AnxA6) to study the effect of AnxA6 during IAV morphogenesis. A431 and A431-AnxA6 cell lines provide a good and well established model to investigate the function of AnxA6 in particular cellular mechanisms which could have an impact on IAV infection. A549 cells and A549 cells stably expressing AnxA6-myc (A549-AnxA6) to study a potential immune response regulated by AnxA6 during influenza infection. Therefore, we started our study by confirming levels of AnxA6 in all 4 cell lines by performing a cell fractionation followed by western blotting in A431 and A431-AnxA6 cells, and flow cytometry in A549 and A549-Anx6 cells (figure 3.1).

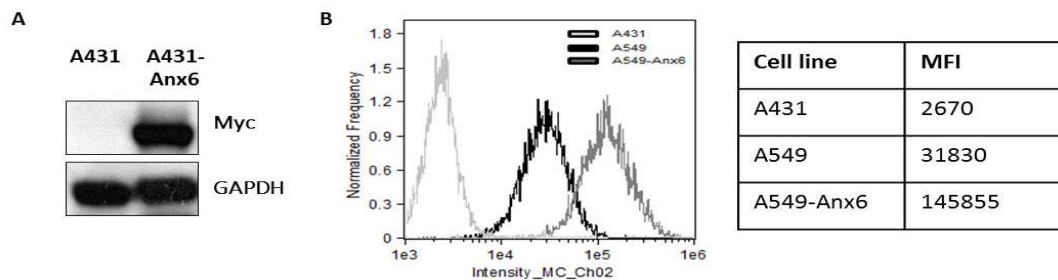


**Figure 3.1 Expression of annexin A6 in A431 and A549 cells.** (A) Expression of AnxA6 in A431 and A549 cells. Cell lysates of A431 and A431 cells expressing a recombinant myc-tagged human AnxA6 (A431-Anx6) were collected and expression levels of AnxA6-myc and GAPDH proteins were determined by Western blotting. (B) Expression of AnxA6 in A549 cells. A431, A549 and A549 cells overexpressing a recombinant myc-tagged human AnxA6 (A549-Anx6) were fixed in 4% paraformaldehyde, permeabilised in 0.05% Triton X-100 for 3 minutes and stained with a mouse anti-AnxA6.

We did not detect any AnxA6 in A431 cells by western blotting, but we detected high levels of AnxA6-myc in A431-AnxA6 cells, showing that our cells exhibit an important difference in AnxA6 expression. After performing a flow cytometry experiment, we compared AnxA6 levels

in A549 and A549-AnxA6. We detected a mean of fluorescence intensity (MFI) of 31830 in A549 cells and of 145855 in A549-Anx6 cells. These results confirm the over-expression of AnxA6 in A549-Anx6 cells compared to A549 cells, being about 5 times higher. Interestingly, we found an MFI of 2670 in A431 cells which correspond to background expression levels as we have already shown that this cell line does not express any AnxA6.

### 3.1.2 Annexin A6 over-expression restricts influenza A virus

In the previous work of our group and another study published later, it was demonstrated that AnxA6 over-expression leads to a reduction in viral titres of different IAV strains. In this study, we have used the filamentous influenza A/Udorn/72 (H3N2) virus and thus we have analysed whether AnxA6 expression also limits viral production of this strain. We have performed a TCID50 after infection with influenza A/Udorn/72 (H3N2) of A431 and A431-AnxA6 cells (figure 3.2).

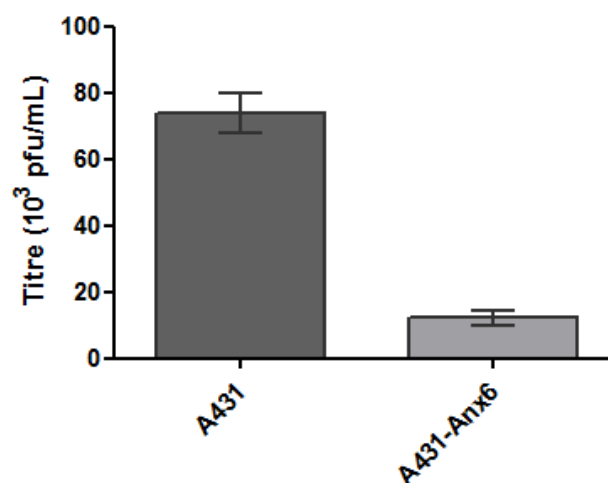


**Figure 3.2. AnxA6 expression leads to a reduction in titres of influenza A/Udorn/72 (H3N2).** A431 and A431-Anx6 cells were infected with influenza A/Udorn/72 (H3N2) virus at an MOI of 0.01, medium of cells was then collected at 72 h p.i., and virus titers were determined by TCID50 on MDCK cells. Data are shown as means + standard deviation from two independent experiments and an unpaired Student's t-test was performed. \*, P<0.05; \*\*, P<0.01; \*\*\*, P<0.001.

Interestingly, we found that human AnxA6 also reduces titers of influenza A/Udorn/72 (H3N2) by about 80%; we have now confirmed that AnxA6 also efficiently restricts influenza A/Udorn/72 (H3N2). However, the effect of AnxA6 expression can vary among IAV strains such as influenza A/WSN/33 (H1N1) or A/HK/1/68 (H3N2) which exhibited differences of about 1 log<sub>10</sub> in titers (Ma et al., 2012). The later study performed by Musiol determined that AnxA6 overexpression resulted in reduced titers, reduced infectivity of viral particles released from infected cells and a reduction in M1 viral protein during infection. It is possible that AnxA6 effect on IAV restriction may differ among strains due to the different selection pressure imposed by the host. In addition, differences in protein sequence and expression may also contribute to differences in virus replication rates and therefore in viral titers.

### 3.1.3 Filamentous influenza A virus particles are readily observed at the surface of infected human epithelial cells

As already mentioned, the filamentous influenza A/Udorn/72 (H3N2) is used in this study to enable distinction between the basis and the elongating bud and to determine whether AnxA6 colocalizes with M2 at the base of budding particles to generate a mechanical restraint on M2 during the scission event. Thus, after confirming differences in AnxA6 expression between cell lines and the reduction of viral titres upon its expression, we performed scanning electron microscopy (SEM) and immunofluorescence assay (IFA) to confirm the production of filamentous IAV from infected human epithelial A431 and A431-AnxA6 cells and their visualisation for convenient observation of budding events at the plasma membrane and distinction between the basis and the elongating bud (figure 3.3).

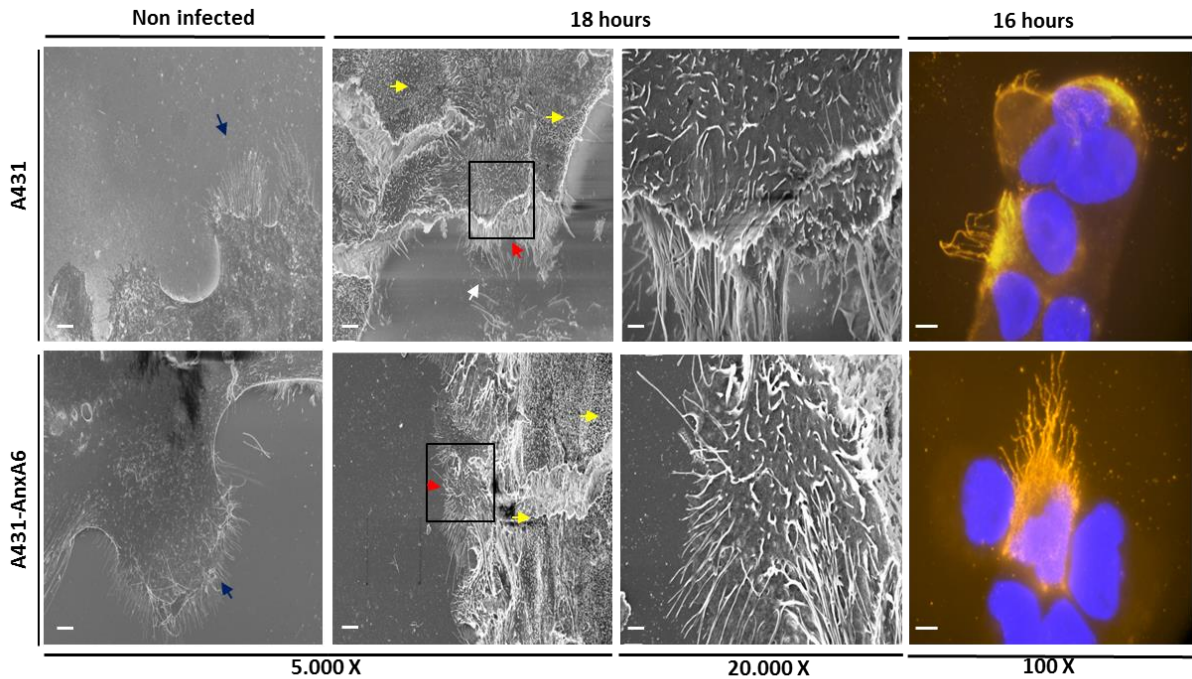


**Figure 3.3. SEM and IFA enable observation of budding of filamentous virions from infected A431 and A431-AnxA6 cells.** (A) 431 (upper panels) and A431-AnxA6 (lower panels) cells were infected with influenza A/Udorn/72(H3N2) for 18h at a MOI=1, fixed first in 2.5% glutaraldehyde for 2 hours and then with 1% osmium tetroxide for 1h at 4°C, critical point dried (K850 Critical Point Dryer) and platinum coated (Sputter Coating; 1kV, 5mA, 30sec). Samples were observed on Zeiss Supra 35VP FEG (field emission gun) scanning electron microscope. Non infected controls are shown on the left panels (blue arrows: filopodia). Filamentous virions bud from the plasma membrane of cells infected for 18 hours (red arrows). Free filaments were observed outside cells in infected samples (white arrows). At 18 hours post-infection, more cells were observed with large budding platforms resulting in the granular aspect of the plasma membrane (yellow arrows) and thicker clusters of filaments. Regions of interest showing budding events are delimited by black frames and shown at higher magnification on the right panels. Scale bars, 10  $\mu\text{m}$  in left and middle panels and 1  $\mu\text{m}$  in right panels. (B) 431 (upper panels) and A431-AnxA6 (lower panels) cells were infected with A/Udorn/72(H3N2) for 16 hours at a MOI=2, fixed in 4% paraformaldehyde and labelled for the staining of nuclei (blue) and H3 (orange) for observation by immunofluorescence microscopy. Virus budding is shown in orange after H3 staining and nuclei are stained in blue. Scale bars, 10  $\mu\text{m}$ .

Indeed, filamentous viral particles were observed budding from the plasma membrane of cells infected for 16 hours and 18 hours, as well free filaments were observed outside the cells. These techniques enabled the visualisation of filamentous IAV budding events in human epithelial cells and confirmed that cells and the viral strain used in this experiment are suitable for our investigations.

#### 3.1.4 Patterns of expression of viral H3 and M2 proteins and cellular human annexin A6 protein

We then performed an immunofluorescence experiment to determine patterns of expression of H3, M2 and AnxA6, in A431 and A431-AnxA6 cells (figure 3.4). As expected, we found that all 3 proteins exhibit a same pattern of expression in the different cell lines. First, H3 staining enabled the visualisation of budding events of filamentous viruses and areas where virus budding occurs are shown with an enrichment of H3 staining in a polarised area of the cell surface. A431 and A431-AnxA6 cells exhibited long viral filaments budding from the cell surface and virions can be observed all around the cells. Also, M2 cellular distribution was very similar in all cell lines as it was mainly found enriched at the plasma membrane. These results are in agreement with previous studies and confirm that both H3 and M2 viral proteins are found during late infection at the cell surface of influenza infected cells as they play an important role in late stages of viral infection such as assembly and budding. Finally, the cellular human AnxA6 was found exhibiting a punctate pattern in the nucleus but mostly in the cytoplasm A431-AnxA6 cells, which is in agreement with previous studies. As previously shown, no AnxA6 could be detected in A431 cells.

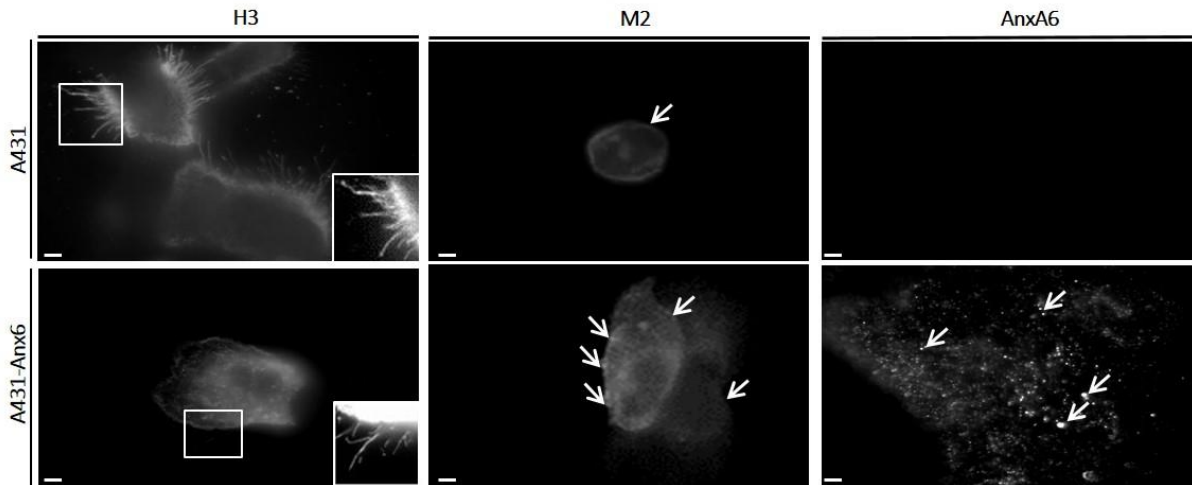


**Figure 3.4. Observation of subcellular localisation of viral H3 and M2 proteins and cellular AnxA6 protein in infected cells by immunofluorescence assay.** A431 (upper panels) and A431-AnxA6 (lower panels) cells were infected with A/Udorn/72(H3N2) for 16 hours at a MOI=2, fixed in 4% paraformaldehyde and labelled for the staining of H3 (left panels), M2 (middle panels) and AnxA6-myc (right panels). Regions of interest showing budding events of filamentous viruses are delimited by white frames on H3 panels and magnified on the right bottom in the panel, white arrows on the M2 and AnxA6 panels show the localisation of M2 at the plasma membrane and that AnxA6 is mainly found in the cell cytoplasm. Scale bars, 10  $\mu$ m.

### 3.1.5 AnxA6 is not enriched together with M2 at the plasma membrane where viral particles bud

As mentioned above, our group has shown that the human AnxA6 interacts with the IAV M2 cytoplasmic tail and one role of M2 in scission of viral particles has been later explained by its location to the basis of budding virions (Ma et al., 2012, Rossman et al., 2010). To verify our first hypothesis, which is that AnxA6 could affect the formation of the viral budding zone by generating a mechanical restraint on M2 during the scission event, we studied the subcellular localisation of viral and cellular proteins by immunostaining and whether AnxA6 colocalizes with M2 at the basis of viral particles budding from the surface of infected cells. We first performed an immunofluorescence experiment to check whether we could detect M2 at the neck of viral filaments (figure 3.5).

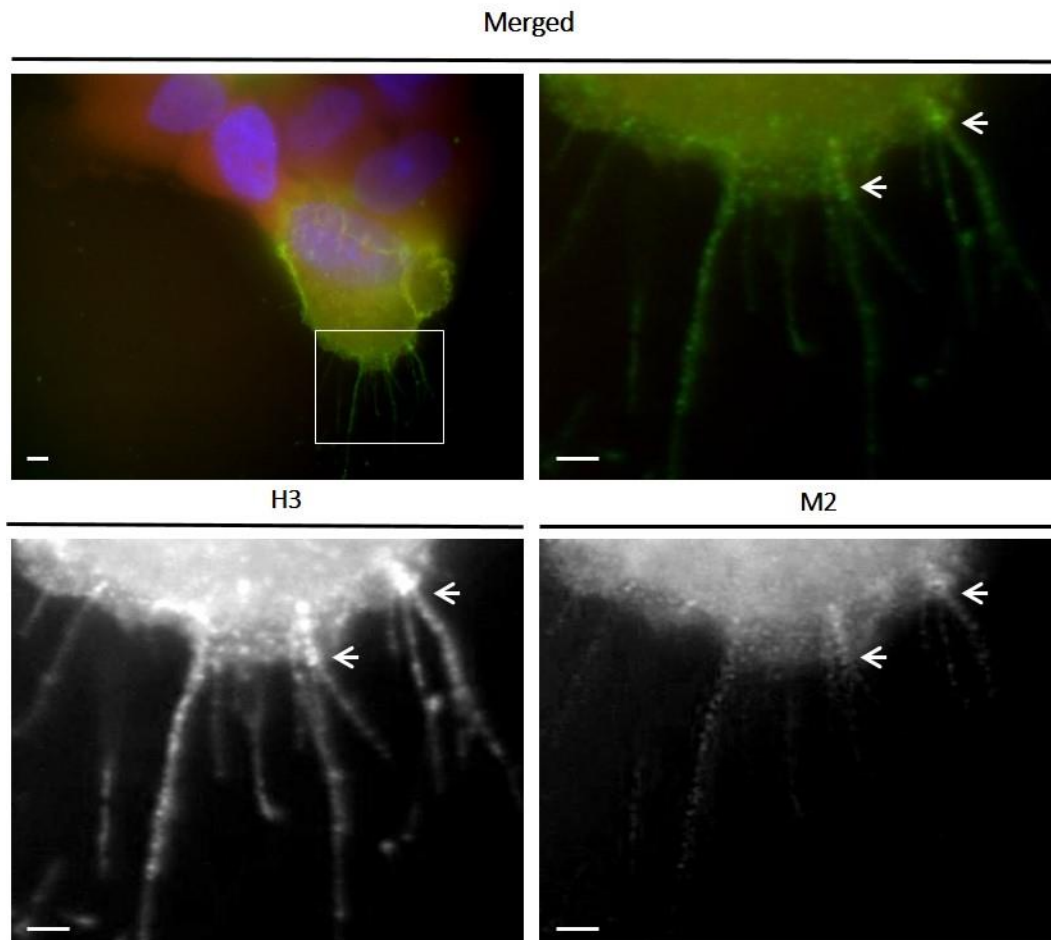


**Figure 3.5. M2 was observed at the basis of budding filamentous particles.** A431-AnxA6 (lower panel) cells were infected with A/Udorn/72(H3N2) for 16 hours at a MOI=2, fixed in 4% paraformaldehyde and labelled for the staining of nuclei (blue), H3 (green) and M2 (red). H3 staining enabled visualisation of filamentous viral particles budding from plasma membrane and M2 was observed at the basis of the elongated virions. White arrows show the basis of filaments where both H3 and M2 were found. Merged cropped picture is shown in the top right panel and individual staining of H3 and M2 proteins is shown in bottom panels. Scale bars, 10  $\mu\text{m}$  top left panel and 5  $\mu\text{m}$  top right and bottom panels.

Indeed, staining of M2 and H3 enabled the visualisation of M2 at the basis of elongating filaments budding from infected cells. These findings are in agreement with the study published by Rossman which showed that M2 was located at the neck of budding particles and induced membrane curvature. They also found that M2 was mainly located in budding sites and contributed in scission and release of virions (Rossman et al., 2010).

We then analysed the subcellular localisation of M2 and AnxA6 to check whether they colocalised at the basis of viral filaments (figure 3.6). Again, for both A431 and A431-AnxA6 cells, M2 was mainly found at the plasma membrane as expected at late stages of the virus life cycle and no differences were observed. Also, staining of H3 enabled the visualisation of viral filaments and was also mainly expressed at the surface of infected cells. For infected A431-AnxA6, no change in both M2 and H3 staining patterns could be observed compared to that of A431 cells with this technique. Finally, AnxA6 exhibited a cytosolic distribution in the cell and no recruitment of AnxA6 to the plasma membrane of infected A431-AnxA6 cells where M2 was localised could be observed.

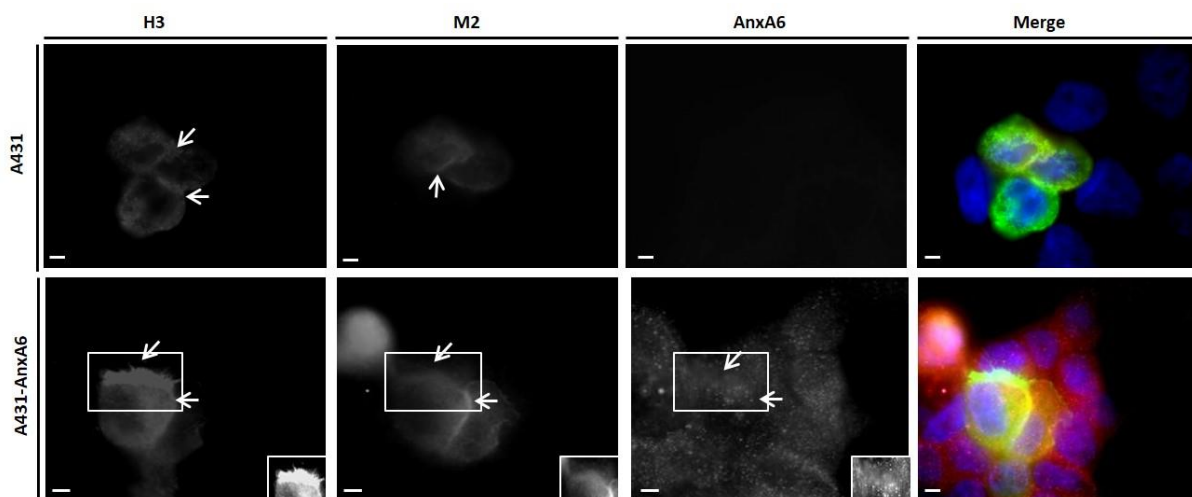


**Figure 3.6. AnxA6 is not enriched together with M2 at the plasma membrane where viral particles bud.** A431 (upper panels) and A431-AnxA6 (lower panel) cells were infected with A/Udorn/72(H3N2) for 16 hours at a MOI=2, fixed in 4% paraformaldehyde and labelled for the staining of nuclei (blue), H3 (green), M2 (orange-red) and AnxA6-myc (far red). Merged images are shown in right panels. White arrows on the M2 and myc panels of A431-AnxA6 cells show the localisation where M2 viral protein is enriched inside the cell and that AnxA6 is not found together with M2. The area where budding of viral filaments takes place is shown with an enrichment of H3 staining in a polarised area of the cell surface. Scale bars, 10  $\mu$ m.

In addition, AnxA6 was not found present in regions of H3 enrichment at the cell surface. Magnified regions of interest show that no enrichment of M2 and AnxA6 was observed where viral filaments bud from the surface of A431-AnxA6 infected cells. From these results, we

conclude that AnxA6 is not enriched at the basis of budding particles and generate a mechanical restraint on M2 during the scission event. These results are partly in disagreement with the data previously published by our group, which demonstrated that M2 and AnxA6 physically interact and are located together near the cell surface of IAV infected cells (Ma et al., 2012).

### 3.1.6 M2 and annexin A6 could colocalize in intracellular vesicular-like compartments.

In addition, the subcellular localisation of H3, M2 and AnxA6 inside infected cells was analysed by immunofluorescence and we studied whether AnxA6 could be found with H3 and M2 viral proteins in same intracellular regions or at the cell periphery. Firstly, we analysed the localisation of H3, M2 and AnxA6 inside the cell and we investigated whether AnxA6 could be found with H3 and M2 viral proteins in same intracellular compartments (figure 3.7).

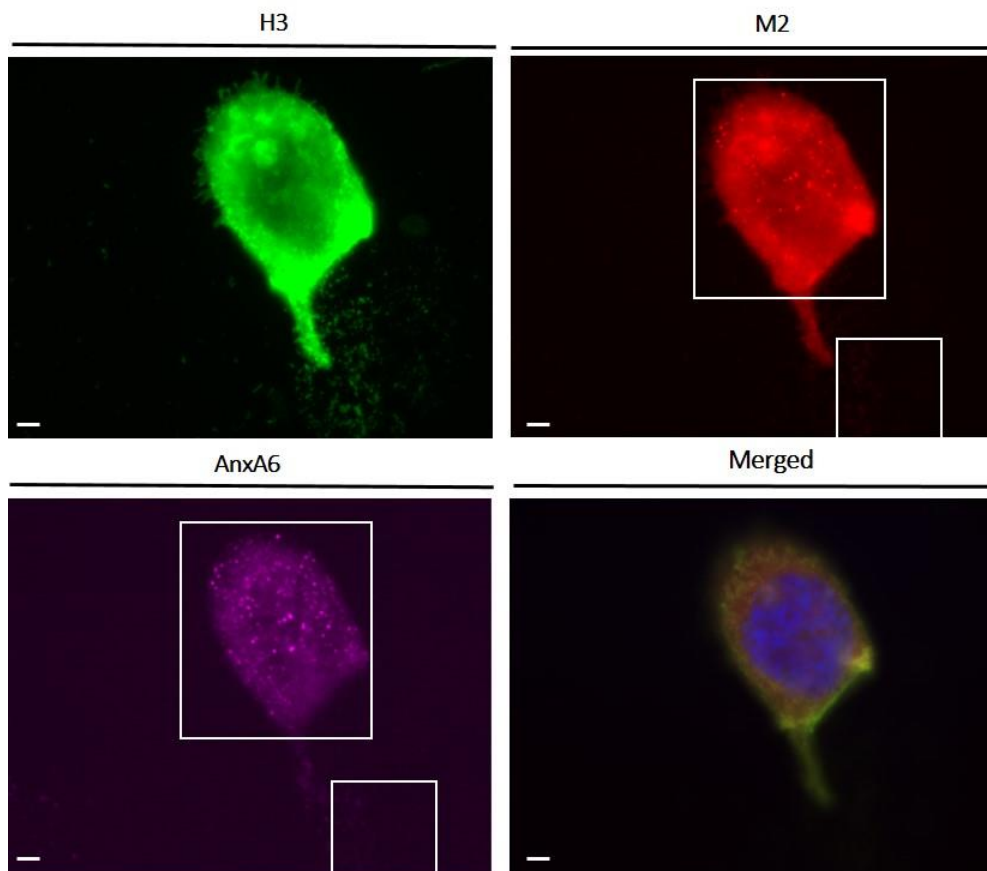


**Figure 3.7. Analysis of annexin A6 subcellular localisation in infected cells.** A431-AnxA6 cells were infected with A/Udorn/72(H3N2) for 16 hours at a MOI=2, fixed in 4% paraformaldehyde and labelled for the staining of nuclei (blue), H3 (green), M2 (red) and AnxA6 (purple). Regions of interest are shown in white frames. Lower protein signals from either released virions or from surrounding cells are also shown in white frames in M2 and AnxA6 panels, which are also shown in figure 3.8. Scale bars, 10  $\mu$ m.

Interestingly, H3 and M2 viral proteins were found in the cytoplasm and enriched in specific intracellular compartments. Also, as already mentioned they were found again at the cell surface where viral particles bud and in released viral particles. AnxA6 was found enriched in intracellular areas which could correlate with regions of M2 but not of H3 presence. Therefore, we analysed in further detail the localisation of both M2 and AnxA6 in the regions of interest from the previous figure (figure 3.8, upper panels). Interestingly, we observed that that M2 and AnxA6 were expressed very similarly and could be found together in some cellular regions in infected cells. We observed that both M2 and AnxA6 proteins exhibit a punctate pattern and we believe they could be found inside vesicular-like compartments. Then, as M2 plays an important role in late stages of viral infection and travels to the cell surface to fulfil its roles, we investigated whether AnxA6 and M2 viral protein could be found together at the cell periphery during apical transport (figure 3.8, lower panels). We detected a low presence of AnxA6 at the cell periphery but in some areas AnxA6 and M2 proteins could be found together; however, H3 viral protein was absent in these areas of possible colocalization. Altogether, our investigation revealed that M2 and AnxA6 exhibited a very similar expression pattern and could colocalize in some cellular regions in infected cells but not where the viral particles bud. These results are in agreement with the study published by Ma, as it was found that M2 and AnxA6 were exhibiting a punctate pattern and colocalised in proximity to the plasma membrane of IAV infected cells (Ma et al., 2012). It is now well known that influenza hijacks the cellular machinery to its own benefit and uses vesicular traffic to transport viral components to site of budding. We therefore suggest that AnxA6 is found in M2-enriched vesicular

structures travelling to the cell surface and interacts with M2 to interfere with the formation of the budzone and the M2-dependent last stages of viral infection.

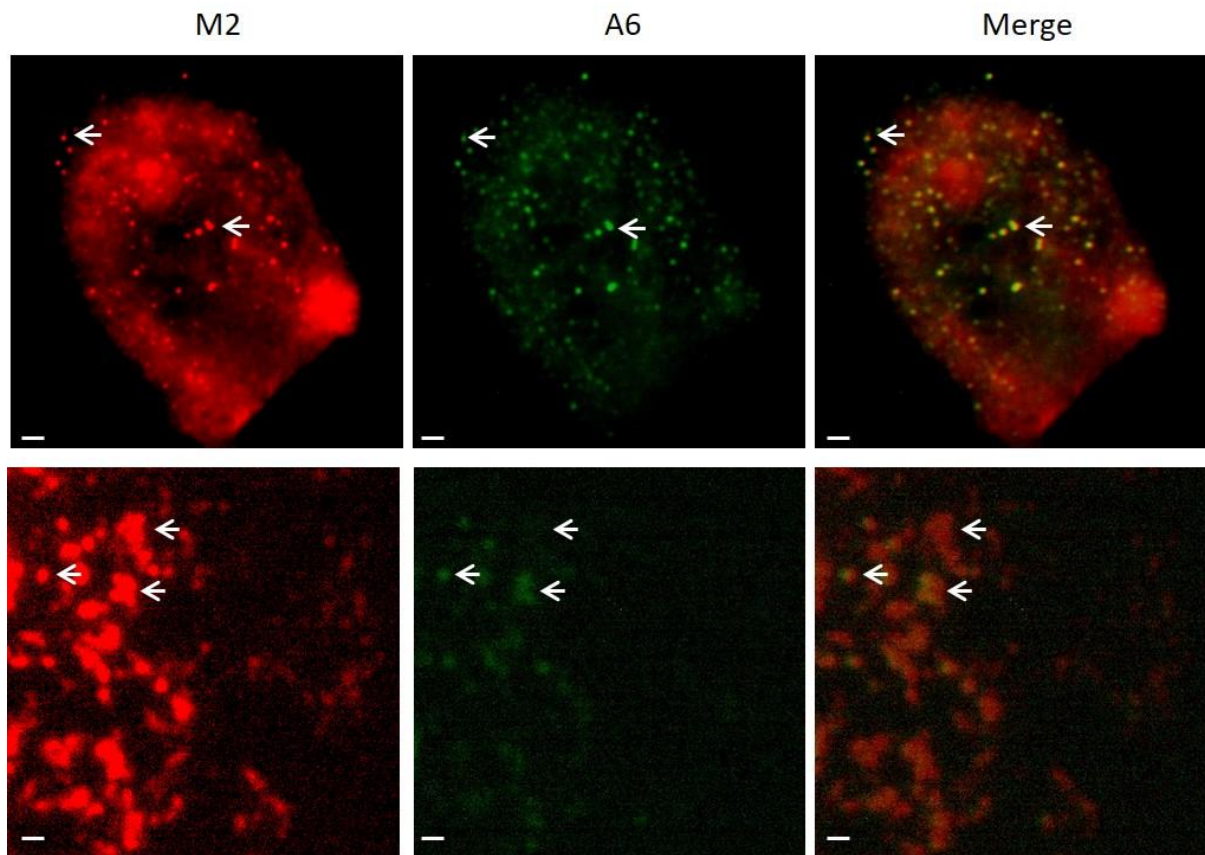


**Figure 3.8. M2 and annexin A6 colocalised in vesicular-like compartments.** A431-AnxA6 cells were infected with A/Udorn/72(H3N2) for 16 hours at a MOI=2, fixed in 4% paraformaldehyde and labelled for the staining of M2 (red) and AnxA6-myc (green). White arrows show regions of M2 and AnxA6 colocalisation in vesicular-like compartments in upper panels and at the cell periphery in lower panels (yellow). Scale bars, 20  $\mu\text{m}$  upper panels and 50  $\mu\text{m}$  bottom panels.

### 3.1.7 AnxA6 expression does not alter the subcellular localisation of M1 during viral infection

As subcellular localisation of H3, M2 and AnxA6 was observed and that enrichment or colocalisation of M2 at the plasma membrane where budding of viral particles occur could not be confirmed, we investigated whether AnxA6 expression alters the subcellular localisation of M1 during infection. It is very well known that M1 is an essential protein responsible for

stabilising all the necessary components required for assembly and budding of newly formed virions, among them viral and cellular proteins but also lipids enriched in rafts. To verify this hypothesis, we performed an immunofluorescence assay and staining of M1 in A431 cells and cells expressing AnxA6 for different times of infection was analysed (figure 3.9).

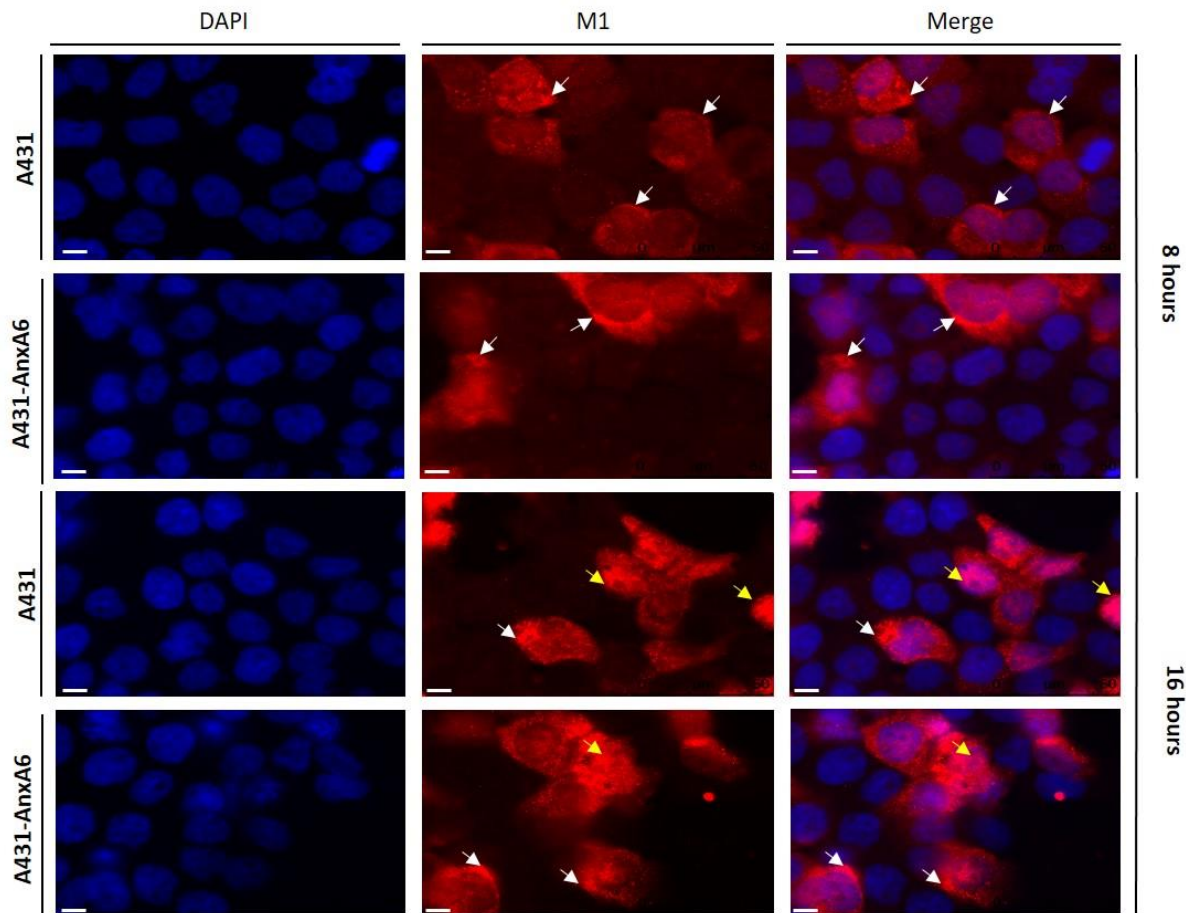


**Figure 3.9. Subcellular localisation of viral M1 protein in infected cells is not altered by AnxA6 expression.** A431 (upper panels) and A431-AnxA6 (lower panel) cells were infected with A/Udorn/72(H3N2) for 8 hours and 16 hours at a MOI=2, fixed in 4% paraformaldehyde and labelled for the staining of nuclei (blue) and M1 (red). Merged images are shown in right panels. White arrows show enrichment of M1 in the perinuclear or membrane regions of infected cells. Yellow arrows indicate nuclear localisation of M1 at 16 hours post-infection. Scale bars, 10  $\mu$ m.

At 8 hours post-infection, we found M1 mainly in the cytoplasm, occasionally in the perinuclear region, and also at the cell surface in both A431 and A431-AnxA6. At 16 hours post-infection, M1 was also similarly in the cytoplasm and at the cell surface, but also inside the nucleus in

both cell lines. We conclude that AnxA6 over-expression does not alter the subcellular localisation of M1 during viral infection as we could not see major changes in M1 expression between cells expressing or not AnxA6.

### 3.1.8 Protein composition of released viral particles

After analysing the subcellular localisation of AnxA6 and viral proteins inside influenza infected cells, we investigated whether over-expression of AnxA6 could lead to changes in protein composition of viral particles released from infected cells. To verify this hypothesis, we performed an immunofluorescence assay on infected A431-AnxA6 cells and also a western blot on purified viral particles released from A431 and A431-AnxA6 cells (figure 3.10). Analysis of viral particles by immunofluorescence determined that both H3 and M2 are present in the entire elongated filaments; however, M2 could be occasionally observed enriched at the basis of virus particles. Surprisingly, no AnxA6 was detected in any virion, which is in agreement with results obtained by western blotting as no AnxA6 could be detected neither by this technique, suggesting that AnxA6 is not a cellular protein incorporated in newly formed virions during assembly and budding (figure 3.10). Also, no M2 protein was detected and similar levels of H3 and M1 expression were obtained in viral particles purified from both A431 and A431-AnxA6 cells. Finally, an accumulation of NP protein in viral particles purified from A431 cells at 48h post-infection was observed when compared to NP protein expression in viral particles purified from A431-AnxA6 cells (figure 3.10). From these experiments, we conclude that AnxA6 is not present in viral particles produced from A431-AnxA6 infected cells and that AnxA6 expression could lead to an imbalance of viral proteins and to a reduction of NP protein incorporation into virions of A431-Anx6 cells. However, this experiment should be repeated to confirm our findings, as only one experiment was successfully performed for detection of viral proteins produced in both cell lines.

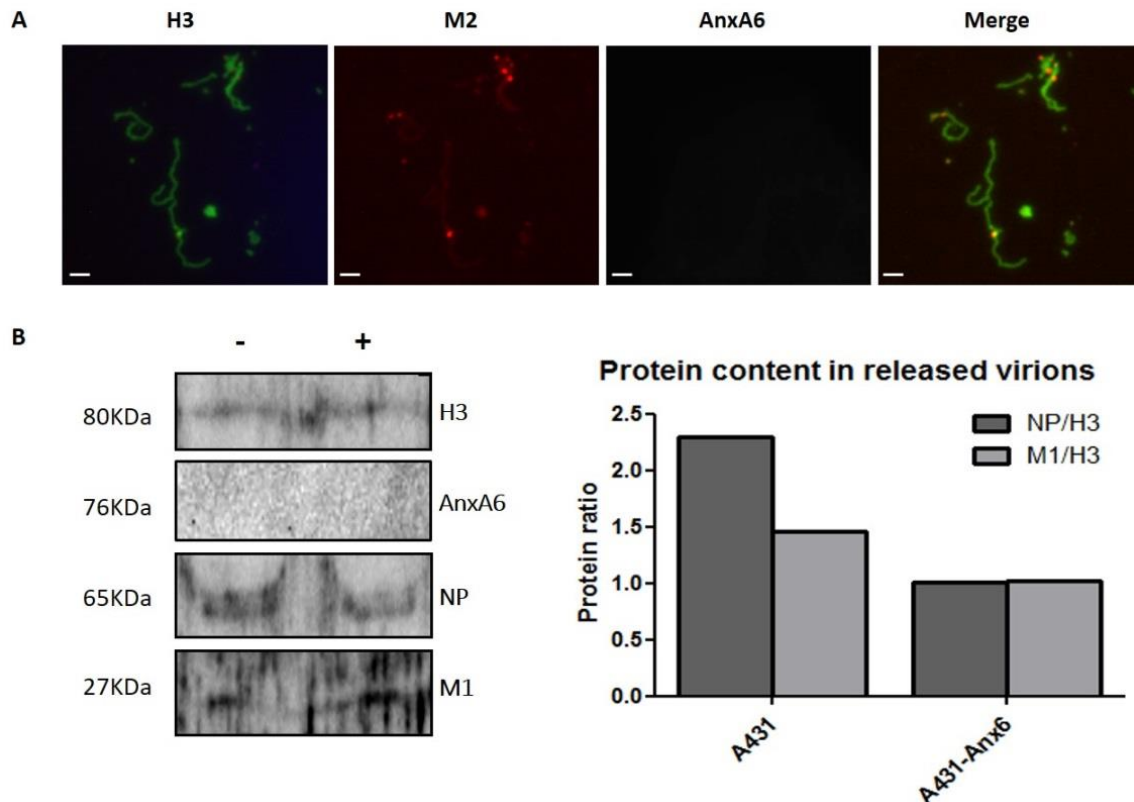


**Figure 3.10. Annexin A6 is not detected in released viral particles.** (A) A431-AnxA6 cells were infected with A/Udorn/72(H3N2) for 16 hours at a MOI=2, fixed in 4% paraformaldehyde and labelled for the staining of H3 (green), M2 (red) and AnxA6 (purple). Only H3 and M2 proteins were detected in released viral particles from the surface of infected cells. Scale bars, 10  $\mu$ m. (B) A431 (-) and A431-AnxA6 (+) cells were infected with influenza A/Udorn/72 (H3N2) virus at an MOI of 0.01, medium of cells was then collected at 48 h p.i., and viral particles were purified by ultracentrifuge. Expression of viral proteins and cellular AnxA6 in virions released from infected A431 and A431-AnxA6 cells were determined by Western blotting. Quantification by densitometry analysis of viral proteins expression for the blot represented enabled calculation of protein ratios in virus particles produced in A431 and A431-AnxA6 cells.

### 3.1.9 Annexin A6 over-expression leads to M2 down-regulation and a defect in expression of viral proteins at the cell surface

As we could not confirm colocalisation of M2 and AnxA6 at the plasma membrane and clarify whether AnxA6 causes a mechanical restraint to virion scission events, we tested our second hypothesis which is that AnxA6 overexpression could affect the trafficking of viral proteins to

site of budding. Enrich and collaborators demonstrated that AnxA6 overexpression induces a retention of cholesterol in endosomes and as a consequence a reduction at membranes of the secretory pathway and at the plasma membrane, which have an important role in IAV infection and trafficking of HA and NA (Enrich et al., 2011, Veit and Thaa, 2011). In addition, these findings are supported by another study showing that AnxA6 has a critical role in the late endosomal cholesterol balance and affects IAV replication and propagation in AnxA6-overexpressing cells. In this study, the authors linked AnxA6 to the imbalance of intracellular cholesterol homeostasis and defective IAV infection (Musiol et al., 2013). Therefore, we thought that AnxA6 overexpression affects the formation of the budding zone, potentially by altering the trafficking of viral proteins to site of budding through regulation of intracellular cholesterol inside the infected cells. To test this hypothesis, we analysed total and surface expression of M2 and the rest of viral proteins (IAV) in A431 and A431-AnxA6 infected cells by flow cytometry (figures 3.11, 3.12 and 3.13). Permeabilisation (P) of cells enabled to measure the total expression of viral proteins whereas the expression at the surface was determined in non permeabilised (NP) cells. As shown in figure 3.11, AnxA6 expression leads to a defect of M2 and viral proteins detected with the polyclonal goat anti-H3N2 (A/Udorn/72) antibody at the surface of infected cells. Total viral protein (IAV) expression levels are similar in A431 and A431-AnxA6 since no significant difference is observed between the mean of fluorescence intensity (MFI) of A431 (20510) and A431-AnxA6 (25675) cells. Nevertheless, MFIs for non permeabilised A431 (26665) and A431-AnxA6 (14475) cells and the shift in surface expression of IAV proteins between A431 and A431-AnxA6 cells determine that expression of all viral proteins detected with the goat anti-H3N2 antibody is reduced at the surface of AnxA6 expressing cells. For M2, total and surface expression is reduced in A431-AnxA6 cells compared to A431 cells; total MFIs of permeabilised A431 (29740) and A431-AnxA6 cells (10970) together with surface MFIs of non permeabilised A431 (14335) and A431-AnxA6 cells (5035) show a very clear reduction of M2 expression. MFIs together with the shift in total and surface expression of M2 between both cell types show that AnxA6 leads to a reduction in total and surface expression of M2 in infected cells.

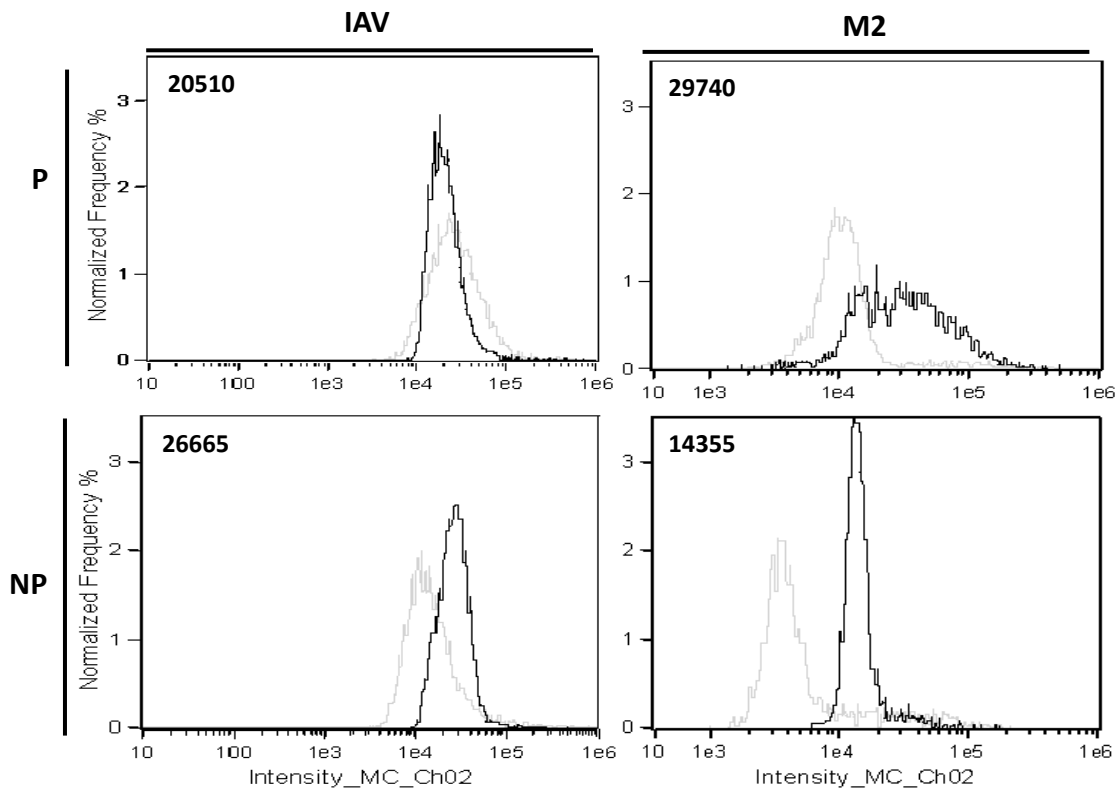


**Figure 3.11. Study of the trafficking of viral proteins to the cell surface by flow cytometry.** A431 and A431-AnxA6 cells were infected with the A/Udorn/72(H3N2) strain for 8 hours at a MOI=3, fixed, permeabilised (P) or not (NP) with Triton-X100 and stained with a polyclonal antibody against influenza A/Udorn/72(H3N2) (IAV) and M2. Histograms show the normalised frequency and the intensity of fluorescence for both viral proteins in the different cell lines. Total and surface mean of fluorescence intensity (MFI) corresponding to expression of viral proteins in both permeabilised and non permeabilised cells are indicated for each cell line. A431 cells are shown in black, A431-AnxA6 cells are shown in light grey. The means of fluorescence intensity presented in this figure are the most representative of 3 independent experiments.

In addition, we found a reduction of 36% in total M2 expression and of 35% in M2 surface expression in A431-AnxA6 cells when compared to A431 cells. Therefore, we believe that due to similar reduction levels observed for total and surface M2 expression, the reduced surface expression could be linked to reduced total expression. These results suggest that AnxA6 down-regulates total expression of M2, and as a consequence, expression of M2 and viral proteins detected with the polyclonal goat anti-H3N2 (A/Udorn/72) antibody is impaired at the surface of infected cells. These data are in disagreement with the study previously published

by our group, in this study no significant changes in M2 expression at the cell surface of infected cells after infectious cycle were observed when A431 cells overexpress AnxA6 (Ma et al., 2012). Representative images of cells sorted during this experiment enabled to show patterns of protein expression in both cell lines (figures 3.12 and 3.13).

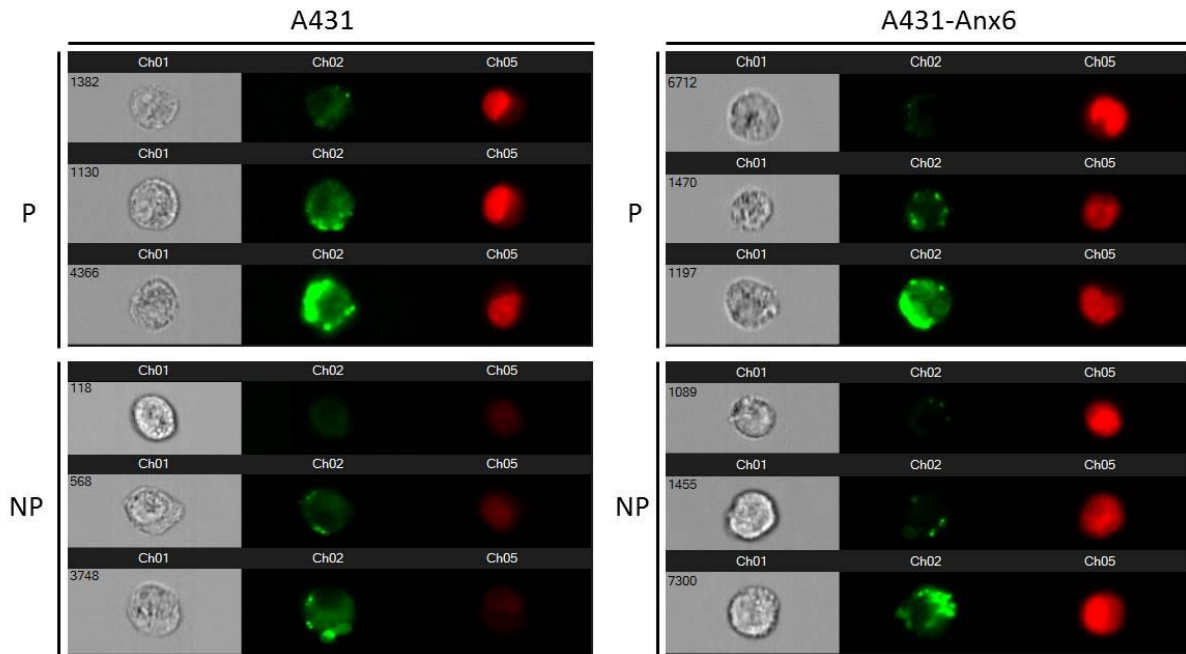


**Figure 3.12. Trafficking of viral proteins to the cell surface by imaging flow cytometry.** A431 and A431-AnxA6 cells were infected with the A/Udorn/72(H3N2) strain for 8 hours at a MOI=3, fixed, permeabilised (P) or not (NP) with Triton-X100 and stained with a polyclonal antibody against the entire virus for the detection of all viral proteins (IAV) and with DraQ5 for the detection of DNA. IAV proteins are shown in green and nuclei in red. Representative images of cells exhibiting negative, low or high levels of protein expression are shown for permeabilised and non permeabilised cells of each cell line.

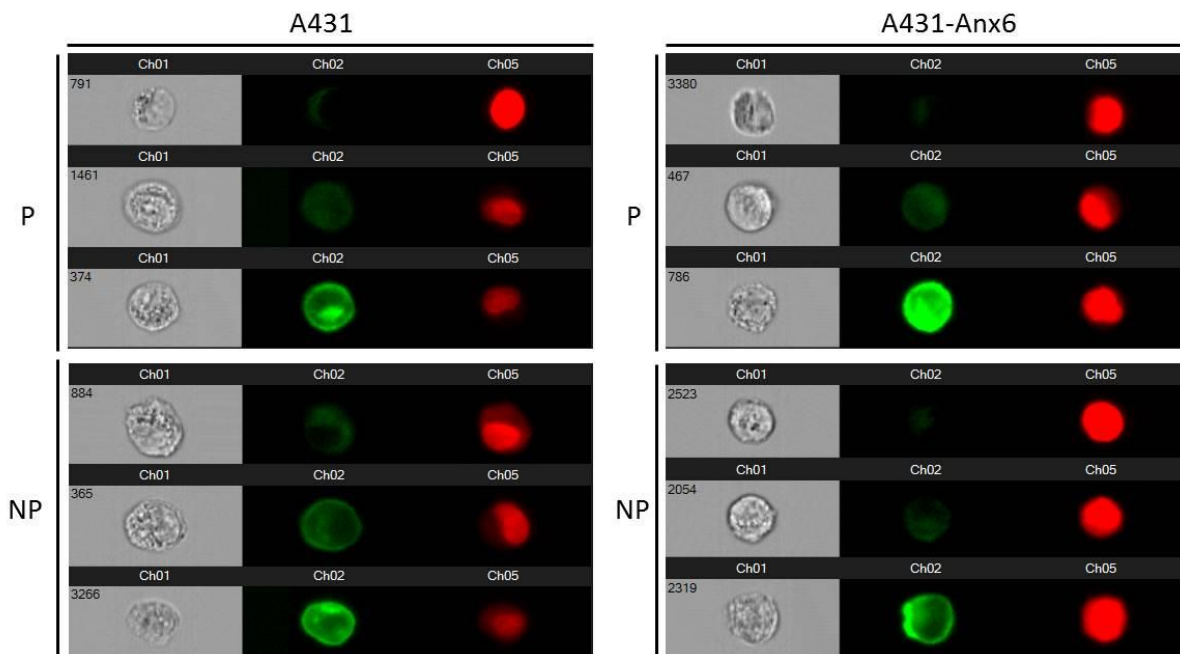


**Figure 3.13. Trafficking of M2 viral protein to the cell surface by imaging flow cytometry.** A431 and A431-AnxA6 cells were infected with the A/Udorn/72(H3N2) strain for 8 hours at a MOI=3, fixed, permeabilised (P) or not (NP) with Triton-X100 and stained with a monoclonal antibody for the detection of M2 viral proteins and Draq5 for the detection of DNA. M2 viral protein is shown in green and nuclei in red. Representative images of cells exhibiting negative, low or high levels of protein expression are shown for permeabilised and non permeabilised cells of each cell line.

### 3.1.10 Alteration of normal expression and subcellular compartmentalisation of viral proteins by annexin A6

Also, we hypothesised that AnxA6 could alter the subcellular localisation of viral proteins during infection and we performed a cellular fractionation followed by western blot on Triton-X100-lysed cells to study changes in expression of viral proteins in different cellular fractions (figure 3.14). Expression levels of viral (H3, NP, M1 and M2) and cellular (AnxA6 and GAPDH) proteins were determined by Western blotting (Figure 3.14). Clearly, AnxA6 overexpression leads to a reduction in expression of M2 at 18 hours post-infection and at 8h p.i in the soluble fraction of A431-AnxA6 cells compared to A431 cells. Also, no M2 protein expression was detected at 5h p.i. This result showing a down-regulation of M2 protein was consistent in several independent experiments (figures 3.14A and 3.14B).

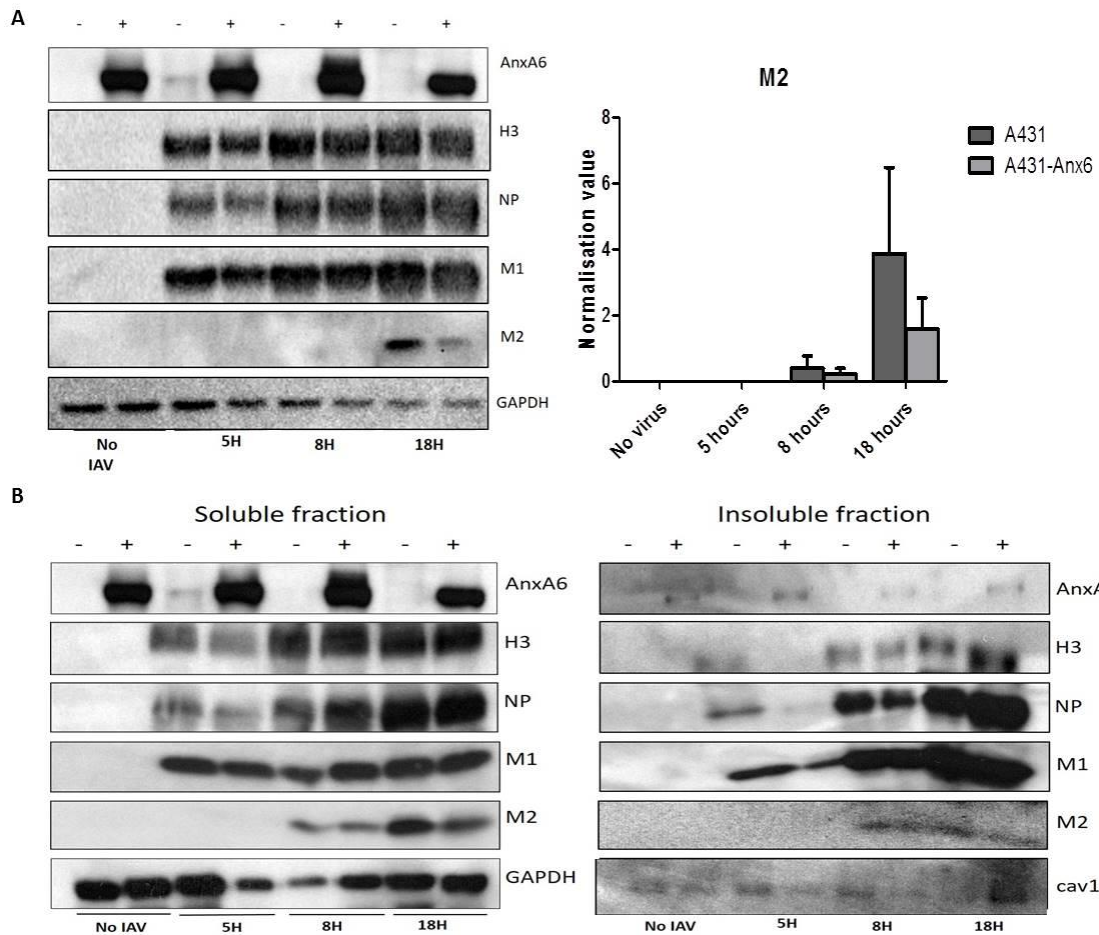


**Figure 3.14. Expression of AnxA6 leads to changes in detection of viral proteins in detergent soluble and insoluble fractions of IAV infected cells.** A431(-) and A431-AnxA6 (+) cells were infected or not with the filamentous influenza A/Udorn/72(H3N2) virus at MOI=3 and lysed in 1% Triton-X100 containing buffer at 5h, 8h and 18h post-infection. Cell lysates were collected and centrifuged for separation of soluble and insoluble fractions. Soluble fractions contain the cell cytosol and insoluble fractions consist of nucleus, detergent resistant membranes/lipid rafts and actin cytoskeleton. (A) Only the soluble fraction is represented for this experiment, the insoluble fraction is not shown but exhibited a similar pattern for expression all viral proteins. Then, M2 protein levels were quantified by densitometry analysis and normalised against GAPDH. Data are shown as means + standard deviation from three independent experiments and an unpaired Student's t-test was performed. \*,  $P < 0.05$ ; \*\*,  $P < 0.01$ ; \*\*\*,  $P < 0.001$ . (B) Both soluble and insoluble fractions are shown for this experiment.

No significant differences in expression of H3, NP and M1 viral proteins with overexpression of AnxA6 could be observed in the experiment shown in figure 3.14A; however, densitometry

analysis of viral proteins expression normalised against cellular GAPDH protein expression for the experiment represented in figure 3.14B revealed some changes in protein levels during infection upon AnxA6 overexpression. Interestingly, cells expressing AnxA6 exhibited an increased expression of all H3, NP and M1 viral proteins at 5h p.i., no M2 protein was detected at this time of infection. Also, less H3 but more NP and more M1 were detected at 8h p.i. in the soluble fraction of cells expressing AnxA6; M2 was again not detected. Interestingly, cells expressing AnxA6 exhibit more H3, NP and M1 but less M2 in their soluble fractions at 18h post-infection, which could be explained by a retention of viral proteins being released from the surface of infected cells. The separation of soluble and insoluble fractions was performed through centrifugation, and detection of GAPDH and caveolin 1 marker proteins was used to identify separated fractions. It is well known that GAPDH is a soluble protein present in the soluble fraction and will not be present in the insoluble fraction; conversely, caveolin 1 is present in detergent resistant rafts microdomains in the insoluble fraction but not in the soluble fraction, which is in agreement with previous studies. Overall, these results suggest that AnxA6 expression alters expression of viral proteins in IAV infected cells. Also, reduced detection of M2 and other viral proteins at 8h post-infection in cells expressing AnxA6 is in agreement with results obtained by flow cytometry on non permeabilised cells at 8h post-infection. Overall, our findings suggest that Annexin A6 overexpression leads to a down-regulation of M2 viral protein, which could subsequently affect expression of M2 and other viral proteins at the cell surface, which is observed by flow cytometry and western blot at 8h post-infection after a first cycle of viral replication. AnxA6 then restricts budding and release of progeny viruses as shown earlier by 2 independent studies, resulting in an accumulation of viral proteins in the cell at later time points, observed by western blot at 18h post-infection.

### 3.1.11 Identification of pathway targeting degradation of M2

Since we demonstrated that AnxA6 down-regulates M2 protein expression as a mechanism of restriction against IAV, we investigated which pathway is targeted by AnxA6 to accomplish its degradation. It has been described that AnxA6 participates in degradation of proteins

through the regulation of proteasome, also called the '26S proteasome' (Guo and Peng, 2013). The proteasome is a multisubunit enzymatic complex, composed of a 20S main protease and of one or two 19S subunits which are responsible for substrate specificity and degradation of targeted proteins into peptides. It is responsible for degradation of cellular components in the cytoplasm and nucleus. It can degrade from small signalling or inhibitory molecules to cell cycle regulators, transcription factors, but also proteins that control cell progression, differentiation, survival or apoptosis. Proteins targeted for degradation by the proteasome are ubiquitinated, or conjugated with an ubiquitin residue, and then recognised for hydrolysis (Guo and Peng, 2013, Adams, 2003). In this study, we used the peptide-aldehyde proteasome inhibitor MG132 (carbobenzoxyl-L-leucyl-L-leucyl-L-leucinal) which binds to active sites of the 20S enzymatic subunits to specifically block the proteolytic activity of the 26S proteasome complex without altering activity of any other cellular components (Guo and Peng, 2013). In addition, it is known that AnxA6 plays an important role in the regulation of endocytic and exocytic pathways, but more importantly regulates the endolysosomal pathway as it participates in the transport of cholesterol, lipids and proteins from late endosomes to lysosomes for degradation (Cubells et al., 2007). Inhibition of the endosome-lysosome compartment acidification is possible with ammonium chloride (NH<sub>4</sub>Cl) treatment, which produces an intracellular alkalinisation leading to an increase of the intralysosomal pH and an alteration of the lysosomal function subsequently affecting protein degradation (Tanaka et al., 1986, Ohkuma and Poole, 1978). To verify whether these pathways are responsible for M2 degradation by AnxA6, we analysed total expression of M2 viral protein in IAV infected A431 cells expressing AnxA6 treated with the MG132 inhibitor and NH<sub>4</sub>Cl by imaging flow cytometry (figure 3.15). Our previous findings showed that cells overexpressing AnxA6 exhibited a reduction in expression of M2 viral protein at 18h p.i. when compared to A431 cells. For this reason, we have treated cells at 7h p.i. with NH<sub>4</sub>Cl and MG132, when protein synthesis occurs during virus life cycle and fixed cells at 24h p.i to investigate whether either the lysosomal or the proteasome pathways are responsible for M2 degradation. Interestingly, we found that M2 protein expression levels increased in cells overexpressing AnxA6 when treated with NH<sub>4</sub>Cl;

however, no significant difference in M2 protein expression was observed when comparing MG132-treated and non-treated samples (figure 3.15). Means of fluorescence intensity (MFI) of M2 expression for samples treated with NH4Cl and not treated were of 537.000 and 460.100 respectively, whereas M2 MFI in non-infected cells was of 3.500 and in cells treated with MG132 of 446.500. Also, we found that no up-regulation of H3 protein expression was observed when cells overexpressing AnxA6 were treated either with NH4Cl or with MG132. Detected MFI of H3 protein expression in NH4Cl-treated samples was of 953.400 whereas MFI was of 948.700 in IAV-infected not treated cells, 9.300 in non-infected cells and 574.400 when cells were treated with MG132. Low MFIs of M2 and H3 in non-infected cells confirm that infection of samples was efficient. From our results, we suggest that AnxA6 targets M2 protein for degradation through the lysosomal pathway as we observed only increased M2 protein expression when inhibiting the lysosomal pathway with NH4Cl, and also that this down-regulation is an M2-specific mechanism as no H3 up-regulation was observed in NH4-treated IAV infected cells.

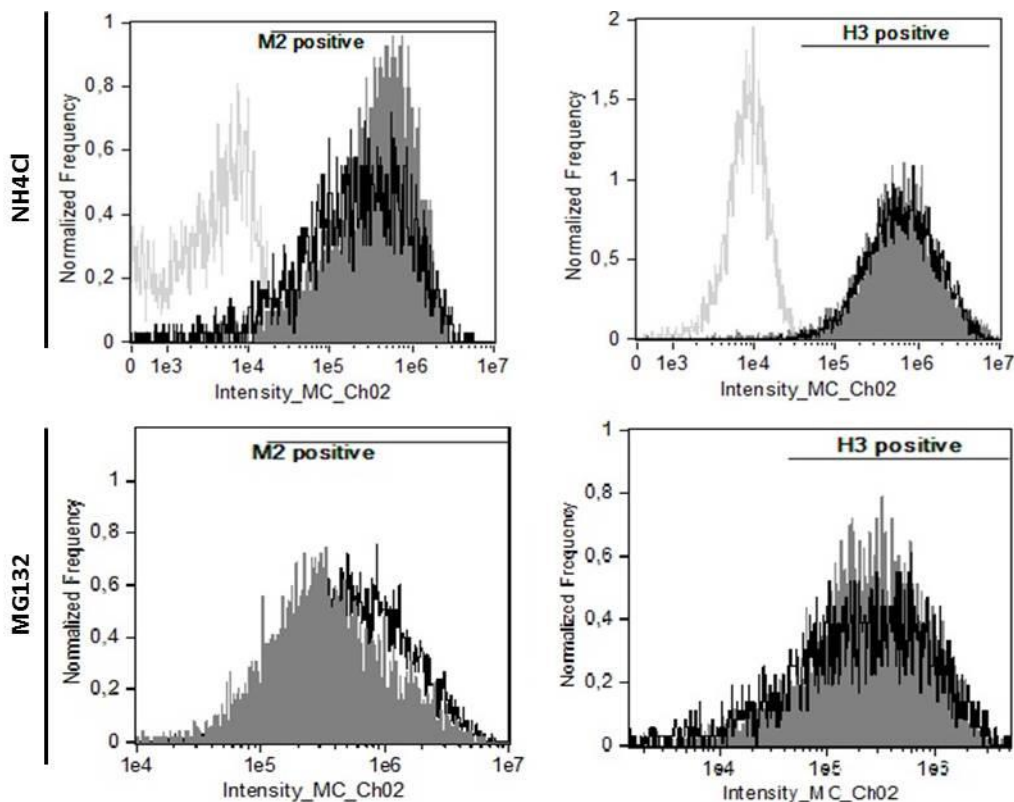


**Figure 3.15. AnxA6 targets M2 degradation through the lysosomal pathway.** A431-AnxA6 cells were infected with the A/Udorn/72(H3N2) strain for 24 hours or not at a MOI=2, treated at 7h post-infection with NH<sub>4</sub>Cl or MG132, fixed with 4% paraformaldehyde, permeabilised with 1% Triton-X100 and stained for the detection of M2 and H3 viral proteins. Histograms show the normalised frequency and the intensity of fluorescence. Non-infected A431-AnxA6 cells are shown in light grey, A431-AnxA6 infected with IAV are shown in black and A431-AnxA6 cells infected with IAV treated with NH<sub>4</sub>Cl or MG132 are shown in dark grey. The means of fluorescence intensity presented in this figure are the most representative of two independent experiments.

### 3.1.12 AnxA6 overexpression impairs morphogenesis of filamentous influenza A virus

We have now demonstrated that annexin A6 overexpression leads to M2 down-regulation and, as a consequence, impaired M2 expression at the cell surface during influenza infection. The previous work of our group determined that AnxA6 overexpression leads to impaired release of viral particles from the surface of cells infected with the spherical influenza A/WSN/33 (H1N1). In this study, we investigated the effect of AnxA6 overexpression on morphogenesis and release from cells infected with the filamentous influenza A/Udorn/72 (H3N2). For this purpose, we performed an experiment of transmission electron microscopy to analyse the structure of budding viral filaments from the surface of infected cells (figures 3.16 and 3.17). Electron microscopy enabled visualisation of the cell's surface when infected for 10 and 20 hours or not. Non infected controls are shown on the left panels and no viral filaments could be observed at the surface of A431 and A431-AnxA6 cells (figure 3.16).

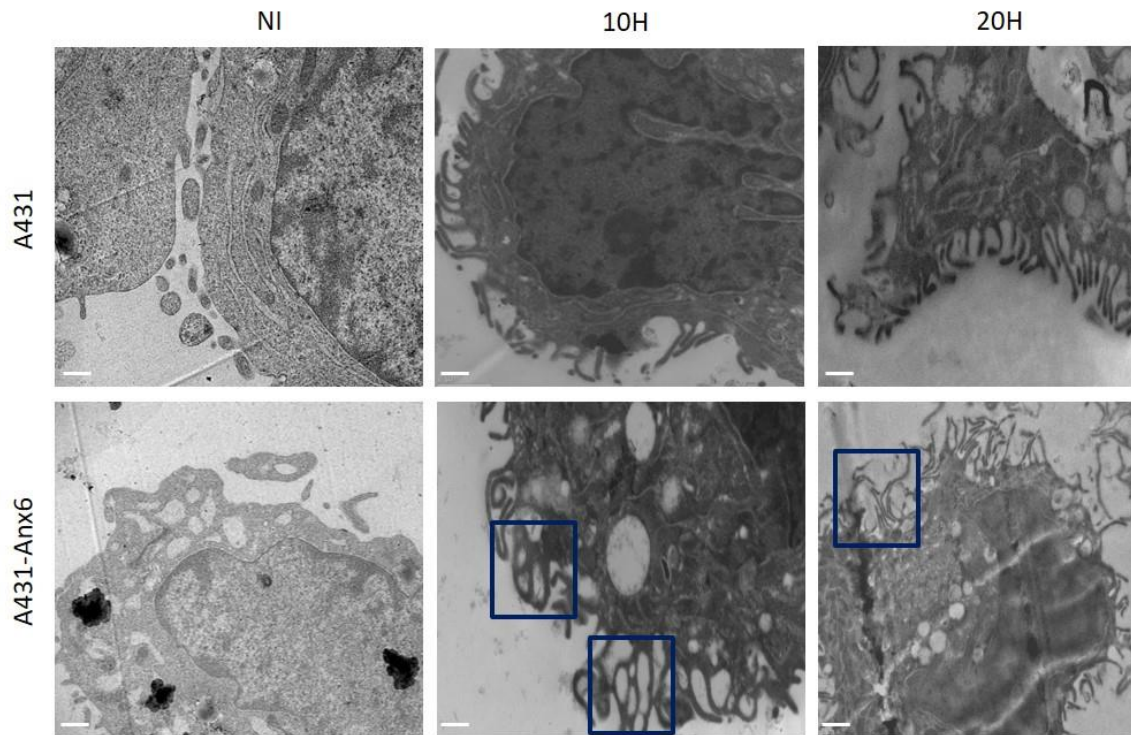


**Figure 3.16. Annexin A6 overexpression impairs morphogenesis of filamentous influenza A virus.** A431 (upper panels) and A431-AnxA6 (lower panels) cells were infected with A/Udorn/72(H3N2) for 10 hours (middle panels) and 20 hours (right panels) at a MOI=5, fixed first in 4% paraformaldehyde/1% glutaraldehyde for 2 hours and with 1% osmium tetroxide for 1h, and then prepared for sectioning. Cells were observed on JEOL 2100 FEG (field emission gun) transmission electron microscope. Regions of interest with interconnected filaments budding from the surface of infected A431-AnxA6 cells are shown in the blue frames. Scale bars, 0.5  $\mu$ m.

In these panels, cells are in a healthy state and filopodia, nuclear membrane and some organelles could be observed. Budding events from the surface of cells infected for 10 and 20 hours were then analysed and differences could be observed between cell types. At 10 and 20 hours p.i., cells seem to look unhealthy and suffering from the cytopathic effect caused by viral infection leading to morphologic changes: infected cells exhibit a rounded shape and an altered nuclear and cytoplasmic structure suggesting their imminent death. In addition, viral filaments are located at the cell surface and released from both A431 and A431-AnxA6 cells. A431 cells exhibited long viral filaments that are well individualised, whereas A431-AnxA6 cells showed longer and interconnected filaments. Also, more filaments could be observed at

the plasma membrane of A431 cells compared to A431-AnxA6 cells. These results suggest that AnxA6 overexpression leads to an impaired release of filamentous viral particles from the surface of infected cells, which is in agreement with the previous work performed by our group as defect in release and morphogenesis of newly formed virions was also observed. In addition, we investigated the aspect of individual viral filaments budding from infected cells as we thought that defect in release could also correlate with alterations of normal virus morphogenesis (figure 3.17). Indeed, closer observation of budding filaments at 10h p.i. suggested that overexpression of AnxA6 leads to an incomplete scission of viral particles. Filaments at the surface of cells expressing AnxA6 were more abundant and not individualised, they were interconnected and exhibiting an abnormal morphology compared to filaments budding from A431 cells. Magnification on filaments are shown on the right panels of figure 3.17. Clearly, three filaments shown on the upper panel are clearly separated from each other, where the end of the filaments and possibly some spikes are well observed. Conversely, filaments from A431-AnxA6 cells shown on the lower panel may not be well separated and there may not be distinction between both ends; however, we cannot confirm this finding due to overstaining of images presented in this figure. These results suggest that AnxA6 overexpression leads to an impaired morphogenesis of newly formed virions and may interfere with scission of virions located at the surface of infected cells, which could be explained by the reduced levels of M2 at the cell surface of infected cells. We believe that further ultrastructural analysis of nascent virions by electron microscopy at higher resolution combined with immune-gold labelling of viral proteins and staining of cholesterol using lipid probes could be used to link annexin A6 overexpression with misbalance of cholesterol, deficiency in morphogenesis and impaired budding of virions. However, it is possible that cholesterol sequestration in intracellular compartments by AnxA6 leads to disruption of endosomal cholesterol egress and reduced levels at the plasma membrane, having an impact on IAV replication (Musiol et al., 2013). Also, reduced levels of cholesterol at the cell surface may inhibit expression of M2 viral protein at budding sites and inhibit IAV release by interfering

with a cholesterol-dependent M2-promoted membrane curvature and posterior scission, as previously suggested by Rossman (Rossman et al., 2010).

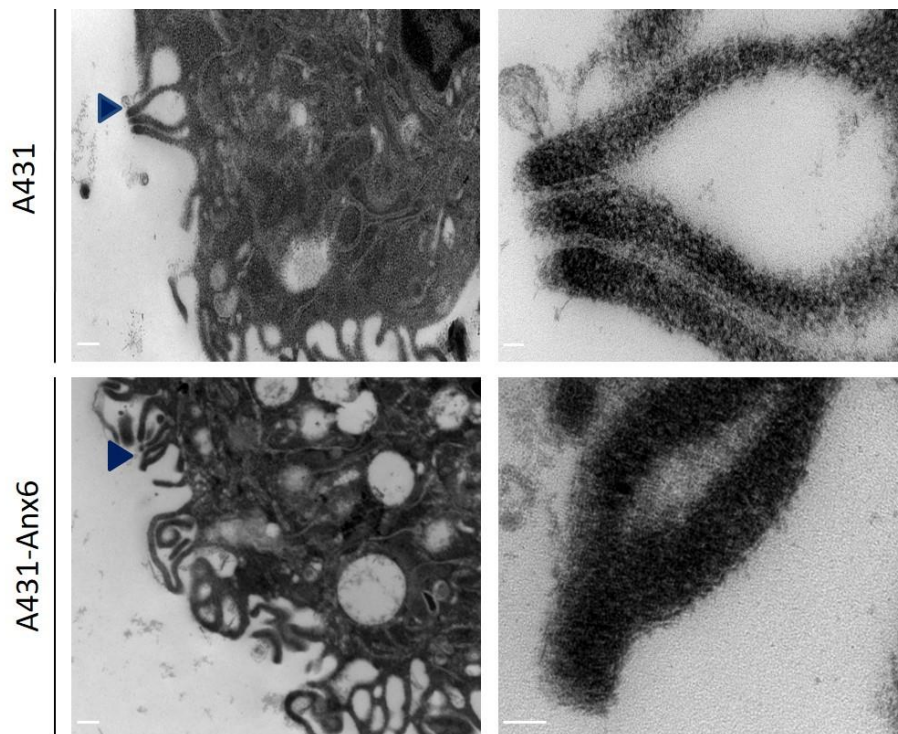


**Figure 3.17. Annexin A6 overexpression leads to budding of interconnected filamentous influenza A virus.** (A) A431 (upper panels) and A431-AnxA6 (lower panels) cells were infected with A/Udorn/72(H3N2) for 10 hours at a MOI=5, fixed first in 4% paraformaldehyde/1% glutaraldehyde for 2 hours and with 1% osmium tetroxide for 1h, and then prepared for sectioning. Cells were observed on JEOL 2100 FEG (field emission gun) transmission electron microscope. Regions of interest showing budding events are presented in left panels, individual budding filaments are shown in the left panels with blue head arrows and are magnified in the right panels. Scale bars, 0.5  $\mu$ m left panels and 50 nm right panels.

In this section, we have now demonstrated that annexin A6 overexpression leads to inhibition of IAV infection. We found that AnxA6 overexpression results in M2 down-regulation and, as a consequence, impaired M2 expression at the cell surface during influenza infection. We also showed that defective expression of M2 at the cell surface leads to a defect in scission and budding of viral particles, which also resulted in abnormal morphology of virions released from the surface of infected cells.

### **3.2 Annexin A6 is implicated in the modulation of important cellular pathways required for viral infection and induction of the anti-IAV innate immune response**

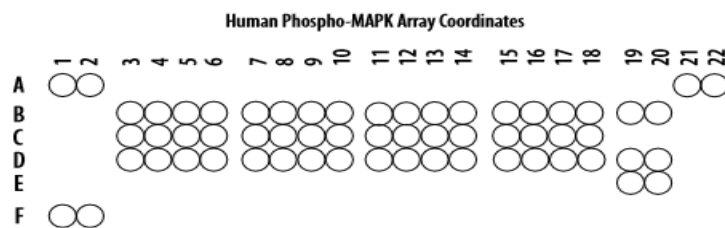
In our previous section, we have used A431 cells and A431 cells stably expressing AnxA6-myc (A431-AnxA6) to study the effect of AnxA6 during IAV morphogenesis. In this chapter, I used A549 lung epithelial cells and A549 cells stably expressing AnxA6-myc (A549-AnxA6) to study a potential immune response regulated by AnxA6 during influenza infection. Our hypothesis is based on previous studies showing that AnxA6 is involved in the regulation of many signalling pathways. For instance, Minashima and collaborators published a study which determined that AnxA6 modulates extracellular signal-regulated kinase (ERK) and p38 mitogen-activated protein kinase (MAPK) activities through regulation of intracellular Ca<sup>2+</sup> concentration and its binding to PKC $\alpha$  (Minashima et al., 2012). Also, Campbell and collaborators found that AnxA6 interacts with p65 subunit of the NF- $\kappa$ B transcription factor to regulate its activation in chondrocytes (Campbell et al., 2013). In addition, several studies have demonstrated that MAPKs and other signalling pathways are activated in response to early influenza infection and play an important role in activation of cytokine and chemokine response (Cannon et al., 2014). In this section, I investigate whether AnxA6 overexpression modulates intracellular signalling pathways during IAV infection and induces an antiviral response.

#### **3.2.1 Annexin A6 regulates important signalling kinases during early IAV infection**

As already mentioned, many studies have already shown that MAPKs are activated in response to early influenza infection. For instance, Cannon and co-workers found that phosphorylation of extracellular regulated kinases 1 and 2 (ERK 1/2), p38 and c-Jun kinases 1 and 2 (JNK 1/2) MAPKs is increased between 15 minutes and 3 hours post-infection to stimulate the production of inflammatory cytokines and chemokines (Cannon et al., 2014). Therefore, we first analysed whether AnxA6 overexpression plays a role in the modulation of MAPK pathways during early influenza infection. For this purpose, we first used a proteome

profiler to test phosphorylation/activation of important MAPKs and other intracellular protein regulators of signal transduction between 30 minutes and 4 hours post-infection (figures 3.18, 3.19 and 3.20). We speculate that strong differences in activation/phosphorylation levels and interval of activity for MAPKs such as Akt, ERK, JNK and p38 between A549 and A549-Anx6 infected cells will be observed; especially at 0.5h and 1h p.i. when innate immune responses occur in the host cell during early entry and post-entry stages of IAV infection to activate defence mechanisms.

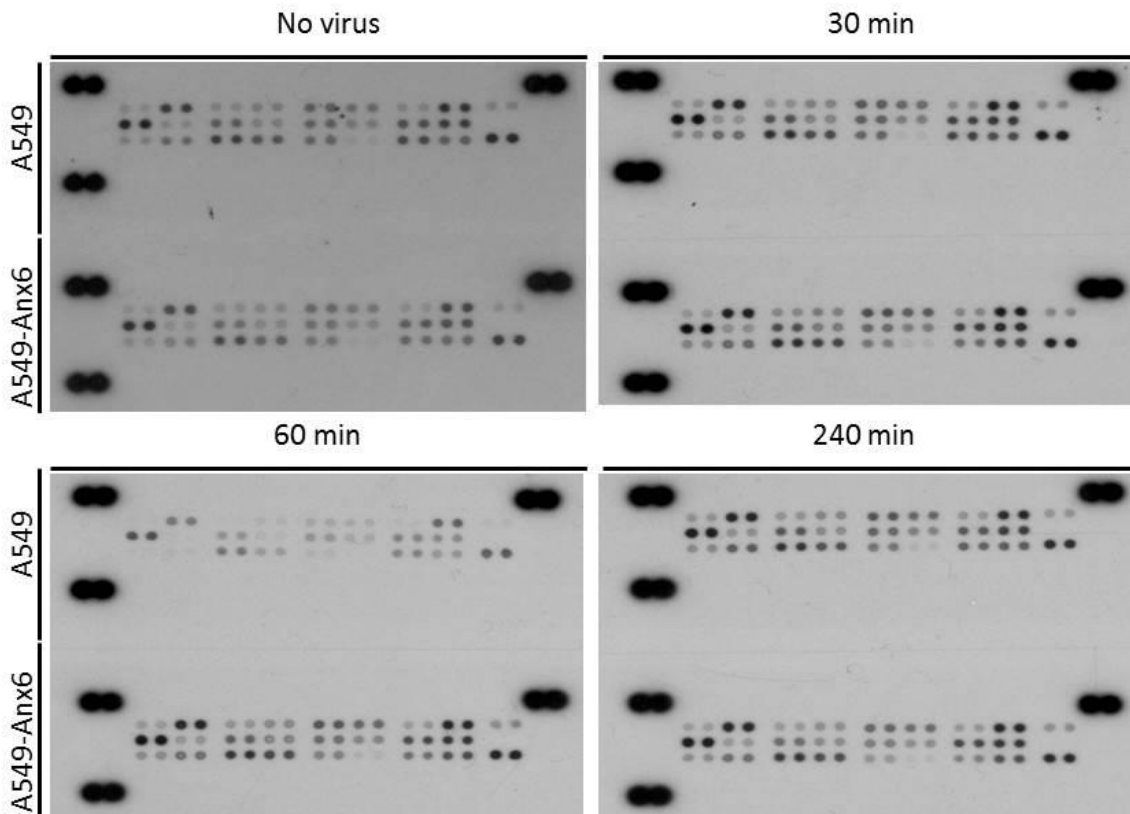
**A**



**B**

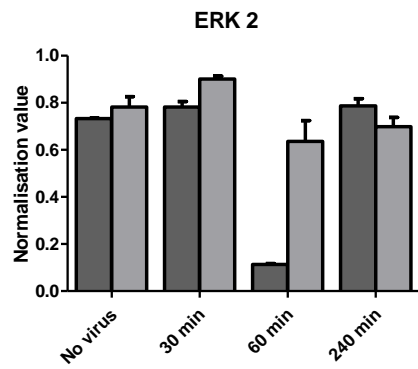
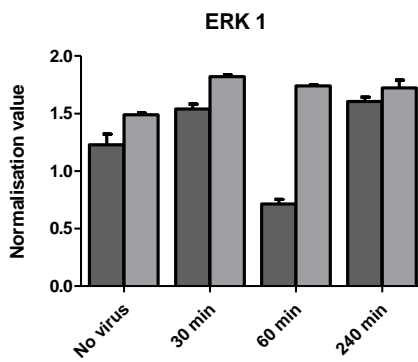
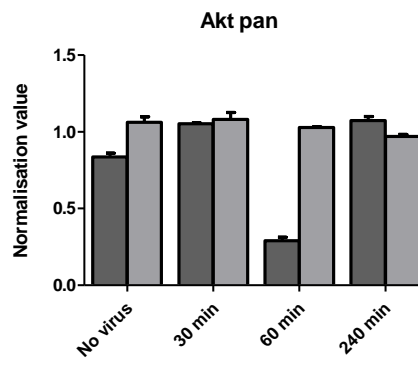
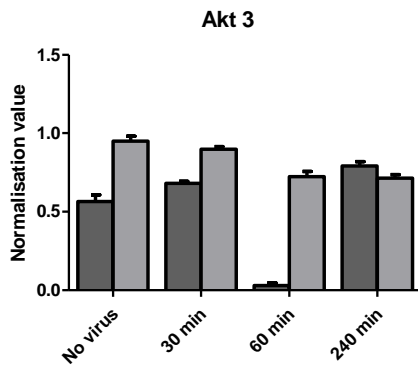
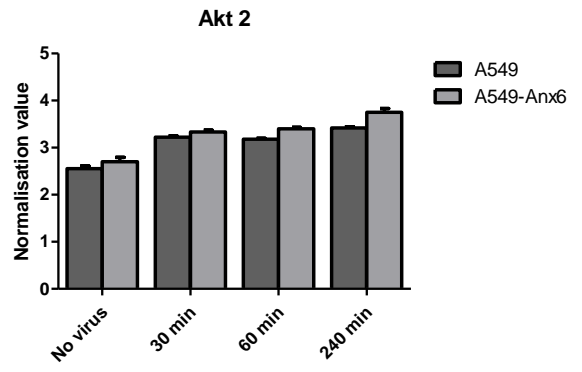
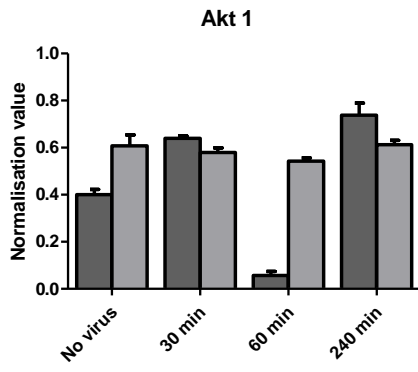
Coordinate	Target/Control	Alternate Nomenclature	Phosphorylation Site Detected
A1, A2	Reference Spots	—	—
A21, A22	Reference Spots	—	—
B3, B4	Akt1	PKB $\alpha$ , RAC $\alpha$	S473
B5, B6	Akt2	PKB $\beta$ , RAC $\beta$	S474
B7, B8	Akt3	PKB $\gamma$ , RAC $\gamma$	S472
B9, B10	Akt pan	—	S473, S474, S472
B11, B12	CREB	—	S133
B13, B14	ERK1	MAPK3, p44 MAPK	T202/Y204
B15, B16	ERK2	MAPK1, p42 MAPK	T185/Y187
B17, B18	GSK-3 $\alpha/\beta$	GSK3A/GSK3B	S21/S9
B19, B20	GSK-3 $\beta$	GSK3B	S9
C3, C4	HSP27	HSPB1, SRP27	S78/S82
C5, C6	JNK1	MAPK8, SAPK1 $\gamma$	T183/Y185
C7, C8	JNK2	MAPK9, SAPK1 $\alpha$	T183/Y185
C9, C10	JNK3	MAPK10, SAPK1 $\beta$	T221/Y223
C11, C12	JNK pan	—	T183/Y185, T221/Y223
C13, C14	MKK3	MEK3, MAP2K3	S218/T222
C15, C16	MKK6	MEK6, MAP2K6	S207/T211
C17, C18	MSK2	RSK $\beta$ , RPS6KA4	S360
D3, D4	p38 $\alpha$	MAPK14, SAPK2A, CSBP1	T180/Y182
D5, D6	p38 $\beta$	MAPK11, SAPK2B, p38-2	T180/Y182
D7, D8	p38 $\delta$	MAPK13, SAPK4	T180/Y182
D9, D10	p38 $\gamma$	MAPK12, SAPK3, ERK6	T183/Y185
D11, D12	p53	—	S46
D13, D14	p70 S6 Kinase	S6K1, p70 $\alpha$ , RPS6KB1	T421/S424
D15, D16	RSK1	MAPKAPK1 $\alpha$ , RPS6KA1	S380
D17, D18	RSK2	ISPK-1, RPS6KA3	S386
D19, D20	TOR	—	S2448
E19, E20	PBS	Control (-)	—
F1, F2	Reference Spots	—	—

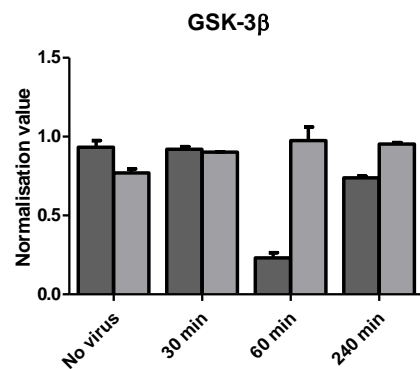
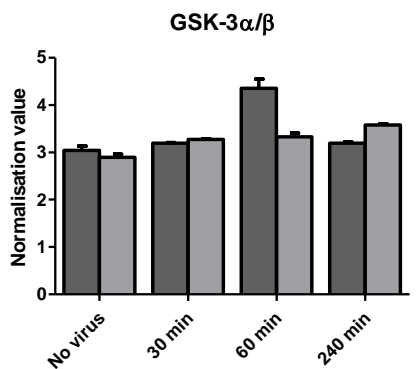
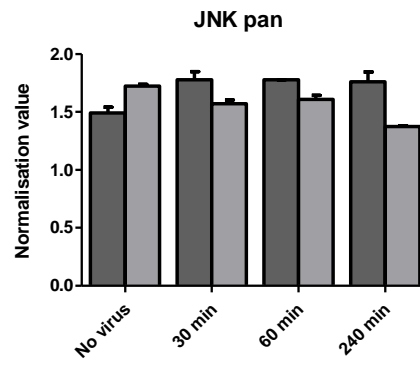
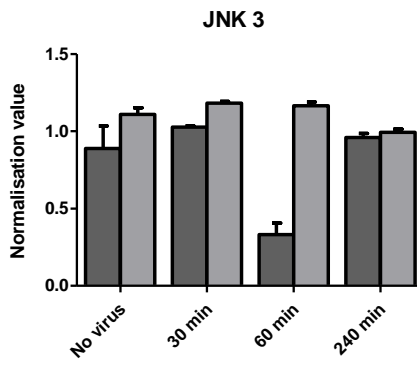
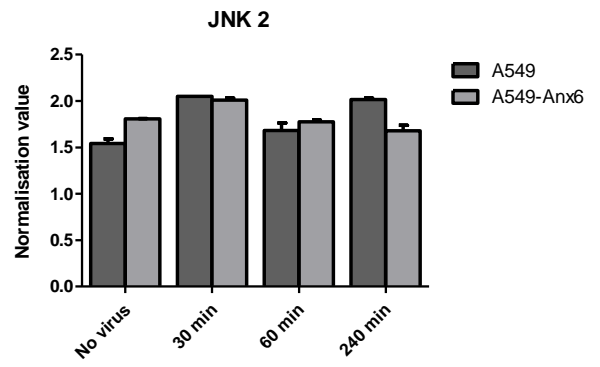
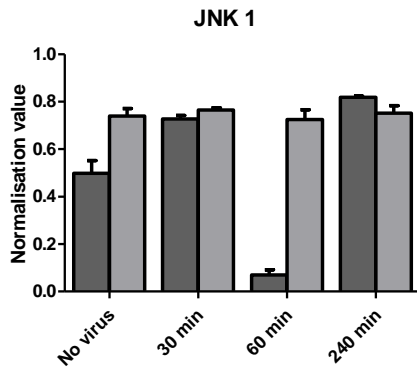
**Figure 3.18. Study of MAPKs and other signalling kinases activation during early influenza infection.** (A) Layout of the human Phospho-MAPK coordinates tested with the proteome profiler array ARY002B. (B) List of target kinases and their phosphorylation sites.

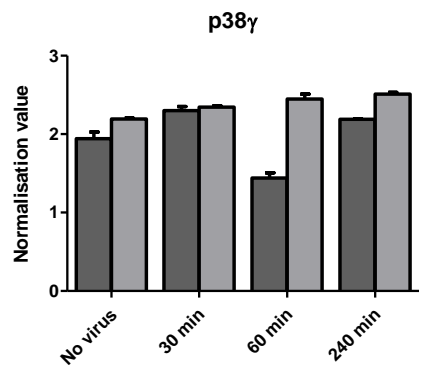
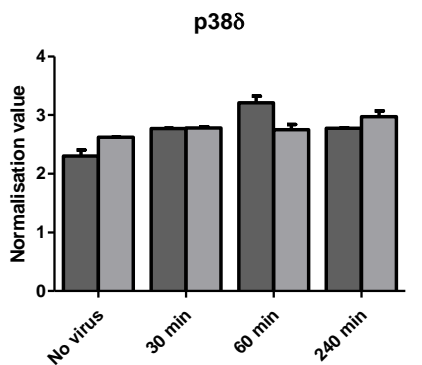
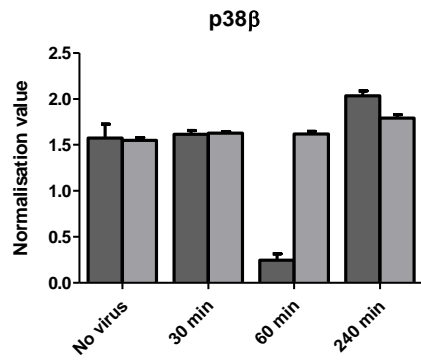
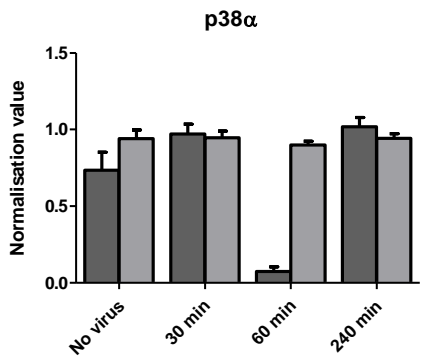
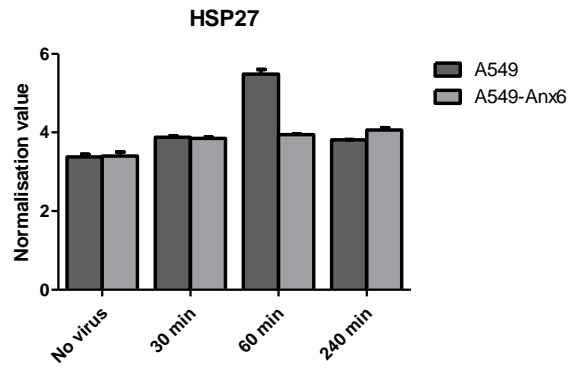
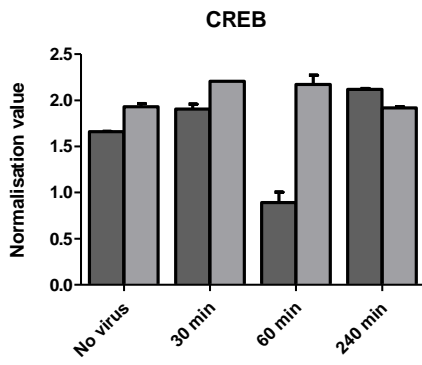


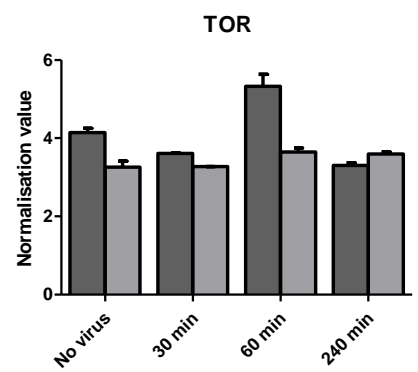
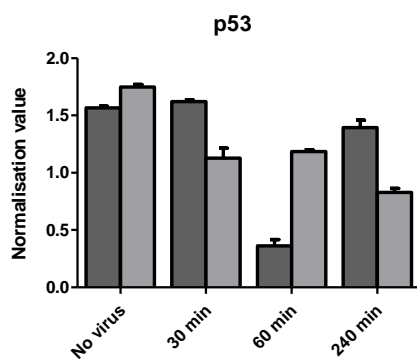
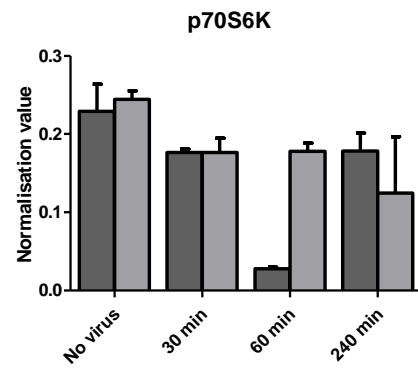
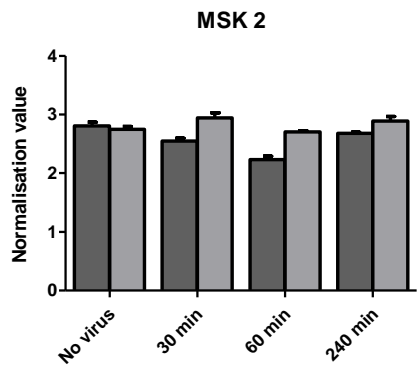
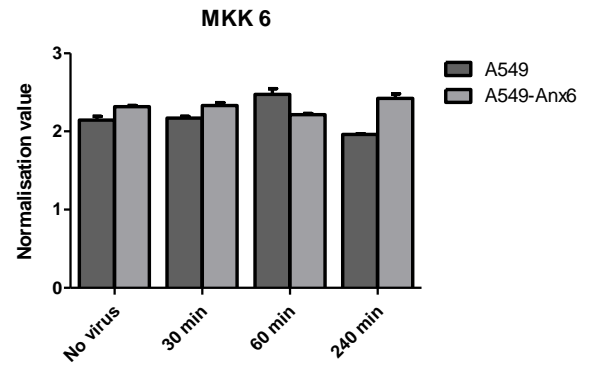
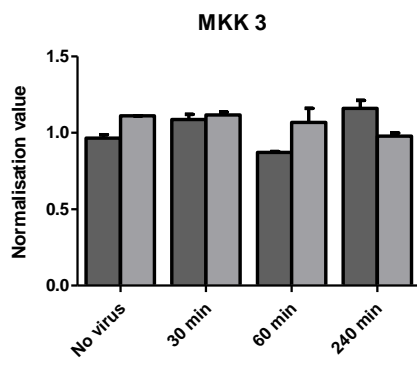
**Figure 3.19. Detection of activated/phosphorylated kinases during influenza infection.** A549 and A549-Anx6 cells were infected with A/Udorn/72(H3N2) at MOI=10 or not for 0.5h, 1h and 4 hours and lysed. Sample mixtures were added to each respective membrane previously blocked, hybridised with detection antibody cocktail against phosphorylated residues in kinases tested and incubated with streptavidin-HRP. Then, membranes were washed and revealed with ECL substrate to detect phosphorylation signals after 15 minutes exposure.

Below are presented the normalised values of all kinases tested in both A549 and A549-AnxA6 cell lines when non-infected and also when infected for 0.5, 1 and 4 hours. Normalisation values were obtained by quantification of all detected signals with ImageJ software after subtraction of the reference spot signal and comparison of each individual signal with the sum of signals in each cell line for each protein in order to compare each individual signal against the total signal for all treatments and both cell lines (figure 3.20).









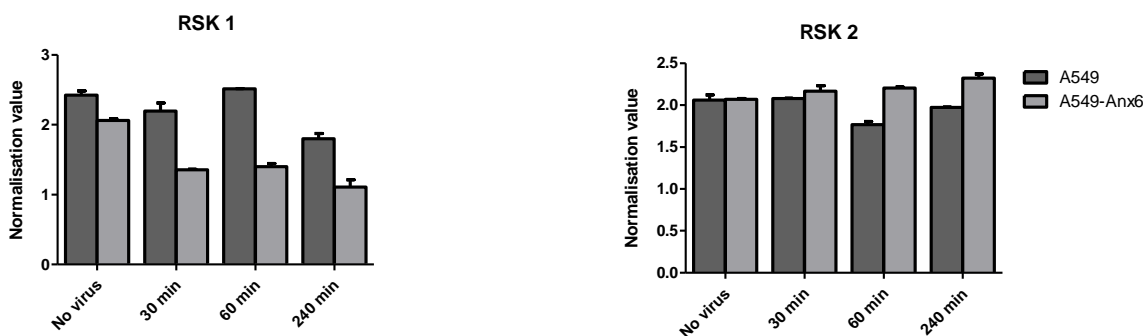


**Figure 3.20. Normalisation of activated/phosphorylated kinases during influenza infection.**

Detection of phosphorylated kinases for each membrane was quantified using ImageJ software after subtraction of the reference spot signal and normalised against the sum of signals in each cell line. Data are shown as means + standard deviation from two reference spot signals calculated of a single experiment.

The proteome profiler revealed different patterns in kinases and other protein regulators phosphorylation during infection between A549 and A549-Anx6 cells. Akt 1/2/3/Pan modules did not exhibit an important difference in expression during early infection as all samples have a similar level of phosphorylation compared to the non-infected control, especially in A549-Anx6 cells. Interestingly, protein phosphorylation of Akt1, Akt3 and Akt-Pan but not Akt2 in A549 cells is clearly lower compared to the non-infected sample at 1h p.i. Then, detection of ERK1 phosphorylation determined its activation is higher in A549-Anx6 cells than in A549 cells and it is also higher for both cell lines at 0.5h, 1h and 4h post-infection compared to non-infected controls but at 1h p.i. in A549 cells exhibit the lowest activation. For ERK2, A549-Anx6 cells show a higher phosphorylation for all time points but at 4h p.i., where A549 cells exhibit more activation than A549-Anx6 cells. Also, A549 cells exhibit a higher activation at 0.5h and 4h post-infection and A549-AnxA6 at 0.5h p.i. only compared to non-infected controls. At 1h post-infection, both cell lines have a lower phosphorylation for ERK2 and again, A549-AnxA6 expresses it more than A549 cells. JNK 1/2/3/Pan modules exhibited no significant differences between cell lines and also between time points as for both A549 and A549-Anx6 cell lines, all samples exhibited similar levels of phosphorylation compared to the

non-treated controls. Only a marked difference between cell lines could be observed at 1h p.i. for JNK1 and JNK3, where A549 cells exhibited a lower activation than A549-Anx6 cells but also compared to the non-infected control. Then, same levels of GSK-3 $\alpha/\beta$  activation were detected in both A549 and A549-Anx6 cell lines and also no differences were observed between infected and non-infected samples. Only, more expression was detected in A549 cells at 1h p.i. For GSK-3 $\beta$ , higher levels at 0.5h p.i. but lower levels of activation at 1h and 4h p.i were found in A549 compared to A549-Anx6 cells. Again, only a marked difference of protein activation was found at 1h p.i, where levels in A549-Anx6 were higher. Other proteins tested with the array were CREB and HSP27, which exhibited no significant differences between cell lines and also between time points as for both A549 and A549-Anx6 cell lines, all samples exhibited similar levels of phosphorylation compared to the non-treated controls. Only a marked difference between cell lines could be observed at 1h p.i. for JNK1 and JNK3, where A549 cells exhibited a lower activation of CREB but higher of HSP27 compared to levels in A549-Anx6 cells. Similarly, no marked differences were detected between cell lines and also between time points between cell lines, only small differences were detected between cell lines at 1h p.i. where less activated levels were detected for p38 $\alpha/\beta/\gamma$  but more important levels were detected for p38 $\delta$  in A549 cells compared to A549-Anx6 cells. Neither were observed important differences in activation of MKK3, MKK6 and MSK2 between cell lines during infection as expression in infected samples were similar in both cell lines and also compared to respective non-infected controls. Only at 1h and 4h p.i. a slight difference was observed for MKK3 between cell lines, where it was more importantly activated in A549 cells at 1h p.i. and in A549-AnxA6 cells at 4h p.i. Similarly, only a difference could be observed at 1h p.i. for MKK6 which was higher expressed in A549 cells compared to A549-Anx6 cells. For MSK2, only a marked difference in activation could be observed at 0.5h p.i. and A549-Anx6 exhibited a higher phosphorylation than A549 cells. Then, it was also observed that infected A549 and A549-Anx6 cells exhibited a reduction in p70S6K and p53 activation compared to non-infected cells and a more marked difference was evident between cell lines at 1h and 4h p.i. We found that both p70S6K and p53 were more activated in A549-Anx6 cells at 1h p.i. and

in A549 cells at 4h p.i. For TOR, we found a very steady expression in all samples in A549-Anx6 cells but a biphasic activation in A549 cells when infection occurs. No differences were observed in A549-Anx6 cells between infected samples and the non-infected control. Conversely, we found a reduced activation at 0.5h and 4h p.i. but a very clear increased activation at 1h p.i. which almost doubled activation levels in A549 cells. Detection of RSK1 activation levels determined that Anx6 overexpression leads to a reduced phosphorylation not only during infection but also compared to A549 cells as all levels of RSK1 activation were decreased in A549 and A549-Anx6 cells compared to non-infected controls and more activation was found in A549 cells than in A549-Anx6 cells. However, an increased activation was found in A549 cells at 1h p.i. Finally, no major differences were observed in RSK2 activation after infection and also between cell lines. Steady levels were observed in both A549 and A549-Anx6 cell lines between 0.5h and 4h p.i.; however a very slight decrease was found with infection in A549 cells and a very slight increase was observed in A549-Anx6 cells. As expected, we showed that that Anx6 is involved in the regulation and activation of many important kinases during early influenza infection. For instance, we found that some Akt, ERK, JNK and p38 modules of MAPKs and other kinases such as CREB, GSK-3 $\beta$ , p70S6K and p53 were up-regulated during infection, which was mainly observed at 1h post-infection. Conversely, we found that activation of other proteins such as GSK-3 $\alpha/\beta$ , HSP27, p38 $\delta$ , MKK6, TOR and RSK1 was down-regulated during early infection. From these results, we suggest that Anx6 may regulate activation of important kinases during early infection and Anx6 could play a role through their modulation in limiting viral replication and propagation. However, a second experiment should be performed to confirm these results, and especially, to clarify whether IAV infection leads to a reduced activation of kinases at 1h p.i. in A549 cells. Surprisingly, we detected lower signals for most of kinases at 1h p.i. in A549 cells, these findings suggest that the membrane used could be defective as it is unlikely that the totality of proteins analysed after treatment are down-regulated at this time of infection in comparison to A549-AnxA6 cells.

### 3.2.2 Annexin A6 regulates expression of ERK and AKT signalling pathways during early infection

To confirm previous results, we also analysed whether AnxA6 overexpression regulates activation of ERK 1/2, JNK 1/2 and AKT pathways during early infection by western blotting. For this purpose, we performed a cell fractionation and a western blot on lysates of A549 and A549-AnxA6 IAV infected cells for 0.5, 1 and 4 hours to test phosphorylation of ERK, JNK and AKT pathways (figure 3.21).

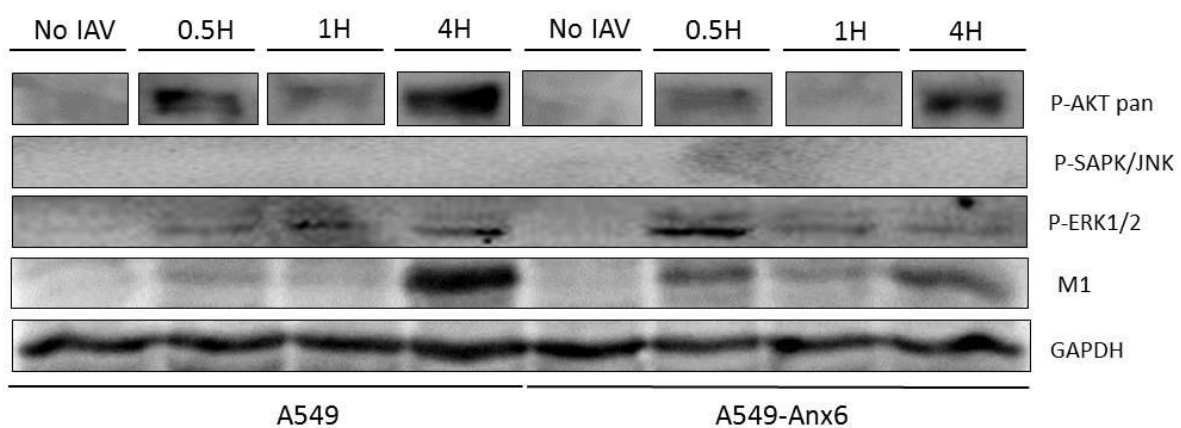


**Figure 3.21. Annexin A6 regulates expression of ERK and AKT signalling pathways during early infection of influenza virus in A549 human lung epithelial cells.** A549 and A549-AnxA6 cells were infected or not with the influenza A/Udorn/72 (H3N2) strain at a MOI=10 and lysed at for 0.5, 1 and 4 hours post-infection. Cell lysates were collected and prepared for loading at a concentration of 1.5mg/ $\mu$ l. Expression levels of M1 viral protein as a control of infection, GAPDH as a loading control, and then phospho-ERK1/2, phospho-SAPK/JNK and phospho-AKT pan cellular proteins were determined by Western blotting.

By western blot, we also found that AnxA6 overexpression leads to differences in activation of ERK and AKT pathways during influenza infection. Firstly, we observed a biphasic modulation of ERK1/2 module by AnxA6 during early infection as more phosphorylated/activated ERK1/2 at 0.5h but less phosphorylated/activated ERK1/2 at 1h and 4h post-infection in A549 cells over-expressing AnxA6 was detected. Interestingly, we found less phosphorylated/activated AKT Pan at 0.5h, 1h and 4h post-infection in A549 cells over-expressing AnxA6. Also, no

phosphorylation of SAPK/JNK 1/2 was detected as no bands appeared after labelling with specific antibody against phospho-SAPK/JNK. Expression of M1 protein is shown as a control of infection and we found that M1 is expressed at 0.5., 1 and 4h p.i. in both cell lines but not in non-infected samples, as expected. The first signals corresponding to 0.5h and 1h p.i. correlate to infection levels, which are higher in A549-Anx6 cells. The last signal, at 4h p.i., corresponds to production of viral proteins and it is lower in cells over-expressing AnxA6. Expression levels of GAPDH protein show that all samples were loaded at the same concentration. From these results, we suggest again that AnxA6 regulates activation of ERK and AKT modules during early infection; however, patterns in activation are not in agreement with the preliminary results obtained with the MAPK proteome profiler as we could not see any biphasic activation of ERK1/2, higher levels of ERK2 activation compared to ERK1 in both cell lines and nor a reduction in Akt activation in cells over-expressing AnxA6 during viral infection. We suggest that AnxA6 is involved in regulation and activation of these pathways during IAV infection; however, further investigation is required to further clarify to which extent AnxA6 is involved and the molecular mechanism underlying AnxA6 role in inhibiting viral replication and propagation by regulation of these pathways. We suggest that AnxA6 is involved in regulation and activation of these pathways during IAV infection; however, further investigation is required to further clarify to which extent AnxA6 is involved and the molecular mechanism underlying AnxA6 role in inhibiting viral replication and propagation by regulation of these pathways.

### 3.2.3 Overexpression of Annexin A6 leads to differential profile of cytokines in A549 human lung epithelial cells

I have already mentioned that some studies have shown the implication of these pathways in the stimulation of inflammatory cytokines during influenza infection. We just showed that AnxA6 over-expression leads to a modulation of signalling pathways during early infection. Therefore, we hypothesised that AnxA6 over-expression could regulate cytokine production during viral infection. To clarify this hypothesis, we performed real-time PCR to test mRNA

levels of pro-inflammatory and anti-inflammatory cytokines and chemokines during infection at different MOIs, first we tested levels at MOI=1 and then at MOI=5 (figures 3.22 and 3.23). Firstly, we found increasing levels of viral M1 mRNA over time and also that cells over-expressing AnxA6 exhibited lower levels of M1 viral protein, showing that AnxA6 expression could lead to limited infection at MOI=1. We also found that AnxA6 over-expression led to significant differences in mRNA levels of many cytokines between cell lines (figure 3.22).

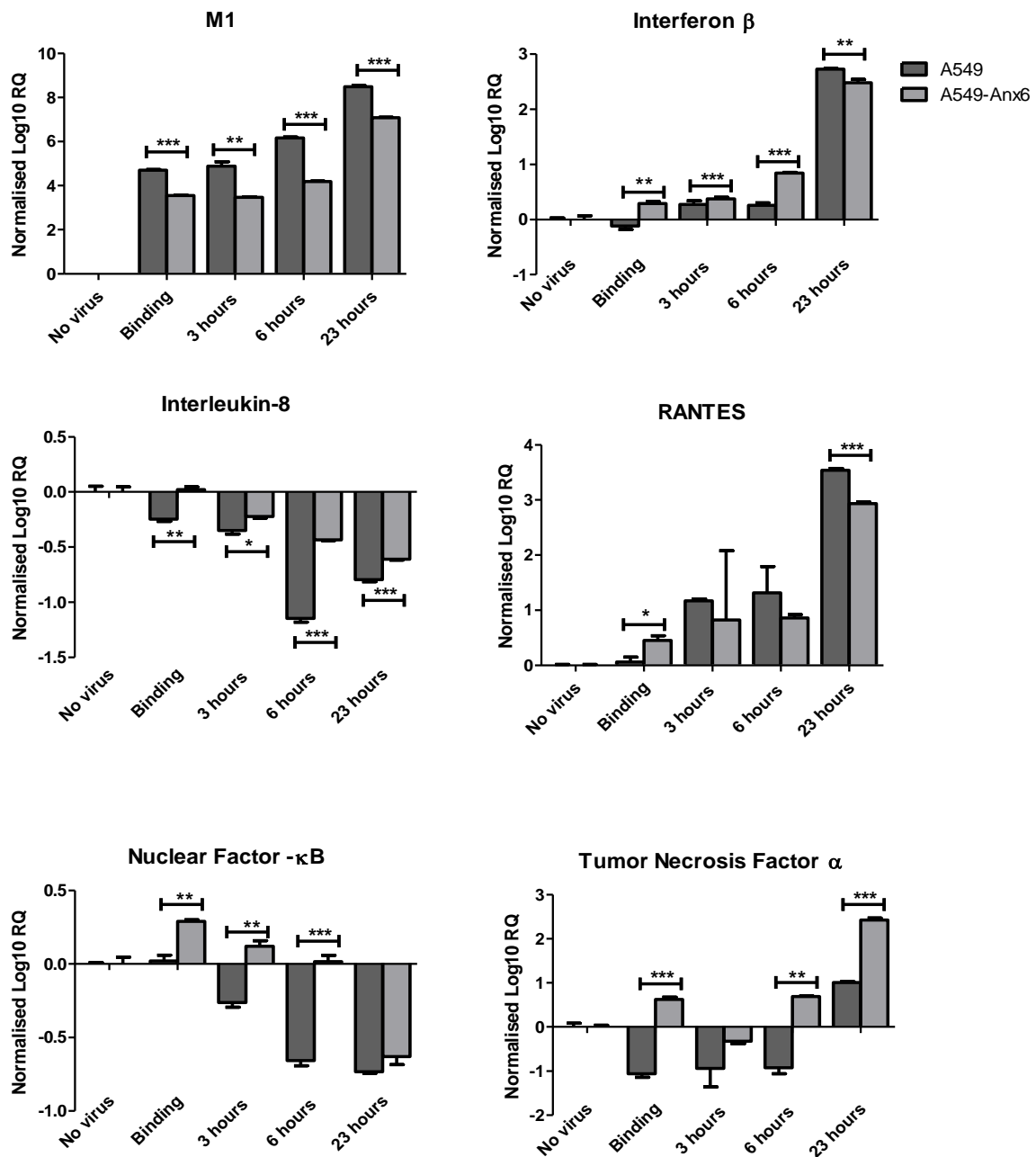


**Figure 3.22. Differential profile of cytokines is expressed upon viral infection in A549 human lung epithelial cells over-expressing Annexin A6.** A549 and A549-AnxA6 cells were infected or not with the A/Udorn/72 (H3N2) strain for 3, 6, 23 hours at a MOI=1. mRNA was purified, reverse-transcribed into cDNA and RT-PCR conducted on interferon beta, IL-8, RANTES, nuclear factor – kappa B and tumor necrosis factor genes. mRNA levels of M1 gene was used to quantify rate of infection. Results are expressed in log<sub>10</sub> of relative quantities (RQ) calculated using the comparative CT method ( $\Delta\Delta CT$ ) from Ct values of samples. 18S RNA gene was used as endogenous control and non-infected sample as the calibrator. Data are shown as means + standard deviation from triplicates of two independent experiments and an unpaired Student's t-test was performed. \*, P<0.05; \*\*, P<0.01; \*\*\*, P<0.001.

Interferon beta mRNA levels also increased over the time of infection and were higher in cells over-expressing AnxA6 when binding of virus to cells occurs and at 3 and 6h p.i. but it is slightly higher in A549 cells at 23h p.i. These results suggest that an interferon producing antiviral activity could be activated by AnxA6 during early infection, especially at 6h p.i. when the most important difference in mRNA levels was observed. For NF- $\kappa$ B, again higher levels of mRNA were found in cells over-expressing AnxA6; however, the fold-difference is very low and a decrease in mRNA in both cell lines could be observed over time: these differences in NF- $\kappa$ B mRNA expression levels were not significant. In addition, mRNA levels of RANTES increased progressively over time of infection and only during virus binding mRNA levels were higher in cells over-expressing AnxA6, as at 3, 6 and 23h p.i., we observed higher levels in A549 cells compared to A549-AnxA6 cells and this difference was only significant at 23h p.i. Therefore, RANTES could play a role in the immune response during late infection. Then, we observed that mRNA levels of interleukin-8 (IL-8) decreased during infection and also cells over-expressing AnxA6 always exhibited higher levels than A549 cells, especially at later stages of infection as the most marked differences in mRNA expression were found at 6 and 23h p.i. and when IL-8 could participate more importantly in the anti-IAV response. Interleukin-1 $\beta$  (IL-1 $\beta$ ) could not be detected in this experiment. Finally, TNF $\alpha$  mRNA levels increased over time of infection and cells over-expressing AnxA6 always exhibited higher mRNA levels than

A549 cells at MOI=1. More important differences could be observed during viral binding, but also at 6 and especially at 23h p.i. From these results, we suggest that AnxA6 could participate in the regulation of anti-IAV innate immune response, by mainly up-regulating mRNA expression of cytokines and chemokines such as TNF $\alpha$ , IL-8 and RANTES during late infection. To confirm the previous results, we performed another real-time PCR to test mRNA levels of inflammatory cytokines and chemokines during infection but at MOI=5 (figure 3.23).

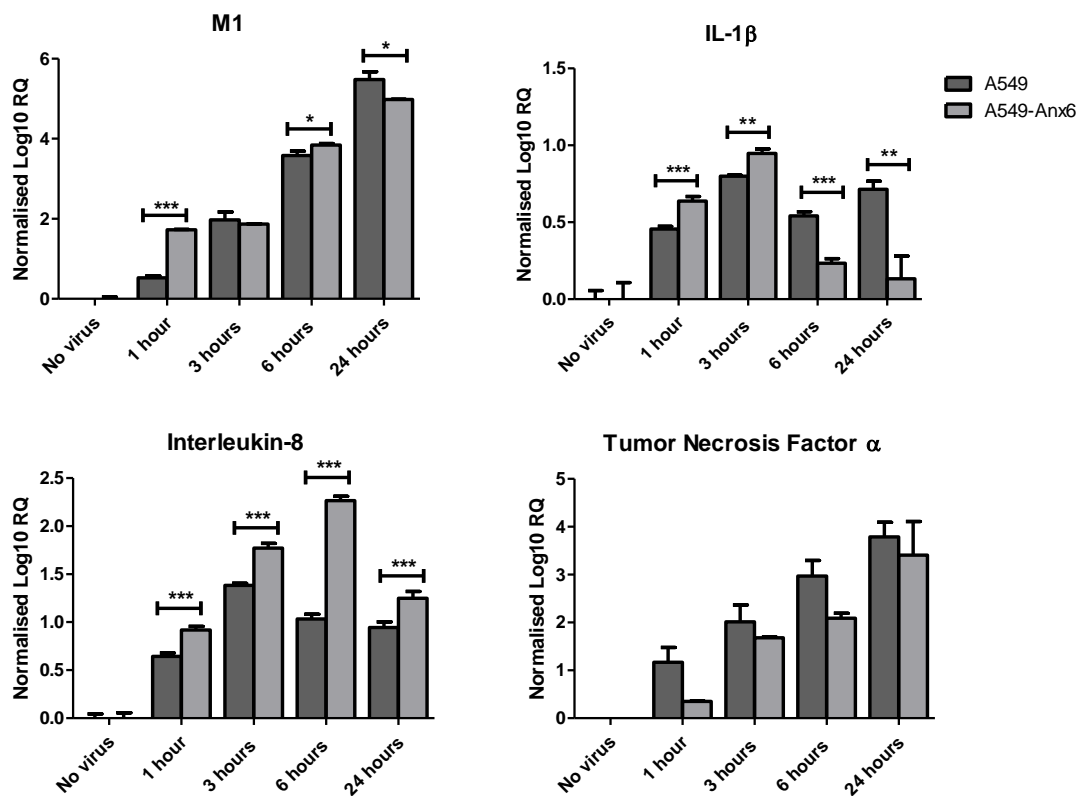


**Figure 3.23. Differential profile of cytokines is expressed upon viral infection in A549 human lung epithelial cells over-expressing Annexin A6.** A549 and A549-AnxA6 cells were infected or not with the A/Udm/72 (H3N2) strain for 1, 3, 6 and 24 hours at a MOI=5. mRNA was purified, retro-transcribed into cDNA and RT-PCR conducted on IL-1 beta, IL-8 and tumor necrosis factor genes. mRNA levels of M1 gene was used to quantify rate of infection. Results are expressed in log<sub>10</sub> of relative quantities (RQ) calculated using the comparative CT method ( $\Delta\Delta$ CT) from Ct values of samples. 18S RNA gene was used as endogenous control and non-infected sample as the calibrator. Data are shown as means + standard deviation from triplicates from two independent experiments and an unpaired Student's t-test was performed. \*, P<0.05; \*\*, P<0.01; \*\*\*, P<0.001.

Firstly, we found increasing levels of viral M1 mRNA over time which show that infection happened but not as efficiently as expected, levels of M1 are lower than in the first experiment at MOI=1. Experiments were performed with different IAV batches and it is likely that the batch used for the experiment at MOI=5 was less infective, leading to a lower infectivity and reduced levels of M1 mRNA levels when compared to M1 mRNA levels at MOI=1. Also, levels of M1 are not consistent with findings at MOI=1 as no down-regulation of M1 was found at all times of infection in cells over-expressing AnxA6. In addition, no significant differences were found at any time point between cell lines. In this experiment, we also found increased mRNA levels of IL-8 in cells over-expressing AnxA6 and we confirm that AnxA6 plays a role in production of IL-8 during infection, especially at 6h p.i. Then, we found increasing mRNA levels in expression of TNF $\alpha$  during infection but also lower levels were observed in A549 cells over-expressing AnxA6: these results are in disagreement with the previous experiment as we found that AnxA6-overexpression led to increased mRNA expression of TNF $\alpha$  at MOI=1. We suggest that differences in batch infectivity used in both experiments may lead to these differences observed in TNF $\alpha$  mRNA levels. Interestingly, we detected mRNA levels of IL-1 $\beta$  in this experiment and we obtained higher expression during early infection but lower at late infection in cells over-expressing AnxA6. Marked differences were observed more importantly during late infection, at 6 and 24h p.i. However, we could not detect expression of NF- $\kappa$ B, RANTES and interferon- $\beta$  in this experiment. Altogether, we suggest that AnxA6 contributes to an anti-IAV innate immune response by potentiating expression of cytokines such as TNF $\alpha$  and IL-8 in A549 human lung epithelial cells, especially at late times of infection.

#### 3.2.4 Over-expression of annexin A6 in A549 lung epithelial cells is associated with higher levels of NF- $\kappa$ B nuclear translocation in IAV infected cells

Finally, we analysed activation of NF- $\kappa$ B during viral infection as it has been described to play a central role in the activation of the innate immune response against IAV and in the production of inflammatory cytokines. For this purpose, we performed immunofluorescence microscopy and flow cytometry experiments on lung epithelial cells during early and late infection and we

analysed levels of NF- $\kappa$ B nuclear translocation. We first tested nuclear translocation of NF- $\kappa$ B by flow cytometry during early infection. For this, we quantified the similarity score of NF- $\kappa$ B to nuclear probe Draq5 at 2, 6 and 9h post-infection in A549 and A549-AnxA6 cells (figure 3.24). We found a higher similarity score in A549-AnxA6 cells compared to A549 cells at all times of infection, but also in non-infected controls meaning that over-expression of AnxA6 leads to a higher translocation of NF- $\kappa$ B into the nucleus and therefore a higher activation. We found a higher activation at 2h and 9h p.i., however no major differences were observed between cell lines as the increase in NF- $\kappa$ B activation at these times of infection are similar to the one observed in non-infected cells. We suggest that AnxA6 over-expression does not lead to an increase in NF- $\kappa$ B activation during early infection. Therefore, we then tested its activation during late infection by immunofluorescence (figure 3.24). Immunostaining of 200 non-infected cells and cells infected for 20h or 46h enabled us to determine the percentage of nuclear and cytosolic NF- $\kappa$ B localisation. In non-infected cells, we found 2% nuclear and 98% cytosolic expression of NF- $\kappa$ B in A549 cells and 14% nuclear and 86% cytosolic expression in A549-AnxA6 cells, suggesting that overexpression of AnxA6 or stable expression of a factor regulated by AnxA6 leads to a higher nuclear translocation and activation of NF- $\kappa$ B. At 20h p.i., we found 28% nuclear and 72% cytosolic expression but 86% nuclear and 14% cytosolic expression in A549 and A549-AnxA6 cells respectively. These results suggest that viral infection for 20h results in an increase in NF- $\kappa$ B activation, which is about three times higher in AnxA6 over-expressing cells as translocation raises about 26% in A549 cells and about 72% in A549-AnxA6 cells. At 46h p.i., we observed 29% nuclear and 71% cytosolic expression but 55% nuclear and 45% cytosolic expression in A549 and A549-AnxA6 cells respectively. These results determined again that an increase in NF- $\kappa$ B activation occurs in A549-AnxA6 cells as we found an increase in nuclear translocation of about 27% in A549 cells and about 41% in A549-AnxA6 cells. We suggest from these results that AnxA6 over-expression leads to an increased activation of NF- $\kappa$ B during late influenza infection, and more importantly at around 20h post-infection. To further confirm these results, we performed a new experiment of flow cytometry and we tested nuclear translocation of NF- $\kappa$ B at 24h p.i. in both cell lines

(figure 3.24). We quantified the similarity score of NF- $\kappa$ B to nuclear probe Draq5 and we found a reduced similarity score in 24h-infected A549 cells compared to non-infected cells, suggesting that influenza virus reduces NF- $\kappa$ B activation at late stages of infection.

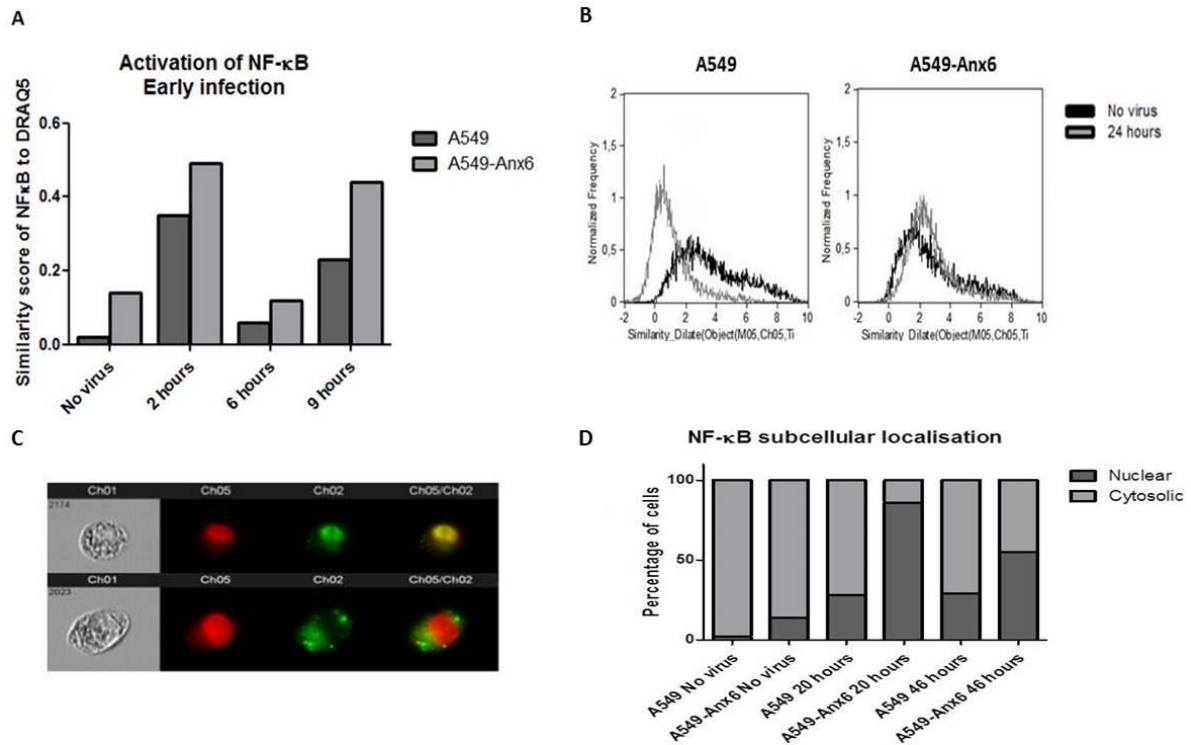


**Figure 3.24. Over-expression of annexin A6 in A549 lung epithelial cells is associated with higher levels of NF- $\kappa$ B nuclear translocation in IAV infected cells.** A, B and C: Imagestream, A549 and A549-AnxA6 cells were infected or not with the influenza A/Udorn/72 (H3N2) strain for 2, 6, 9 hours at MOI=2 and 24 hours at a MOI=1, fixed in 4% paraformaldehyde and stained with a polyclonal antibody for the detection of NF- $\kappa$ B p65 and Draq5 for the detection of DNA. NF- $\kappa$ B p65 protein is shown in green and nuclei in red. Nuclear translocation of NF- $\kappa$ B was analysed by the Amnis Ideas software for image analysis and represented as similarity score of NF- $\kappa$ B to Draq5 or similarity dilate in A and B, respectively. Images of cells with and without NF- $\kappa$ B translocation to the nucleus are shown. D: Immunofluorescence: A549 and A549-AnxA6 cells were infected with the A/Udorn/72 (H3N2) strain for 20 and 46 hours at a MOI=1, fixed in 4% paraformaldehyde and stained with a polyclonal antibody for the detection of NF- $\kappa$ B p65 and DAPI for the detection of DNA.. At least 200 cells were counted by 3 independent people.

Interestingly, similar scores were obtained from non-infected and 24h-infected cells over-expressing AnxA6. We therefore conclude that AnxA6 over-expression in lung epithelial cells is associated with higher levels of NF- $\kappa$ B nuclear translocation in IAV infected cells during late infection and contributes to the regulation of an innate antiviral response. These findings together with up-regulation of cytokines such as IL-8 and TNF $\alpha$  at 24h p.i. suggest that AnxA6 participates in an antiviral response against IAV and limits viral propagation during late infection.

### 3.3 Influenza A virus down-regulates Annexin A6 expression

#### 3.3.1 Annexin A6 is down-regulated upon IAV infection at the mRNA level

In this chapter, I analysed whether IAV regulates AnxA6 gene and protein expression in order to counteract its restrictive role during infection. For this purpose, we have analysed mRNA expression of different isoforms of AnxA6 in A549 lung epithelial cells during infection with different strains and MOIs by real-time PCR and also AnxA6 protein expression by flow cytometry. As a test experiment, I first analysed AnxA6 gene expression during infection with the influenza A/HK/98 (H3N2) strain for 3h, 6h and 12h at a MOI=5 and when virus is left binding to cells for 1h (figure 3.25).

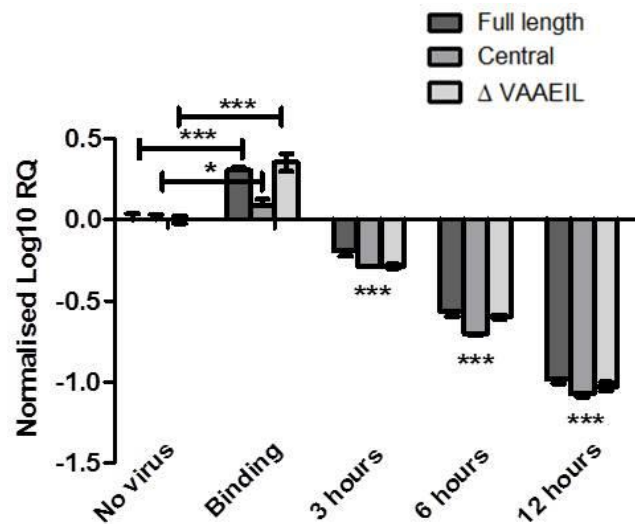


**Figure 3.25. Endogenous annexin A6 is down-regulated upon IAV infection at the mRNA level.**

A549 cells were infected or not with A/HK/98 (H3N2) strain for 3, 6 and 12 hours at a MOI=5. mRNA was purified, reverse-transcribed into cDNA and RT-PCR conducted on different isoforms of endogenous AnxA6. Results are expressed in log<sub>10</sub> of relative quantities (RQ) calculated using the comparative CT method ( $\Delta\Delta CT$ ) from Ct values of samples. 18S RNA gene was used as endogenous control and non-infected sample as the calibrator. Data are shown as means + standard deviation from triplicates from two independent experiments and an ANOVA test was performed. \*, P<0.05; \*\*, P<0.01; \*\*\*, P<0.001.

When cells were infected with A/HK/98 (H3N2) strain for 3h, 6h and 12h at a MOI=5, an evident down-regulation could be observed. Treatment of 1h virus binding to the cells led to up-regulation of all isoforms of about a 0.3-0.4 10-fold difference when compared to non-infected controls. Then, at 3h, 6h and 12h p.i., a progressive down-regulation at mRNA levels was observed, being of about 0.3, 0.6 and 1 10-fold difference respectively compared to non-infected controls, which was very significant at each time of infection. To confirm these preliminary data, we then analysed AnxA6 gene expression after 1h of virus binding and also in cells infected with the influenza A/Udorn/72 (H3N2) for 3h, 6h and 23h at MOI=1 (figure 3.26).

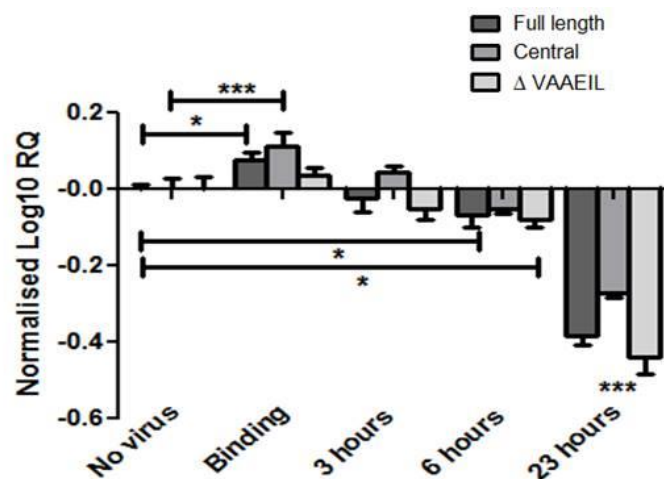


**Figure 3.26. Endogenous annexin A6 is down-regulated upon IAV infection at the mRNA level.** A549 cells were infected or not with the A/Udorn/72 (H3N2) strain for 3, 6, 23 hours at a MOI=1. mRNA was purified, reverse-transcribed into cDNA and RT-PCR conducted on different isoforms of endogenous AnxA6. Results are expressed in log10 of relative quantities (RQ) calculated using the comparative CT method ( $\Delta\Delta CT$ ) from Ct values of samples. 18S RNA gene was used as endogenous control and non-infected sample as the calibrator. Data are shown as means + standard deviation from triplicates from two independent experiments and an ANOVA test was performed. \*, P<0.05; \*\*, P<0.01; \*\*\*, P<0.001.

We found that all isoforms tested were slightly up-regulated compared to non-infected controls when 1h of virus binding to the cells surface occurred, which is in agreement with results

obtained after infection with influenza A/HK/98 (H3N2). At 3h p.i., both the full length isoform and the isoform lacking VAAEIL amino acids were slightly down-regulated, whereas the isoform detected with primers binding to the central region of the gene was up-regulated. At 6 and 23h p.i., all isoforms were found to be down-regulated; however, levels are lower at later time points as the relative quantification falls from about 0.1 log<sub>10</sub> to about 0.4 log<sub>10</sub>. In this experiment, we found that IAV infection leads to AnxA6 gene down-regulation but in a less significant fashion, as only a 0.4 log<sub>10</sub> difference was found at 23h p.i. Clearly, IAV targets down-regulation of endogenous AnxA6 gene expression during infection; however, further investigation on AnxA6 gene expression is required as I have used different IAV strains and MOIs. In addition, it is not clear whether this down-regulation is due to IAV and AnxA6 interaction or whether IAV shuts down AnxA6 gene expression indirectly by regulating other host genes during infection. It will be of critical importance to clarify whether IAV controls regulatory regions of AnxA6 gene promoter driven repression. Therefore, we suggest that differences in gene regulation may be due to the ability of viral strains to shut down expression of restriction factors and further investigation is critical to decipher the molecular mechanism employed by IAV to target AnxA6 down-regulation. We then investigated whether exogenous AnxA6, which is expressed in AnxA6 over-expressing A549 cells, is also down-regulated by IAV (figure 3.27). To test this hypothesis, we performed again a real-time PCR and we analysed mRNA expression of the different isoforms of AnxA6 in A549-AnxA6 cells during infection with the filamentous A/Udorn/72 (H3N2) strain at MOI=5. We found no down-regulation of exogenous AnxA6 gene expression, except for the isoform lacking the VAAEIL sequence which was very slightly down-regulated upon virus binding, all isoforms are stable and up-regulated at 3, 6 and 24h post-infection but also after binding when compared to non-infected controls.

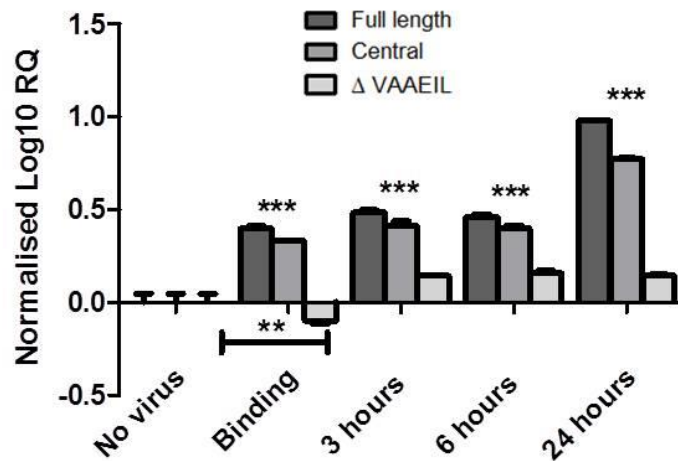


**Figure 3.27. Exogenous annexin A6 gene expression is up-regulated by influenza A virus.** A549-Anx6 cells were infected or not with A/Udorn/72 (H3N2) strain for 3, 6 and 24 hours at a MOI=5. mRNA was purified, reverse-transcribed into cDNA and RT-PCR conducted on different isoforms of AnxA6 to detect endogenous and exogenous AnxA6 gene expression. Results are expressed in log<sub>10</sub> of relative quantities (RQ) calculated using the comparative CT method ( $\Delta\Delta CT$ ) from Ct values of samples. 18S RNA gene was used as endogenous control and non-infected sample as the calibrator. Data are shown as means + standard deviation from triplicates from two independent experiments and an ANOVA test was performed. \*, P<0.05; \*\*, P<0.01; \*\*\*, P<0.001.

### 3.3.2 Annexin A6 protein is also down-regulated during IAV infection

As we found that IAV down-regulates gene expression of endogenous AnxA6, we then tested whether protein levels are also down-regulated when cells were infected with the filamentous A/Udorn/72 (H3N2) strain and we tested protein expression by flow cytometry on A549 lung epithelial cells during early and late infection. We first analysed AnxA6 protein levels in A549 cells during early infection (figure 3.28).

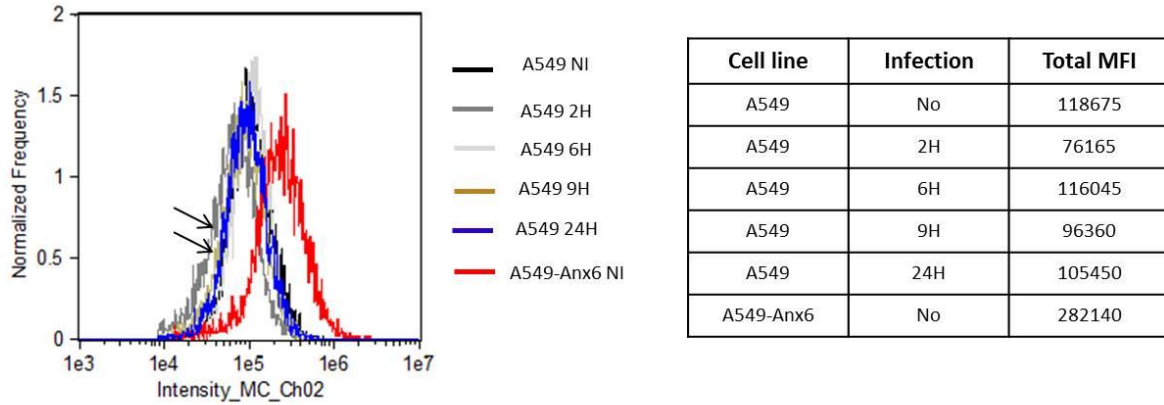


**Figure 3.28. Annexin A6 is slightly down-regulated upon IAV infection at the protein level during early infection.** A549 cells were infected or not with the influenza A/Udorn/72 (H3N2) strain for 2, 6, 9 hours at MOI=2 and 24 hours at a MOI=1, fixed in 4% paraformaldehyde and labelled for detection of endogenous annexin A6 by flow cytometry. Black arrows show AnxA6 protein down-regulation at 2h and 6h post-infection.

We tested levels of AnxA6 expression in A549 cells infected for 2, 6 and 9 hours in addition to A549 and A549-AnxA6 non-infected cells. We found a mean of fluorescence of 118.675 in non-infected A549 cells, corresponding to normal levels of protein expression and of 282.140 in non-infected A549-AnxA6 cells, showing that over-expression of AnxA6 in A549 cells led to an increase of more than twice in protein levels. When infected with the filamentous A/Udorn/72 (H3N2) strain at MOI=2, A549 cells exhibited a mean of fluorescence of 76.165, 116.045 and 96.360 at 2, 6 and 9h p.i. These results suggest that an important down-regulation in protein levels occurs at 2h p.i. and again at 9h p.i. in a less important manner. No down-regulation could be observed at 6h p.i. as protein expression at this time point is very similar to expression found in non-infected control. We also analysed whether IAV down-regulates protein levels of endogenous AnxA6 at late times of infection and we found that infection for 24h at MOI=1 did not lead to protein down-regulation of AnxA6. This result is in disagreement with levels of gene mRNA expression, which could be explained by experiments variability or by other cellular processes occurring during infection. It is known that many cellular processes can lead to discrepancies between mRNA and protein levels. For instance,

mRNA transcription is not as efficient as protein translation, but also protein half-life and stability of AnxA6 could explain why protein expression did not correlate with gene expression during early stages of IAV infection. Therefore, further experiments are required to confirm whether IAV down-regulates protein expression of endogenous AnxA6 during early infection. We then analysed AnxA6 protein expression during late stages of viral infection, and after several cycles of replication (figure 3.29). To test whether AnxA6 protein is down-regulated by IAV during late infection, we have analysed protein levels of endogenous AnxA6 at 22, 48 and 70h p.i. and compared them to A549 non-infected cells. A431 cells, which do not express AnxA6, are used as negative controls and we found a mean of fluorescence of 2.670 determining that very low background levels were obtained in this cell line. A549 cells exhibited a mean of fluorescence of 31.830 in non-infected A549 cells, corresponding to normal levels of protein expression in this experiment and of 145.855 in non-infected A549-AnxA6 cells, showing again a higher protein expression in our positive control with AnxA6 over-expression.

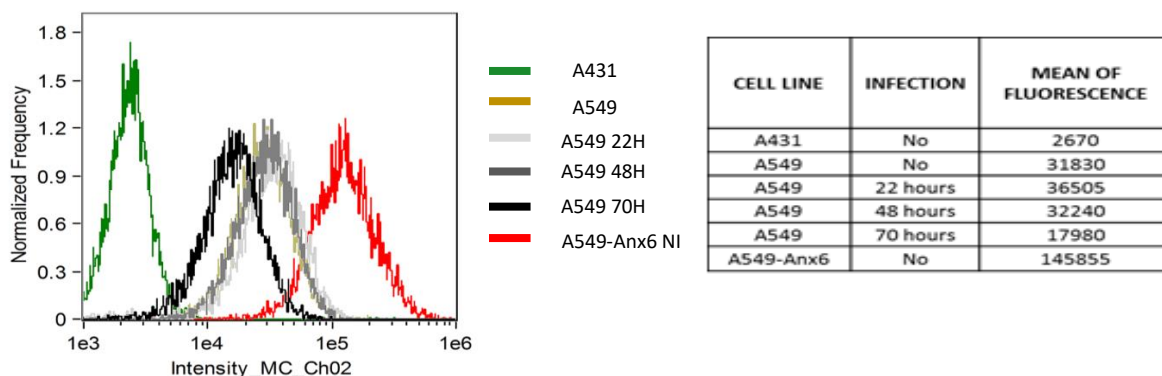


**Figure 3.29. Annexin A6 protein is down-regulated at very late IAV infection.** A549 cells were infected when required with the A/Udorn/72 (H3N2) strain for 24, 48 and 70 hours at a MOI=2, fixed, permeabilised with Triton-X100 and stained for the detection of the endogenous AnxA6 protein by flow cytometry. A431 cells were used as a negative control and A549-Anx6 cells were used as a positive control for AnxA6 expression.

Then, when infected with the filamentous A/Udorn/72 (H3N2) strain at MOI=1, A549 cells exhibited a mean of fluorescence of 36.505, 32.240 and 17.980 at 22, 48 and 70h p.i. These results suggest AnxA6 protein is stably expressed during late infection and only an important

down-regulation in protein levels occurred at 70h p.i. as protein expression at this time point was reduced of about nearly 50% when compared to non-infected control. To conclude, we suggest that IAV down-regulates AnxA6 mRNA expression during early infection and protein expression during late infection as a mechanism of defence against viral restriction.

### 3.3.3 Influenza A virus does not down-regulate exogenous annexin A6 protein during infection

Finally, we analysed whether IAV also down-regulates protein expression of exogenous AnxA6 during early and late infection (figures 3.30 and 3.31). To test whether AnxA6 protein is down-regulated by IAV during early infection, we have analysed protein levels of exogenous AnxA6 at 5h, 8h and 18h p.i. and compared them to A549-AnxA6 non-infected cells (figure 3.30). We found an MFI of 29855 for exogenous AnxA6 protein in non-infected cells. MFIs in infected cells were of 22065 at 5h p.i., 24165 at 8h p.i. and 27.850 at 18h p.i., suggesting that no significant down-regulation of AnxA6 exogenous protein expression occurred during early infection.

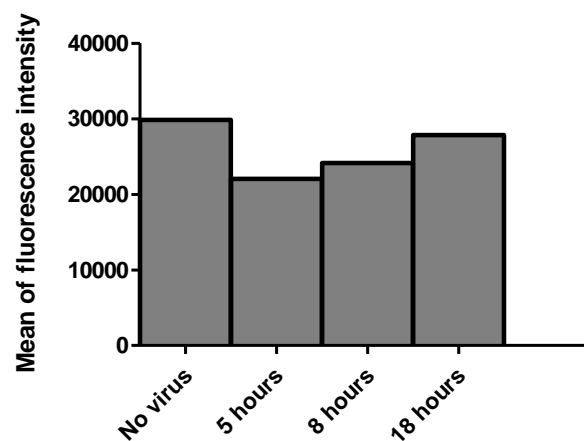


**Figure 3.30. Exogenous annexin A6 protein is not down-regulated during early IAV infection.**

A549-AnxA6 cells were infected when required with the A/Udorn/72 (H3N2) strain for 5, 8 and 18 hours at a MOI=1, fixed, permeabilised with Triton-X100 and stained for the detection of the exogenous AnxA6 protein with an anti-myc antibody by flow cytometry.

In addition, we tested levels of exogenous AnxA6 at 16h p.i. in 3 independent experiments (figure 3.31). In non-infected A549-AnxA6 cells, an MFI was 50.720 with a SD of 28.580 whereas in infected cells an MFI of 152580 was found with a SD of 150320. These results suggest that influenza virus infection does not lead to down-regulation of the exogenous AnxA6 protein during early or late infection. These results are in disagreement with the data presented in figure 3.30. Again, as experiments were performed with different IAV batches, differences in virus infectivity could explain these discrepancies.

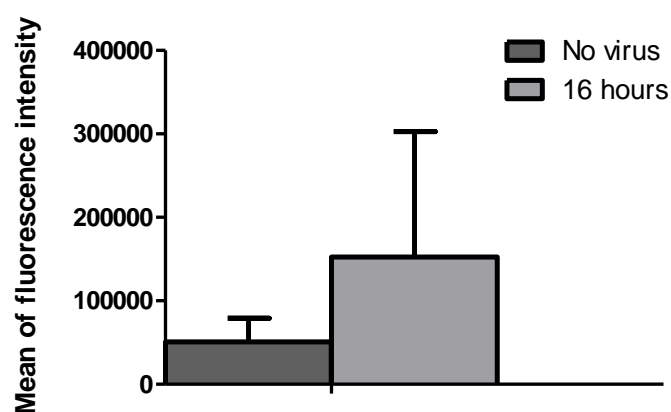


**Figure 3.31. Exogenous annexin A6 protein is not down-regulated during late viral infection.**

A549-AnxA6 cells were infected when required with the A/Udorn/72 (H3N2) strain for 16 hours at a MOI=1, fixed, permeabilised with Triton-X100 and stained for the detection of the exogenous AnxA6 protein with an anti-myc antibody by flow cytometry. Data are shown as means + standard deviation from three independent experiments. 10.000 cells were analysed in each experiment.

To conclude, we suggest that IAV down-regulates expression of endogenous AnxA6 at mRNA levels during early infection and at protein levels during late infection as a mechanism of defence against viral restriction. As no physical interaction between AnxA6 and entering virions has been described, we speculate that IAV manipulates host gene expression during early infection to limit AnxA6 gene expression. However, investigation is still required to clarify whether IAV targets AnxA6 gene promoter to specifically down-regulate its gene expression or whether it is a result of the general shutdown occurring during viral infection. Finally, AnxA6 protein degradation was mainly observed at late stages of infection. AnxA6 lifespan of 48-72h

limits protein degradation during early stages of infection and may explain why no marked effect of IAV infection on AnxA6 protein expression could be detected earlier.

## 4 DISCUSSION

### 4.1 Molecular mechanism of influenza A virus restriction by Annexin A6

Late stages of the IAV life cycle leading to the morphogenesis and release of virions from infected cells are a well-orchestrated mechanism and occur at apical domains of the plasma membrane (Rossman and Lamb, 2011). As in the case of IAV, HIV and Ebola virus are also enveloped viruses that bud from cholesterol-enriched lipid rafts and their envelope is derived from the host cell plasma membrane; unlike HIV and Ebola virus, IAV release is not dependent on the endosomal sorting complex required for transport (ESCRT) pathway for membrane scission and budding (Rossman et al., 2010). Recently, the M2 viral protein has been identified as an important factor for the release of IAV virions since it is located at the basis of budding particles in low cholesterol-containing membrane domains and it has been suggested to drive a force able to create a negative membrane curvature and the pinching off of budding viral particles (Rossman et al., 2010, Schmidt et al., 2013). Specifically, the M2 CT contains a CRAC motif which has been suggested to bind to cholesterol at the periphery of lipid rafts during budding and participates in membrane curvature leading to membrane scission and release of progeny viruses (Schroeder et al., 2005). In the previous study of our group, the human AnxA6 was identified as a cellular factor interacting with the M2 CT and also a restriction factor of influenza infection (Ma et al., 2012). AnxA6 is a phospholipid-binding protein that is recruited to cellular membranes enriched in polar phospholipids (PS, PE). Therefore AnxA6 could be translocated to plasma membrane when infection occurs due to elevated levels of intracellular calcium and interact with the M2 viral protein (Lizarbe et al., 2013, Ma et al., 2012, Gerke et al., 2005). One hypothesis in the present study was that AnxA6 is recruited to the cell plasma membrane and colocalizes with the M2 viral protein at the neck of budding particles generating a mechanical restraint on M2 during the scission event. To verify this hypothesis we performed an immunofluorescence experiment using a filamentous influenza strain for convenient observation of budding events at the plasma membrane and distinction between the neck and the elongating filamentous bud. As in the study published by

Rossman, we found that M2 is located at the basis of budding virions; however, our preliminary results show that AnxA6 is not recruited to the plasma membrane where viral filaments bud and therefore it does not colocalize with M2 at the neck of budding particles (figures 3.5 and 3.6). This led us to analyse the subcellular localisation of AnxA6 and IAV viral proteins inside the cell during late stages of infection. Interestingly, we observed that AnxA6 and M2 colocalised at the cell periphery in close proximity to the cell surface, but also in vesicular-like structures (figure 3.8).

Several studies led us to think that AnxA6 could affect the formation of the viral budding zone by regulating cholesterol homeostasis. For instance, Cubells et al. demonstrated that AnxA6 leads to a sequestration of cholesterol in late endosomes leading to decreased levels in other cellular compartments like the Golgi complex and the plasma membrane (Cubells et al., 2007). Musiol et al. showed that correct transport of cholesterol from late endosomes to the plasma membrane is important for IAV replication and suggest that intracellular cholesterol imbalance produced by the overexpression of AnxA6 has an antiviral activity (Musiol et al., 2013). Reverter et al. indicated that transport of cholesterol from late endosomes to the Golgi complex regulates trafficking and localisation of t-SNAREs whereas Cornely et al. showed that AnxA6 interacts with membrane microdomains and regulate the localisation of cell surface receptors (Cornely et al., 2011, Reverter et al., 2011). This latter study together with previous investigations identify cholesterol as a critical factor during IAV infection which is very interesting since it is one major component of the lipid rafts where viral budding occurs (Musiol et al., 2013, Veit and Thaa, 2011, Sun and Whittaker, 2003). However, cholesterol is not only critical for IAV life cycle but it is also for other viruses such as enteroviruses and the Andes Virus (ANDV) belonging to the Bunyaviridae family. Enteroviruses are able to regulate the intracellular cholesterol through the cellular endocytic machinery for efficient replication whereas inhibition of genes participating in cholesterol synthesis and uptake was blocking the ANDV infection identifying the major cellular sterol regulatory pathway as essential for ANDV (Petersen et al., 2014, Ilnytska et al., 2013). In addition, it was suggested that cholesterol-enriched rafts behave as signalling platforms that link intracellular signalling pathways with

extracellular processes (Munro, 2003). Thus, targeting cellular factors which regulate the transport of cholesterol and phospholipids inside the cell will help to identify key molecules responsible for the negative modulation of IAV infection by AnxA6. For instance, an extremely interesting factor to target would be the sterol carrier protein-2 (SCP-2), a protein that binds and transfers cholesterol and phospholipids inside the cell to regulate multiple signalling pathways in lipid rafts/caveolae. In vitro experiments with cells overexpressing SCP-2 showed that SCP-2 could determine the structure and function of lipid rafts/caveolae by redistributing signalling lipids between rafts and other intracellular sites. SCP-2 has a central role in the enrichment of raft-associated signalling lipids such as cholesterol, ceramide, fatty acids or phosphatidylinositol (PI) (Schroeder et al., 2007). SCP-2 is known to have a high affinity for lipid molecules that participate in intracellular signalling and regulates their transport between cellular compartments by controlling either vesicle trafficking or protein-mediated lipid transport. For instance, SCP-2 could bind PIs to present them as signalling lipid substrates and their transport within rafts/caveolae (Schroeder et al., 2007). In a recent study, phosphatidylinositol 4,5 bisphosphate (PI(4,5)P<sub>2</sub>) was described as a low abundant lipid present in membranes involved in many cellular events such as membrane curvature, fission of endosomes or exocytosis. It has been shown to be required for internalisation and infection of foot-and-mouth disease virus and of vesicular stomatitis virus and as well to participate in HIV assembly by recruiting the Gag viral protein to the plasma membrane. In this study, the authors suggest the modulation of PI(4,5)P<sub>2</sub> and the activity of the phosphatidylinositol-4-phosphate-5-kinase (PIP5K), which produces PI(4,5)P<sub>2</sub>, as a new antiviral strategy (Vazquez-Calvo et al., 2012). Therefore, it would be interesting to verify whether PI(4,5)P<sub>2</sub> also affects IAV infection. Also, the vesicle-associated membrane protein (VAMP)-associated protein A (VAPA) and oxysterol-binding protein (OSBP) are additional factors to study since they have been recently described to participate in the transport of cholesterol from endoplasmic reticulum to the plasma membrane and other organelles and therefore they could also be involved in the restriction of IAV. Action of VAPA and OSBP is coordinated by the ceramide-transfer protein (CERT), which transfers ceramide between ER and Golgi complex (Peretti et

al., 2008). Ceramide is a lipid involved in several biological processes that has recently been described to be present and to displace cholesterol and other sterols in lipid rafts and could have a repercussion on proteins that bind with cholesterol in these membrane domains (Castro et al., 2014, Megha and London, 2004). Finally, factors previously described such as caveolin-1 and cPLA2 could also be of interest together with syntaxin 6 whose inhibition leads to a reduction of caveolin-1/caveolae at the plasma membrane and the polymerase I and transcript release factor (PITRF) (called as well Cav-p60 or Cavin) which regulate the structure and function of caveolae after being recruited to membrane domains with cholesterol, PS and caveolin (Hill et al., 2008, Choudhury et al., 2006). These previous investigations led us to study a second hypothesis which is that AnxA6 might indirectly regulate IAV infection through imbalance in cholesterol homeostasis, which affects the formation of the viral budzone by altering the trafficking of viral proteins to the cell surface. We first studied the total and surface expression of M2 and other structural proteins by flow cytometry. We found that total expression of M2 decreased in infected cells over-expressing AnxA6 contrarily to the rest of viral proteins which were not affected by AnxA6 expression; but also and more importantly that expression of M2 and other viral proteins at the surface was reduced in the presence of AnxA6 (figure 3.11). These results determined that AnxA6 down-regulates total expression of M2, and as a consequence, expression of M2 and other viral proteins is impaired at the surface of infected cells. These results are in agreement with the western blot experiments carried out to study whether AnxA6 affects the association of cellular AnxA6 and viral M2, M1, NP and H3 proteins with Triton X-100 soluble versus insoluble cellular fractions (figure 3.14). We demonstrated that AnxA6 has an effect on the association of M2 viral protein with detergent resistant membranes (DRM) since a noticeable difference of expression was observed between A431 and A431-AnxA6 cells upon infection. Interestingly, reduced levels of M2 were detected in both soluble and insoluble fractions in A431-Anx6 cells compared to A431 cells. However, no major changes were found in association of other viral proteins such as M1, NP and H3 to soluble and insoluble fractions when AnxA6 over-expression. This is also in agreement with an immunofluorescence experiment performed to study whether AnxA6 over-

expression leads to a change in subcellular localisation of M1 viral protein as we could not observe differences in M1 localisation which was mainly found in the nucleus and perinuclear region in both cell lines due to its role in viral replication and transcription (figure 3.9) (Martin and Helenius, 1991). Altogether, these results suggest that AnxA6 down-regulates total expression of M2, which subsequently affects M2 protein levels at the cell surface. We also observed that in addition to M2, expression of other viral proteins were reduced at the surface of infected cells. It is now very clear that AnxA6 regulates total M2 expression and drives an M2-dependent mechanism of IAV restriction. As we found that M2 down-regulation is very evident, we tried to identify which pathway is targeted by AnxA6 for M2 degradation. AnxA6 is implicated in the regulation of the endosomal/lysosomal pathway as it controls trafficking of endo- and exocytic vesicles along the secretory pathway. It was found that AnxA6 is responsible for the endocytosis of low-density lipoproteins (LDL) and its transport to lysosomes for degradation (Cubells et al., 2007; Grewal et al., 2000). To date, no link between AnxA6 expression and regulation of proteasome pathway activation has been found; however, it has already been described that proteasome is involved in regulation of sorting of cytosolic, nuclear or membrane proteins to lysosomes which can then be degraded when ubiquitinated (Dong et al., 2004, van Kerkhof et al., 2001). Protein synthesis, transport and degradation are tightly regulated to maintain cellular homeostasis. Cells have developed many ways of degrading proteins; however, the proteasome is the most important pathway participating in protein sorting. The proteasome is activated when target nuclear and cytosolic proteins become polyubiquitinated. Ubiquitin is a polypeptide that binds to the amino group of the side chain of a lysine residue on a target protein; and attachment of multiple ubiquitins results in the formation of a multiubiquitin chain that acts as a signal for protein recognition by the proteasome system and subsequent degradation (Lecker et al., 2006). In addition, single ubiquitination of membrane proteins such as cell surface receptors leads to endocytosis and subsequent endosomal sorting for degradation in lysosomes (van Kerkhof et al., 2001). Interestingly, several studies have shown the importance of the ubiquitin/proteasome during viral infection: the ubiquitin/proteasome system was found to participate in the entry and

endosomal trafficking of Kaposi's Sarcoma-associated Herpesvirus in endothelial cells, to assist in infection and propagation of dengue virus in mosquitoes and also in replication of coxsackievirus in mouse cardiomyocytes (Choy et al., 2015, Greene et al., 2012, Gao et al., 2008a, Luo et al., 2003). Infection of other viruses such as hepatitis A virus, hepatitis C virus, vesicular stomatitis virus, poliovirus or HIV-1 is also dependent on the proteasome system (Choi et al., 2013, Neznanov et al., 2008). Therefore, we performed a flow cytometry experiment to investigate whether blockage of lysosomal and proteasome pathways were responsible for M2 degradation in cells over-expressing AnxA6, and to understand the mechanism behind its down-regulation (figure 3.15). We found that blockage of proteasome by the MG132 inhibitor did not lead to an accumulation of M2; however, blockage of lysosomal pathway by ammonium chloride resulted in the accumulation of M2 protein at 24h post-infection. Also, we found that blockage of these pathways did not translate in H3 protein accumulation, suggesting that M2 down-regulation by AnxA6 is a protein-specific mechanism. As it is possible that a compensation mechanism could happen inside host cells enabling M2 to escape from degradation when any of these pathways is inhibited individually, we also studied levels of M2 expression when both pathways are simultaneously inhibited and we found that M2 protein expression was reduced, suggesting that these pathways are essential for cell viability and normal function. We concluded that AnxA6 inhibits IAV infection by targeting M2 protein down-regulation by regulating the lysosomal pathway. As already described, M2 also plays an important role in release and budding of viral particles, it regulates a negative membrane curvature which leads to the pinching off virions from the surface of infected cells (Roberts et al., 2013). We therefore analysed the consequences of M2 down-regulation at the cell surface by transmission electron microscopy (figures 3.16 and 3.17). We found that long viral filaments, well individualised were budding from A431 cells, whereas interconnected viral filaments were observed in A431-AnxA6 cells. In addition, a more important number of viral particles were found in cells over-expressing AnxA6. These findings led us to conclude that AnxA6 overexpression leads to an impaired viral release due to an incomplete scission of filamentous virus particles (figure 4.1).

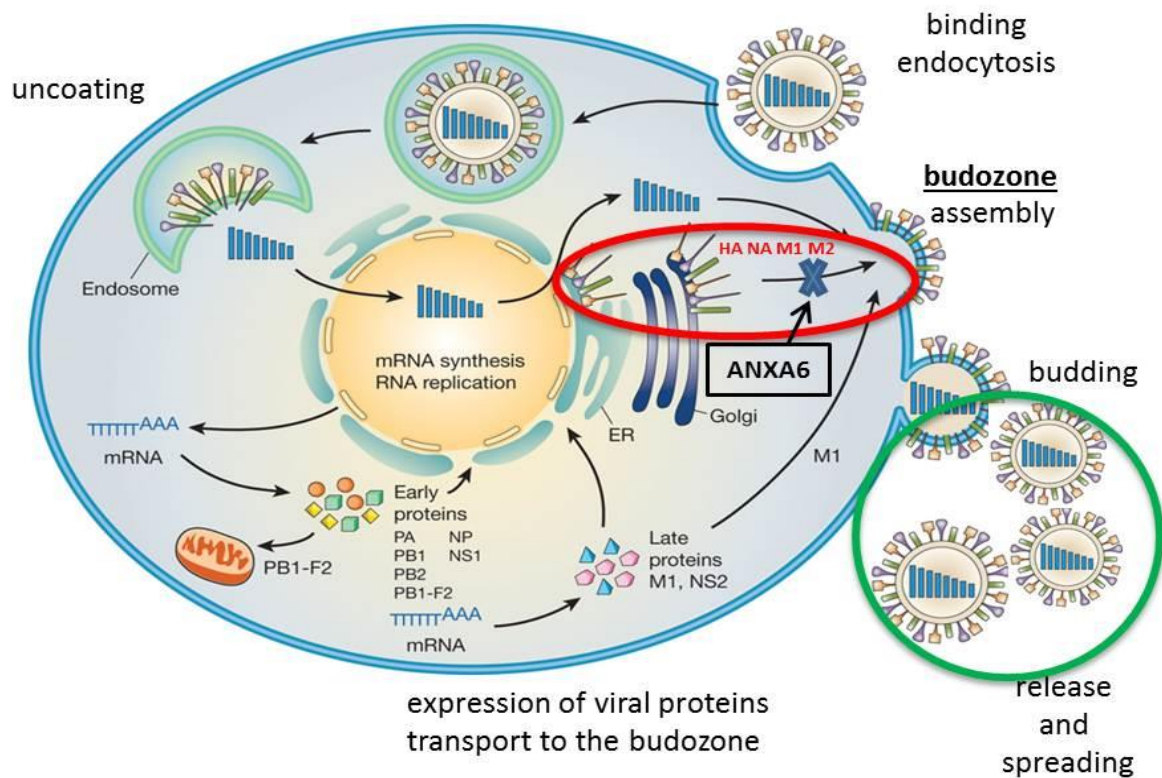


**Figure 4.1. Suggested model of the restriction molecular mechanism of influenza A virus by human annexin A6.** Annexin A6 affects late stages of virus life cycle by interfering with the formation of the viral budozone. It alters the trafficking of viral proteins to the cell surface (indicated in red), and especially M2 protein which plays a role in scission and budding of viral particles from the plasma membrane of infected cells. Reduced expression of M2 at the cell surface leads to a defect in virus morphogenesis and in incomplete scission of virions, resulting in the tethering of budding virions (indicated in green). Adapted from Neumann et al., 2009.

However, events of colocalisation of annexin A6 and M2 have already been observed in Ma's study and therefore further analysis by confocal microscopy and also by transmission electron microscopy after the labelling of AnxA6 and the M2 viral proteins with the specific antibodies will further clarify whether these proteins colocalize to the basis of budding filaments as we believe that higher resolution is required to conclude on this hypothesis. Also, analysis of the morphogenesis of the virus by TEM will enable to further understand the defects in viral assembly and clustering of viral proteins during their trafficking to lipid rafts. Combination of ultrastructural analysis of nascent virions and immuno-labelling of viral proteins and staining

of cholesterol using lipid probes such as filipin will also be used by TEM to link annexin A6 overexpression with misbalance of cholesterol, defect of compartmentalisation of viral proteins and deficiency in morphogenesis. Also, the misbalance of viral proteins in cells over-expressing annexin A6 could be analysed by photoactivated localization microscopy (PALM), which combines fluorescence and high-resolution microscopy. This approach could be used to analyse and quantify maps of clustered proteins and to observe differences in cells expressing Annexin A6 using specific probes against cholesterol and other lipids inside infected cells. To further understand the mechanism of viral restriction by Annexin A6, it would be interesting to perform a cell fractionation assay on IAV infected cells to clarify whether Annexin A6 expression leads to a retention of viral proteins in specific cellular compartments. Finally, western blot and immunofluorescence experiments demonstrated that no AnxA6 was found in purified viral particles of influenza A/Udorn/72 (H3N2) suggesting that it is not recruited with other viral and cellular components into newly formed virions, which reinforces the hypothesis of an indirect virus restriction by an imbalanced cholesterol homeostasis produced by AnxA6 during IAV infection (figure 3.10). However, samples containing higher titres of purified viral particles may be required for AnxA6 detection by western blot as it has already been detected in purified viral particles of influenza A/WSN/33 (H1N1), a more pathogenic strain.

## **4.2 Annexin A6 modulates important intracellular signalling pathways required for influenza A virus infection**

The role of Annexin A6 in the regulation of intracellular signalling pathways is still poorly understood, only few studies have described AnxA6 involvement in their modulation. A study performed by Minashima identified AnxA6 as a modulator of ERK and p38 MAPKs by binding to PKC $\alpha$  upon changes in intracellular Ca<sup>(2+)</sup> concentration and another study led by Campbell identified AnxA6 interaction with p65 subunit of the NF- $\kappa$ B transcription factor to regulate its activation in chondrocytes (Campbell et al., 2013; Minashima et al., 2012). Interestingly, several studies have demonstrated MAPKs and other intracellular protein regulators of signal transduction activation during early influenza infection. Cannon and co-workers showed that different MAPKs are activated during early infection in mouse macrophages. They found that phosphorylation of extracellular regulated kinases 1 and 2 (ERK 1/2), p38 and c-Jun kinases 1 and 2 (JNK 1/2) MAPKs is increased between 15 minutes and 3 hours post-infection (Cannon et al., 2014). Also, a later study determined that inhibition of Akt kinase activity suppresses entry and replication of influenza virus and exhibits an antiviral activity during early phase of infection (Hirata et al., 2014). Another study showed that Akt is up-regulated during early influenza infection and suggested that activation of PI3k-Akt signalling has a protective role against viral replication. This study also showed an up-regulation of p53 pathway in late infection inducing apoptosis and cell death to reduce virus propagation (Zhirnov and Klenk, 2007). Nailwal and co-workers found that NP viral protein is responsible for p53 modulation by their direct interaction (Nailwal et al., 2015). Then, the heat shock protein 27 (HSP27) was found to interact with the IAV NS1 protein and their interaction led to a reduced expression of interferon beta (Li et al., 2012). Finally, mTOR and p70S6K kinases have been described to participate in the interplay between apoptosis and autophagy during IAV infection (Datan et al., 2014). Therefore, we investigated whether AnxA6 overexpression modulates intracellular signalling pathways during IAV infection to induce an antiviral response. We first analysed phosphorylation/activation of important MAPKs and other

intracellular protein regulators of signal transduction between 30 minutes and 4 hours post-infection with a phospho-proteome profiler (figures 3.19 and 3.20) and by western blot (figure 3.21). We found no important differences in phosphorylation of Akt modules between cell lines with the proteome profiler, which was in disagreement with results obtained by western blot as no activation was observed in non-infected samples and less activation was found at 0.5, 1 and 4h p.i. in cells over-expressing AnxA6. Several studies have shown that PI3K/Akt pathway plays an important role during IAV infection. Hirata and co-workers demonstrated that inhibition of Akt kinase activity reduces uptake and virus replication (Hirata et al., 2014). Also, it was previously found that IAV NS1 protein can bind to and activate PI3K, which subsequently activates Akt leading to suppression of antiapoptotic signals through inhibition of GSK-3 $\beta$  and caspase 9. This study showed the modulation of Akt activation by NS1 protein in order to prevent apoptosis and ensure efficient virus replication (Ehrhardt et al., 2007). Therefore, we suggest that AnxA6 reduces activation of Akt during early infection to limit PI3K/Akt virus-supporting activity and limit viral replication and propagation. It would be very interesting to check expression levels of Akt regulators such as phosphoinositide-3 kinase (PI3K), activator, and phosphatase and tensin homology (PTEN), repressor, during IAV infection in AnxA6 overexpressing cells. The study of IAV replication capacity when inhibitors of these factors are used would enable to better understand the tight regulation of these pathways by AnxA6 during infection (Hers et al., 2011). Also, cleavage of PARP could be investigated to determine the effect of AnxA6 regulation of apoptosis during infection as performed by Ehrhardt in the study of Akt regulation by NS1 (Ehrhardt et al., 2007). This investigation would enable to decipher the link between AnxA6 modulation of Akt signalling and its implication in viral restriction. In addition, ERK 1/2 are well activated between 15 minutes and 3 hours post-infection and have been identified as important regulators in the production of inflammatory cytokines and chemokines (Cannon et al., 2014). We found with the proteome profiler increased ERK1 phosphorylation in cells over-expressing AnxA6 upon influenza infection, whereas ERK2 was exhibiting higher levels of phosphorylation at 0.5h p.i. in cells over-expressing AnxA6 only (figure 3.20). These results are not in agreement with the

western blot as we found a biphasic ERK1/2 activation by AnxA6 as more phosphorylated ERK1/2 at 0.5h but less phosphorylated/activated ERK1/2 at 1 and 4 hours post-infection in A549 cells over-expressing AnxA6 was detected (figure 3.21). These results suggest that AnxA6 over-expression leads to an increased activation of ERK 1/2 at 0.5h p.i. to stimulate the production of pro-inflammatory cytokines during early infection. By using MAPKs inhibitors, Cannon demonstrated that ERK and JNK are responsible for the production of TNF $\alpha$ , MCP-1, CCL2, MIP-1 $\alpha$ , CCL4 and IP-10 between 3 and 24h post-infection in murine macrophages (Cannon et al., 2014). However, another study found an important function of ERK during early infection: its activation together with PI3K enables acidification in intracellular compartments through vacuolar ATP-dependent proton pumps (V-ATPase) activity which promoted fusion of viral and cellular membranes for the release of vRNA during infection (Marjuki et al., 2011). In this study, it was shown that IAV manipulates ERK and PI3K pathways to facilitate early stages of viral infection. Marjuki and collaborators showed that IAV infection led to early activation of ERK and PI3K signalling cascades, which mediated intracellular acidification by stimulation of vATPase and membranes fusion. They found that activated ERK and PI3K colocalize and interact with subunit E of the V-ATPase V1 domain upon IAV infection to stimulate V-ATPase activity. V-ATPase activation also resulted in increased RNP import into the nucleus, virus replication and transcription. Altogether, they suggested that IAV-dependent activation of ERK and PI3K-mediated V-ATPase activity is essential for virus replication and propagation (Marjuki et al., 2011). In addition, no activation of JNK was observed by western blot but the proteome profiler showed more activation of JNK1/3 but less JNK2/Pan in cells over-expressing AnxA6 (figure 3.20). These results need to be confirmed as JNK was already found to be activated in order to stimulate production of cytokines. Our preliminary results and the findings previously published led us to investigate whether changes in MAPKs activation regulated by AnxA6 could also translate into changes in cytokines expression. We therefore performed real-time PCRs to study transcription levels of cytokines well known to be produced during IAV infection. We analysed mRNA levels of cytokines at MOI=1 and MOI=5: no important differences in mRNA expression of interferon- $\beta$ , IL-1 $\beta$ , RANTES and NF- $\kappa$ B were observed;

however, AnxA6 over-expression led to significant increased mRNA levels of TNF $\alpha$  and IL-8 (figures 3.22 and 3.23). These results suggest that AnxA6 expression potentiates the production of cytokines during infection. It would be interesting to study mRNA levels of TNF $\alpha$  and IL-8 when using specific MAPK inhibitors in order to confirm whether their regulation is MAPK dependent, especially ERK inhibitors are likely to affect cytokines production as it has already shown in the study carried out by Cannon (Cannon et al., 2014). Finally, we have already mentioned that NF- $\kappa$ B activation is regulated by AnxA6 and that NF- $\kappa$ B contributes to the innate immune response against IAV by regulating many signalling pathways leading to production of interferons and many other cytokines. However, many studies have shown the controversial manipulation of NF- $\kappa$ B by influenza virus, as it has also been shown that its activation is required for viral infection (Nimmerjahn et al., 2004). Therefore, we tested activation of NF- $\kappa$ B during early and late infection by imaging flow cytometry and immunofluorescence. We found that AnxA6 over-expression in lung epithelial cells leads to higher NF- $\kappa$ B nuclear translocation in IAV infected cells during late but not during early infection and we suggest that AnxA6 potentiates the NF- $\kappa$ B-dependent innate antiviral response (figure 3.24). However, future experiments should be performed in order to study changes in NF- $\kappa$ B gene expression between cell lines, as an example it would be very interesting to perform a luciferase reporter assay using an expression vector with the regulatory region of NF- $\kappa$ B upstream of the luciferase reporter gene to analyse the increase in NF- $\kappa$ B gene expression and transcription in AnxA6 over-expressing cells during infection. Also, Pinto and collaborators demonstrated the NF- $\kappa$ B-dependent stimulation of IL-6, IL-8 and RANTES upon infection of different IAV strains in A549 lung epithelial cells also used in our study, thus analysis of changes in transcriptional levels of cytokines when using NF- $\kappa$ B inhibitors in cells over-expressing AnxA6 would enable to confirm whether AnxA6 regulates synthesis of cytokines via NF- $\kappa$ B activation (figure 4.2). As already mentioned, we found an increase in IL-8 mRNA levels in AnxA6 over-expressing cells during viral infection, which could suggest that AnxA6 could promote neutrophil recruitment to sites of infection by up-regulating IL-8 production (Pinto et al., 2011).

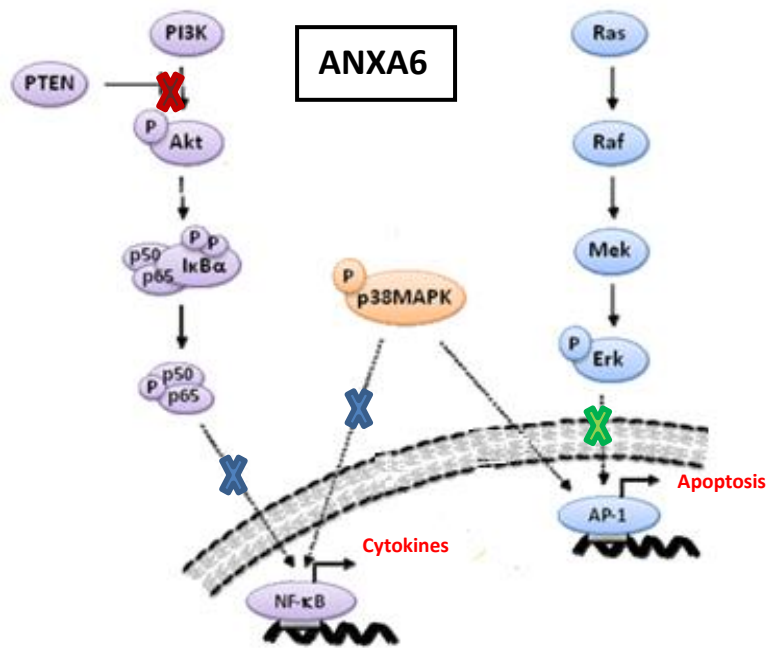


**Figure 4.2. Targeting intracellular pathways to clarify the role of AnxA6 in their regulation during influenza infection.** Different pathways playing a role during viral infection could be targeted with pharmacological drugs at different levels to understand their regulation by human AnxA6. For instance, Akt could be targeted by inhibiting either PTEN or PI3K as they are the upstream regulators of this pathway (indicated in red). Also, NF-κB and ERK MAPK can be inhibited with specific inhibitors to block their activation (indicated in blue and green respectively). Adapted from Campbell et al., 2013.

### **4.3 Influenza A virus down-regulates annexin A6**

We have already mentioned that viruses have developed strategies to counteract the host innate and adaptive immune responses. Influenza virus is able to encode proteins that limit antiviral immunity during infection. The non-structural protein 1 (NS1), both PB2 and PB1-F2 components of the polymerase complex and M2 are the main proteins playing a role in the defeat of immune responses. These proteins interact with host factors at different levels and inhibit signalling pathways regulating an antiviral response to infection such as RIG-I, IFNs or autophagy and cell death pathways (Goraya et al., 2015; Zhirnov and Klenk, 2013; Van de Sandt et al., 2012; Sharma et al., 2011; Guan et al., 2011; Gack et al., 2009; Li et al., 2006; Ludwig et al., 2002; Talon et al., 2000; Wang et al., 2000). In addition, we speculated that IAV could also regulate other host factors executing a restriction on viral infection and propagation. As our study aims at deciphering the molecular mechanism of viral restriction by AnxA6 and its involvement in an antiviral immune response, we suspected that IAV could repress AnxA6 expression as a strategy of defence. We therefore first analysed endogenous and exogenous AnxA6 mRNA levels after infection with different viral strains and we found a clear down-regulation of endogenous AnxA6 gene expression during infection (figures 3.25 and 3.26). However, no down-regulation in mRNA levels was observed for the exogenous AnxA6, which increased in A549 cells over-expressing AnxA6 upon infection when compared to non-infected cells. We then analysed protein levels of endogenous and exogenous AnxA6 and we found that endogenous AnxA6 protein is only down-regulated at around 70-72 h p.i. unlike exogenous AnxA6 protein which is up-regulated during infection (figures 3.29 and 3.31). Lifespan of AnxA6 protein is of about 48-72 hours, which could be the reason why reduction in AnxA6 protein expression is only significant at 70h p.i.. However, these results led us to study by qPCR whether infection has a bystander effect on AnxA6 mRNA gene expression and also mRNA expression levels of IL-1 $\beta$  and TNF $\alpha$ . Again, we did not see significant changes in cytokines and AnxA6 gene expression suggesting that no bystander effect happens during infection. Furthermore, it is now well known that a general shutdown occurs

in the cell during infection, which results in the inhibition of host cell transcription, mRNA degradation and cell protein synthesis. It is then necessary to study transcription levels of AnxA6-neighbouring genes as it would clarify whether AnxA6 down-regulation is specifically targeted by the virus or it is a consequence of the general shut down. As an example, it would be interesting to study the changes in mRNA levels of glutathione peroxidase 3 (GPX3) and TNF-alpha induced protein 3 interacting protein 1 (TNIP1) genes, which are located in close proximity to AnxA6 in the chromosome 5 (figure 4.3). Finally, a study led by Wang and collaborators indicated that AnxA6 gene expression is down-regulated in gastric cancer cells and its promoter region can be methylated. Therefore, it would be very interesting to study whether AnxA6 DNA promoter is also methylated during viral infection, which would clarify whether methylation is the cause for a delay in protein down-regulation and explain its expression changes (Wang et al., 2013). Interestingly, other genes have been shown to be methylated during IAV infection: proinflammatory cytokines CXCL14, CCL25, CXCL6, and interleukines IL13, IL17C, IL4R were exhibiting changes in their promoter methylation which could regulate their expression to limit viral infection (Mukherjee et al., 2013). We conclude that IAV down-regulates AnxA6 gene expression during early infection and AnxA6 protein during late infection as a mechanism of defence against AnxA6.

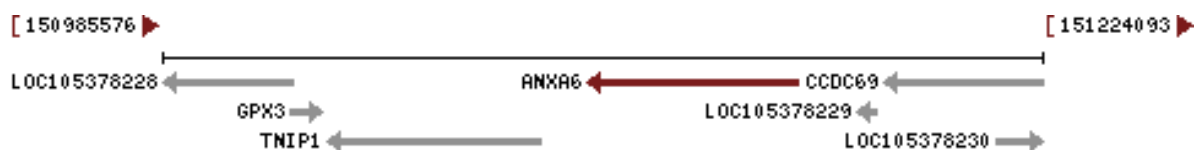


**Figure 4.3. Map of the AnxA6-related region on chromosome 5.** Annexin A6 is located in the locus 5q33.1, in close proximity to genes GPX3 and TNIP1. From NCBI.

In conclusion, we confirm that AnxA6 restricts IAV infection by down-regulating total M2 protein expression, and as a consequence affects expression of M2 and other viral proteins at the cell surface. In addition, we have found that inhibition of the lysosomal pathway leads to an increased total M2 protein expression, suggesting its involvement in IAV restriction by AnxA6. We therefore suggest that AnxA6 targets M2 protein degradation by regulating the

lysosomal pathway, which results in defective IAV morphogenesis and budding from infected cells. Also, we found that AnxA6 modulates activation of signalling pathways to limit virus propagation and potentiates an innate immune response, it is necessary to confirm by which molecular mechanism AnxA6 regulates this antiviral response. Finally, we show that IAV down-regulates AnxA6 expression at mRNA and protein levels during early and late infection respectively, and it is necessary to further study the cross-talk between the virus and the host.

## 5 CONCLUSIONS AND PERSPECTIVES

In the previous study performed by our group, it was found that human AnxA6 interacts with the IAV M2 proton channel and limits production of progeny IAV from infected cells. They found that depletion of AnxA6 led to increased viral titers and overexpression of AnxA6 correlated with reduced viral titers. Also, it was found that overexpression of AnxA6 impairs morphogenesis and release of progeny viruses as infection of AnxA6-overexpressing cells with a spherical strain led to budding of elongated and interconnected virions (Ma et al., 2012). These findings were supported by a later study which determined that AnxA6 has a critical role in the late endosomal cholesterol balance and affects viral replication and propagation in AnxA6-overexpressing cells infected with IAV, suggesting that AnxA6 is the link between the cholesterol homeostasis in the cell and IAV infection cycle (Musiol et al., 2013). In this work, we further analysed the effect of AnxA6 on the negative modulation of influenza virus infection and investigated the molecular mechanism responsible for restriction of IAV morphogenesis by AnxA6 by using the filamentous influenza A/Udorn/72 (H3N2) strain. Interestingly, we found by flow cytometry and western blot that AnxA6 leads to M2 down-regulation, and as a consequence, M2 protein expression at the cell surface was also impaired. In addition, we suggest that AnxA6 over-expression targets M2 viral protein for degradation through the lysosomal pathway as we found that blockage of this pathway with NH<sub>4</sub>Cl in AnxA6 over-expressing cells resulted in increased total M2 protein expression. Also, we observed that both M2 and AnxA6 proteins were present in the cytosol and we believe they could be found together inside vesicular-like compartments. By electron microscopy, we found more important number of viral particles in cells over-expressing AnxA6, which were interconnected and attached at the surface of infected cells suggesting that AnxA6 overexpression leads to an impaired viral release due to an incomplete scission of filamentous virus particles. Altogether, these results suggest that AnxA6 impairs total and surface expression of M2 protein, which subsequently has an impact in the normal morphogenesis and release of IAV. Our study reveals the molecular mechanism of restriction of IAV morphogenesis and release

by AnxA6; however, further investigation is required to better understand the deficit in expression of viral proteins to cell surface and degradation of M2 protein, a key viral component for the completion of IAV life cycle. In the future, we intend to better understand AnxA6 involvement in the regulation of the pathways responsible for M2 protein degradation. Also, we will confirm by higher resolution microscopy followed by the immune-gold labelling of cellular AnxA6 and viral M2 proteins whether they colocalize at the plasma membrane and we will clarify whether AnxA6 interferes with the formation of the IAV budzone by physically interacting with M2 cytoplasmic tail at the neck of budding particles and by generating a mechanical restraint on M2 during the scission event. Confocal microscopy, transmission electron microscopy or photoactivated localization microscopy could be used to analyse localisation of these proteins in addition to cholesterol and other lipids and will be essential to further understand the AnxA6-dependent mechanism of IAV restriction and to provide the link of annexin A6 overexpression with misbalance of cholesterol, defect of compartmentalisation of viral proteins and deficiency in morphogenesis.

In our study, we also investigated AnxA6 implication in the modulation of important cellular pathways required for influenza virus infection and in the regulation of an inflammatory response. We based our study on the fact that even though the role of Annexin A6 in the regulation of intracellular signalling pathways is still poorly understood, some studies have shown that AnxA6 is involved in the modulation of ERK and p38 MAPKs by binding to PKC $\alpha$  and of NF- $\kappa$ B transcription factor through its interaction with p65 subunit (Campbell et al., 2013; Minashima et al., 2012). In addition, many studies have demonstrated the link between activation of these pathways and the synthesis of pro-inflammatory cytokines during IAV infection (Cannon et al., 2014). We found that AnxA6 reduces activation of Akt and increases activation of ERK signalling pathways during early infection. Also, we observed that AnxA6 overexpression leads to higher activation of NF- $\kappa$ B at late times of infection. Furthermore, differences in cytokine expression were observed during IAV infection between lung epithelial cells which express endogenous levels of AnxA6 and cells overexpressing AnxA6. Differences

were especially important in expression of TNF $\alpha$  and IL-8 cytokines. We concluded that regulation of these pathways by AnxA6 enable to build a pro-inflammatory innate immune response to limit viral replication and propagation. In the future, we intend to use specific inhibitors to block activation of these pathways and we will demonstrate the AnxA6-dependent regulation and its impact on the stimulation of an innate immune response during IAV infection.

Finally, we investigated whether AnxA6 is down-regulated by IAV during infection as it is well known that viruses have developed new strategies to evade host immune responses (Van de Sandt et al., 2012). We found that mRNA levels of AnxA6 were down-regulated during early and late infection, whereas protein levels were only reduced at late times of infection. We suggested that IAV has established a mechanism which enables to limit AnxA6 restriction during viral propagation. In the future, we will clarify whether AnxA6 down-regulation is due to a general shutdown state which is induced by the virus upon host infection or whether it is a specific and targeted down-regulation. For that, we will analyse mRNA and protein expression levels of host cellular factors such as GPX3 and TNIP1 as they are found in close proximity to AnxA6 gene in the chromosomal location. Also, it will be interesting to analyse whether this down-regulation is regulated by AnxA6 interaction with M2 cytoplasmic tail.

## 6 BIBLIOGRAPHY

- ADAMS, J. 2003. The proteasome: structure, function, and role in the cell. *Cancer Treat Rev*, 29 Suppl 1, 3-9.
- ALI, A., AVALOS, R. T., PONIMASKIN, E. & NAYAK, D. P. 2000. Influenza virus assembly: effect of influenza virus glycoproteins on the membrane association of M1 protein. *J Virol*, 74, 8709-19.
- ALMOND, J. W. & FELSENREICH, V. 1982. Phosphorylation of the nucleoprotein of an avian influenza virus. *J Gen Virol*, 60, 295-305.
- ALVAREZ-GUAITA, A., VILA DE MUGA, S., OWEN, D. M., WILLIAMSON, D., MAGENAU, A., GARCIA-MELERO, A., REVERTER, M., HOQUE, M., CAIRNS, R., CORNELLY, R., TEBAR, F., GREWAL, T., GAUS, K., AYALA-SANMARTIN, J., ENRICH, C. & RENTERO, C. 2015. Evidence for annexin A6-dependent plasma membrane remodelling of lipid domains. *Br J Pharmacol*, 172, 1677-90.
- AMORIM, M. J., BRUCE, E. A., READ, E. K., FOEGLEIN, A., MAHEN, R., STUART, A. D. & DIGARD, P. 2011. A Rab11- and microtubule-dependent mechanism for cytoplasmic transport of influenza A virus viral RNA. *J Virol*, 85, 4143-56.
- ANEGON, I., CUTURI, M. C., TRINCHIERI, G. & PERUSSIA, B. 1988. Interaction of Fc receptor (CD16) ligands induces transcription of interleukin 2 receptor (CD25) and lymphokine genes and expression of their products in human natural killer cells. *J Exp Med*, 167, 452-72.
- ARIMORI, Y., NAKAMURA, R., YAMADA, H., SHIBATA, K., MAEDA, N., KASE, T. & YOSHIKAI, Y. 2013. Type I interferon limits influenza virus-induced acute lung injury by regulation of excessive inflammation in mice. *Antiviral Res*, 99, 230-7.
- ARNON, T. I., LEV, M., KATZ, G., CHERNOBROV, Y., PORGADOR, A. & MANDELBOIM, O. 2001. Recognition of viral hemagglutinins by NKp44 but not by NKp30. *Eur J Immunol*, 31, 2680-9.
- ARRANZ, R., COLOMA, R., CHICHON, F. J., CONESA, J. J., CARRASCOSA, J. L., VALPUESTA, J. M., ORTIN, J. & MARTIN-BENITO, J. 2012. The structure of native influenza virion ribonucleoproteins. *Science*, 338, 1634-7.
- ARRESE, M. & PORTELA, A. 1996. Serine 3 is critical for phosphorylation at the N-terminal end of the nucleoprotein of influenza virus A/Victoria/3/75. *J Virol*, 70, 3385-91.
- ASAI, Y., HASHIMOTO, S., KUJIME, K., GON, Y., MIZUMURA, K., SHIMIZU, K. & HORIE, T. 2001. Amantadine inhibits RANTES production by influenzavirus-infected human bronchial epithelial cells. *Br J Pharmacol*, 132, 918-24.
- AVILA-SAKAR, A. J., CREUTZ, C. E. & KRETSINGER, R. H. 1998. Crystal structure of bovine annexin VI in a calcium-bound state. *Biochim Biophys Acta*, 1387, 103-16.
- BABIYCHUK, E. B. & DRAEGER, A. 2000. Annexins in cell membrane dynamics. Ca(2+)-regulated association of lipid microdomains. *J Cell Biol*, 150, 1113-24.
- BALCAROVA-STANDER, J., PFEIFFER, S. E., FULLER, S. D. & SIMONS, K. 1984. Development of cell surface polarity in the epithelial Madin-Darby canine kidney (MDCK) cell line. *EMBO J*, 3, 2687-94.
- BARMAN, S., ADHIKARY, L., CHAKRABARTI, A. K., BERNAS, C., KAWAOKA, Y. & NAYAK, D. P. 2004. Role of transmembrane domain and cytoplasmic tail amino acid sequences of influenza A virus neuraminidase in raft association and virus budding. *J Virol*, 78, 5258-69.
- BARMAN, S., ALI, A., HUI, E. K., ADHIKARY, L. & NAYAK, D. P. 2001. Transport of viral proteins to the apical membranes and interaction of matrix protein with glycoproteins in the assembly of influenza viruses. *Virus Res*, 77, 61-9.
- BARMAN, S. & NAYAK, D. P. 2007. Lipid raft disruption by cholesterol depletion enhances influenza A virus budding from MDCK cells. *J Virol*, 81, 12169-78.
- BATRA, J., TRIPATHI, S., KUMAR, A., KATZ, J. M., COX, N. J., LAL, R. B., SAMBHARA, S. & LAL, S. K. 2016. Human Heat shock protein 40 (Hsp40/DnaJ1) promotes influenza A virus replication by assisting nuclear import of viral ribonucleoproteins. *Sci Rep*, 6, 19063.

- BAUDIN, F., PETIT, I., WEISSEHORN, W. & RUIGROK, R. W. 2001. In vitro dissection of the membrane and RNP binding activities of influenza virus M1 protein. *Virology*, 281, 102-8.
- BEALE, R., WISE, H., STUART, A., RAVENHILL, B. J., DIGARD, P. & RANDOW, F. 2014. A LC3-interacting motif in the influenza A virus M2 protein is required to subvert autophagy and maintain virion stability. *Cell Host Microbe*, 15, 239-47.
- BERGGARD, T., LINSE, S. & JAMES, P. 2007. Methods for the detection and analysis of protein-protein interactions. *Proteomics*, 7, 2833-42.
- BERTRAM, S., GLOWACKA, I., BLAZEJEWSKA, P., SOILLEUX, E., ALLEN, P., DANISCH, S., STEFFEN, I., CHOI, S. Y., PARK, Y., SCHNEIDER, H., SCHUGHART, K. & POHLMANN, S. 2010. TMPRSS2 and TMPRSS4 facilitate trypsin-independent spread of influenza virus in Caco-2 cells. *J Virol*, 84, 10016-25.
- BILLIAU, A. 2006. Interferon: the pathways of discovery I. Molecular and cellular aspects. *Cytokine Growth Factor Rev*, 17, 381-409.
- BOLIAR, S. & CHAMBERS, T. M. 2010. A new strategy of immune evasion by influenza A virus: inhibition of monocyte differentiation into dendritic cells. *Vet Immunol Immunopathol*, 136, 201-10.
- BOTTCHER-FRIEBERTSHAUSER, E., FREUER, C., SIELAFF, F., SCHMIDT, S., EICKMANN, M., UHLENDORFF, J., STEINMETZER, T., KLENK, H. D. & GARTEN, W. 2010. Cleavage of influenza virus hemagglutinin by airway proteases TMPRSS2 and HAT differs in subcellular localization and susceptibility to protease inhibitors. *J Virol*, 84, 5605-14.
- BOTTCHER, E., FREUER, C., STEINMETZER, T., KLENK, H. D. & GARTEN, W. 2009. MDCK cells that express proteases TMPRSS2 and HAT provide a cell system to propagate influenza viruses in the absence of trypsin and to study cleavage of HA and its inhibition. *Vaccine*, 27, 6324-9.
- BOULO, S., AKARSU, H., RUIGROK, R. W. & BAUDIN, F. 2007. Nuclear traffic of influenza virus proteins and ribonucleoprotein complexes. *Virus Res*, 124, 12-21.
- BRASS, A. L., HUANG, I. C., BENITA, Y., JOHN, S. P., KRISHNAN, M. N., FEELEY, E. M., RYAN, B. J., WEYER, J. L., VAN DER WEYDEN, L., FIKRIG, E., ADAMS, D. J., XAVIER, R. J., FARZAN, M. & ELLEDGE, S. J. 2009. The IFITM proteins mediate cellular resistance to influenza A H1N1 virus, West Nile virus, and dengue virus. *Cell*, 139, 1243-54.
- BRUCE, E. A., DIGARD, P. & STUART, A. D. 2010. The Rab11 pathway is required for influenza A virus budding and filament formation. *J Virol*, 84, 5848-59.
- BUI, M., WILLS, E. G., HELENIUS, A. & WHITTAKER, G. R. 2000. Role of the influenza virus M1 protein in nuclear export of viral ribonucleoproteins. *J Virol*, 74, 1781-6.
- BURGUI, I., ARAGON, T., ORTIN, J. & NIETO, A. 2003. PABP1 and eIF4G1 associate with influenza virus NS1 protein in viral mRNA translation initiation complexes. *J Gen Virol*, 84, 3263-74.
- CADY, S. D., LUO, W., HU, F. & HONG, M. 2009. Structure and function of the influenza A M2 proton channel. *Biochemistry*, 48, 7356-64.
- CALDER, L. J., WASILEWSKI, S., BERRIMAN, J. A. & ROSENTHAL, P. B. 2010. Structural organization of a filamentous influenza A virus. *Proc Natl Acad Sci U S A*, 107, 10685-90.
- CAMPBELL, K. A., MINASHIMA, T., ZHANG, Y., HADLEY, S., LEE, Y. J., GIOVINAZZO, J., QUIRNO, M. & KIRSCH, T. 2013. Annexin A6 interacts with p65 and stimulates NF-kappaB activity and catabolic events in articular chondrocytes. *Arthritis Rheum*, 65, 3120-9.
- CANNON, G., CALLAHAN, M. A., GRONEMUS, J. Q. & LOWY, R. J. 2014. Early activation of MAP kinases by influenza A virus X-31 in murine macrophage cell lines. *PLoS One*, 9, e105385.
- CAO, X., SURMA, M. A. & SIMONS, K. 2012. Polarized sorting and trafficking in epithelial cells. *Cell Res*, 22, 793-805.
- CASTRO, B. M., PRIETO, M. & SILVA, L. C. 2014. Ceramide: a simple sphingolipid with unique biophysical properties. *Prog Lipid Res*, 54, 53-67.
- CHEN, C. & ZHUANG, X. 2008. Epsin 1 is a cargo-specific adaptor for the clathrin-mediated endocytosis of the influenza virus. *Proc Natl Acad Sci U S A*, 105, 11790-5.

- CHEN, W., CALVO, P. A., MALIDE, D., GIBBS, J., SCHUBERT, U., BACIK, I., BASTA, S., O'NEILL, R., SCHICKLI, J., PALESE, P., HENKLEIN, P., BENNINK, J. R. & YEWDELL, J. W. 2001. A novel influenza A virus mitochondrial protein that induces cell death. *Nat Med*, 7, 1306-12.
- CHEN, Z., LI, Y. & KRUG, R. M. 1999. Influenza A virus NS1 protein targets poly(A)-binding protein II of the cellular 3'-end processing machinery. *EMBO J*, 18, 2273-83.
- CHENAVAS, S., CREPIN, T., DELMAS, B., RUIGROK, R. W. & SLAMA-SCHWOK, A. 2013. Influenza virus nucleoprotein: structure, RNA binding, oligomerization and antiviral drug target. *Future Microbiol*, 8, 1537-45.
- CHLANDA, P., SCHRAIDT, O., KUMMER, S., RICHES, J., OBERWINKLER, H., PRINZ, S., KRAUSSLICH, H. G. & BRIGGS, J. A. 2015. Structural Analysis of the Roles of Influenza A Virus Membrane-Associated Proteins in Assembly and Morphology. *J Virol*, 89, 8957-66.
- CHLYSTUN, M., CAMPANELLA, M., LAW, A. L., DUCHEN, M. R., FATIMATHAS, L., LEVINE, T. P., GERKE, V. & MOSS, S. E. 2013. Regulation of mitochondrial morphogenesis by annexin A6. *PLoS One*, 8, e53774.
- CHOI, A. G., WONG, J., MARCHANT, D. & LUO, H. 2013. The ubiquitin-proteasome system in positive-strand RNA virus infection. *Rev Med Virol*, 23, 85-96.
- CHOU, Y. Y., VAFABAKHSH, R., DOGANAY, S., GAO, Q., HA, T. & PALESE, P. 2012. One influenza virus particle packages eight unique viral RNAs as shown by FISH analysis. *Proc Natl Acad Sci U S A*, 109, 9101-6.
- CHOUDHURY, A., MARKS, D. L., PROCTOR, K. M., GOULD, G. W. & PAGANO, R. E. 2006. Regulation of caveolar endocytosis by syntaxin 6-dependent delivery of membrane components to the cell surface. *Nat Cell Biol*, 8, 317-28.
- CHOY, M. M., SESSIONS, O. M., GUBLER, D. J. & OOI, E. E. 2015. Production of Infectious Dengue Virus in *Aedes aegypti* Is Dependent on the Ubiquitin Proteasome Pathway. *PLoS Negl Trop Dis*, 9, e0004227.
- CHUTIWITOONCHAI, N., KAKISAKA, M., YAMADA, K. & AIDA, Y. 2014. Comparative analysis of seven viral nuclear export signals (NESs) reveals the crucial role of nuclear export mediated by the third NES consensus sequence of nucleoprotein (NP) in influenza A virus replication. *PLoS One*, 9, e105081.
- COHEN, M., ZHANG, X. Q., SENAATI, H. P., CHEN, H. W., VARKI, N. M., SCHOOLEY, R. T. & GAGNEUX, P. 2013. Influenza A penetrates host mucus by cleaving sialic acids with neuraminidase. *Virology*, 45, 317-321.
- COLOMA, R., VALPUESTA, J. M., ARRANZ, R., CARRASCOSA, J. L., ORTIN, J. & MARTIN-BENITO, J. 2009. The structure of a biologically active influenza virus ribonucleoprotein complex. *PLoS Pathog*, 5, e1000491.
- COMPANS, R. W., CONTENT, J. & DUESBERG, P. H. 1972. Structure of the ribonucleoprotein of influenza virus. *J Virol*, 10, 795-800.
- COOMBS, K. M., BERARD, A., XU, W., KROKHIN, O., MENG, X., CORTENS, J. P., KOBASA, D., WILKINS, J. & BROWN, E. G. 2010. Quantitative proteomic analyses of influenza virus-infected cultured human lung cells. *J Virol*, 84, 10888-906.
- CORNELY, R., RENTERO, C., ENRICH, C., GREWAL, T. & GAUS, K. 2011. Annexin A6 is an organizer of membrane microdomains to regulate receptor localization and signalling. *IUBMB Life*, 63, 1009-17.
- CREUTZ, C. E., HIRA, J. K., GEE, V. E. & EATON, J. M. 2012. Protection of the membrane permeability barrier by annexins. *Biochemistry*, 51, 9966-83.
- CUBELLS, L., VILA DE MUGA, S., TEBAR, F., BONVENTRE, J. V., BALSINDE, J., POL, A., GREWAL, T. & ENRICH, C. 2008. Annexin A6-induced inhibition of cytoplasmic phospholipase A2 is linked to caveolin-1 export from the Golgi. *J Biol Chem*, 283, 10174-83.
- CUBELLS, L., VILA DE MUGA, S., TEBAR, F., WOOD, P., EVANS, R., INGELMO-TORRES, M., CALVO, M., GAUS, K., POL, A., GREWAL, T. & ENRICH, C. 2007. Annexin A6-induced alterations in cholesterol transport and caveolin export from the Golgi complex. *Traffic*, 8, 1568-89.

- DATAN, E., SHIRAZIAN, A., BENJAMIN, S., MATASSOV, D., TINARI, A., MALORNI, W., LOCKSHIN, R. A., GARCIA-SASTRE, A. & ZAKERI, Z. 2014. mTOR/p70S6K signaling distinguishes routine, maintenance-level autophagy from autophagic cell death during influenza A infection. *Virology*, 452-453, 175-90.
- DE VRIES, E., TSCHERNE, D. M., WIENHOLTS, M. J., COBOS-JIMENEZ, V., SCHOLTE, F., GARCIA-SASTRE, A., ROTTIER, P. J. & DE HAAN, C. A. 2011. Dissection of the influenza A virus endocytic routes reveals macropinocytosis as an alternative entry pathway. *PLoS Pathog*, 7, e1001329.
- DEMIROV, D., GABRIEL, G., SCHNEIDER, C., HOHENBERG, H. & LUDWIG, S. 2012. Interaction of influenza A virus matrix protein with RACK1 is required for virus release. *Cell Microbiol*, 14, 774-89.
- DESJARDINS, M., CELIS, J. E., VAN MEER, G., DIEPLINGER, H., JAHRAUS, A., GRIFFITHS, G. & HUBER, L. A. 1994. Molecular characterization of phagosomes. *J Biol Chem*, 269, 32194-200.
- DESSELBERGER, U., RACANIELLO, V. R., ZAZRA, J. J. & PALESE, P. 1980. The 3' and 5'-terminal sequences of influenza A, B and C virus RNA segments are highly conserved and show partial inverted complementarity. *Gene*, 8, 315-28.
- DIAS, A., BOUVIER, D., CREPIN, T., MCCARTHY, A. A., HART, D. J., BAUDIN, F., CUSACK, S. & RUIGROK, R. W. 2009. The cap-snatching endonuclease of influenza virus polymerase resides in the PA subunit. *Nature*, 458, 914-8.
- DIEBOLD, S. S., KAISHO, T., HEMMI, H., AKIRA, S. & REIS E SOUSA, C. 2004. Innate antiviral responses by means of TLR7-mediated recognition of single-stranded RNA. *Science*, 303, 1529-31.
- DIENZ, O., RUD, J. G., EATON, S. M., LANTHIER, P. A., BURG, E., DREW, A., BUNN, J., SURATT, B. T., HAYNES, L. & RINCON, M. 2012. Essential role of IL-6 in protection against H1N1 influenza virus by promoting neutrophil survival in the lung. *Mucosal Immunol*, 5, 258-66.
- DONG, X., LIU, J., ZHENG, H., GLASFORD, J. W., HUANG, W., CHEN, Q. H., HARDEN, N. R., LI, F., GERDES, A. M. & WANG, X. 2004. In situ dynamically monitoring the proteolytic function of the ubiquitin-proteasome system in cultured cardiac myocytes. *Am J Physiol Heart Circ Physiol*, 287, H1417-25.
- DOSS, M., WHITE, M. R., TECLE, T., GANTZ, D., CROUCH, E. C., JUNG, G., RUCHALA, P., WARING, A. J., LEHRER, R. I. & HARTSHORN, K. L. 2009. Interactions of alpha-, beta-, and theta-defensins with influenza A virus and surfactant protein D. *J Immunol*, 182, 7878-87.
- DREUX, M. & CHISARI, F. V. 2010. Viruses and the autophagy machinery. *Cell Cycle*, 9, 1295-1307.
- DUBOIS, J., TERRIER, O. & ROSA-CALATRAVA, M. 2014. Influenza viruses and mRNA splicing: doing more with less. *MBio*, 5, e00070-14.
- EHRHARDT, C., WOLFF, T., PLESCHKA, S., PLANZ, O., BEERMANN, W., BODE, J. G., SCHMOLKE, M. & LUDWIG, S. 2007. Influenza A virus NS1 protein activates the PI3K/Akt pathway to mediate antiapoptotic signaling responses. *J Virol*, 81, 3058-67.
- EIERHOFF, T., HRINCIUS, E. R., RESCHER, U., LUDWIG, S. & EHRHARDT, C. 2010. The epidermal growth factor receptor (EGFR) promotes uptake of influenza A viruses (IAV) into host cells. *PLoS Pathog*, 6, e1001099.
- EISFELD, A. J., KAWAKAMI, E., WATANABE, T., NEUMANN, G. & KAWAOKA, Y. 2011a. RAB11A is essential for transport of the influenza virus genome to the plasma membrane. *J Virol*, 85, 6117-26.
- EISFELD, A. J., NEUMANN, G. & KAWAOKA, Y. 2011b. Human immunodeficiency virus rev-binding protein is essential for influenza a virus replication and promotes genome trafficking in late-stage infection. *J Virol*, 85, 9588-98.
- EL BAKKOURI, K., DESCAMPS, F., DE FILETTE, M., SMET, A., FESTJENS, E., BIRKETT, A., VAN ROOIJEN, N., VERBEEK, S., FIERS, W. & SAELENS, X. 2011. Universal vaccine based on ectodomain of matrix protein 2 of influenza A: Fc receptors and alveolar macrophages mediate protection. *J Immunol*, 186, 1022-31.
- ELLEMAN, C. J. & BARCLAY, W. S. 2004. The M1 matrix protein controls the filamentous phenotype of influenza A virus. *Virology*, 321, 144-53.

- ENRICH, C., RENTERO, C., DE MUGA, S. V., REVERTER, M., MULAY, V., WOOD, P., KOESE, M. & GREWAL, T. 2011. Annexin A6-Linking Ca(2+) signaling with cholesterol transport. *Biochim Biophys Acta*, 1813, 935-47.
- FALCON, A. M., FORTES, P., MARION, R. M., BELOSO, A. & ORTIN, J. 1999. Interaction of influenza virus NS1 protein and the human homologue of Staufen in vivo and in vitro. *Nucleic Acids Res*, 27, 2241-7.
- FEELEY, E. M., SIMS, J. S., JOHN, S. P., CHIN, C. R., PERTEL, T., CHEN, L. M., GAIHA, G. D., RYAN, B. J., DONIS, R. O., ELLEDGE, S. J. & BRASS, A. L. 2011. IFITM3 inhibits influenza A virus infection by preventing cytosolic entry. *PLoS Pathog*, 7, e1002337.
- FERGUSON, L., OLIVIER, A. K., GENOVA, S., EPPERSON, W. B., SMITH, D. R., SCHNEIDER, L., BARTON, K., MCCUAN, K., WEBBY, R. J. & WAN, X. F. 2016. Pathogenesis of Influenza D Virus in Cattle. *J Virol*, 90, 5636-42.
- FERNANDEZ-SESMA, A., MARUKIAN, S., EBERSOLE, B. J., KAMINSKI, D., PARK, M. S., YUEN, T., SEALFON, S. C., GARCIA-SASTRE, A. & MORAN, T. M. 2006. Influenza virus evades innate and adaptive immunity via the NS1 protein. *J Virol*, 80, 6295-304.
- FISLOVA, T., THOMAS, B., GRAEF, K. M. & FODOR, E. 2010. Association of the influenza virus RNA polymerase subunit PB2 with the host chaperonin CCT. *J Virol*, 84, 8691-9.
- FOURNIER, E., MOULES, V., ESSERE, B., PAILLART, J. C., SIRBAT, J. D., ISEL, C., CAVALIER, A., ROLLAND, J. P., THOMAS, D., LINA, B. & MARQUET, R. 2012. A supramolecular assembly formed by influenza A virus genomic RNA segments. *Nucleic Acids Res*, 40, 2197-209.
- FUJII, Y., GOTO, H., WATANABE, T., YOSHIDA, T. & KAWAOKA, Y. 2003. Selective incorporation of influenza virus RNA segments into virions. *Proc Natl Acad Sci U S A*, 100, 2002-7.
- FUKUDA, M., ASANO, S., NAKAMURA, T., ADACHI, M., YOSHIDA, M., YANAGIDA, M. & NISHIDA, E. 1997. CRM1 is responsible for intracellular transport mediated by the nuclear export signal. *Nature*, 390, 308-11.
- GABRIEL, G., KLINGEL, K., OTTE, A., THIELE, S., HUDJETZ, B., ARMAN-KALCEK, G., SAUTER, M., SHMIDT, T., ROTHER, F., BAUMGARTE, S., KEINER, B., HARTMANN, E., BADER, M., BROWNLEE, G. G., FODOR, E. & KLENK, H. D. 2011. Differential use of importin-alpha isoforms governs cell tropism and host adaptation of influenza virus. *Nat Commun*, 2, 156.
- GACK, M. U., ALBRECHT, R. A., URANO, T., INN, K. S., HUANG, I. C., CARNERO, E., FARZAN, M., INOUE, S., JUNG, J. U. & GARCIA-SASTRE, A. 2009. Influenza A virus NS1 targets the ubiquitin ligase TRIM25 to evade recognition by the host viral RNA sensor RIG-I. *Cell Host Microbe*, 5, 439-49.
- GACK, M. U., SHIN, Y. C., JOO, C. H., URANO, T., LIANG, C., SUN, L., TAKEUCHI, O., AKIRA, S., CHEN, Z., INOUE, S. & JUNG, J. U. 2007. TRIM25 RING-finger E3 ubiquitin ligase is essential for RIG-I-mediated antiviral activity. *Nature*, 446, 916-920.
- GAMBLIN, S. J., HAIRE, L. F., RUSSELL, R. J., STEVENS, D. J., XIAO, B., HA, Y., VASISHT, N., STEINHAEUER, D. A., DANIELS, R. S., ELLIOT, A., WILEY, D. C. & SKEHEL, J. J. 2004. The structure and receptor binding properties of the 1918 influenza hemagglutinin. *Science*, 303, 1838-42.
- GAMBLIN, S. J. & SKEHEL, J. J. 2010. Influenza hemagglutinin and neuraminidase membrane glycoproteins. *J Biol Chem*, 285, 28403-9.
- GANNAGE, M., DORMANN, D., ALBRECHT, R., DENGJEL, J., TOROSSO, T., RAMER, P. C., LEE, M., STROWIG, T., ARREY, F., CONENELLO, G., PYPART, M., ANDERSEN, J., GARCIA-SASTRE, A. & MUNZ, C. 2009. Matrix protein 2 of influenza A virus blocks autophagosome fusion with lysosomes. *Cell Host Microbe*, 6, 367-80.
- GAO, G., ZHANG, J., SI, X., WONG, J., CHEUNG, C., MCMANUS, B. & LUO, H. 2008a. Proteasome inhibition attenuates coxsackievirus-induced myocardial damage in mice. *Am J Physiol Heart Circ Physiol*, 295, H401-8.
- GAO, Q., BRYDON, E. W. & PALESE, P. 2008b. A seven-segmented influenza A virus expressing the influenza C virus glycoprotein HEF. *J Virol*, 82, 6419-26.
- GARFINKEL, M. S. & KATZE, M. G. 1992. Translational control by influenza virus. Selective and cap-dependent translation of viral mRNAs in infected cells. *J Biol Chem*, 267, 9383-90.

- GERKE, V., CREUTZ, C. E. & MOSS, S. E. 2005. Annexins: linking Ca<sup>2+</sup> signalling to membrane dynamics. *Nat Rev Mol Cell Biol*, 6, 449-61.
- GERKE, V. & MOSS, S. E. 2002. Annexins: from structure to function. *Physiol Rev*, 82, 331-71.
- GOG, J. R., AFONSO EDOS, S., DALTON, R. M., LECLERCQ, I., TILEY, L., ELTON, D., VON KIRCHBACH, J. C., NAFFAKH, N., ESCRIOU, N. & DIGARD, P. 2007. Codon conservation in the influenza A virus genome defines RNA packaging signals. *Nucleic Acids Res*, 35, 1897-907.
- GONZALEZ-NAVAJAS, J. M., LEE, J., DAVID, M. & RAZ, E. 2012. Immunomodulatory functions of type I interferons. *Nat Rev Immunol*, 12, 125-35.
- GORAYA, M. U., WANG, S., MUNIR, M. & CHEN, J. L. 2015. Induction of innate immunity and its perturbation by influenza viruses. *Protein Cell*, 6, 712-21.
- GOTO, H., MURAMOTO, Y., NODA, T. & KAWAOKA, Y. 2013. The genome-packaging signal of the influenza A virus genome comprises a genome incorporation signal and a genome-bundling signal. *J Virol*, 87, 11316-22.
- GRAEF, K. M., VREEDE, F. T., LAU, Y. F., MCCALL, A. W., CARR, S. M., SUBBARAO, K. & FODOR, E. 2010. The PB2 subunit of the influenza virus RNA polymerase affects virulence by interacting with the mitochondrial antiviral signaling protein and inhibiting expression of beta interferon. *J Virol*, 84, 8433-45.
- GRAYSON, M. H. & HOLTZMAN, M. J. 2007. Emerging role of dendritic cells in respiratory viral infection. *J Mol Med (Berl)*, 85, 1057-68.
- GREENE, W., ZHANG, W., HE, M., WITT, C., YE, F. & GAO, S. J. 2012. The ubiquitin/proteasome system mediates entry and endosomal trafficking of Kaposi's sarcoma-associated herpesvirus in endothelial cells. *PLoS Pathog*, 8, e1002703.
- GREWAL, T. & ENRICH, C. 2006. Molecular mechanisms involved in Ras inactivation: the annexin A6-p120GAP complex. *Bioessays*, 28, 1211-20.
- GREWAL, T. & ENRICH, C. 2009. Annexins--modulators of EGF receptor signalling and trafficking. *Cell Signal*, 21, 847-58.
- GREWAL, T., EVANS, R., RENTERO, C., TEBAR, F., CUBELLS, L., DE DIEGO, I., KIRCHHOFF, M. F., HUGHES, W. E., HEEREN, J., RYE, K. A., RINNINGER, F., DALY, R. J., POL, A. & ENRICH, C. 2005. Annexin A6 stimulates the membrane recruitment of p120GAP to modulate Ras and Raf-1 activity. *Oncogene*, 24, 5809-20.
- GREWAL, T., HEEREN, J., MEWAWALA, D., SCHNITGERHANS, T., WENDT, D., SALOMON, G., ENRICH, C., BEISIEGEL, U. & JACKLE, S. 2000. Annexin VI stimulates endocytosis and is involved in the trafficking of low density lipoprotein to the prelysosomal compartment. *J Biol Chem*, 275, 33806-13.
- GREWAL, T., KOESE, M., RENTERO, C. & ENRICH, C. 2010. Annexin A6-regulator of the EGFR/Ras signalling pathway and cholesterol homeostasis. *Int J Biochem Cell Biol*, 42, 580-4.
- GUAN, R., MA, L. C., LEONARD, P. G., AMER, B. R., SRIDHARAN, H., ZHAO, C., KRUG, R. M. & MONTELLIONE, G. T. 2011. Structural basis for the sequence-specific recognition of human ISG15 by the NS1 protein of influenza B virus. *Proc Natl Acad Sci U S A*, 108, 13468-73.
- GUARDA, G., BRAUN, M., STAEHLI, F., TARDIVEL, A., MATTMANN, C., FORSTER, I., FARLIK, M., DECKER, T., DU PASQUIER, R. A., ROMERO, P. & TSCHOPP, J. 2011. Type I interferon inhibits interleukin-1 production and inflammasome activation. *Immunity*, 34, 213-23.
- GUILLOT, L., LE GOFFIC, R., BLOCH, S., ESCRIOU, N., AKIRA, S., CHIGNARD, M. & SI-TAHAR, M. 2005. Involvement of toll-like receptor 3 in the immune response of lung epithelial cells to double-stranded RNA and influenza A virus. *J Biol Chem*, 280, 5571-80.
- GUNTESKI-HAMBLIN, A. M., SONG, G., WALSH, R. A., FRENZKE, M., BOIVIN, G. P., DORN, G. W., 2ND, KAETZEL, M. A., HORSEMAN, N. D. & DEDMAN, J. R. 1996. Annexin VI overexpression targeted to heart alters cardiomyocyte function in transgenic mice. *Am J Physiol*, 270, H1091-100.
- GUO, N. & PENG, Z. 2013. MG132, a proteasome inhibitor, induces apoptosis in tumor cells. *Asia Pac J Clin Oncol*, 9, 6-11.

- HAO, L., SAKURAI, A., WATANABE, T., SORENSEN, E., NIDOM, C. A., NEWTON, M. A., AHLQUIST, P. & KAWAOKA, Y. 2008. Drosophila RNAi screen identifies host genes important for influenza virus replication. *Nature*, 454, 890-3.
- HARTSHORN, K. L., CROUCH, E. C., WHITE, M. R., EGGLETON, P., TAUBER, A. I., CHANG, D. & SASTRY, K. 1994. Evidence for a protective role of pulmonary surfactant protein D (SP-D) against influenza A viruses. *J Clin Invest*, 94, 311-9.
- HARTSHORN, K. L., WHITE, M. R., MOGUES, T., LIGTENBERG, T., CROUCH, E. & HOLMSKOV, U. 2003. Lung and salivary scavenger receptor glycoprotein-340 contribute to the host defense against influenza A viruses. *Am J Physiol Lung Cell Mol Physiol*, 285, L1066-76.
- HASHIMOTO, G., WRIGHT, P. F. & KARZON, D. T. 1983. Antibody-dependent cell-mediated cytotoxicity against influenza virus-infected cells. *J Infect Dis*, 148, 785-94.
- HASHIMOTO, Y., MOKI, T., TAKIZAWA, T., SHIRATSUCHI, A. & NAKANISHI, Y. 2007. Evidence for phagocytosis of influenza virus-infected, apoptotic cells by neutrophils and macrophages in mice. *J Immunol*, 178, 2448-57.
- HATTA, M. & KAWAOKA, Y. 2003. The NB protein of influenza B virus is not necessary for virus replication in vitro. *J Virol*, 77, 6050-4.
- HAUSE, B. M., DUCATEZ, M., COLLIN, E. A., RAN, Z., LIU, R., SHENG, Z., ARMIEN, A., KAPLAN, B., CHAKRAVARTY, S., HOPPE, A. D., WEBBY, R. J., SIMONSON, R. R. & LI, F. 2013. Isolation of a novel swine influenza virus from Oklahoma in 2011 which is distantly related to human influenza C viruses. *PLoS Pathog*, 9, e1003176.
- HAWGOOD, S., BROWN, C., EDMONDSON, J., STUMBAUGH, A., ALLEN, L., GOERKE, J., CLARK, H. & POULAIN, F. 2004. Pulmonary collectins modulate strain-specific influenza a virus infection and host responses. *J Virol*, 78, 8565-72.
- HE, J., SUN, E., BUJNY, M. V., KIM, D., DAVIDSON, M. W. & ZHUANG, X. 2013. Dual function of CD81 in influenza virus uncoating and budding. *PLoS Pathog*, 9, e1003701.
- HENKEL, J. R. & WEISZ, O. A. 1998. Influenza virus M2 protein slows traffic along the secretory pathway. pH perturbation of acidified compartments affects early Golgi transport steps. *J Biol Chem*, 273, 6518-24.
- HERS, I., VINCENT, E. E. & TAVARE, J. M. 2011. Akt signalling in health and disease. *Cell Signal*, 23, 1515-27.
- HILL, M. M., BASTIANI, M., LUETTERFORST, R., KIRKHAM, M., KIRKHAM, A., NIXON, S. J., WALSER, P., ABANKWA, D., OORSCHOT, V. M., MARTIN, S., HANCOCK, J. F. & PARTON, R. G. 2008. PTRF-Cavin, a conserved cytoplasmic protein required for caveola formation and function. *Cell*, 132, 113-24.
- HILSCH, M., GOLDENBOGEN, B., SIEBEN, C., HOFER, C. T., RABE, J. P., KLIPP, E., HERRMANN, A. & CHIANTIA, S. 2014. Influenza A matrix protein M1 multimerizes upon binding to lipid membranes. *Biophys J*, 107, 912-23.
- HIRATA, N., SUIZU, F., MATSUDA-LENNIKOV, M., EDAMURA, T., BALA, J. & NOGUCHI, M. 2014. Inhibition of Akt kinase activity suppresses entry and replication of influenza virus. *Biochem Biophys Res Commun*, 450, 891-8.
- HO, L. P., DENNEY, L., LUHN, K., TEOH, D., CLELLAND, C. & MCMICHAEL, A. J. 2008. Activation of invariant NKT cells enhances the innate immune response and improves the disease course in influenza A virus infection. *Eur J Immunol*, 38, 1913-22.
- HOLSINGER, L. J., NICHANI, D., PINTO, L. H. & LAMB, R. A. 1994. Influenza A virus M2 ion channel protein: a structure-function analysis. *J Virol*, 68, 1551-63.
- HONDA, K., YANAI, H., NEGISHI, H., ASAGIRI, M., SATO, M., MIZUTANI, T., SHIMADA, N., OHBA, Y., TAKAOKA, A., YOSHIDA, N. & TANIGUCHI, T. 2005. IRF-7 is the master regulator of type-I interferon-dependent immune responses. *Nature*, 434, 772-7.
- HU, Y. 2010. Two special topics on the avian influenza virus and on epigenetics, have drawn much attention. *Sci China Life Sci*, 53, 1483-4.

- HUANG, S., CHEN, J., CHEN, Q., WANG, H., YAO, Y., CHEN, J. & CHEN, Z. 2013. A second CRM1-dependent nuclear export signal in the influenza A virus NS2 protein contributes to the nuclear export of viral ribonucleoproteins. *J Virol*, 87, 767-78.
- HUBER, L. A., PIMPLIKAR, S., PARTON, R. G., VIRTÀ, H., ZERIAL, M. & SIMONS, K. 1993. Rab8, a small GTPase involved in vesicular traffic between the TGN and the basolateral plasma membrane. *J Cell Biol*, 123, 35-45.
- HUI, E. K. & NAYAK, D. P. 2002. Role of G protein and protein kinase signalling in influenza virus budding in MDCK cells. *J Gen Virol*, 83, 3055-66.
- HUTCHINSON, E. C., VON KIRCHBACH, J. C., GOG, J. R. & DIGARD, P. 2010. Genome packaging in influenza A virus. *J Gen Virol*, 91, 313-28.
- IBRICEVIC, A., PEKOSZ, A., WALTER, M. J., NEWBY, C., BATTAILE, J. T., BROWN, E. G., HOLTZMAN, M. J. & BRODY, S. L. 2006. Influenza virus receptor specificity and cell tropism in mouse and human airway epithelial cells. *J Virol*, 80, 7469-80.
- ICHINOHE, T., PANG, I. K. & IWASAKI, A. 2010. Influenza virus activates inflammasomes via its intracellular M2 ion channel. *Nat Immunol*, 11, 404-10.
- ILNYTSKA, O., SANTIANA, M., HSU, N. Y., DU, W. L., CHEN, Y. H., VIKTOROVA, E. G., BELOV, G., BRINKER, A., STORCH, J., MOORE, C., DIXON, J. L. & ALTAN-BONNET, N. 2013. Enteroviruses harness the cellular endocytic machinery to remodel the host cell cholesterol landscape for effective viral replication. *Cell Host Microbe*, 14, 281-93.
- IMAI, M., WATANABE, S., NINOMIYA, A., OBUCHI, M. & ODAGIRI, T. 2004. Influenza B virus BM2 protein is a crucial component for incorporation of viral ribonucleoprotein complex into virions during virus assembly. *J Virol*, 78, 11007-15.
- IMAI, Y., KUBA, K., NEELY, G. G., YAGHUBIAN-MALHAMI, R., PERKMANN, T., VAN LOO, G., ERMOLAEVA, M., VELDHIJZEN, R., LEUNG, Y. H., WANG, H., LIU, H., SUN, Y., PASPARAKIS, M., KOPF, M., MECH, C., BAVARI, S., PEIRIS, J. S., SLUTSKY, A. S., AKIRA, S., HULTQVIST, M., HOLMDAHL, R., NICHOLLS, J., JIANG, C., BINDER, C. J. & PENNINGER, J. M. 2008. Identification of oxidative stress and Toll-like receptor 4 signaling as a key pathway of acute lung injury. *Cell*, 133, 235-49.
- ITO, Y., SHINYA, K., KISO, M., WATANABE, T., SAKODA, Y., HATTA, M., MURAMOTO, Y., TAMURA, D., SAKAI-TAGAWA, Y., NODA, T., SAKABE, S., IMAI, M., HATTA, Y., WATANABE, S., LI, C., YAMADA, S., FUJII, K., MURAKAMI, S., IMAI, H., KAKUGAWA, S., ITO, M., TAKANO, R., IWATSUKI-HORIMOTO, K., SHIMOJIMA, M., HORIMOTO, T., GOTO, H., TAKAHASHI, K., MAKINO, A., ISHIGAKI, H., NAKAYAMA, M., OKAMATSU, M., TAKAHASHI, K., WARSHAUER, D., SHULT, P. A., SAITO, R., SUZUKI, H., FURUTA, Y., YAMASHITA, M., MITAMURA, K., NAKANO, K., NAKAMURA, M., BROCKMAN-SCHNEIDER, R., MITAMURA, H., YAMAZAKI, M., SUGAYA, N., SURESH, M., OZAWA, M., NEUMANN, G., GERN, J., KIDA, H., OGASAWARA, K. & KAWAOKA, Y. 2009. In vitro and in vivo characterization of new swine-origin H1N1 influenza viruses. *Nature*, 460, 1021-5.
- IWAI, A., SHIOZAKI, T., KAWAI, T., AKIRA, S., KAWAOKA, Y., TAKADA, A., KIDA, H. & MIYAZAKI, T. 2010. Influenza A virus polymerase inhibits type I interferon induction by binding to interferon beta promoter stimulator 1. *J Biol Chem*, 285, 32064-74.
- JACKLE, S., BEISIEGEL, U., RINNINGER, F., BUCK, F., GRIGOLEIT, A., BLOCK, A., GROGER, I., GRETEN, H. & WINDLER, E. 1994. Annexin VI, a marker protein of hepatocytic endosomes. *J Biol Chem*, 269, 1026-32.
- JANG, H., BOLTZ, D., STURM-RAMIREZ, K., SHEPHERD, K. R., JIAO, Y., WEBSTER, R. & SMEYNE, R. J. 2009. Highly pathogenic H5N1 influenza virus can enter the central nervous system and induce neuroinflammation and neurodegeneration. *Proc Natl Acad Sci U S A*, 106, 14063-8.
- JAYASEKERA, J. P., MOSEMAN, E. A. & CARROLL, M. C. 2007. Natural antibody and complement mediate neutralization of influenza virus in the absence of prior immunity. *J Virol*, 81, 3487-94.

- JEWELL, N. A., VAGHEFI, N., MERTZ, S. E., AKTER, P., PEEBLES, R. S., JR., BAKALETZ, L. O., DURBIN, R. K., FLANO, E. & DURBIN, J. E. 2007. Differential type I interferon induction by respiratory syncytial virus and influenza A virus in vivo. *J Virol*, 81, 9790-800.
- JOB, E. R., DENG, Y. M., TATE, M. D., BOTTAZZI, B., CROUCH, E. C., DEAN, M. M., MANTOVANI, A., BROOKS, A. G. & READING, P. C. 2010. Pandemic H1N1 influenza A viruses are resistant to the antiviral activities of innate immune proteins of the collectin and pentraxin superfamilies. *J Immunol*, 185, 4284-91.
- JORBA, N., COLOMA, R. & ORTIN, J. 2009. Genetic trans-complementation establishes a new model for influenza virus RNA transcription and replication. *PLoS Pathog*, 5, e1000462.
- KAETZEL, M. A. & DEDMAN, J. R. 2004. Annexin VI regulation of cardiac function. *Biochem Biophys Res Commun*, 322, 1171-7.
- KAINOV, D. E., MULLER, K. H., THEISEN, L. L., ANASTASINA, M., KALOINEN, M. & MULLER, C. P. 2011. Differential effects of NS1 proteins of human pandemic H1N1/2009, avian highly pathogenic H5N1, and low pathogenic H5N2 influenza A viruses on cellular pre-mRNA polyadenylation and mRNA translation. *J Biol Chem*, 286, 7239-47.
- KALTHOFF, D., GLOBIG, A. & BEER, M. 2010. (Highly pathogenic) avian influenza as a zoonotic agent. *Vet Microbiol*, 140, 237-45.
- KAMAL, A., YING, Y. & ANDERSON, R. G. 1998. Annexin VI-mediated loss of spectrin during coated pit budding is coupled to delivery of LDL to lysosomes. *J Cell Biol*, 142, 937-47.
- KARLAS, A., MACHUY, N., SHIN, Y., PLEISSNER, K. P., ARTARINI, A., HEUER, D., BECKER, D., KHALIL, H., OGILVIE, L. A., HESS, S., MAURER, A. P., MULLER, E., WOLFF, T., RUDEL, T. & MEYER, T. F. 2010. Genome-wide RNAi screen identifies human host factors crucial for influenza virus replication. *Nature*, 463, 818-22.
- KASH, J. C., CUNNINGHAM, D. M., SMIT, M. W., PARK, Y., FRITZ, D., WILUSZ, J. & KATZE, M. G. 2002. Selective translation of eukaryotic mRNAs: functional molecular analysis of GRSF-1, a positive regulator of influenza virus protein synthesis. *J Virol*, 76, 10417-26.
- KAWAGUCHI, A., MOMOSE, F. & NAGATA, K. 2011. Replication-coupled and host factor-mediated encapsidation of the influenza virus genome by viral nucleoprotein. *J Virol*, 85, 6197-204.
- KAWAI, N., IKEMATSU, H., IWAKI, N., SATOH, I., KAWASHIMA, T., MAEDA, T., MIYACHI, K., HIROTSU, N., SHIGEMATSU, T. & KASHIWAGI, S. 2005. Factors influencing the effectiveness of oseltamivir and amantadine for the treatment of influenza: a multicenter study from Japan of the 2002-2003 influenza season. *Clin Infect Dis*, 40, 1309-16.
- KAWAI, T. & AKIRA, S. 2007. Antiviral signaling through pattern recognition receptors. *J Biochem*, 141, 137-45.
- KELLER, P. & SIMONS, K. 1998. Cholesterol is required for surface transport of influenza virus hemagglutinin. *J Cell Biol*, 140, 1357-67.
- KENWORTHY, A. K. 2008. Have we become overly reliant on lipid rafts? Talking Point on the involvement of lipid rafts in T-cell activation. *EMBO Rep*, 9, 531-5.
- KIDD, V. J., LAHTI, J. M. & TEITZ, T. 2000. Proteolytic regulation of apoptosis. *Semin Cell Dev Biol*, 11, 191-201.
- KIEN, F., MA, H., DIAZ GAISENBAND, S. & B., N. 2013. VIROPORINS: Differential Functions at Late Stages of Viral Life Cycles.
- KINOSHITA, Y., UO, T., JAYADEV, S., GARDEN, G. A., CONRADS, T. P., VEENSTRA, T. D. & MORRISON, R. S. 2006. Potential applications and limitations of proteomics in the study of neurological disease. *Arch Neurol*, 63, 1692-6.
- KNOWLES, M. R. & BOUCHER, R. C. 2002. Mucus clearance as a primary innate defense mechanism for mammalian airways. *J Clin Invest*, 109, 571-7.
- KOESE, M., RENTERO, C., KOTA, B. P., HOQUE, M., CAIRNS, R., WOOD, P., VILA DE MUGA, S., REVERTER, M., ALVAREZ-GUAITA, A., MONASTYRSKAYA, K., HUGHES, W. E., SWARBRICK, A., TEBAR, F., DALY, R. J., ENRICH, C. & GREWAL, T. 2013. Annexin A6 is a scaffold for PKC $\alpha$  to promote EGFR inactivation. *Oncogene*, 32, 2858-72.

- KOHIO, H. P. & ADAMSON, A. L. 2013. Glycolytic control of vacuolar-type ATPase activity: a mechanism to regulate influenza viral infection. *Virology*, 444, 301-9.
- KOLUMAM, G. A., THOMAS, S., THOMPSON, L. J., SPRENT, J. & MURALI-KRISHNA, K. 2005. Type I interferons act directly on CD8 T cells to allow clonal expansion and memory formation in response to viral infection. *J Exp Med*, 202, 637-50.
- KONIG, R., STERTZ, S., ZHOU, Y., INOUE, A., HOFFMANN, H. H., BHATTACHARYYA, S., ALAMARES, J. G., TSCHERNE, D. M., ORTIGOZA, M. B., LIANG, Y., GAO, Q., ANDREWS, S. E., BANDYOPADHYAY, S., DE JESUS, P., TU, B. P., CACHE, L., SHIH, C., ORTH, A., BONAMY, G., MIRAGLIA, L., IDEKER, T., GARCIA-SASTRE, A., YOUNG, J. A., PALESE, P., SHAW, M. L. & CHANDA, S. K. 2010. Human host factors required for influenza virus replication. *Nature*, 463, 813-7.
- KUNDU, A., AVALOS, R. T., SANDERSON, C. M. & NAYAK, D. P. 1996. Transmembrane domain of influenza virus neuraminidase, a type II protein, possesses an apical sorting signal in polarized MDCK cells. *J Virol*, 70, 6508-15.
- LAI, J. C., CHAN, W. W., KIEN, F., NICHOLLS, J. M., PEIRIS, J. S. & GARCIA, J. M. 2010. Formation of virus-like particles from human cell lines exclusively expressing influenza neuraminidase. *J Gen Virol*, 91, 2322-30.
- LAUDER, S. N., JONES, E., SMART, K., BLOOM, A., WILLIAMS, A. S., HINDLEY, J. P., ONDONDO, B., TAYLOR, P. R., CLEMENT, M., FIELDING, C., GODKIN, A. J., JONES, S. A. & GALLIMORE, A. M. 2013. Interleukin-6 limits influenza-induced inflammation and protects against fatal lung pathology. *Eur J Immunol*, 43, 2613-25.
- LE GOFFIC, R., ARSHAD, M. I., RAUCH, M., L'HELGOUALC'H, A., DELMAS, B., PIQUET-PELLORCE, C. & SAMSON, M. 2011. Infection with influenza virus induces IL-33 in murine lungs. *Am J Respir Cell Mol Biol*, 45, 1125-32.
- LE GOFFIC, R., BOUGUYON, E., CHEVALIER, C., VIDIC, J., DA COSTA, B., LEYMARIE, O., BOURDIEU, C., DECAMPS, L., DHORNE-POLLET, S. & DELMAS, B. 2010. Influenza A virus protein PB1-F2 exacerbates IFN-beta expression of human respiratory epithelial cells. *J Immunol*, 185, 4812-23.
- LEE, S. H., JUNG, J. U. & MEANS, R. E. 2003. 'Complementing' viral infection: mechanisms for evading innate immunity. *Trends Microbiol*, 11, 449-52.
- LEI, Y., MOORE, C. B., LIESMAN, R. M., O'CONNOR, B. P., BERGSTRALH, D. T., CHEN, Z. J., PICKLES, R. J. & TING, J. P. 2009. MAVS-mediated apoptosis and its inhibition by viral proteins. *PLoS One*, 4, e5466.
- LI, S., MIN, J. Y., KRUG, R. M. & SEN, G. C. 2006. Binding of the influenza A virus NS1 protein to PKR mediates the inhibition of its activation by either PACT or double-stranded RNA. *Virology*, 349, 13-21.
- LI, Z., LIU, X., ZHAO, Z. & LIU, W. 2012. [Heat shock protein 27 enhances the inhibitory effect of influenza A virus NS1 on the expression of interferon-beta]. *Sheng Wu Gong Cheng Xue Bao*, 28, 1205-15.
- LIEMANN, S. & LEWIT-BENTLEY, A. 1995. Annexins: a novel family of calcium- and membrane-binding proteins in search of a function. *Structure*, 3, 233-237.
- LIN, H. C., SUDHOF, T. C. & ANDERSON, R. G. 1992. Annexin VI is required for budding of clathrin-coated pits. *Cell*, 70, 283-91.
- LIU, G., XIANG, Y., GUO, C., PEI, Y., WANG, Y. & KITAZATO, K. 2014a. Cofilin-1 is involved in regulation of actin reorganization during influenza A virus assembly and budding. *Biochem Biophys Res Commun*, 453, 821-5.
- LIU, Q., BAWA, B., MA, J., LI, F., MA, W. & RICHT, J. A. 2014b. A crucial role of N-terminal domain of influenza A virus M1 protein in interaction with swine importin alpha1 protein. *Virus Genes*, 49, 157-62.
- LIZARBE, M. A., BARRASA, J. I., OLMO, N., GAVILANES, F. & TURNAY, J. 2013. Annexin-phospholipid interactions. Functional implications. *Int J Mol Sci*, 14, 2652-83.

- LONGHI, M. P., WRIGHT, K., LAUDER, S. N., NOWELL, M. A., JONES, G. W., GODKIN, A. J., JONES, S. A. & GALLIMORE, A. M. 2008. Interleukin-6 is crucial for recall of influenza-specific memory CD4 T cells. *PLoS Pathog*, 4, e1000006.
- LOU, Z., SUN, Y. & RAO, Z. 2014. Current progress in antiviral strategies. *Trends Pharmacol Sci*, 35, 86-102.
- LUDWIG, S., WANG, X., EHRHARDT, C., ZHENG, H., DONELAN, N., PLANZ, O., PLESCHKA, S., GARCIA-SASTRE, A., HEINS, G. & WOLFF, T. 2002. The influenza A virus NS1 protein inhibits activation of Jun N-terminal kinase and AP-1 transcription factors. *J Virol*, 76, 11166-71.
- LUO, H., ZHANG, J., CHEUNG, C., SUAREZ, A., MCMANUS, B. M. & YANG, D. 2003. Proteasome inhibition reduces coxsackievirus B3 replication in murine cardiomyocytes. *Am J Pathol*, 163, 381-5.
- MA, H., KIEN, F., MANIERE, M., ZHANG, Y., LAGARDE, N., TSE, K. S., POON, L. L. & NAL, B. 2012. Human annexin A6 interacts with influenza a virus protein M2 and negatively modulates infection. *J Virol*, 86, 1789-801.
- MANDELBOIM, O., LIEBERMAN, N., LEV, M., PAUL, L., ARNON, T. I., BUSHKIN, Y., DAVIS, D. M., STROMINGER, J. L., YEWDELL, J. W. & PORGADOR, A. 2001. Recognition of haemagglutinins on virus-infected cells by Nkp46 activates lysis by human NK cells. *Nature*, 409, 1055-60.
- MANZOOR, R., KURODA, K., YOSHIDA, R., TSUDA, Y., FUJIKURA, D., MIYAMOTO, H., KAJIHARA, M., KIDA, H. & TAKADA, A. 2014. Heat shock protein 70 modulates influenza A virus polymerase activity. *J Biol Chem*, 289, 7599-614.
- MARJUKI, H., GORNITZKY, A., MARATHE, B. M., ILYUSHINA, N. A., ALDRIDGE, J. R., DESAI, G., WEBBY, R. J. & WEBSTER, R. G. 2011. Influenza A virus-induced early activation of ERK and PI3K mediates V-ATPase-dependent intracellular pH change required for fusion. *Cell Microbiol*, 13, 587-601.
- MARJUKI, H., YEN, H. L., FRANKS, J., WEBSTER, R. G., PLESCHKA, S. & HOFFMANN, E. 2007. Higher polymerase activity of a human influenza virus enhances activation of the hemagglutinin-induced Raf/MEK/ERK signal cascade. *Virology*, 4, 134.
- MARTIN, K. & HELENIUS, A. 1991. Nuclear transport of influenza virus ribonucleoproteins: the viral matrix protein (M1) promotes export and inhibits import. *Cell*, 67, 117-30.
- MATROSOVICH, M. N., MATROSOVICH, T. Y., GRAY, T., ROBERTS, N. A. & KLENK, H. D. 2004. Human and avian influenza viruses target different cell types in cultures of human airway epithelium. *Proc Natl Acad Sci U S A*, 101, 4620-4.
- MATSUKURA, S., KOKUBU, F., KUBO, H., TOMITA, T., TOKUNAGA, H., KADOKURA, M., YAMAMOTO, T., KUROIWA, Y., OHNO, T., SUZAKI, H. & ADACHI, M. 1998. Expression of RANTES by normal airway epithelial cells after influenza virus A infection. *Am J Respir Cell Mol Biol*, 18, 255-64.
- MATSUOKA, Y., MATSUMAE, H., KATOH, M., EISFELD, A. J., NEUMANN, G., HASE, T., GHOSH, S., SHOEMAKER, J. E., LOPES, T. J., WATANABE, T., WATANABE, S., FUKUYAMA, S., KITANO, H. & KAWAOKA, Y. 2013. A comprehensive map of the influenza A virus replication cycle. *BMC Syst Biol*, 7, 97.
- MCCAFFREY, L. M. & MACARA, I. G. 2012. Signaling pathways in cell polarity. *Cold Spring Harb Perspect Biol*, 4.
- MCCULLOUGH, C., WANG, M., RONG, L. & CAFFREY, M. 2012. Characterization of influenza hemagglutinin interactions with receptor by NMR. *PLoS One*, 7, e33958.
- MEDINA, R. A. & GARCIA-SASTRE, A. 2011. Influenza A viruses: new research developments. *Nat Rev Microbiol*, 9, 590-603.
- MEGHA & LONDON, E. 2004. Ceramide selectively displaces cholesterol from ordered lipid domains (rafts): implications for lipid raft structure and function. *J Biol Chem*, 279, 9997-10004.
- MINASHIMA, T., SMALL, W., MOSS, S. E. & KIRSCH, T. 2012. Intracellular modulation of signaling pathways by annexin A6 regulates terminal differentiation of chondrocytes. *J Biol Chem*, 287, 14803-15.

- MIRSAEIDI, M., GIDFAR, S., VU, A. & SCHRAUFNAGEL, D. 2016. Annexins family: insights into their functions and potential role in pathogenesis of sarcoidosis. *J Transl Med*, 14, 89.
- MOELLER, A., KIRCHDOERFER, R. N., POTTER, C. S., CARRAGHER, B. & WILSON, I. A. 2012. Organization of the influenza virus replication machinery. *Science*, 338, 1631-4.
- MOMOSE, F., KIKUCHI, Y., KOMASE, K. & MORIKAWA, Y. 2007. Visualization of microtubule-mediated transport of influenza viral progeny ribonucleoprotein. *Microbes Infect*, 9, 1422-33.
- MOMOSE, F., NAITO, T., YANO, K., SUGIMOTO, S., MORIKAWA, Y. & NAGATA, K. 2002. Identification of Hsp90 as a stimulatory host factor involved in influenza virus RNA synthesis. *J Biol Chem*, 277, 45306-14.
- MONASTYRSKAYA, K., BABIYCHUK, E. B. & DRAEGER, A. 2009. The annexins: spatial and temporal coordination of signaling events during cellular stress. *Cell Mol Life Sci*, 66, 2623-42.
- MONASTYRSKAYA, K., BABIYCHUK, E. B., HOSTETTLER, A., RESCHER, U. & DRAEGER, A. 2007. Annexins as intracellular calcium sensors. *Cell Calcium*, 41, 207-19.
- MUKHERJEE, S., VIPAT, V. C. & CHAKRABARTI, A. K. 2013. Infection with influenza A viruses causes changes in promoter DNA methylation of inflammatory genes. *Influenza Other Respir Viruses*, 7, 979-86.
- MULLER, K. H., KAKKOLA, L., NAGARAJ, A. S., CHELTSOV, A. V., ANASTASINA, M. & KAINOV, D. E. 2012. Emerging cellular targets for influenza antiviral agents. *Trends Pharmacol Sci*, 33, 89-99.
- MUNRO, S. 2003. Lipid rafts: elusive or illusive? *Cell*, 115, 377-88.
- MUSIOL, A., GRAN, S., EHRHARDT, C., LUDWIG, S., GREWAL, T., GERKE, V. & RESCHER, U. 2013. Annexin A6-balanced late endosomal cholesterol controls influenza A replication and propagation. *MBio*, 4, e00608-13.
- NAILWAL, H., SHARMA, S., MAYANK, A. K. & LAL, S. K. 2015. The nucleoprotein of influenza A virus induces p53 signaling and apoptosis via attenuation of host ubiquitin ligase RNF43. *Cell Death Dis*, 6, e1768.
- NAITO, T., MOMOSE, F., KAWAGUCHI, A. & NAGATA, K. 2007. Involvement of Hsp90 in assembly and nuclear import of influenza virus RNA polymerase subunits. *J Virol*, 81, 1339-49.
- NAKASHIMA, S. 2002. Protein kinase C alpha (PKC alpha): regulation and biological function. *J Biochem*, 132, 669-75.
- NAYAK, D. P., HUI, E. K. & BARMAN, S. 2004. Assembly and budding of influenza virus. *Virus Res*, 106, 147-65.
- NEMEROFF, M. E., BARABINO, S. M., LI, Y., KELLER, W. & KRUG, R. M. 1998. Influenza virus NS1 protein interacts with the cellular 30 kDa subunit of CPSF and inhibits 3' end formation of cellular pre-mRNAs. *Mol Cell*, 1, 991-1000.
- NEWCOMB, L. L., KUO, R. L., YE, Q., JIANG, Y., TAO, Y. J. & KRUG, R. M. 2009. Interaction of the influenza A virus nucleocapsid protein with the viral RNA polymerase potentiates unprimed viral RNA replication. *J Virol*, 83, 29-36.
- NEZNANOV, N., DRAGUNSKY, E. M., CHUMAKOV, K. M., NEZNANOVA, L., WEK, R. C., GUDKOV, A. V. & BANERJEE, A. K. 2008. Different effect of proteasome inhibition on vesicular stomatitis virus and poliovirus replication. *PLoS One*, 3, e1887.
- NG, A. K., WANG, J. H. & SHAW, P. C. 2009. Structure and sequence analysis of influenza A virus nucleoprotein. *Sci China C Life Sci*, 52, 439-49.
- NGUYEN, K. B., WATFORD, W. T., SALOMON, R., HOFMANN, S. R., PIEN, G. C., MORINOBU, A., GADINA, M., O'SHEA, J. J. & BIRON, C. A. 2002. Critical role for STAT4 activation by type 1 interferons in the interferon-gamma response to viral infection. *Science*, 297, 2063-6.
- NIMMERJAHN, F., DUDZIAK, D., DIRMEIER, U., HOBOM, G., RIEDEL, A., SCHLEE, M., STAUDT, L. M., ROSENWALD, A., BEHREND, U., BORNKAMM, G. W. & MAUTNER, J. 2004. Active NF-kappaB signalling is a prerequisite for influenza virus infection. *J Gen Virol*, 85, 2347-56.
- NODA, T., SUGITA, Y., AOYAMA, K., HIRASE, A., KAWAKAMI, E., MIYAZAWA, A., SAGARA, H. & KAWAOKA, Y. 2012. Three-dimensional analysis of ribonucleoprotein complexes in influenza A virus. *Nat Commun*, 3, 639.

- NOTON, S. L., MEDCALF, E., FISHER, D., MULLIN, A. E., ELTON, D. & DIGARD, P. 2007. Identification of the domains of the influenza A virus M1 matrix protein required for NP binding, oligomerization and incorporation into virions. *J Gen Virol*, 88, 2280-90.
- O'BRIEN, K. B., MORRISON, T. E., DUNDORE, D. Y., HEISE, M. T. & SCHULTZ-CHERRY, S. 2011. A protective role for complement C3 protein during pandemic 2009 H1N1 and H5N1 influenza A virus infection. *PLoS One*, 6, e17377.
- O'NEILL, R. E., TALON, J. & PALESE, P. 1998. The influenza virus NEP (NS2 protein) mediates the nuclear export of viral ribonucleoproteins. *EMBO J*, 17, 288-96.
- OECKINGHAUS, A. & GHOSH, S. 2009. The NF-kappaB family of transcription factors and its regulation. *Cold Spring Harb Perspect Biol*, 1, a000034.
- OHKUMA, S. & POOLE, B. 1978. Fluorescence probe measurement of the intralysosomal pH in living cells and the perturbation of pH by various agents. *Proc Natl Acad Sci U S A*, 75, 3327-31.
- PALESE, P. & SCHULMAN, J. L. 1976. Mapping of the influenza virus genome: identification of the hemagglutinin and the neuraminidase genes. *Proc Natl Acad Sci U S A*, 73, 2142-6.
- PAN, Q., CHEN, H., WANG, F., JEZA, V. T., HOU, W., ZHAO, Y., XIANG, T., ZHU, Y., ENDO, Y., FUJITA, T. & ZHANG, X. L. 2012. L-ficolin binds to the glycoproteins hemagglutinin and neuraminidase and inhibits influenza A virus infection both in vitro and in vivo. *J Innate Immun*, 4, 312-24.
- PEIRIS, J. S., DE JONG, M. D. & GUAN, Y. 2007. Avian influenza virus (H5N1): a threat to human health. *Clin Microbiol Rev*, 20, 243-67.
- PERETTI, D., DAHAN, N., SHIMONI, E., HIRSCHBERG, K. & LEV, S. 2008. Coordinated lipid transfer between the endoplasmic reticulum and the Golgi complex requires the VAP proteins and is essential for Golgi-mediated transport. *Mol Biol Cell*, 19, 3871-84.
- PEREZ-GONZALEZ, A., RODRIGUEZ, A., HUARTE, M., SALANUEVA, I. J. & NIETO, A. 2006. hCLE/CGI-99, a human protein that interacts with the influenza virus polymerase, is a mRNA transcription modulator. *J Mol Biol*, 362, 887-900.
- PEREZ, J. T., VARBLE, A., SACHIDANANDAM, R., ZLATEV, I., MANOHARAN, M., GARCIA-SASTRE, A. & TENOVER, B. R. 2010. Influenza A virus-generated small RNAs regulate the switch from transcription to replication. *Proc Natl Acad Sci U S A*, 107, 11525-30.
- PETERSEN, J., DRAKE, M. J., BRUCE, E. A., RIBLETT, A. M., DIDIGU, C. A., WILEN, C. B., MALANI, N., MALE, F., LEE, F. H., BUSHMAN, F. D., CHERRY, S., DOMS, R. W., BATES, P. & BRILEY, K., JR. 2014. The major cellular sterol regulatory pathway is required for Andes virus infection. *PLoS Pathog*, 10, e1003911.
- PIELAK, R. M. & CHOU, J. J. 2011. Influenza M2 proton channels. *Biochim Biophys Acta*, 1808, 522-9.
- PINTO, L. H., HOLSINGER, L. J. & LAMB, R. A. 1992. Influenza virus M2 protein has ion channel activity. *Cell*, 69, 517-28.
- PINTO, L. H. & LAMB, R. A. 2006a. Influenza virus proton channels. *Photochem Photobiol Sci*, 5, 629-32.
- PINTO, L. H. & LAMB, R. A. 2006b. The M2 proton channels of influenza A and B viruses. *J Biol Chem*, 281, 8997-9000.
- PINTO, R., HEROLD, S., CAKAROVA, L., HOEGNER, K., LOHMEYER, J., PLANZ, O. & PLESCHKA, S. 2011. Inhibition of influenza virus-induced NF-kappaB and Raf/MEK/ERK activation can reduce both virus titers and cytokine expression simultaneously in vitro and in vivo. *Antiviral Res*, 92, 45-56.
- PIQUERAS, B., CONNOLLY, J., FREITAS, H., PALUCKA, A. K. & BANCHEREAU, J. 2006. Upon viral exposure, myeloid and plasmacytoid dendritic cells produce 3 waves of distinct chemokines to recruit immune effectors. *Blood*, 107, 2613-8.
- PONS, M., IHRKE, G., KOCH, S., BIERMER, M., POL, A., GREWAL, T., JACKLE, S. & ENRICH, C. 2000. Late endocytic compartments are major sites of annexin VI localization in NRK fibroblasts and polarized WIF-B hepatoma cells. *Exp Cell Res*, 257, 33-47.

- PUIG, O., CASPARY, F., RIGAUT, G., RUTZ, B., BOUVERET, E., BRAGADO-NILSSON, E., WILM, M. & SERAPHIN, B. 2001. The tandem affinity purification (TAP) method: a general procedure of protein complex purification. *Methods*, 24, 218-29.
- RAO, V. S., SRINIVAS, K., SUJINI, G. N. & KUMAR, G. N. 2014. Protein-protein interaction detection: methods and analysis. *Int J Proteomics*, 2014, 147648.
- REINHARDT, J. & WOLFF, T. 2000. The influenza A virus M1 protein interacts with the cellular receptor of activated C kinase (RACK) 1 and can be phosphorylated by protein kinase C. *Vet Microbiol*, 74, 87-100.
- RENTERO, C., EVANS, R., WOOD, P., TEBAR, F., VILA DE MUGA, S., CUBELLS, L., DE DIEGO, I., HAYES, T. E., HUGHES, W. E., POL, A., RYE, K. A., ENRICH, C. & GREWAL, T. 2006. Inhibition of H-Ras and MAPK is compensated by PKC-dependent pathways in annexin A6 expressing cells. *Cell Signal*, 18, 1006-16.
- REVERTER, M., RENTERO, C., DE MUGA, S. V., ALVAREZ-GUAITA, A., MULAY, V., CAIRNS, R., WOOD, P., MONASTYRSKAYA, K., POL, A., TEBAR, F., BLASI, J., GREWAL, T. & ENRICH, C. 2011. Cholesterol transport from late endosomes to the Golgi regulates t-SNARE trafficking, assembly, and function. *Mol Biol Cell*, 22, 4108-23.
- RICHARDSON, J. C. & SIMMONS, N. L. 1979. Demonstration of protein asymmetries in the plasma membrane of cultured renal (MDCK) epithelial cells by lactoperoxidase-mediated iodination. *FEBS Lett*, 105, 201-4.
- ROBERTS, K. L., LESER, G. P., MA, C. & LAMB, R. A. 2013. The amphipathic helix of influenza A virus M2 protein is required for filamentous bud formation and scission of filamentous and spherical particles. *J Virol*, 87, 9973-82.
- ROBERTS, P. C., LAMB, R. A. & COMPANS, R. W. 1998. The M1 and M2 proteins of influenza A virus are important determinants in filamentous particle formation. *Virology*, 240, 127-37.
- ROBERTSON, J. S. 1979. 5' and 3' terminal nucleotide sequences of the RNA genome segments of influenza virus. *Nucleic Acids Res*, 6, 3745-57.
- ROSSMAN, J. S., JING, X., LESER, G. P. & LAMB, R. A. 2010. Influenza virus M2 protein mediates ESCRT-independent membrane scission. *Cell*, 142, 902-13.
- ROSSMAN, J. S. & LAMB, R. A. 2011. Influenza virus assembly and budding. *Virology*, 411, 229-36.
- ROSSMAN, J. S., LESER, G. P. & LAMB, R. A. 2012. Filamentous influenza virus enters cells via macropinocytosis. *J Virol*, 86, 10950-60.
- RUIGROK, R., BAUDIN, F., PETIT, I. & WEISSENHORN, W. 2001. Role of influenza virus M1 protein in the viral budding process. *International Congress Series*, 1219, 397-404.
- RUIGROK, R. W. & BAUDIN, F. 1995. Structure of influenza virus ribonucleoprotein particles. II. Purified RNA-free influenza virus ribonucleoprotein forms structures that are indistinguishable from the intact influenza virus ribonucleoprotein particles. *J Gen Virol*, 76 ( Pt 4), 1009-14.
- RUST, M. J., LAKADAMYALI, M., ZHANG, F. & ZHUANG, X. 2004. Assembly of endocytic machinery around individual influenza viruses during viral entry. *Nat Struct Mol Biol*, 11, 567-73.
- SADLER, A. J. & WILLIAMS, B. R. 2008. Interferon-inducible antiviral effectors. *Nat Rev Immunol*, 8, 559-68.
- SAKAGUCHI, T., LESER, G. P. & LAMB, R. A. 1996. The ion channel activity of the influenza virus M2 protein affects transport through the Golgi apparatus. *J Cell Biol*, 133, 733-47.
- SAMJI, T. 2009. Influenza A: understanding the viral life cycle. *Yale J Biol Med*, 82, 153-9.
- SANDERS, C. J., DOHERTY, P. C. & THOMAS, P. G. 2011. Respiratory epithelial cells in innate immunity to influenza virus infection. *Cell Tissue Res*, 343, 13-21.
- SATTERLY, N., TSAI, P. L., VAN DEURSEN, J., NUSSENZVEIG, D. R., WANG, Y., FARIA, P. A., LEVAY, A., LEVY, D. E. & FONTOURA, B. M. 2007. Influenza virus targets the mRNA export machinery and the nuclear pore complex. *Proc Natl Acad Sci U S A*, 104, 1853-8.
- SCHMIDT, N. W., MISHRA, A., WANG, J., DEGRADO, W. F. & WONG, G. C. 2013. Influenza virus A M2 protein generates negative Gaussian membrane curvature necessary for budding and scission. *J Am Chem Soc*, 135, 13710-9.

- SCHMITT, A. P. & LAMB, R. A. 2005. Influenza virus assembly and budding at the viral budzone. *Adv Virus Res*, 64, 383-416.
- SCHMITZ, N., KURRER, M., BACHMANN, M. F. & KOPF, M. 2005. Interleukin-1 is responsible for acute lung immunopathology but increases survival of respiratory influenza virus infection. *J Virol*, 79, 6441-8.
- SCHROEDER, C., HEIDER, H., MONCKE-BUCHNER, E. & LIN, T. I. 2005. The influenza virus ion channel and maturation cofactor M2 is a cholesterol-binding protein. *Eur Biophys J*, 34, 52-66.
- SCHROEDER, F., ATSHAVES, B. P., MCINTOSH, A. L., GALLEGOS, A. M., STOREY, S. M., PARR, R. D., JEFFERSON, J. R., BALL, J. M. & KIER, A. B. 2007. Sterol carrier protein-2: new roles in regulating lipid rafts and signaling. *Biochim Biophys Acta*, 1771, 700-18.
- SCHULTZ-CHERRY, S., DYBDAHL-SISSOKO, N., NEUMANN, G., KAWAOKA, Y. & HINSHAW, V. S. 2001. Influenza virus ns1 protein induces apoptosis in cultured cells. *J Virol*, 75, 7875-81.
- SCHUMACHER, C., CLARK-LEWIS, I., BAGGIOLINI, M. & MOSER, B. 1992. High- and low-affinity binding of GRO alpha and neutrophil-activating peptide 2 to interleukin 8 receptors on human neutrophils. *Proc Natl Acad Sci U S A*, 89, 10542-6.
- SELADI-SCHULMAN, J., STEEL, J. & LOWEN, A. C. 2013. Spherical influenza viruses have a fitness advantage in embryonated eggs, while filament-producing strains are selected in vivo. *J Virol*, 87, 13343-53.
- SEN, G. C. 2001. Viruses and interferons. *Annu Rev Microbiol*, 55, 255-81.
- SEO, S. H. & WEBSTER, R. G. 2002. Tumor necrosis factor alpha exerts powerful anti-influenza virus effects in lung epithelial cells. *J Virol*, 76, 1071-6.
- SHAPIRA, S. D., GAT-VIKS, I., SHUM, B. O., DRICOT, A., DE GRACE, M. M., WU, L., GUPTA, P. B., HAO, T., SILVER, S. J., ROOT, D. E., HILL, D. E., REGEV, A. & HACHOEN, N. 2009. A physical and regulatory map of host-influenza interactions reveals pathways in H1N1 infection. *Cell*, 139, 1255-67.
- SHARMA, K., TRIPATHI, S., RANJAN, P., KUMAR, P., GARTEN, R., DEYDE, V., KATZ, J. M., COX, N. J., LAL, R. B., SAMBHARA, S. & LAL, S. K. 2011. Influenza A virus nucleoprotein exploits Hsp40 to inhibit PKR activation. *PLoS One*, 6, e20215.
- SHAW, M. L. 2011. The host interactome of influenza virus presents new potential targets for antiviral drugs. *Rev Med Virol*, 21, 358-69.
- SHAW, M. L., STONE, K. L., COLANGELO, C. M., GULCICEK, E. E. & PALESE, P. 2008. Cellular proteins in influenza virus particles. *PLoS Pathog*, 4, e1000085.
- SHISHKOV, A., BOGACHEVA, E., FEDOROVA, N., KSENOFONTOV, A., BADUN, G., RADYUKHIN, V., LUKASHINA, E., SEREBRYAKOVA, M., DOLGOV, A., CHULICHKOV, A., DOBROV, E. & BARATOVA, L. 2011. Spatial structure peculiarities of influenza A virus matrix M1 protein in an acidic solution that simulates the internal lysosomal medium. *FEBS J*, 278, 4905-16.
- SHTYKOVA, E. V., BARATOVA, L. A., FEDOROVA, N. V., RADYUKHIN, V. A., KSENOFONTOV, A. L., VOLKOV, V. V., SHISHKOV, A. V., DOLGOV, A. A., SHILOVA, L. A., BATISHCHEV, O. V., JEFFRIES, C. M. & SVERGUN, D. I. 2013. Structural analysis of influenza A virus matrix protein M1 and its self-assemblies at low pH. *PLoS One*, 8, e82431.
- SHTYRYA, Y. A., MOCHALOVA, L. V. & BOVIN, N. V. 2009. Influenza virus neuraminidase: structure and function. *Acta Naturae*, 1, 26-32.
- SIECZKARSKI, S. B. & WHITTAKER, G. R. 2005. Characterization of the host cell entry of filamentous influenza virus. *Arch Virol*, 150, 1783-96.
- SIMPSON-HOLLEY, M., ELLIS, D., FISHER, D., ELTON, D., MCCAULEY, J. & DIGARD, P. 2002. A functional link between the actin cytoskeleton and lipid rafts during budding of filamentous influenza virions. *Virology*, 301, 212-25.
- SKEHEL, J. J. & WILEY, D. C. 2000. Receptor binding and membrane fusion in virus entry: the influenza hemagglutinin. *Annu Rev Biochem*, 69, 531-69.
- SMITH, P. D., DAVIES, A., CRUMPTON, M. J. & MOSS, S. E. 1994. Structure of the human annexin VI gene. *Proc Natl Acad Sci U S A*, 91, 2713-7.

- STAGLIAR, I., KOROSTENSKY, C., JOHANSSON, N. & TE HEESSEN, S. 1998. A genetic system based on split-ubiquitin for the analysis of interactions between membrane proteins in vivo. *Proc Natl Acad Sci U S A*, 95, 5187-92.
- STEINHAUER, D. A. 1999. Role of hemagglutinin cleavage for the pathogenicity of influenza virus. *Virology*, 258, 1-20.
- SUGUITAN, A. L., JR., MATSUOKA, Y., LAU, Y. F., SANTOS, C. P., VOGEL, L., CHENG, L. I., ORANDLE, M. & SUBBARAO, K. 2012. The multibasic cleavage site of the hemagglutinin of highly pathogenic A/Vietnam/1203/2004 (H5N1) avian influenza virus acts as a virulence factor in a host-specific manner in mammals. *J Virol*, 86, 2706-14.
- SUN, X. & WHITTAKER, G. R. 2003. Role for influenza virus envelope cholesterol in virus entry and infection. *J Virol*, 77, 12543-51.
- TAKAHASHI, T., SUZUKI, Y. & SUZUKI, T. 2006. [Role of influenza virus sialidase]. *Seikagaku*, 78, 409-13.
- TAKEDA, M., LESER, G. P., RUSSELL, C. J. & LAMB, R. A. 2003. Influenza virus hemagglutinin concentrates in lipid raft microdomains for efficient viral fusion. *Proc Natl Acad Sci U S A*, 100, 14610-7.
- TAKEUCHI, O. & AKIRA, S. 2009. Innate immunity to virus infection. *Immunol Rev*, 227, 75-86.
- TALON, J., HORVATH, C. M., POLLEY, R., BASLER, C. F., MUSTER, T., PALESE, P. & GARCIA-SASTRE, A. 2000. Activation of interferon regulatory factor 3 is inhibited by the influenza A virus NS1 protein. *J Virol*, 74, 7989-96.
- TANAKA, R. D., LI, A. C., FOGELMAN, A. M. & EDWARDS, P. A. 1986. Inhibition of lysosomal protein degradation inhibits the basal degradation of 3-hydroxy-3-methylglutaryl coenzyme A reductase. *J Lipid Res*, 27, 261-73.
- TANG, Y., ZAITSEVA, F., LAMB, R. A. & PINTO, L. H. 2002. The gate of the influenza virus M2 proton channel is formed by a single tryptophan residue. *J Biol Chem*, 277, 39880-6.
- TANIDA, I., UENO, T. & KOMINAMI, E. 2008. LC3 and Autophagy. *Methods Mol Biol*, 445, 77-88.
- TARUS, B., CHEVALIER, C., RICHARD, C. A., DELMAS, B., DI PRIMO, C. & SLAMA-SCHWOK, A. 2012. Molecular dynamics studies of the nucleoprotein of influenza A virus: role of the protein flexibility in RNA binding. *PLoS One*, 7, e30038.
- TAUBER, S., LIGERTWOOD, Y., QUIGG-NICOL, M., DUTIA, B. M. & ELLIOTT, R. M. 2012. Behaviour of influenza A viruses differentially expressing segment 2 gene products in vitro and in vivo. *J Gen Virol*, 93, 840-9.
- TECLE, T., WHITE, M. R., SORENSEN, G., GANTZ, D., KACAK, N., HOLMSKOV, U., SMITH, K., CROUCH, E. C. & HARTSHORN, K. L. 2008. Critical role for cross-linking of trimeric lectin domains of surfactant protein D in antiviral activity against influenza A virus. *Biochem J*, 412, 323-9.
- TONG, S., LI, Y., RIVAILLER, P., CONRARDY, C., CASTILLO, D. A., CHEN, L. M., RECUENCO, S., ELLISON, J. A., DAVIS, C. T., YORK, I. A., TURMELLE, A. S., MORAN, D., ROGERS, S., SHI, M., TAO, Y., WEIL, M. R., TANG, K., ROWE, L. A., SAMMONS, S., XU, X., FRACE, M., LINDBLADE, K. A., COX, N. J., ANDERSON, L. J., RUPPRECHT, C. E. & DONIS, R. O. 2012. A distinct lineage of influenza A virus from bats. *Proc Natl Acad Sci U S A*, 109, 4269-74.
- TONG, S., ZHU, X., LI, Y., SHI, M., ZHANG, J., BOURGEOIS, M., YANG, H., CHEN, X., RECUENCO, S., GOMEZ, J., CHEN, L. M., JOHNSON, A., TAO, Y., DREYFUS, C., YU, W., MCBRIDE, R., CARNEY, P. J., GILBERT, A. T., CHANG, J., GUO, Z., DAVIS, C. T., PAULSON, J. C., STEVENS, J., RUPPRECHT, C. E., HOLMES, E. C., WILSON, I. A. & DONIS, R. O. 2013. New world bats harbor diverse influenza A viruses. *PLoS Pathog*, 9, e1003657.
- TRIPATHI, S., WHITE, M. R. & HARTSHORN, K. L. 2015. The amazing innate immune response to influenza A virus infection. *Innate Immun*, 21, 73-98.
- TSFASMAN, T., KOST, V., MARKUSHIN, S., LOTTE, V., KOPTIAEVA, I., BOGACHEVA, E., BARATOVA, L. & RADYUKHIN, V. 2015. Amphipathic alpha-helices and putative cholesterol binding domains of the influenza virus matrix M1 protein are crucial for virion structure organisation. *Virus Res*, 210, 114-8.

- TUVIM, M. J., GILBERT, B. E., DICKEY, B. F. & EVANS, S. E. 2012. Synergistic TLR2/6 and TLR9 activation protects mice against lethal influenza pneumonia. *PLoS One*, 7, e30596.
- UNTERHOLZNER, L. & BOWIE, A. G. 2008. The interplay between viruses and innate immune signaling: recent insights and therapeutic opportunities. *Biochem Pharmacol*, 75, 589-602.
- VAN DE SANDT, C. E., KREIJTZ, J. H. & RIMMELZWAAN, G. F. 2012. Evasion of influenza A viruses from innate and adaptive immune responses. *Viruses*, 4, 1438-76.
- VAN KERKHOFF, P., ALVES DOS SANTOS, C. M., SACHSE, M., KLUMPERMAN, J., BU, G. & STROUS, G. J. 2001. Proteasome inhibitors block a late step in lysosomal transport of selected membrane but not soluble proteins. *Mol Biol Cell*, 12, 2556-66.
- VARGA, Z. T. & PALESE, P. 2011. The influenza A virus protein PB1-F2: killing two birds with one stone? *Virulence*, 2, 542-6.
- VARGA, Z. T., RAMOS, I., HAI, R., SCHMOLKE, M., GARCIA-SASTRE, A., FERNANDEZ-SESMA, A. & PALESE, P. 2011. The influenza virus protein PB1-F2 inhibits the induction of type I interferon at the level of the MAVS adaptor protein. *PLoS Pathog*, 7, e1002067.
- VAZQUEZ-CALVO, A., SOBRINO, F. & MARTIN-ACEBES, M. A. 2012. Plasma membrane phosphatidylinositol 4,5 bisphosphate is required for internalization of foot-and-mouth disease virus and vesicular stomatitis virus. *PLoS One*, 7, e45172.
- VECKMAN, V., OSTERLUND, P., FAGERLUND, R., MELEN, K., MATIKAINEN, S. & JULKUNEN, I. 2006. TNF-alpha and IFN-alpha enhance influenza-A-virus-induced chemokine gene expression in human A549 lung epithelial cells. *Virology*, 345, 96-104.
- VEIT, M., ENGEL, S., THAA, B., SCOLARI, S. & HERRMANN, A. 2013. Lipid domain association of influenza virus proteins detected by dynamic fluorescence microscopy techniques. *Cell Microbiol*, 15, 179-89.
- VEIT, M. & THAA, B. 2011. Association of influenza virus proteins with membrane rafts. *Adv Virol*, 2011, 370606.
- VELJKOVIC, V., VELJKOVIC, N., MULLER, C. P., MULLER, S., GLISIC, S., PEROVIC, V. & KOHLER, H. 2009. Characterization of conserved properties of hemagglutinin of H5N1 and human influenza viruses: possible consequences for therapy and infection control. *BMC Struct Biol*, 9, 21.
- VERBIST, K. C., ROSE, D. L., COLE, C. J., FIELD, M. B. & KLONOWSKI, K. D. 2012. IL-15 participates in the respiratory innate immune response to influenza virus infection. *PLoS One*, 7, e37539.
- VERMA, A., WHITE, M., VATHIPADIEKAL, V., TRIPATHI, S., MBIANDA, J., IEONG, M., QI, L., TAUBENBERGER, J. K., TAKAHASHI, K., JENSENIUS, J. C., THIEL, S. & HARTSHORN, K. L. 2012. Human H-ficolin inhibits replication of seasonal and pandemic influenza A viruses. *J Immunol*, 189, 2478-87.
- VILA DE MUGA, S., TIMPSON, P., CUBELLS, L., EVANS, R., HAYES, T. E., RENTERO, C., HEGEMANN, A., REVERTER, M., LESCHNER, J., POL, A., TEBAR, F., DALY, R. J., ENRICH, C. & GREWAL, T. 2009. Annexin A6 inhibits Ras signalling in breast cancer cells. *Oncogene*, 28, 363-77.
- WANG, C., LAMB, R. A. & PINTO, L. H. 1995. Activation of the M2 ion channel of influenza virus: a role for the transmembrane domain histidine residue. *Biophys J*, 69, 1363-71.
- WANG, M. & VEIT, M. 2016. Hemagglutinin-esterase-fusion (HEF) protein of influenza C virus. *Protein Cell*, 7, 28-45.
- WANG, S., CHI, X., WEI, H., CHEN, Y., CHEN, Z., HUANG, S. & CHEN, J. L. 2014. Influenza A virus-induced degradation of eukaryotic translation initiation factor 4B contributes to viral replication by suppressing IFITM3 protein expression. *J Virol*, 88, 8375-85.
- WANG, W., BUTLER, E. N., VEGUILLA, V., VASSELL, R., THOMAS, J. T., MOOS, M., JR., YE, Z., HANCOCK, K. & WEISS, C. D. 2008. Establishment of retroviral pseudotypes with influenza hemagglutinins from H1, H3, and H5 subtypes for sensitive and specific detection of neutralizing antibodies. *J Virol Methods*, 153, 111-9.
- WANG, X., HINSON, E. R. & CRESSWELL, P. 2007a. The interferon-inducible protein viperin inhibits influenza virus release by perturbing lipid rafts. *Cell Host Microbe*, 2, 96-105.

- WANG, X., LI, M., ZHENG, H., MUSTER, T., PALESE, P., BEG, A. A. & GARCIA-SASTRE, A. 2000. Influenza A virus NS1 protein prevents activation of NF-kappaB and induction of alpha/beta interferon. *J Virol*, 74, 11566-73.
- WANG, X., ZHANG, S., ZHANG, J., LAM, E., LIU, X., SUN, J., FENG, L., LU, H., YU, J. & JIN, H. 2013. Annexin A6 is down-regulated through promoter methylation in gastric cancer. *Am J Transl Res*, 5, 555-62.
- WANG, X. Q., YAN, Q., SUN, P., LIU, J. W., GO, L., MCDANIEL, S. M. & PALLER, A. S. 2007b. Suppression of epidermal growth factor receptor signaling by protein kinase C-alpha activation requires CD82, caveolin-1, and ganglioside. *Cancer Res*, 67, 9986-95.
- WATANABE, S., WATANABE, T. & KAWAOKA, Y. 2009. Influenza A virus lacking M2 protein as a live attenuated vaccine. *J Virol*, 83, 5947-50.
- WHO. 2016. *World Health Organisation* [Online]. Available: <http://www.who.int/mediacentre/factsheets/fs211/en/>.
- WIDJAJA, I., DE VRIES, E., TSCHERNE, D. M., GARCIA-SASTRE, A., ROTTIER, P. J. & DE HAAN, C. A. 2010. Inhibition of the ubiquitin-proteasome system affects influenza A virus infection at a postfusion step. *J Virol*, 84, 9625-31.
- WILEY, D. C. & SKEHEL, J. J. 1987. The structure and function of the hemagglutinin membrane glycoprotein of influenza virus. *Annu Rev Biochem*, 56, 365-94.
- WIRAWAN, E., VANDEN BERGHE, T., LIPPENS, S., AGOSTINIS, P. & VANDENABEELE, P. 2012. Autophagy: for better or for worse. *Cell Res*, 22, 43-61.
- WISE, H. M., FOEGLEIN, A., SUN, J., DALTON, R. M., PATEL, S., HOWARD, W., ANDERSON, E. C., BARCLAY, W. S. & DIGARD, P. 2009. A complicated message: Identification of a novel PB1-related protein translated from influenza A virus segment 2 mRNA. *J Virol*, 83, 8021-31.
- WOLFF, T., O'NEILL, R. E. & PALESE, P. 1998. NS1-Binding protein (NS1-BP): a novel human protein that interacts with the influenza A virus nonstructural NS1 protein is relocalized in the nuclei of infected cells. *J Virol*, 72, 7170-80.
- WOODFIN, B. M. & KAZIM, A. L. 1993. Interaction of the amino-terminus of an influenza virus protein with mitochondria. *Arch Biochem Biophys*, 306, 427-30.
- WU, W. W., SUN, Y. H. & PANTE, N. 2007. Nuclear import of influenza A viral ribonucleoprotein complexes is mediated by two nuclear localization sequences on viral nucleoprotein. *Virology*, 4, 49.
- WU, Y., WU, Y., TEFSSEN, B., SHI, Y. & GAO, G. F. 2014. Bat-derived influenza-like viruses H17N10 and H18N11. *Trends Microbiol*, 22, 183-91.
- XU, X., SONG, Y., LI, Y., CHANG, J., ZHANG, H. & AN, L. 2010. The tandem affinity purification method: an efficient system for protein complex purification and protein interaction identification. *Protein Expr Purif*, 72, 149-56.
- YANG, M. L., CHEN, Y. H., WANG, S. W., HUANG, Y. J., LEU, C. H., YEH, N. C., CHU, C. Y., LIN, C. C., SHIEH, G. S., CHEN, Y. L., WANG, J. R., WANG, C. H., WU, C. L. & SHIAU, A. L. 2011. Galectin-1 binds to influenza virus and ameliorates influenza virus pathogenesis. *J Virol*, 85, 10010-20.
- YI, M., CROSS, T. A. & ZHOU, H. X. 2008. A secondary gate as a mechanism for inhibition of the M2 proton channel by amantadine. *J Phys Chem B*, 112, 7977-9.
- YONDOLA, M. A., FERNANDES, F., BELICHA-VILLANUEVA, A., UCCELINI, M., GAO, Q., CARTER, C. & PALESE, P. 2011. Budding capability of the influenza virus neuraminidase can be modulated by tetherin. *J Virol*, 85, 2480-91.
- YOO, J. K., KIM, T. S., HUFFORD, M. M. & BRACIALE, T. J. 2013. Viral infection of the lung: host response and sequelae. *J Allergy Clin Immunol*, 132, 1263-76; quiz 1277.
- YU, M., LIU, X., CAO, S., ZHAO, Z., ZHANG, K., XIE, Q., CHEN, C., GAO, S., BI, Y., SUN, L., YE, X., GAO, G. F. & LIU, W. 2012. Identification and characterization of three novel nuclear export signals in the influenza A virus nucleoprotein. *J Virol*, 86, 4970-80.
- YU, W. C., CHAN, R. W., WANG, J., TRAVANTY, E. A., NICHOLLS, J. M., PEIRIS, J. S., MASON, R. J. & CHAN, M. C. 2011. Viral replication and innate host responses in primary human alveolar epithelial

- cells and alveolar macrophages infected with influenza H5N1 and H1N1 viruses. *J Virol*, 85, 6844-55.
- ZAMARIN, D., GARCIA-SASTRE, A., XIAO, X., WANG, R. & PALESE, P. 2005. Influenza virus PB1-F2 protein induces cell death through mitochondrial ANT3 and VDAC1. *PLoS Pathog*, 1, e4.
- ZAMARIN, D., ORTIGOZA, M. B. & PALESE, P. 2006. Influenza A virus PB1-F2 protein contributes to viral pathogenesis in mice. *J Virol*, 80, 7976-83.
- ZAMBON, M. 2011. Assessment of the burden of influenza in children. *Lancet*, 378, 1897-8.
- ZHANG, K., WANG, Z., FAN, G. Z., WANG, J., GAO, S., LI, Y., SUN, L., YIN, C. C. & LIU, W. J. 2015. Two polar residues within C-terminal domain of M1 are critical for the formation of influenza A Virions. *Cell Microbiol*, 17, 1583-93.
- ZHANG, R., CHI, X., WANG, S., QI, B., YU, X. & CHEN, J. L. 2014. The regulation of autophagy by influenza A virus. *Biomed Res Int*, 2014, 498083.
- ZHANG, S., WANG, J., WANG, Q. & TOYODA, T. 2010. Internal initiation of influenza virus replication of viral RNA and complementary RNA in vitro. *J Biol Chem*, 285, 41194-201.
- ZHENG, W. & TAO, Y. J. 2013. Structure and assembly of the influenza A virus ribonucleoprotein complex. *FEBS Lett*, 587, 1206-14.
- ZHIRNOV, O. P. & KLENK, H. D. 2007. Control of apoptosis in influenza virus-infected cells by up-regulation of Akt and p53 signaling. *Apoptosis*, 12, 1419-32.
- ZHIRNOV, O. P. & KLENK, H. D. 2013. Influenza A virus proteins NS1 and hemagglutinin along with M2 are involved in stimulation of autophagy in infected cells. *J Virol*, 87, 13107-14.
- ZHIRNOV, O. P., KONAKOVA, T. E., WOLFF, T. & KLENK, H. D. 2002. NS1 protein of influenza A virus down-regulates apoptosis. *J Virol*, 76, 1617-25.
- ZHOU, S., LIU, R., ZHAO, X., HUANG, C. & WEI, Y. 2011. Viral proteomics: the emerging cutting-edge of virus research. *Sci China Life Sci*, 54, 502-12.
- ZHOU, Z., JIANG, X., LIU, D., FAN, Z., HU, X., YAN, J., WANG, M. & GAO, G. F. 2009. Autophagy is involved in influenza A virus replication. *Autophagy*, 5, 321-8.

## **7 APPENDIX: Study of an engineered Annexin A1-derived peptide as a modulator of influenza A virus infection**

### **7.1 Introduction**

During my PhD studies I had the opportunity to attend several international conferences and interact with many well-known scientists. For instance, I had the opportunity to discuss with Professor Mauro Peretti, from Queen Mary University of London, who generously provided our group with an engineered annexin A1 (AnxA1)-derived peptide, containing 250aa from the N-terminal domain which mimics the role of the Annexin A1 full-length protein. As AnxA6, AnxA1 is a protein that binds to phospholipids in a calcium-dependent manner. It has been previously described to be expressed abundantly in the cytoplasm of many immune cell types and travels to the cell plasma membrane when cell activation or a specific stimulus occurs. It is known to be a regulator of inflammation; however, the molecular mechanism is still poorly understood. AnxA1 has been implicated in the modulation of both innate and adaptive immunity (D'Acquisto et al., 2008). For instance, AnxA1 acts as a potent anti-inflammatory factor when administered in mice, it limits neutrophil adhesion and migration to cellular tissues and inhibits chemoattractant response. It is also known that AnxA1 initiates signalling through the formyl peptide receptor 2 (FPR2), a G-protein-coupled receptor which is also the receptor for the anti-inflammatory lipoxin A4. Annexin A1, peptides derived from its N-terminal region, lipoxin A4 and other host factors are in competition to bind to FPR2 and activate downstream signalling and regulate anti-inflammatory responses (Perretti and D'Acquisto, 2009). It was also determined recently that AnxA1 overexpression leads to reduction of pro-inflammatory factors in PC12 neuronal cells. AnxA1 overexpression resulted in reduced reactive oxygen species production and pro-inflammatory factors such as IL-6, inducible nitric oxide synthase (iNOS) and NF- $\kappa$ B protein (Kiani-Esfahani et al., 2016). Finally, another recent study showed AnxA1 involvement in IAV infection. Arora and collaborators found that AnxA1 expression increased during IAV infection, promoting virus replication and virus-mediated

apoptosis. Also, they showed that mice deficient in AnxA1 presented a reduced viral load and increased survival (Arora et al., 2016).

## **7.2 Hypothesis and aim of the study**

We hypothesized that AnxA1 may act as a soluble factor regulating IAV infection. In this study, we investigated the role of an engineered AnxA1-derived peptide during IAV infection and whether it is beneficial or detrimental to IAV. To investigate our hypothesis, I used a combination of serological techniques such as haemagglutination assay and haemagglutination inhibition assay with the AnxA1 peptide to test whether it prevents virus attachment to red blood cells and limits IAV infection.

## **7.3 Materials and methods**

### **7.3.1 Haemagglutination assay**

The haemagglutination assay is a serological technique which enables to quantify viruses based on their ability to bind to molecules present on the surface of red blood cells (RBCs). The titre of virus was estimated by serial dilutions of virus added to wells containing red blood cells. First, a 10% solution of guinea pig red blood cells (TCS Biosciences Ltd) in PBS was prepared by centrifuging twice at 800g or 1200rpm for 10min and 5min, and removing the supernatant. After the second spin, the supernatant was removed and PBS was added to make the 10% stock cell solution. Before the experiment, a 0.75% solution of red blood cells in PBS is prepared. Then, a serial dilution of each virus was prepared in a round-bottom U-shape 96-well dish (Fisher scientific, UK). 50µl of PBS were first added to each well, 50µl of virus sample were added to the first column, mixed well and 50µl transferred to the next well on the right till the last column of the plate. 50µl from the wells of the last column were discarded into 1% Virkon (Fisher Scientific, UK). Finally, 50µl of the 0.75% red blood cell solution were added to each well. After shaking gently, the plates were left at room temperature for 2h. Haemagglutination of the red blood cells produced a uniform reddish

colour across the well and the lack of haemagglutination produced a halo at the bottom of the well. The virus HA titre is the highest dilution factor with a positive result.

### 7.3.2 Haemagglutination assay inhibition

This technique is a modification of the haemagglutination assay which enables to measure the level of proteins of interest reacting with IAV, inhibiting its attachment to red blood cells and subsequent haemagglutination when present at a sufficient concentration. A 0.75% guinea pig red blood cell solution was prepared in PBS together with the viruses at the titres determined by the HA test. A serial dilution of our AnxA1 peptide was prepared by adding 25µl of peptide sample at the desired concentration to the first column of wells containing 25µl of PBS, mixing well and transferring 25µl to each well of the next column on the right. 25µl were discarded from the wells of the last column. In this technique, the virus dilution was left for 60min at 37°C to interact with the serial dilution of AnxA1 peptide and then 50µl of 0.75% guinea pig red blood cells were added to each well for 60min. If inhibition of haemagglutination occurred, a halo of settled cells in the centre of the wells appeared.

## 7.4 Results

Several studies have already demonstrated the role of AnxA1 and its derived peptides in the modulation of inflammation. It has already been mentioned that AnxA1 participates in the regulation of innate and adaptive immune responses, and also to play an anti-inflammatory role in mice. AnxA1 expression also leads to inhibition of pro-inflammatory mediators in neurons. In addition, a study recently published showed AnxA1 involvement in the regulation of IAV infection as its overexpression translated in enhanced virus replication and apoptosis, whereas its knock-out from mice decreased viral titers and increased survival (Arora et al., 2016, Kiani-Esfahani et al., 2016, Perretti and D'Acquisto, 2009, D'Acquisto et al., 2008). In this section, we used several viruses to investigate whether AnxA1-derived peptide acts as a modulator of IAV infection. We first performed an haemagglutination assay to determine HA titers of influenza A/WSN/33 (H1N1), pandemic A/England/2009 (H1N1), A/HK/99 (H3N2) and A/Udorn/72 (H3N2), and tested their ability to bind to red blood cells (figure 7.1). As already

mentioned, haemagglutination of the red blood cells produced a uniform reddish colour across the well and the lack of haemagglutination produced a halo at the bottom of the well. The virus HA titre is the highest dilution factor with a positive result. When performing HA test on both influenza A/WSN/33 and pandemic A/England/2009 (H1N1) viruses, we found that dilutions from 1:4 to 1:256 exhibited a uniform reddish colour corresponding to haemagglutination of RBCs. From dilutions 1:512 to 1:8.092, we observed a halo corresponding to no haemagglutination. Negative control wells with PBS only also exhibited a halo, suggesting that there was no haemagglutination. Also, the wells with low virus concentration exhibited a similar result to negative controls with PBS as a halo could be observed. These results determine that HA titer for both H1N1 viruses was of 256. All conditions were performed in duplicate to confirm HA titers.

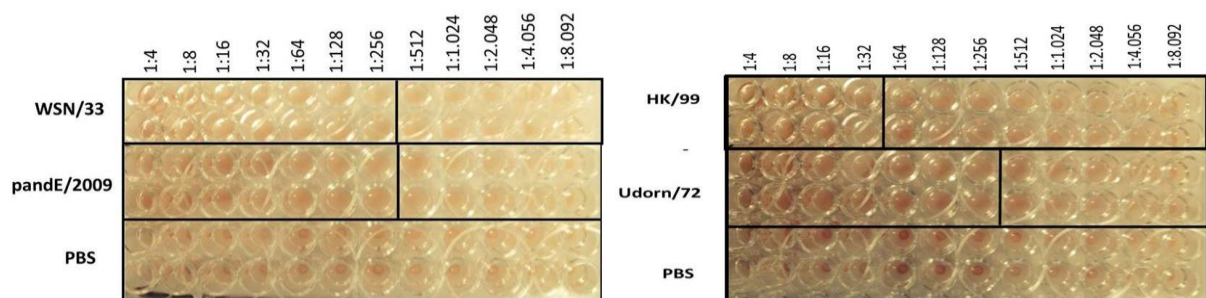


**Figure 7.1. Haemagglutination assays of H1N1 and H3N2 influenza viruses using guinea pig red blood cells.** Panels show HA titers after 2-fold serial dilutions of used H1N1 (left) and H3N2 (right) viruses in PBS and red blood cells in duplicates. PBS and virus were added to the first well, mixed and transferred into the next well for virus dilution from 1:4 to 1:8.092. 0.75% RBCs were then added to all wells and left at room temperature for 2h. Bottom rows containing only PBS were used as negative controls.

In addition, we found haemagglutination for influenza A/HK/99 (H3N2) in dilutions from 1:4 to 1:32 and in dilutions 1:4 to 1:256 for influenza A/Udorn/72 (H3N2), whereas a halo could be observed from dilutions 1:64 and 1:512 for influenza A/HK/99 and A/Udorn/72 (H3N2) viruses respectively. Therefore, HA titers were of 32 and 256 for H3N2 viruses. Again, we observed a halo in negative control wells with PBS, suggesting that there was no haemagglutination,

which was also very similar to result observed in wells with low virus concentration. After obtaining HA titers for all viruses, I performed a haemagglutination inhibition assay with our AnxA1-derived peptide to investigate whether it reacts with IAV, inhibits virus attachment to RBCs and also to determine at which concentration it is required for its inhibitory effect (figure 7.2). In order to test this hypothesis, we adjusted all virus samples to corresponding HA titers found by haemagglutination test and then added different concentrations of AnxA1-derived peptide to wells.

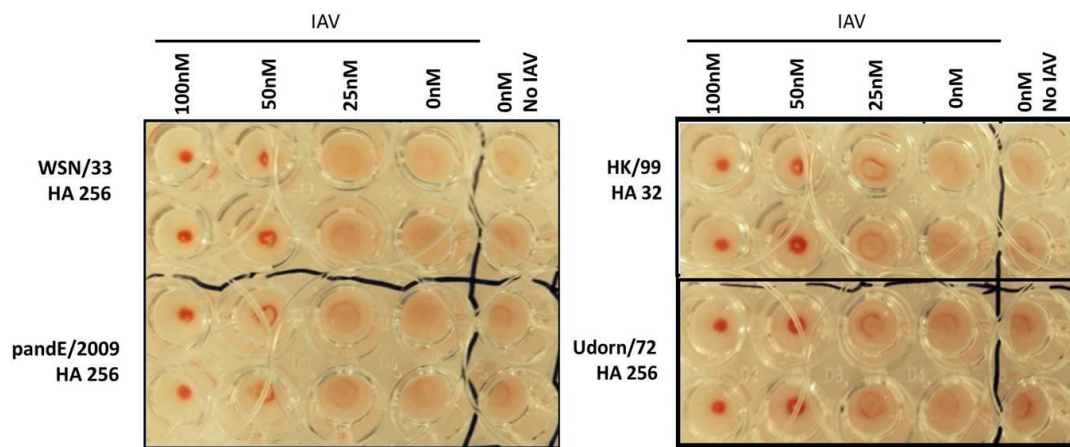


**Figure 7.2. Haemagglutination inhibition assays of H1N1 and H3N2 influenza viruses using guinea pig red blood cells.** Panels show wells a serial dilution of AnxA1-derived peptides from 100nM to 25nM in PBS. Then, H1N1 (left) and H3N2 (right) viruses were added to each corresponding well at the concentrations determined by the HA test and left incubating at 37°C for 1h. Finally, 0.75% RBCs were added to all wells and left at 37°C for 1h. Negative control wells of the last column of each plate contained neither peptide nor IAV.

In this experiment, we observed a same pattern for both H1N1 and H3N2 viruses used. We first observed a very clear halo in wells with 100 nM and 50 nM of the AnxA1-derived peptide, suggesting that these wells contain a sufficient concentration of peptide to interact with viral particles and effectively block their haemagglutination. Conversely, we observed a uniform reddish colour across the wells with 25 nM and 0 nM of peptide, possibly due to a lower concentration of AnxA1 peptide which was not sufficient to interfere with haemagglutination of RBCs. Surprisingly, a similar colour and pattern was observed in negative control samples

with PBS only when compared to wells with low concentrations of peptide, these results were unexpected in controls as we should have observed a halo like in wells with high concentrations of peptide where no haemagglutination is visible. However, it may be possible that there is a slightly darker halo which could correspond to a lack of haemagglutination which is especially observed in rows incubated with the pandemic influenza A/England/2009 (H1N1) and both influenza A/HK/99 and A/Udorn/72 (H3N2) viruses. Altogether, these results indicate that 50nM of AnxA1-derived peptide are sufficient to inhibit IAV haemagglutination as a very clear halo appeared in wells of all strains used in our experiment. We suggest that AnxA1 peptide interferes with IAV ability to bind to RBCs and may act as a soluble inhibitor of IAV infection, by preventing its attachment to receptors at the surface of cells and blocking its propagation.

## **7.5 Discussion and conclusion**

The role of AnxA1 in the modulation in IAV infection is poorly understood, only one study has described its involvement during the virus life cycle. Arora and collaborators described that AnxA1 expression is increased during infection, resulting in virus replication and apoptosis. They also showed that mice deficient in AnxA1 exhibited a lower viral load and an increased survival (Arora et al., 2016). From this study, it is evident that AnxA1 is a host factor that facilitates replication and promotes IAV propagation. Other studies have shown that AnxA1 can also regulate an anti-inflammatory response. AnxA1 plays a role innate and adaptive immune responses, regulates an anti-inflammatory response in mice and can induce down-regulation of pro-inflammatory factors such as iNOS and NF- $\kappa$ B in neurons (Kiani-Esfahani et al., 2016; Perretti and D'Acquisto, 2009; D'Acquisto et al., 2008). In this section, I investigated whether an engineered AnxA1-derived peptide modulates IAV infection and whether it either assists or restricts viral life cycle. To study this hypothesis, I first performed a haemagglutination assay to obtain HA titers of the 4 different IAV strains used. The HA titer of for both H1N1 viruses was of 256; whereas HA titer was of 32 and 256 for influenza A/HK/99 and A/Udorn/72 (H3N2) viruses respectively (figure 7.1). I then used the titers found by

haemagglutination assay to investigate by haemagglutination inhibition assay whether the AnxA1-derived peptide prevents virus attachment to red blood cells and limits IAV propagation. We found that AnxA1 peptide could interfere with IAV binding to guinea pig RBCs (figure 7.2). Wells incubated with IAV and 50nM of peptide exhibited a halo, suggesting that 50nM of our peptide were sufficient to inhibit IAV haemagglutination. We suggest that AnxA1 peptide interferes with IAV ability to bind to RBCs and may inhibit IAV infection, by preventing its attachment to receptors at the surface of cells and blocking its propagation. We suspect AnxA1 peptide could act as soluble mediator to inhibit IAV in the respiratory tract in a similar fashion to other host factors, such as SP-A, SP-D or other sialic acid inhibitors which exert their antiviral activity by preventing binding of IAV to sialic-acids at the surface of susceptible cells and block virus propagation (Tripathi et al., 2015, Tecele et al., 2008, Hawgood et al., 2004). These results are in disagreement with the study performed by Arora and collaborators as they determined that AnxA1 promotes IAV replication and facilitate infection (Arora et al., 2016). However, it could be possible that AnxA1 plays a pivotal role during infection and could act as an inhibitor prior to IAV entry into a host cell and an assisting factor during infection. This has already been suggested for other important factors; for instance, it was suggested that the transcription factor NF- $\kappa$ B is a pre-requisite for IAV infection but it can also regulate an anti-inflammatory response by activating the synthesis of cytokines (Nimmerjahn et al., 2004). Finally, it would be interesting to test whether the AnxA1-peptide virus has an antiviral effect during early stages of infection; it is worth to test whether incubation of virus with our peptide of interest would translate in reduced virus titers and also whether it interferes with replication or early stages of infection. For instance, we could also investigate whether virus entry or M1/M2 gene and protein expression are impaired upon peptide incubation during early infection. We conclude that AnxA1 may act as a soluble mediator of IAV infection and could inhibit virus propagation; however, further investigation is required to confirm our preliminary results and to further understand the possible mechanism underlying virus restriction by our AnxA1-derived peptide.